Alma Mater Studiorum – Università di Bologna

DOTTORATO DI RICERCA IN

Beni Culturali e Ambientali

Ciclo 34

Settore Concorsuale: 05/C1 Ecologia

Settore Scientifico Disciplinare: BIO/07 ECOLOGIA

The mesophotic zone of the Mediterranean Sea: spatial definition, biodiversity, and predictive models

Presentata da: Giorgio Castellan

Coordinatore Dottorato

Prof. Roberto Pasini

Supervisore

Dr. Federica Foglini

Co-supervisori

Prof. Marco Abbiati
Dr. Marco Taviani
Dr. Lorenzo Angeletti

Esame finale anno 2022

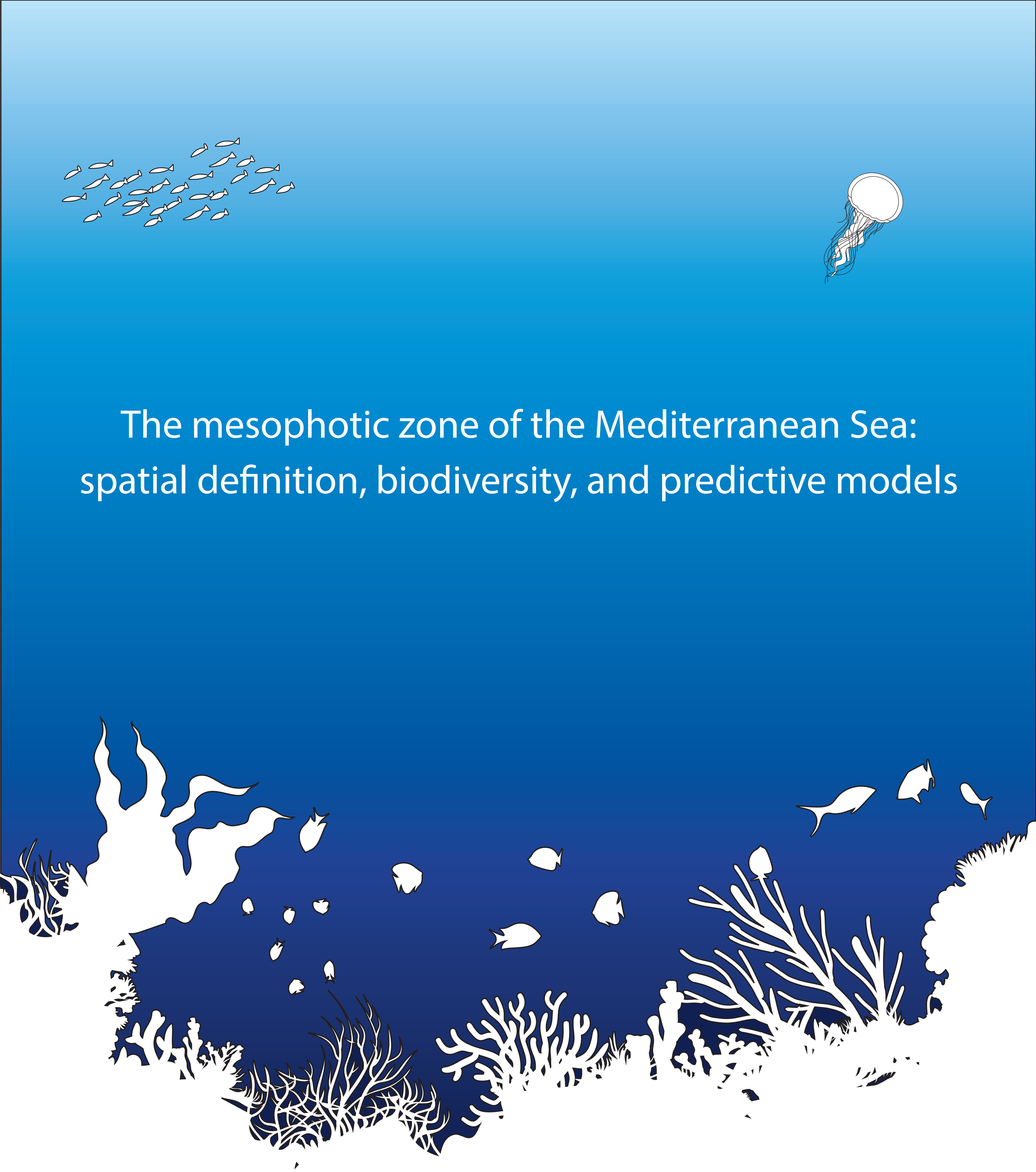

The mesophotic zone of the Mediterranean Sea: spatial definition, biodiversity, and predictive models

Giorgio Castellan

Bologna 2022

Ph.D. Thesis

Table of contents

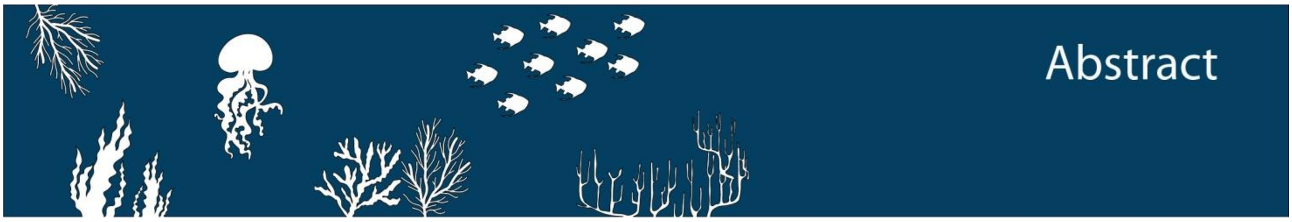

Abstract

Below the shallow waters up to where the sunlight turns out is where the mesophotic zone extends. Although long since recognized, the mesophotic zone has been largely ignored by the scientific community in favor of the shallower and deeper counterparts.

The mesophotic zone is mostly defined as ranging between 30 and 150 m depth. However, these borders are necessarily imprecise due to variations in the penetration of light along the water column related to local factors, mainly solar radiation incidence and water clarity. The Mediterranean Sea, for instance, represents a case in point, being characterized by complex oceanographic dynamics, strong climatic (e.g., rainfalls, sunlight), oceanographic (e.g., water temperature and salinity) and bio-geochemical (e.g., nutrients) gradients, which generate an alternation of temperate- or tropical-like situations within a limited spatial scale (about 4,000 km from the Strait of Gibraltar to the Gulf of Iskenderun, southeastern coast of Turkey). If we were able to integrate the light regime into the definition of the mesophotic zone, we could provide a robust estimation of its bathymetric range and spatial extent not only for the Mediterranean Sea but for any geographical location.

A better understanding of the mesophotic domain of the Mediterranean Sea, starting from its spatial and bathymetric definition, is, moreover, crucial to orient future research and explorations, and support proper management plans and conservation actions.

From late 90s, the advances in underwater technologies along with the growth in computing performances permitted the direct observation of benthic ecosystems populating intermediate to deep situations. Visual surveys performed with manned and unmanned vehicles represent plastic

data that can be used for different purposes and processed following different approaches to convert video recordings and images into spatial information. In the last two decades, the exploration of mesophotic ecosystems is largely increased, documenting the biodiversity associated to ecosystems at mesophotic depths along with their ecological importance, including the ability to provide refuges, and areas for spawning, breeding, feeding, and growth to maturity. Much of the biodiversity characterizing the Mediterranean benthic ecosystems at mesophotic depths is, however, largely undisclosed, with most of the information mainly focused on situations dominated by cnidarians. To some extent, the spectrum of the different biological assemblages that occur at mesophotic depths represents a gap in our knowledge of the mesophotic zone in the Mediterranean Sea, with only a few studies documenting situations dominated by taxonomic components other than cnidarians. To a larger extent, the patterns of diversity and biogeographic processes related to mesophotic ecosystems is still in its infancy. Nevertheless, much of this information are fundamental for more robust ecological characterization and to orient conservation measures.

This thesis provides a quantitative assessment of bathymetric and spatial extent of the mesophotic zone in the Mediterranean Sea applying an approach based on the light regime, using literature information to valide the estimation. The results show that 15% of the entire basin might be under mesophotic conditions, which likely occur between ca. 10-0.005% of surface Photosynthetically Active Radiation (PAR) in a depth range of 30-175.5 m, on average.

To aid the choice of the most accurate method to process visual benthic surveys collected in mesophotic and deep-sea situations, different techniques are tested within the thesis to identify the best compromise between analytic effort and the quality of results. Methods for video-frame extraction at fixed time intervals are compared with method based on distance intervals. The results suggest that time-based extraction methods might be more appropriate for the study of assemblages composition whilst distance-based methods ensure higher accuracy in estimating the extent of substrate covers.

The most conservative time-based method (with intervals of 10 s) is, then, used to analyze a set of 25 visual surveys collected at mesophotic depth in the Mediterranean Sea with the aim of characterizing their taxonomic and functional diversity. More than 290 taxa are identified, occurring in 5 categories of assemblages presenting different levels of both taxonomic and functional diversity. The role of environmental variables and geographic location in influencing the presence and the composition of the surveyed mesophotic assemblages is also explored, highlighting that the environmental setting might be the primary factor controlling the distribution and the structure of the assemblages at mesophotic depths.

A predictive model is, successively, implemented and used to predict the distribution of areas suitable for the presence of deep-water oyster reefs assemblages, which show high levels of taxonomic and functional diversity but are still largely unexplored in the Mediterranean Sea.

Finally, the Gulf of Mexico is used as case study to test if the physical approach to map the mesophotic zone could be applied to different geographical location and whether the environmental setting influences the composition of mesophotic assemblages also beyond the Mediterranean borders. The results suggests that the proposed light-based method can be successfully applied also to estimate the bathymetric and spatial extent of the mesophotic zone in extra-Mediterranean regions and that environmental variables might play a central role in shaping mesophotic assemblages structure on a global scale.

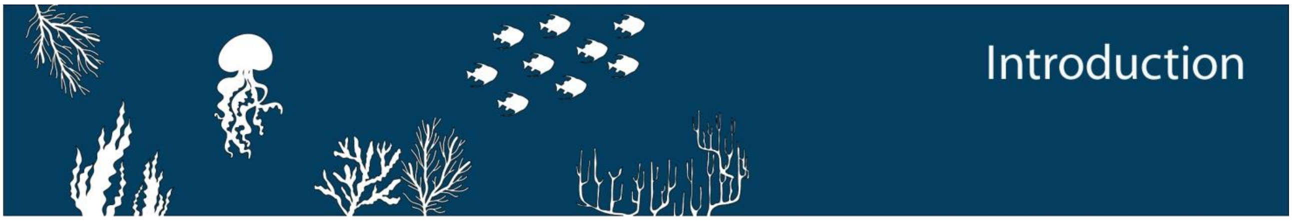

Introduction

Oceans are three-dimensional spaces where physical, chemical, and biological factors vary widely across depths, generating a vertical succession of diverse environmental niches suitable for different biological components (Levin et al., 2018). Of the factors co-varying with depth, the gradient of light plays a major role in structuring communities, controlling the vertical zonation of obligate phototrophic organisms (Markager & Sand-Jensen, 1992). The uppermost part of the water column, the photic zone (Tett, 1990), is characterized by light in the wavelength between 400 and 700 nm, Photosynthetically Active Radiation (PAR), enough intense to sustain photosynthetic metabolism. Traveling through the water column, the light is absorbed and scattered by dissolved and suspended particles that reduce its intensity and change its spectral composition (Fig. 1). The portion between where light (in terms of intensity or composition) begins to be deficient for shallow-water photophilous species down to where photosynthesis fails is known as the mesophotic zone (e.g., Lesser, et al., 2009; Hinderstein et al., 2010; Kahng et al., 2019).

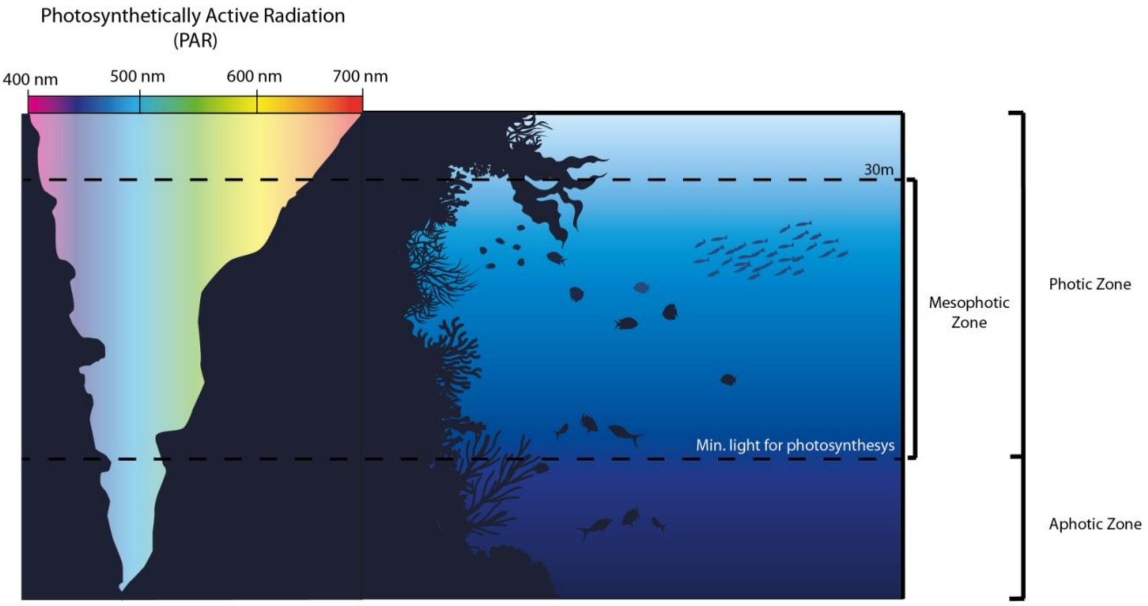

Fig. 1. Schematic representation of water column zonation from shallow to aphotic depths based on the gradient of light with depth.

In the literature, the mesophotic zone is frequently defined as ranging between 30-40 and ca. 150 m depth (e.g., Lesser et al., 2009; Hinderstein et al., 2010; Kahng et al., 2010; Pyle & Copus, 2019). Many publications emphasize these borders, however, rely upon operational limitations or local biological situations hardly to extend to a larger scale. The upper boundary, indeed, was established as a function of the lower limits of conventional SCUBA, whilst the lower derives from the deepest occurrences of tropical zooxanthellate corals, among the first mesophotic ecosystems documented in the late 80s (e.g., Baker et al., 2016).

If the transition from photophilous to sciaphilous organisms has been documented occurring at 30-40 m depth for many taxonomic groups (Weiss, 2017), zooxanthellate scleractinian corals are not necessarily the best reference to define lower boundaries for the mesophotic zone on a global scale. Mesophotic situations dominated by scleractinian corals, in fact, exist (Mesophotic Coral Ecosystems, MCE, Lesser et al., 2009) but are limited to tropical-subtropical latitudes, representing a minority in benthic habitats at mesophotic depths worldwide (e.g., Pyle & Copus, 2019). The main mesophotic actors, in fact, change depending on the geographical position.

Globally, mesophotic ecosystems are dominated by octocorals, mainly gorgonians and antipatharians (Kahng et al., 2017), macroalgae (Spalding, 2012; Spalding et al., 2019) and coralline algae and rhodoliths (Harvey et al., 2016; Basso et al., 2017).

The lack of a global-scale definition of the borders of the mesophotic zone may not pose much of a problem as long as the term “mesophotic” is adopted to refer to intermediate-depth biological situations. Problems arise when scientific information must be transferred to the policy that requires a coherent spatial definition to plan proper management and conservation measures (Cvitanovic et al., 2015).

In the last decades, the improvement of underwater technologies including remotely operated vehicles (ROVs), autonomous underwater vehicles (AUVs), drop cameras, and high-resolution bathymetry mapping techniques have dramatically increased the number of information from direct observation on mesophotic ecosystems together with the awareness of both the biological richness and ecological importance of mesophotic ecosystems (e.g., Hinderstein et al., 2010).

Information on mesophotic ecosystems are, nevertheless, unequally distributed among taxonomic groups, with the overwhelming majority of the studies focusing on cnidarians (Lesser et al., 2009; Kahng et al., 2010; Bridge, 2011; Kahng et al., 2014; Boavida et al., 2016; Cánovas-Molina et al., 2016; Pyle et al., 2016 and many other). Also, density of data on mesophotic ecosystems vary along geographical distance, with temperate latitudes largely less explored that tropical situations (e.g., Turner et al., 2019).

This is the case of the Mediterranean Sea, where the volume of information on mesophotic ecosystems is largely lower with respect to that of tropical and subtropical MCEs (see review in Cerrano et al., 2019). Evidence of the diversity associated with ecosystems characterizing the mesophotic depth range are increasing in the recent, documenting new species (Idan et al., 2018; Bo et al., 2019a), a consistent number of highly biodiverse associations (e.g., Enrichetti et al., 2019; Chimienti, 2020; Chimienti et al., 2020 amongst other) and seldom explored habitats (e.g., Corriero et al., 2019; Albano et al., 2020; Angeletti et al., 2020).

However, the ecological aspects of mesophotic ecosystems are still unexplored at both Mediterranean and global scales. If many publications started exploring the ecology of mesophotic ecosystems dominated by cnidarians (Lesser et al., 2009; Boavida et al., 2016; Cánovas-Molina et al., 2016; Enrichetti et al., 2019; Lesser et al., 2019) the same it is not true for situations characterized by other taxonomic components, whose community structure, biogeography and biodiversity are largely undisclosed. A better understanding of the diversity, distribution and composition of mesophotic ecosystems is crucial to increase the knowledge on the dynamics influencing their presence but also to support management plans and conservation measures aiming at preserving the mesophotic natural heritage.

To do so, modeling techniques, such as Habitat Suitability Models (HSM), are increasingly used to integrate on-field observations (Robert et al., 2016). By analyzing the environmental setting of sites of occurrence of species or assemblage, these models convert local data into large-scale maps of the potential presence of sensitive species and ecologically relevant ecosystems (e.g., Giusti et al., 2014; Guinotte & Davies, 2014; Bargain et al., 2017, 2018; Georgian et al., 2020;), furnishing spatial information at support of conservation actions.

The present thesis, constituted in five main chapters, aims at providing a quantitative and more robust definition of the mesophotic zone in the Mediterranean Sea but also explores the biodiversity and the distribution of the ecosystems colonizing the mesophotic depth range.

The first chapter analyzes the information on mesophotic ecosystems in the Mediterranean Sea to identify the most studied taxonomic groups and how the term “mesophotic” is used in the literature. To help overcoming discrepancies in its definition, a spatial and bathymetric estimation of the mesophotic zone in the Mediterranean Sea is provided by calculating the light penetration along the water column through a modeling approach.

In the second chapter, a comparison among different techniques to process visual surveys collected at mesophotic and deep-sea situations is performed to explore how the analytical method might influence the estimation of diversity and the quantification of habitat extension.

The most conservative technique is then used, in the third chapter, to analyze a set of 25 ROV surveys performed in correspondence of mesophotic assemblages in the Mediterranean Sea, providing a description of their taxonomic and functional diversity. Also, patterns in the distribution of the different assemblages together with the environmental factors influencing their structure are explored.

Using deep-water oyster reefs assemblages as case study, a HSM is developed in the fourth chapter to map the distribution of areas suitable for the presence of these mesophotic assemblages in the Adriatic Sea and north-Ionian Sea area.

The fifth chapter explores the mesophotic zone in the northern Gulf of Mexico as an insight on extra-Mediterranean mesophotic situations. The spatial and vertical extension of the mesophotic zone is provided by applying the modeling approach used in chapter 1. The diversity associated with mesophotic ecosystems is explored by analyzing a set of 8 ROV performed in the north-western area of the Gulf. Also, the environmental factors influencing the structure of the assemblgaes are explored.

The results of this work are expected to help overcoming discrepancies in the definition of the mesophotic zone, increase the knowledge on the diversity of mesophotic ecosystems in the Mediterranean Sea and the factors shaping their composition. Also, HSMs are used to map the potential presence of highly diverse and ecologically relevant mesophotic assemblages and provide spatial information to support future conservation actions. The variability in the spatial and vertical extension of the mesophotic zone between intra- and extra-Mediterranean situations as well as the composition of assemblages populating this depth range are explored using the Gulf of Mexico as a case study.

Reference

Albano, P.G., Azzarone, M., Amati, B., Bogi, C., Sabelli, B., Rilov, G. (2020). Low diversity or poorly explored? Mesophotic molluscs highlight undersampling in the Eastern Mediterranean. *Biodiversity and Conservation*, 29(14), 4059–4072. https://doi.org/10.1007/s10531-020-02063-w

Angeletti, L., Canese, S., Cardone, F., Castellan, G., Foglini, F., Taviani, M. (2020). A brachiopod biotope associated with rocky bottoms at the shelf break in the central Mediterranean Sea: geobiological traits and conservation aspects. *Aquatic Conservation: Marine and Freshwater Ecosystems*, 30(2), 402–411. https://doi.org/10.1002/aqc.3255

Baker, E.K., Puglise, K.A., Harris, P.T. (2016). *Mesophotic coral ecosystems: a lifeboat for coral reefs?* The United Nations Environment Programme and GRID-Arendal, Nairobi and Arenal: Nairobi, Kenya, 98 pp.

Bargain, A., Foglini, F., Pairaud, I., Bonaldo, D., Carniel, S., Angeletti, L., Taviani, M., Rochette, S., Fabri, M.C. (2018). Predictive habitat modeling in two Mediterranean canyons including hydrodynamic variables. *Progress in Oceanography*, 169, 151–168. https://doi.org/10.1016/j.pocean.2018.02.015

Bargain, A., Marchese, F., Savini, A., Taviani, M., Fabri, M.-C. (2017). Santa Maria di Leuca Province (Mediterranean Sea): identification of suitable mounds for Cold-Water Coral settlement using geomorphometric proxies and MaxEnt methods. *Frontiers in Marine Science*, 4. https://doi.org/10.3389/fmars.2017.00338

Basso, D., Babbini, L., Ramos-Esplá, A.A., Salomidi, M. (2017). Mediterranean rhodolith beds. In: *Rhodolith/Maërl Beds: A Global Perspective*. Riosmena-Rodríguez R, Nelson W, Aguirre J (Eds). Springer International Publishing: Cham, pp. 281–298.

Bo, M., Bavestrello, G., Di Muzio, G., Canese, S., Betti, F. (2019). First record of a symbiotic relationship between a polyclad and a black coral with description of *Anthoplana antipathellae* gen. et sp. nov. (Acotylea, Notoplanidae). *Marine Biodiversity*, 49(6), 2549–2570. https://doi.org/10.1007/s12526-019-00982-8

Boavida, J., Assis, J., Silva, I., Serrão, E.A. (2016). Overlooked habitat of a vulnerable gorgonian revealed in the Mediterranean and Eastern Atlantic by ecological niche modelling. *Scientific Reports*, 6, 36460. https://doi.org/10.1038/srep36460

Bridge, T. (2011). Habitats and sessile benthic megafaunal communities in the mesophotic zone of the Great Barrier Reef World Heritage Area, Australia. Ph.D. Dissertation, James Cook University, Australia.

Cánovas-Molina, A., Montefalcone, M., Bavestrello, G., Cau, A., Bianchi, C.N., Morri, C., Canese S., Bo, M. (2016). A new ecological index for the status of mesophotic megabenthic assemblages in the Mediterranean based on ROV photography and video footage. *Continental Shelf Research*, 121, 13–20. https://doi.org/10.1016/j.csr.2016.01.008

Cerrano, C., Bastari, A., Calcinai, B., Camillo, C.D., Pica, D., Puce, S., Valisano, L., Torsani, F. (2019). Temperate mesophotic ecosystems: gaps and perspectives of an emerging conservation challenge for the Mediterranean Sea. *The European Zoological Journal*, 86(1), 370–388. https://doi.org/10.1080/24750263.2019.1677790

Chimienti, G. (2020). Vulnerable Forests of the Pink Sea Fan *Eunicella verrucosa* in the Mediterranean Sea. *Diversity*, 12(5), 176. https://doi.org/10.3390/d12050176

Chimienti, G., De Padova, D., Mossa, M., Mastrototaro, F. (2020). A mesophotic black coral forest in the Adriatic Sea. *Scientific Reports*, 10(1), 8504. https://doi.org/10.1038/s41598-020-65266-9

Corriero, G., Pierri, C., Mercurio, M., Marzano, C.N., Tarantini, S.O., Gravina, M.F., Lisco S., Moretti M., De Giosa F., Valenzano E., Giangrande A., Mastrodonato M., Longo C., Cardone F. (2019). A Mediterranean mesophotic coral reef built by non-symbiotic scleractinians. *Scientific Reports*, 9(1), 3601. https://doi.org/10.1038/s41598-019-40284-4

Cvitanovic, C., Hobday, A.J., van Kerkhoff, L., Wilson, S.K., Dobbs, K., Marshall, N.A. (2015). Improving knowledge exchange among scientists and decision-makers to facilitate the adaptive governance of marine resources: A review of knowledge and research needs. *Ocean, Coastal Management*, 112, 25–35. https://doi.org/10.1016/j.ocecoaman.2015.05.002

Enrichetti, F., Dominguez-Carrió, C., Toma, M., Bavestrello, G., Betti, F., Canese, S., Bo, M. (2019). Megabenthic communities of the Ligurian deep continental shelf and shelf break (NW Mediterranean Sea). *PLOS ONE*, 14(10), e0223949. https://doi.org/10.1371/journal.pone.0223949

Georgian, S.E., Kramer, K., Saunders, M., Shedd, W., Roberts, H., Lewis, C., Fisher C., Cordes E. 2020 (2020). Habitat suitability modelling to predict the spatial distribution of cold-water coral communities affected by the Deepwater Horizon oil spill. *Journal of Biogeography*, 47(7), 1455–1466. https://doi.org/10.1111/jbi.13844

Giusti, M., Innocenti, C., Canese, S. (2014). Predicting suitable habitat for the gold coral *Savalia savaglia* (Bertoloni, 1819) (Cnidaria, Zoantharia) in the South Tyrrhenian Sea. *Continental Shelf Research*, 81, 19–28. https://doi.org/10.1016/j.csr.2014.03.011

Guinotte, J.M., Davies, A.J. (2014). Predicted deep-sea coral habitat suitability for the U.S. West Coast. *PLOS ONE*, 9(4), e93918. https://doi.org/10.1371/journal.pone.0093918

Harvey, A.S., Harvey, R.M., Merton, E., Harvey, A.S., Harvey, R.M., Merton, E. (2016). The distribution, significance and vulnerability of Australian rhodolith beds: a review. *Marine and Freshwater Research*, 68(3), 411–428. https://doi.org/10.1071/MF15434

Hinderstein, L.M., Marr, J.C.A., Martinez, F.A., Dowgiallo, M.J., Puglise, K.A., Pyle, R.L., Zawada, D.G., Appeldoorn, R. (2010). Theme section on "Mesophotic coral ecosystems: characterization, ecology, and management". *Coral Reefs*, 29(2), 247–251. https://doi.org/10.1007/s00338-010-0614-5

Idan, T., Shefer, S., Feldstein, T., Yahel, R., Huchon, D., Ilan, M. (2018). Shedding light on an East-Mediterranean mesophotic sponge ground community and the regional sponge fauna. *Mediterranean Marine Science*, 19(1), 84–106. https://doi.org/10.12681/mms.13853

Kahng, S.E., Garcia-Sais, J.R., Spalding, H.L., Brokovich, E., Wagner, D., Weil, E., Hinderstein, L., Toonen, R.J. (2010). Community ecology of mesophotic coral reef ecosystems. *Coral Reefs*, 29(2), 255–275. https://doi.org/10.1007/s00338-010-0593-6

Kahng, S., Copus, J., Wagner, D. (2014). Recent advances in the ecology of mesophotic coral ecosystems (MCEs). *Current Opinion in Environmental Sustainability*, 7, 72–81. https://doi.org/10.1016/j.cosust.2013.11.019

Kahng, S., Copus, J.M., Wagner, D. (2017). Mesophotic coral ecosystems. In: *Marine animal forests: the ecology of benthic biodiversity hotspots*. Rossi S, Bramanti L, Gori A, Orejas C (Eds). Springer International Publishing: Cham, pp. 185–206.

Kahng, S.E., Akkaynak, D., Shlesinger, T., Hochberg, E.J., Wiedenmann, J., Tamir, R., Tchernov, D. (2019). Light, temperature, photosynthesis, heterotrophy, and the lower depth limits of mesophotic coral ecosystems. In: *Mesophotic coral ecosystems*. Loya Y, Puglise KA, Bridge TCL (Eds). Springer International Publishing: Cham, pp. 801–828.

Lesser, M.P., Slattery, M., Laverick, J.H., Macartney, K.J., Bridge, T.C. (2019). Global community breaks at 60 m on mesophotic coral reefs. J Pandolfi, Ed. *Global Ecology and Biogeography*, 28(10), 1403–1416. https://doi.org/10.1111/geb.12940

Lesser, M.P., Slattery, M., Leichter, J.J. (2009). Ecology of mesophotic coral reefs. *Journal of Experimental Marine Biology and Ecology*, 375(1), 1–8. https://doi.org/10.1016/j.jembe.2009.05.009

Levin, N., Kark, S., Danovaro, R. (2018). Adding the Third Dimension to Marine Conservation. *Conservation Letters*, 11(3), e12408. https://doi.org/10.1111/conl.12408

Markager, S., Sand-Jensen, K. (1992). Light requirements and depth zonation of marine macroalgae. *Marine Ecology Progress Series*, 88, 83–92. https://doi.org/10.3354/meps088083

Matos, F.L., Company, J.B., Cunha, M.R. (2021). Mediterranean seascape suitability for *Lophelia pertusa*: living on the edge. *Deep Sea Research Part I: Oceanographic Research Papers*, 170, 103496. https://doi.org/10.1016/j.dsr.2021.103496

Pyle, R.L., Copus, J.M. (2019). Mesophotic coral ecosystems: introduction and overview. In: *Mesophotic coral ecosystems*. Loya Y, Puglise KA, Bridge TCL (Eds). Springer International Publishing: Cham, pp. 3–27.

Pyle, R.L., Boland, R., Bolick, H., Bowen, B.W., Bradley, C.J., Kane, C., Kosaki, R.K., Langston, R., Longenecker, K., Montgomery, A., Parrish, F.A., Popp, B.N., Rooney, J., Smith, C.M., Wagner, D., Spalding, H. (2016). A comprehensive investigation of mesophotic coral ecosystems in the Hawaiian Archipelago. *PeerJ*, 4, e2475. https://doi.org/10.7717/peerj.2475

Robert, K., Jones, D.O., Roberts, J.M., Huvenne, V.A. (2016). Improving predictive mapping of deep-water habitats: considering multiple model outputs and ensemble techniques. *Deep Sea Research Part I: Oceanographic Research Papers*, 113, 80–89.

Spalding, H.L. (2012). Ecology of mesophotic macroalgae and *Halimeda kanaloana* meadows in the main Hawaiian Islands. Ph.D. Thesis. University of Hawaii at Manoa, Hawaii.

Spalding, H.L., Amado-Filho, G.M., Bahia, R.G., Ballantine, D.L., Fredericq, S., Leichter, J.J., et al. (2019). Macroalgae. In: *Mesophotic coral ecosystems*. Loya Y, Puglise KA, Bridge TCL (Eds). Springer International Publishing: Cham, pp. 507–536.

Tett, P. (1990). The photic zone. In: *Light and life in the sea*. Herring, P.J., Campbell, A.K., Whitfield, M, Maddock, L. (Eds.). Cambridge University Press: Cambridge, pp. 59–87.

Turner, J.A., Andradi-Brown, D.A., Gori, A., Bongaerts, P., Burdett, H.L., Ferrier-Pagès, C., Voolstra, C.R., Weinstein, D.K., Bridge, T., Costantini, F., Gress, E., Laverick, J., Loya, Y., Goodbody-Gringley, G., Rossi, S., Taylor, M.L., Viladrich, N., Voss, J., Williams, J., Woodall, L.C., Eyal, G. (2019). Key questions for research and conservation of mesophotic coral ecosystems and temperate mesophotic ecosystems. In: *Mesophotic coral ecosystems*. Loya Y, Puglise KA, Bridge TCL (Eds). Springer International Publishing: Cham, pp. 989–1003.

Weiss, K.R. (2017). Into the Twilight Zone. *Science*, 355(6328), 900–904. https://doi.org/10.1126/science.355.6328.900

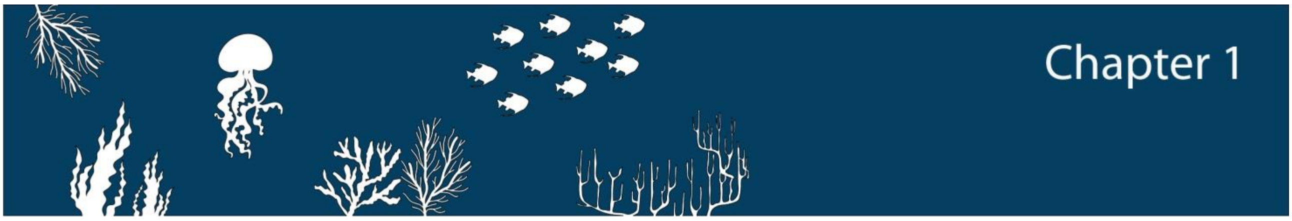

1. The Mesophotic Zone of the Mediterranean Sea: knowledge and uncertainties

1.1 Introduction

The steadily increase in the volume of scientific literature about the mesophotic zone taking place in the last two decades has provided an insight of the biodiversity that benthic mesophotic ecosystems may host on a global scale (Pyle and Copus, 2019). Most of this information on, however, comes from the study of mesophotic coral ecosystems (MCE, Lesser et al., 2009) whilst other biological components remain largely unexplored. The Mediterranean Sea does not represent an exception, with the overwhelming majority of studies focusing on situations dominated by cnidarians (Cerrano et al., 2019).

Despite representing a relevant taxonomic component at mesophotic depths (Bo et al., 2014; Gori et al., 2014; Bramanti et al., 2017; Cau et al., 2017; Capdevila et al., 2018; Enrichetti et al., 2019; Chimienti, 2020 among others), cnidarians are not necessarily the main actor at mesophotic depth in the Mediterranean Sea. Evidence of ecosystems dominated by other taxonomic components, indeed, exists (Castellan et al., 2019; Corriero et al., 2019; Angeletti & Taviani, 2020; Angeletti et al., 2020). Some authors suggest that the lack of information on the diverse mesophotic components in the Mediterranean Sea (Cerrano et al., 2019) and at temperate latitudes in general (Pyle and Copus, 2019) might be related to the incoherent use of the term "mesophotic". Situations where ecosystems occurring at mesophotic conditions are not defined as such or that adopt terms such as “deep-water” or just “deep” as synonymous for “mesophotic” are common. Moreover, some biological situations are deliberately considered as independent features despite present in conditions and depth range typically mesophotic (Littler et al., 1991; Ballesteros, 2006). This is the case of rhodolith beds and coralligenous formations which have been widely studied in the Mediteranean Sea (>300 documentations since 1965; source: www.scopus.com). The formers are increasingly accounted as mesophotic (e.g., Foster et al., 2013; Basso et al., 2017) but opinions differ on whether coralligenous associations should be considered an independent biological feature or under the mesophotic domain (e.g., Cerrano et al., 2019).

Part of the information on Mediterranean mesophotic ecosystems might, thus, be just concealed behind an incoherent use of terminology.

The lack of obvious boundaries has undoubtedly complicated the spatial definition of the mesophotic zone (Pyle & Copus, 2019), leading to defining as "mesophotic" only the ecosystems between the depth range from 30-40 m to ca. 150 m (Hinderstein et al., 2010). Evidence of macroalgae assemblages (mainly coralline algae) able to maintain their photosynthetic metabolism up to 0.0005% PAR (Markager & Sand-Jensen, 1992; Runcie et al., 2008), much below the value of 1% PAR commonly used to define the limit of the photic zone, suggest, for instance, that photic conditions might entend much deeper than what previously thought.

If the upper limit of "30 m" may be representative the characteristics of the Mediterranean Sea by excluding shallow-water zooxanthellate coral communities (e.g., Rodolfo-Metalpa et al., 2015), the same is not necessarily true for the lower border that might significantly differ from that of tropical latitudes (i.e., 150 m). As a case in point, the Mediterranean Sea is a semi-enclosed oligotrophic basin with complex physical and biological dynamics, seasonality (D'Ortenzio & Ribera d'Alcalà, 2009; Christaki et al., 2011), and biophysical processes (Basterretxea et al., 2018). Strong climatic (e.g., rainfalls, sunlight), physical (e.g., water temperature and salinity) and biochemical (e.g., nutrients) gradients characterize this basin (Bethoux, 1979; Azov, 1991; Pinardi et al., 2006), generating an alternation of temperate- or tropical-like situations within a limited spatial scale that influences the penetration of light along the water column.

If we would imagine setting the upper border of the mesophotic zone at 30 m depth, and the lower limit at the lowest value of PAR quantity that sustains photic metabolism, we would be able to provide information about the bathymetric limits of the mesophotic zone and spatially estimate the portion of seafloor falling under mesophotic conditions at any latitude.

In this chapter, the literature about the mesophotic zone is analyzed to explore how its definition vary between Mediterranean and extra-Mediterranean areas and which taxonomic groups are most studied. In addition, the quantity of PAR reaching the seabed is estimated from 17-year (2002-2018) average surface Chlorophyll-a (Chl-a) concentration from open-access repository (NASA Ocean Color: https://oceancolor.gsfc.nasa.gov/). The minimum value of light intensity able to sustain photosynthetic metabolism is obtained by analyzing information on photosynthetic components and used to set the lower border of the mesophotic zone and provide its spatial extent in the Mediterranean Sea. The values of PAR and depth at the borders are then extracted to explore the ranges that might be related to mesophotic conditions in the Mediterranean basin. The variability of the estimation across the basin is also explored by dividing the basin into subregions delineated in the Marine Strategy Framework Directive (MSFD: Directive 2008/56/EC). Finally, the spatial definition of the mesophotic zone is compared with the distribution of benthic mesophotic assemblages from available literature to validate the estimation.

1.2 Materials and methods

1.2.1 Analysis of the literature on mesophotic zone

An extensive bibliographic search was conducted with a cut-off date of 31 January 2021. To identify documents regarding mesophotic ecosystems on a global scale, the information stored in the www.mesophotic.org database was compared to records obtained from Elsevier’s Scopus database (www.scopus.com) using "mesophotic" as a filter.

For the Mediterranean Sea, the query “Mediterranean” was used in the mesophotic.org database (http://www.mesophotic.org/), while “twilight AND Mediterranean” and “mesophotic AND

Mediterranean” were used for Elsevier’s Scopus database. A cross-check between the results from these two databases was performed to exclude duplicates. The records were, then, screened to remove non-benthic studies (e.g., regarding fish fauna). Whenever specified, the depth range adopted to define the mesophotic zone was extracted. Also, the taxonomic group investigated in the records located in the Mediterranean Sea was extracted.

For model validation, literature records were integrated with the distribution of coralligenous and rhodolith beds habitats from the MEDISEH database (see Martin et al., 2014). The literature records were classified as “mono-species / mixed-assemblage”, while the classes “Coralligenous” and “Rhodolith beds” were assigned to the relative occurrences from MEDISEH database. In total, 1407 locations relevant to the study were selected. Among these, 38 records wrongly located on land and 317 falling outside the extent of satellite data (e.g., too close to coastline) were removed. Finally, 55 sites deeper than 500 m were not considered, representing potential outliers. The final dataset consisted in 997 locations of mesophotic assemblages covering the entire Mediterranean Sea. The dataset was converted into spatial data and the depth for each location was extracted by using ArcGIS 10.5 (ESRI©) software.

1.2.2 Estimation of PAR reaching the seabed

The quantity of PAR reaching the seabed for the whole Mediterranean Sea was estimated by using the methodology proposed by Morel et al., 2007 and more recently compared to other estimation methods (Saulquin et al., 2013). This method derives the diffuse attenuation coefficient for 490 nm (K_{d490}) from surface Chlorophyll-a concentration (1) and then calculates the diffuse attenuation coefficient (2) for PAR (K_{dPAR}):

$$K_{d490} = 0.0166 + 0.0773 * [\text{Chl-a}] * 0.6715 \tag{1}$$

$$K_{dPAR} = 0.0665 + 0.874 * K_{d490} - 0.00137 * K_{d490}^{-1} \tag{2}$$

This method does not account for the directionality of the light field for the calculation of K_{dPAR} and K_{d490}, but this dependence has been documented to be weak at mesophotic depths (Mobley & Mobley, 1994; Kahng et al., 2019).

The intensity of light (Ez) at bottom depth (z) is then estimated from the intensity of light entering the ocean (PAR at surface, E0) and K_{dPAR} by applying Beer's Law (Kahng et al., 2019) (3):

$$Ez = E0e^{-Kd\,z} \tag{3}$$

The yearly average of surface Chl-a and PAR in the Mediterranean Sea for the period 2002-2018 were calculated from monthly data obtained from the open-access repository NASA Ocean Colour (https://oceancolor.gsfc.nasa.gov/). The open-access repository EMODnet (https://www.emodnet-bathymetry.eu/) provided the bathymetric data for the Mediterranean Sea. Chlorophyll-a and surface PAR data were downloaded at a horizontal resolution of 4x4 km and transformed to match the resolution of the bathymetry (115 m) using an upscaling approach. This technique has been demonstrated to work effectively for many global- and regional-scale variables (e.g., Davies & Guinotte, 2011; Georgian et al., 2020). The 17-years mean Chl-a concentration was then used to estimate K_{d490} (1), K_{dPAR} (2), and then, the quantity of light reaching the seabed (3). The percent PAR at seabed was calculated as the ratio between the value of light at the seabed and the correspondent value of surface PAR in each pixel, multiplied by 100. All calculations were performed in R software (R Core Team 2020) using package "raster" (version 3.3-13, Hijmans et al., 2015).

1.2.3 Borders of the Mediterranean mesophotic zone

The upper limit for the mesophotic zone was set at 30 m depth according to the information on the distribution of shallow-water zooxanthellate corals in the Mediterranean Sea (e.g., Rodolfo-Metalpa et al., 2015). Thus, the portions of the basin shallower than 30 m were excluded to further analysis.

Since 0.0005% of surface PAR resulted as the minimum value able to support photosynthetic metabolisms from the literature analysis, this value was used as the lower border of the mesophotic zone. The layer of the estimated percent surface PAR at seabed was then classified using the tool "Reclassify" in ArcGIS 10.5 (ESRI©), setting a lower limit at 0.0005, and then, converted to a polygon using the "Raster to Polygon" tool.

To investigate the range of percent PAR and the bathymetric interval of the estimated mesophotic zone in the Mediterranean Sea, a point every 20 km along the upper and the lower borders of the estimated polygon was generated and used to extract the value of percent PAR and depth, respectively.

Every estimation and result were then referred to the Mediterranean marine subregions identified by the MSFD: Western Mediterranean Sea, Adriatic Sea, Ionian Sea and Central Mediterranean Sea, and the Aegean-Levantine Sea, to investigate for differences across the Mediterranean basin.

1.2.4 Statistical Analysis

The values of depth and percent PAR at seabed extracted along the mesophotic borders did not meet the assumptions of normality and homoscedasticity verified by using the Shapiro-Wilk test (package "stats", version 4.2.0) and Levene's test (package "car", version 3.0, Fox et al., 2012), respectively. Nonparametric Kruskal–Wallis tests were performed followed by post hoc pairwise comparisons using a Dunn test with Bonferroni adjusted p-values to analyze the differences among the Mediterranean subregions.

1.3 Results

1.3.1 Literature on the mesophotic zone

1.3.1.1 Bathymetric definition

The bibliographic search isolated more than 700 scientific documents regarding mesophotic ecosystems on a global scale (Fig.1.1). From 1980, the number of records shows an exponential growth with a sudden increase around 2010. Among this huge volume of records, a small group of documents was frequently used as a reference for defining the bathymetric range of the mesophotic zone, counting more than 1080 citations (i.e., Lesser et al., 2009; Puglise et al., 2009; Bongaerts et al., 2010; Hinderstein et al., 2010; Kahng et al., 2010, Slattery et al., 2011; Baker et al., 2016). With just one exception, these studies adopted 30-150 m as the bathymetric range for the mesophotic zone (Fig.1.2A).

In the Mediterranean Sea, the number of available information on mesophotic ecosystems over time presented a trend similar to that observed at global scale (Fig.1.1). The bibliographic search extracted

193 records with 21 reporting the bathymetric definition of the mesophotic zone (Fig. 1.2B). The depth values adopted as limits of the mesophotic zone were more variable compared to extra-Mediterranean studies, with the upper border mostly set at 30-50 m depth. The lower border presented higher uncertainty, ranging from 100 to more than 200 m. Noteworthy is that nearly all publications defining the mesophotic zone within 30-150 m depth supported the definition with extra-Mediterranean references.

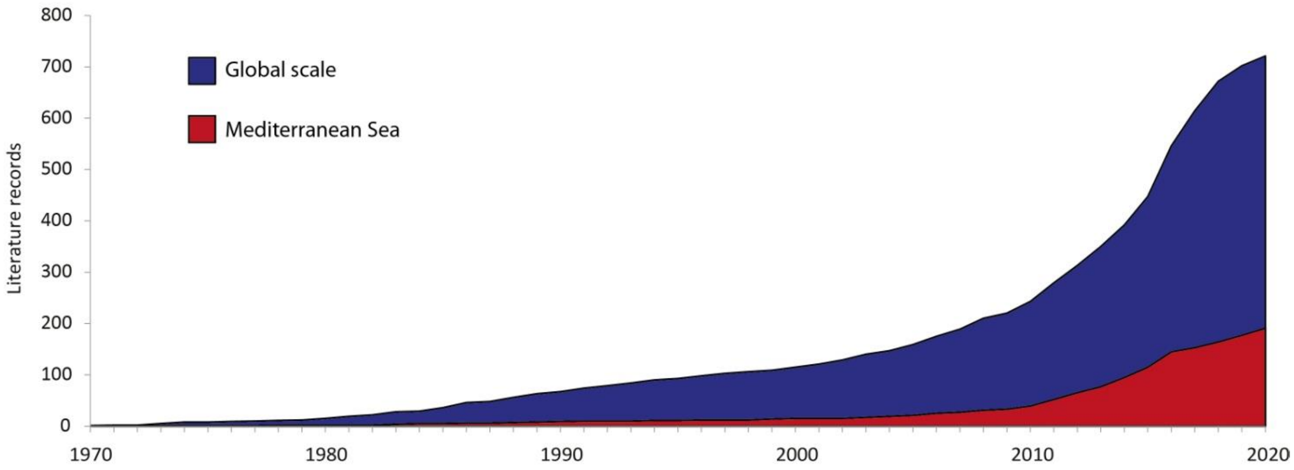

Fig. 1.1. Historical pattern of scientific publications focused on benthic mesophotic ecosystems represented as the cumulative number of publications. Blue area: Global; Red area: Mediterranean Sea.

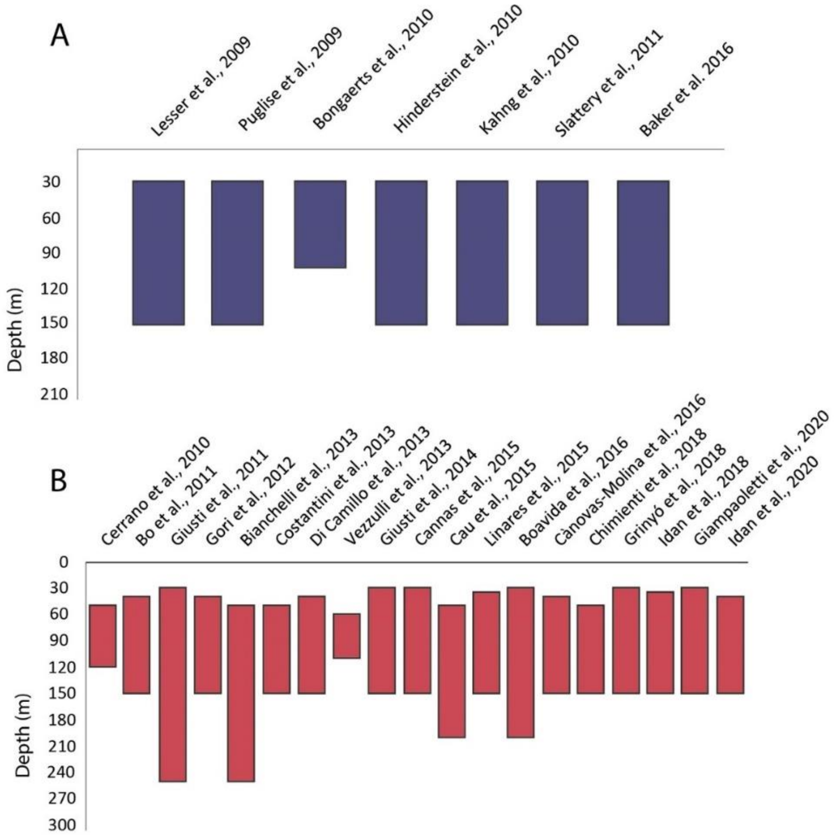

Fig. 1.2. Depth ranges considered as mesophotic zone in the analyzed papers: A) extra-Mediterranean Sea; B) Mediterranean Sea. For extra-Mediterranean Sea only the most cited studies are reported.

1.3.1.2 Main taxonomic targets in the Mediterranean mesophotic literature

The search identified 108 records investigating benthic mesophotic ecosystems in the Mediterranean Sea. Most of the studies were focalized on single taxon (89.3%), while the rest considered multi-taxa assemblages (10.7%). Among single-taxon studies, cnidarians were the most studied taxonomic group being the main subject of more than 75% of records (Fig.1.3). Albeit much smaller, a relevant part of the records was focused on mollusks and sponges, that resulted as the main subject of 4.8% and 3.9% of the records, respectively. Studies on mesophotic macroalgae were uncommon (1.9%) together with those targeting bryozoans, meiofauna, and tunicates (ca. 1%).

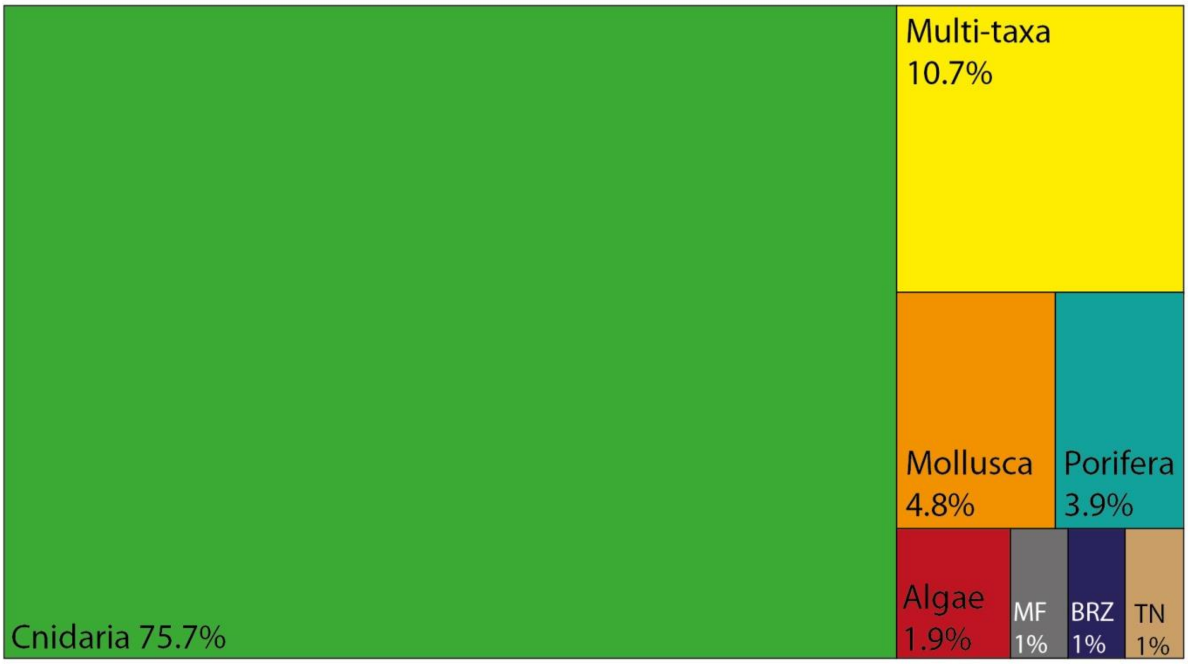

Fig. 1.3. Proportion of the target taxa or multi-taxa assemblages investigated in the records. MF = meiofauna; BRZ = Bryozoa; TN = Tunicata.

1.3.2 The mesophotic zone of the Mediterranean Sea

1.3.2.1 Spatial extension

The average values of Chl-a concentrations and PAR at the surface for the period 2002-2018 showed patterns from north-west to south-east consistent with information from in situ bio-optical observations (Marty & Chiavérini, 2002) and ocean colour data (Morel & André, 1991; Antoine et al., 1995; D'Ortenzio & Ribera d'Alcalà, 2009; Mayot et al., 2016; Fig.1.4A, B). The highest values of Chl-a concentration were registered in the north-western part of the Mediterranean Sea and in the northern Adriatic Sea that decreased moving toward south-east. On the contrary, the highest values of surface PAR intensities were observed along the African coasts and in the Levantine basin. Similarly, the estimated attenuation coefficients (K_{d490} and K_{dPAR}) showed lower values in the south-eastern sector of the Mediterranean Sea (Fig.1.4C, D). Consequently, higher values of PAR reaching the seabed in terms of both intensities (Fig.1.4E) and percent surface PAR (Fig.1.4F) were obtained in the southern and eastern part of the basin.

In total, the 15.01% of the Mediterranean Sea resulted as under mesophotic condition. The Ionian Sea and Central Mediterranean Sea and the Aegean-Levantine Sea subregions presented the largest portions of seabed under mesophotic conditions with 126,003 km^2 and 92,901 km^2, corresponding to 16.31 % and 12.28% of the subregions (Fig. 1.5). Although being the most extended subregion (844,417 km^2, Fig.1.5B), the Western Mediterranean Sea presented a slightly lower portion of seabed under mesophotic conditions (86,656 km^2, 10.27%) with respect to the Ionian Sea and the central Mediterranean Sea and the Aegean-Levantine Sea (Fig 1.5B). In the Adriatic Sea, 71,889 km^2 resulted as presenting mesophotic conditions corresponding to 51.61% of the subregion (Fig. 1.5B).

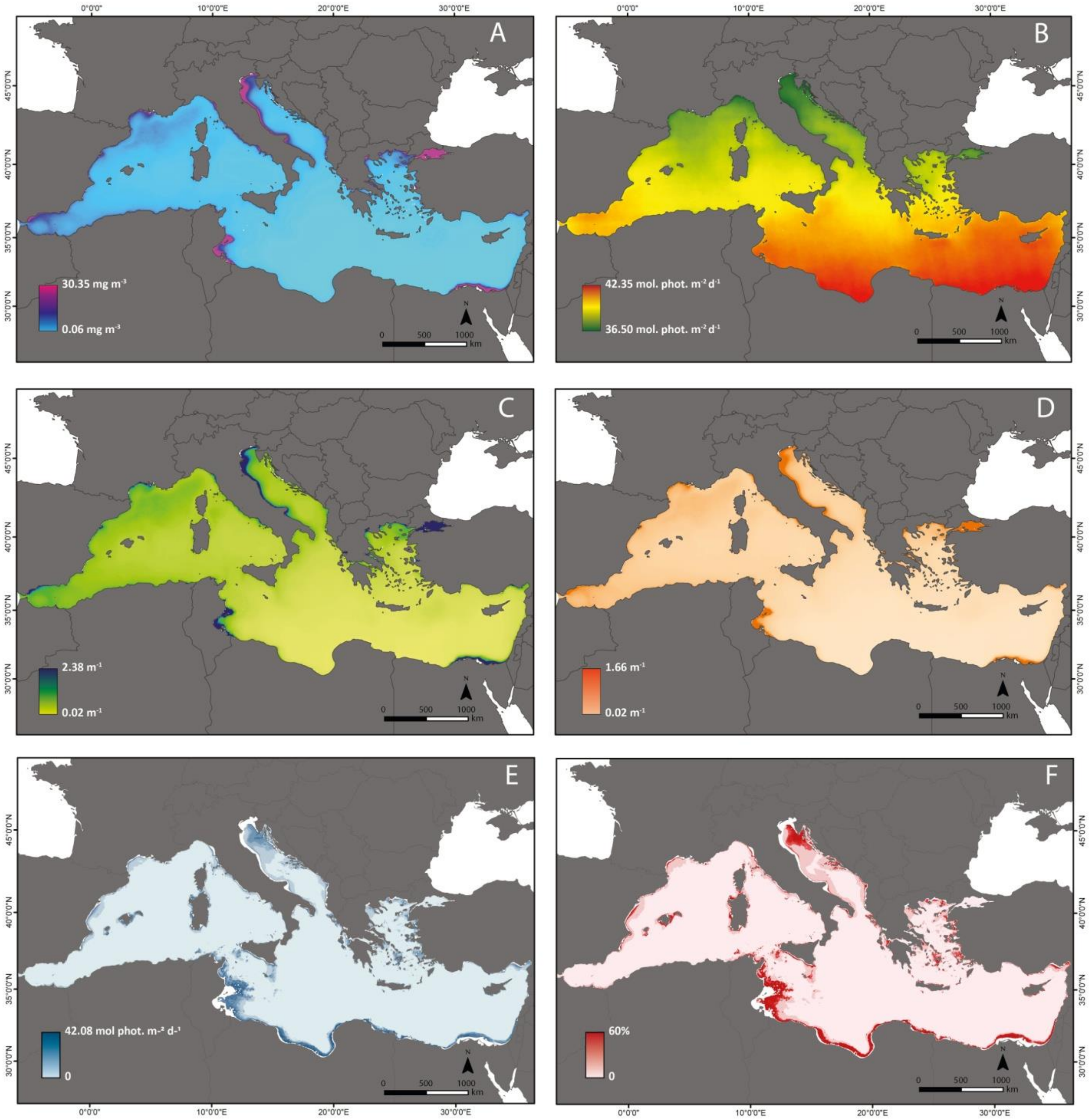

Fig. 1.4. Satellite data on (A) surface concentration of Chlorophyll-a and (B) surface PAR in the Mediterranean Sea. C) Diffuse attenuation coefficient at 490 nm (K_{d490}) and (D) diffuse attenuation coefficient for PAR (K_{dPAR}) calculated from concentration of Chl-a and PAR, according to method proposed by Morel et al., 2007. Quantity (E) and fraction of surface PAR reaching the seabed (F) are also reported.

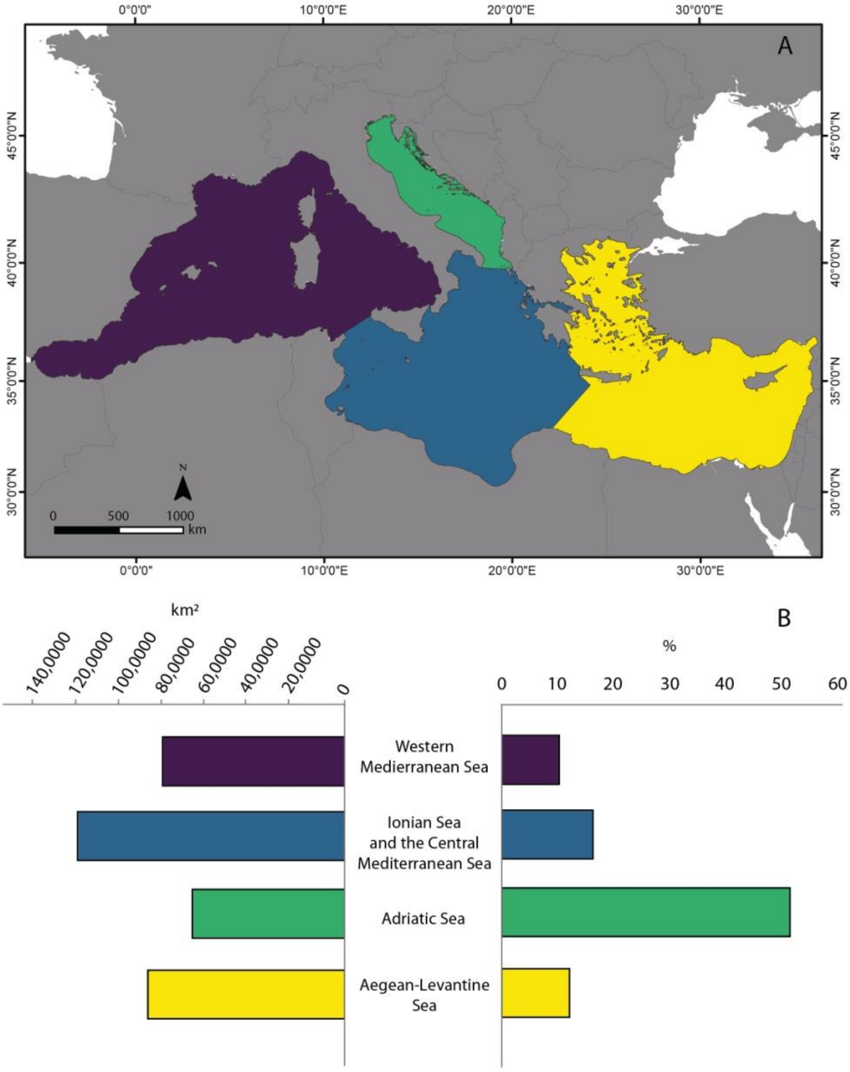

Fig. 1.5 A) Sub-regions of the Mediterranean Sea according to the MSFD (2008/56/EC); Western Mediterranean Sea (purple): ca. 844,417 km^2; Ionian and the Central Mediterranean Sea (blue): 772,705 km^2; Adriatic Sea (green): 139,300 km^2; Aegean-Levantine Sea (yellow):756,642 km^2. B) Bar plot showing the portion of seabed under mesophotic conditions in the different MSFD sub-regions in terms of km^2 and areal percentage.

1.3.2.2 Light and depth ranges

The analysis of percent surface PAR extracted in correspondence of the upper border (i.e., 30 m depth) of the portion of seafloor estimated as under mesophotic conditions revealed an evident difference between north-west and south-east subregions of the Mediterranean Sea (Fig.1.6A), consistent to gradients showed by Chl-a, attenuation coefficients and PAR at seabed. The Aegean-Levantine Sea subregion presented the highest values, reporting an average of 13.30% ± 0.5 surface PAR in correspondence of the upper border (Fig.1.6A). Slightly lower values were obtained for the Ionian and Central Mediterranean Sea subregion, where the percent surface PAR was 12.22% ± 0.5, on average. In the north-western part of the basin, the Western Mediterranean Sea subregion reported an average value of 6.41% ± 0.3 of PAR at the upper border, while the lowest average percent surface PAR was documented in the Adriatic Sea subregion (5.02% ± 0.3, Fig.1.6A). These differences were statistically significant as reported by the Kruskal-Wallis test ($p < 0.01$) and Dunn test post hoc pairwise comparison (Fig. 1.6A). No differences were detected between the Ionian and Central Mediterranean Sea and the Aegean-Levantine Sea subregions. The average value of percent surface PAR at the upper mesophotic border for the whole Mediterranean was 9.79% ± 0.23.

The analysis of depth values extracted at the lower border (i.e., 0.0005% of surface PAR) among Mediterranean subregions showed a pattern similar to that of light reaching the seabed, decreasing from north-west to south-east (Fig. 1.6B). The highest value was detected in the Aegean-Levantine Sea subregion, where the lower border of the estimated mesophotic zone reached a depth of 198 m ± 1.9 on average (Fig.1.6B). The Ionian and Central Mediterranean Sea subregion presented a slightly lower average value, with a depth of 190 m ± 2.5 (Fig.1.6B). The Western Mediterranean Sea and the Adriatic Sea subregions showed similar depth values of the lower mesophotic border, reaching 152 m ± 1.3 and 154 m ± 1.2, respectively. The Kruskal-Wallis and post hoc pairwise tests provided further support to the observed trend, reporting significant differences between north-west and south-east subregions (Fig.1.6B). For the entire Mediterranean Sea, the average depth of the lower mesophotic border was 175.5 m ± 1.2.

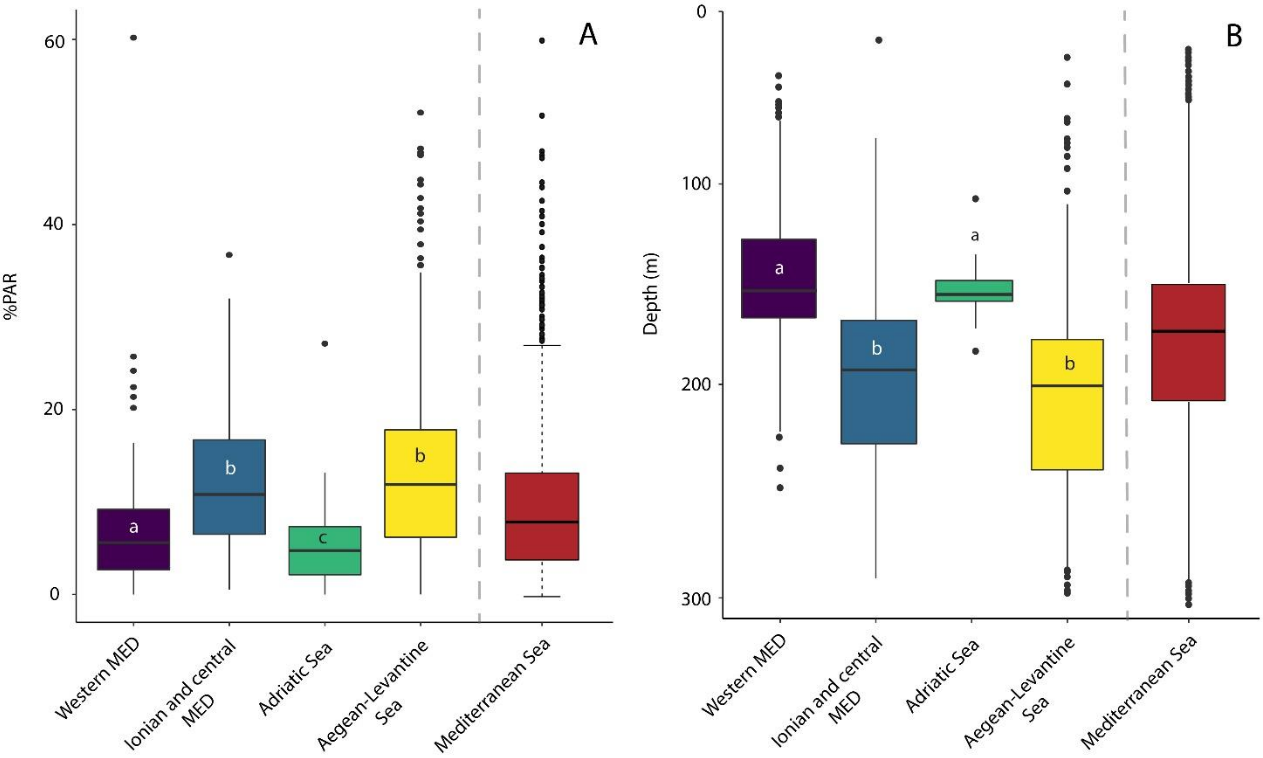

Fig. 1.6. Boxplots displaying the differences in the percent surface PAR at the mesophotic upper border (A) and in the depth of the lower mesophotic border (B) among Mediterranean MSFD subregions. The red box refers to the value for the whole basin. Within each box the horizontal line represents median value. Boxes extend from the 25th to the 75th percentile. The vertical lines indicate the most extreme values within 1.5 interquartile range of the 25th and 75th percentile. Letters refer to significant differences.

1.3.2.3 Distribution of literature records on benthic mesophotic assemblages

The georeferencing of records on Mediterranean benthic mesophotic assemblages from the literature showed that 685 occurrences (68.7%) of the 997 extracted fell within the portion of seafloor estimated as under mesophotic conditions (Fig.1.7A).

A consistent part of occurrences (246, 24.7%) resulted located above 30 m depth, largely represented by coralligenous formations sightings (>80%). The 6.6% of records was located below the lower limit of mesophotic conditions (i.e., below 0.0005% PAR), corresponding to 66 records (Fig.1.7B).

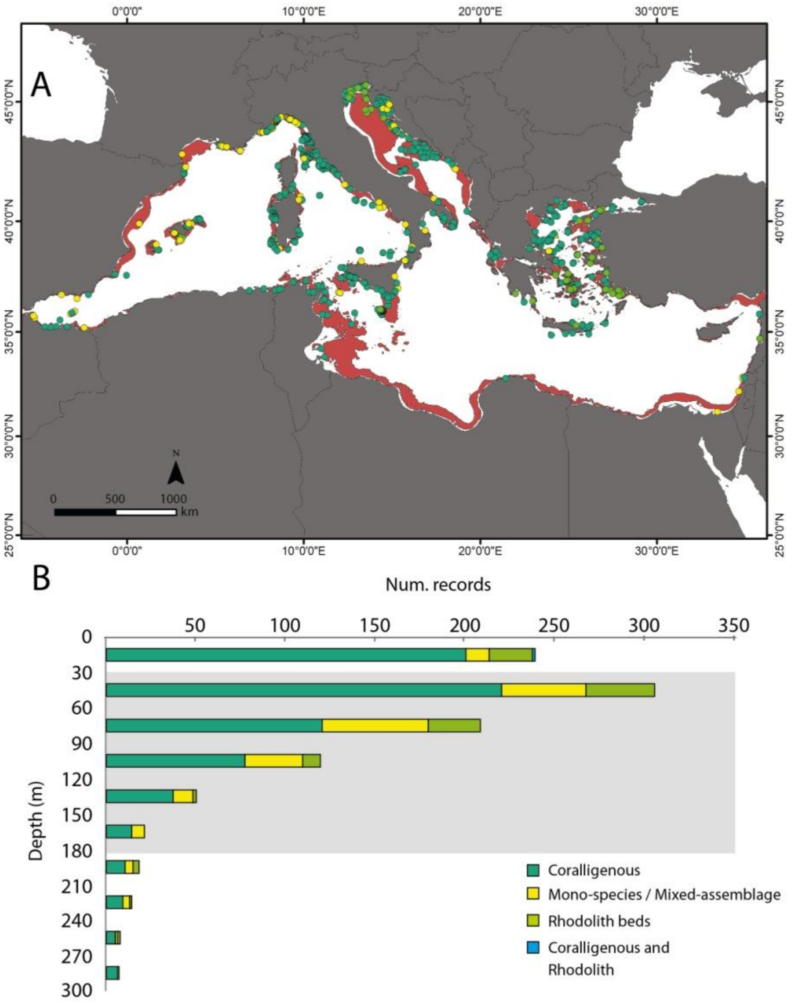

Fig.1.7. A) Map showing the distribution and (B) the depth ranges of published records on benthic mesophotic assemblages, and coralligenous formations and rhodolith beds from the MEDISEH database. Grey shaded bar refers to the depth range estimated as under mesophotic conditions (30-175.5 m).

1.4 Discussion

In the last 40 years, the rapid development of underwater technologies, such as remotely operated vehicles (ROVs) and autonomous underwater vehicles (AUVs), allowed to explore the mesophotic depth and provide information on the biodiversity populating this portion of the water column (Pyle and Copus, 2019). Furthermore, the idea that reefs at moderate depths might be less impacted by thermal stress than shallow reefs (i.e., deep reef refugia hypothesis (DRRH), Bongaerts et al., 2010) has arguably contributed to attracting additional interest from the marine scientific community

(Kahng et al., 2010 among others). As a confirm, an exponential increase in the volume of scientific literature was observed at a global scale, with more than 700 publications from 1970. A significant contribution was provided by studies located in the Mediterranean Sea with more than 190 documents on mesophotic ecosystems detected in the same time range.

The analysis of the mostly investigated taxonomic groups in the Mediterranean literature confirmed the disproportion in the information regarding the main mesophotic actors already highlighted globally (Pyle and Copus, 2019) and in the Mediterranean Sea (Cerrano et al., 2019). Cnidarians were the most frequent targets, representing the main subjects in more than 75% of studies. The charismatic value of coral species and the ecological relevance of their assemblages may potentially have channelled the interest of the scientific community, diverting the attention from situations dominated by different taxonomic groups. Corals surely represent an iconic benthic component, building three-dimensional habitats capable of modifying the near-bottom conditions (Buhl-Mortensen et al., 2010; Bramanti et al., 2017) and acting as important nurseries and refuges for invertebrates and fishes (Bo et al., 2009, 2011; Cerrano et al., 2015; Rossi et al., 2017; D’Onghia, 2019). However, the little evidence available to date on mesophotic ecosystems dominated by other taxonomic groups, such as sponges and mollusk (e.g., Idan et al., 2018; Angeletti & Taviani, 2020; Cardone et al., 2020), suggests that these situations might present levels of biodiversity comparable to those documented for cnidarians assemblages (Maldonado et al., 2017).

The limited number of studies focused on such mesophotic situations might, nevertheless, not necessarily reflect a lower interest from the scientific community but rather that assemblages without a coral component are hardly defined as “mesophotic”. The study of the mesophotic zone originates at tropical latitudes, where deep reefs built by zooxanthellate corals (i.e., MCE) constitute the main biological features (e.g., Lesser et al., 2009, Khang et al., 2010, Hinderstein et al., 2010 and many others). The use of MCE as indicator of intermediate-light conditions has surely concurred to generate a more robust definition of the mesophotic zone in tropical areas over time. By analysing the literature on mesophotic ecosystems at the global scale, in fact, the depth interval of 30-150 m resulted widely used, with a few exceptions, to define the bathymetric range presenting mesophotic conditions (Fig.1.2A).

Problems arise in temperate situations, such as the Mediterranean Sea, where not only a light-dependent coral component that could aid identifying areas under mesophotic conditions is missing but also the physical conditions of the water column are largely different from those at tropical latitudes, resulting in a different degree of light penetration (e.g., Khang et al., 2019).

Adopting a bathymetric definition for the mesophotic zone based on parameters from tropical regions not only might, thus, not fit with the characteristics of the Mediterranean basin but also prevent exploring how different mesophotic conditions influence the distribution and composition of Mediterranean mesophotic communities.

The intensity of light plays a relevant role in this context by delineating the borders of the zone, influencing the ecology but also determining the main actors of mesophotic assemblages (Lesser et al., 2019). The integration of the information regarding the lowest documented percent PAR able to sustain photic metabolism with the PAR reaching the seabed enabled to spatially identify the Mediterranean mesophotic zone. Potentially, more than 377,000 km^2 of the Mediterranean seafloor, corresponding to ca. 15% of the whole basin, might be under mesophotic conditions.

In terms of the light field, the analysis of the percent PAR at the upper border (i.e., 30 m depth) allowed to provide the maximum value of light intensity characterizing the mesophotic zone in the Mediterranean Sea, reporting an average value of 9.79% ± 0.23, suggesting that mesophotic conditions might occur between ca. 10-0.0005% of surface PAR. This range is coherent with available information on coralligenous formations and rhodolith beds, which are commonly found in dim light conditions with irradiance down to 0.05% and 0.0005% of surface light, respectively (Littler et al., 1991; Ballesteros, 2006).

The attenuation of solar radiation increases with increasing depth and is affected by the amount of dissolved and particulate matter suspended in the water column, which is correlated with primary productivity, hydrodynamic conditions, and terrigenous influences (Saulquin et al., 2013).

Moreover, freshwater inputs (e.g., rivers and precipitations) can channel substantial quantities of terrigenous organic and mineral particles, dissolved organic matter, and release large amounts of nutrients to the sea. In the Western Mediterranean Sea, for instance, the estimated portion of seabed under mesophotic conditions is lower with respect to south-eastern subregions although being the largest Mediterranean subregion (Fig.1.3A). Here, intense algal blooms occur in spring when the surface layer stabilizes and sometimes to a less intense in autumn when the thermocline is eroded (Morel & André, 1991). These factors can increase the attenuation of light penetration along the water column, as confirmed by the analysis of K_{dPAR}, which showed higher values in the north-western Mediterranean Sea.

The extension of seabed reached by light can be also influenced by the morphology of the seafloor, with areas characterized by vertical or highly steep sloping bottoms that present reduced extensions when projected on a horizontal axis. In the Western Mediterranean Sea, several mesophotic communities populating rocky vertical bottoms have been documented (e.g., Bo et al., 2014; Enrichetti et al., 2019a; Grinyó et al., 2020), suggesting that the estimated extension of the mesophotic zone may be underrepresented in this geomorphologic setting. Similarly, although the extension of the mesophotic zone of the Adriatic Sea was the lowest observed, more than 50% of the subregion was under mesophotic conditions. Here, the northern sector is very shallow with gentle slopes, reporting an average bottom depth of about 35 m that increase moving towards the south (140 m on average, central Adriatic), with the Pomo/Jabuka Pit reaching 260 m (Artegiani et al., 1997).

The estimated average depth of the lower border of the mesophotic zone was 175.5 m ± 1.2 for the whole basin, which is coherent with the theoretical bathymetric definition provided by previous studies (Cerrano et al., 2019). The threshold of 0.0005% of surface PAR used as the lower limit for mesophotic conditions ensures to comprise also portions of seabed characterized by weak light fields but avoids trespassing into the “deep-sea”, commonly confined below 200 m depth (Spalding et al., 2007; Danovaro et al., 2020) that might potentially cause an overlap between the domains.

Further support to the reliability of the estimation here reported is provided by the high percentage of georeferenced mesophotic studies falling within the proposed area (67%, Fig.1.4B), also considering that more than 80% of those located above 30 m depth were coralligenous formations records, known to occur also shallower than 30 m.

Adopting a deterministic approach to set rigid limits and bound the occurrence of abiotic conditions might appear weak from an ecological perspective. Estimating the spatial extent of the mesophotic zone using the penetration of light in the water column can only identify areas with mesophotic light regime, whilst a complex combination of variables concurs in determining the presence of mesophotic communities, such as biogeochemical factors, type of substrate, biological interactions and stochastic processes. Consequently, the extent of seabed under mesophotic conditions does not necessarily represent the probability of finding mesophotic communities nor strictly describe the composition of communities.

In the literature, efforts have been profused to identify patterns of distribution and community breaks in mesophotic associations on a global scale based on literature review and successively put in relation with the light regime (Lesser et al., 2019). In this sense, estimating the penetration of light along the water column from satellite data is a valid tool to not only bound the depth range likely presenting mesophotic conditions but provides also information on irradiance that might in the future be used to identify patterns in the structure of mesophotic assemblages in the Mediterranean Sea.

Moreover, the presented approach can also be used to estimate the spatial and bathymetric extension of the mesophotic zone in situations characterized by data deficiency. For instance, the southern Mediterranean would appear devoid of mesophotic assemblages from an analysis of the literature due to the few accounts available to date. Large portions of this sector of the Mediterranean Sea likely presenting mesophotic conditions have been, instead, highlighted by the method, enabling their inclusion in the quantitative assessment of the mesophotic zone at the basin scale.

Even it might not represent the most accurate estimation, the results suggest that calculating the penetration of light along the water column from satellite Chl-a concentration might be used to estimate the depth range associated with mesophotic conditions, guaranteeing also to appreciate variations related to local factors and seasonal variability. Moreover, the potential applications of the method extend much beyond the Mediterranean area, allowing to estimate the extension of the mesophotic zone in different geographical situations.

References

Angeletti, L., Taviani, M. (2020). Offshore *Neopycnodonte* oyster reefs in the Mediterranean Sea. *Diversity*, 12(3), 92. https://doi.org/10.3390/d12030092

Angeletti, L., Canese, S., Cardone, F., Castellan, G., Foglini, F., Taviani, M. (2020). A brachiopod biotope associated with rocky bottoms at the shelf break in the central Mediterranean Sea: geobiological traits and conservation aspects. *Aquatic Conservation: Marine and Freshwater Ecosystems*, 30(2), 402–411. https://doi.org/10.1002/aqc.3255

Antoine, D., Morel, A., André, J-M. (1995). Algal pigment distribution and primary production in the eastern Mediterranean as derived from coastal zone color scanner observations. *Journal of Geophysical Research: Oceans*, 100(C8), 16193–16209. https://doi.org/10.1029/95JC00466

Artegiani, A., Paschini, E., Russo, A., Bregant, D., Raicich, F., Pinardi, N. (1997). The Adriatic Sea general circulation. Part I: air–sea interactions and water mass structure. *Journal of Physical Oceanography*, 27(8), 1492–1514. https://doi.org/10.1175/1520-0485(1997)027<1492:TASGCP>2.0.CO;2

Azov, Y. (1991). Eastern Mediterranean—a marine desert? *Marine Pollution Bulletin*, 23, 225–232. https://doi.org/10.1016/0025-326X(91)90679-M

Baker, E.K., Puglise, K.A., Harris, P.T. (2016). *Mesophotic coral ecosystems: a lifeboat for coral reefs?* The United Nations Environment Programme and GRID-Arendal, Nairobi and Arenal: Nairobi, Kenya, 98 pp.

Ballesteros, E. (2006). Mediterranean coralligenous assemblages: a synthesis of present knowledge. *Oceanography and Marine Biology: An Annual Review*, 123–195.

Basterretxea, G., Font-Muñoz, J.S., Salgado-Hernanz, P.M., Arrieta, J., Hernández-Carrasco, I. (2018). Patterns of chlorophyll interannual variability in Mediterranean biogeographical regions. *Remote Sensing of Environment*, 215, 7–17. https://doi.org/10.1016/j.rse.2018.05.027

Bethoux, J.P. (1979). Budgets of the Mediterranean Sea-their dependance on the local climate and on the characteristics of the Atlantic waters. *Oceanologici acta*, 2(2), 157–163.

Bo, M., Bava, S., Canese, S., Angiolillo, M., Cattaneo-Vietti, R., Bavestrello, G. (2014). Fishing impact on deep Mediterranean rocky habitats as revealed by ROV investigation. *Biological Conservation*, 171, 167–176.

Bo, M., Bavestrello, G., Canese, S., Giusti, M., Salvati, E., Angiolillo, M., Greco, S. (2009). Characteristics of a black coral meadow in the twilight zone of the central Mediterranean Sea. *Marine Ecology Progress Series*, 397, 53–61. https://doi.org/10.3354/meps08185

Bo, M., Bertolino, M., Borghini, M., Castellano, M., Harriague, A.C., Di Camillo, C.G., Gasparini, G.P., Misic, C., Povero, P., Schroeder, K., Bavestrello, G. (2011). Characteristics of the mesophotic megabenthic assemblages of the Vercelli Seamount (North Tyrrhenian Sea). *PLOS ONE*, 6(2), e16357. https://doi.org/10.1371/journal.pone.0016357

Bongaerts, P., Ridgway, T., Sampayo, E.M., Hoegh-Guldberg, O. (2010). Assessing the 'deep reef refugia' hypothesis: focus on Caribbean reefs. *Coral Reefs*, 29(2), 309–327. https://doi.org/10.1007/s00338-009-0581-x

Bramanti, L., Benedetti, M.C., Cupido, R., Cocito, S., Priori, C., Erra, F., Iannelli, M., Santangelo, G. (2017). Demography of animal forests: the example of Mediterranean gorgonians. In: *Marine Animal Forests: The Ecology of Benthic Biodiversity Hotspots*. Rossi S, Bramanti L, Gori A, Orejas C (Eds). Springer International Publishing: Cham, pp. 529–548.

Buhl-Mortensen, L., Vanreusel, A., Gooday, A.J., Levin, L.A., Priede, I.G., Buhl-Mortensen, P., Gheerardyn, H., King, N.J., Raes, M. (2010). Biological structures as a source of habitat heterogeneity and biodiversity on the deep ocean margins. *Marine Ecology*, 31(1), 21–50. https://doi.org/10.1111/j.1439-0485.2010.00359.x

Capdevila, P., Linares, C., Aspillaga, E., Riera, J.L., Hereu, B. (2018). Effective dispersal and density-dependence in mesophotic macroalgal forests: Insights from the Mediterranean species *Cystoseira zosteroides*. *PLOS ONE*, 13(1), e0191346. https://doi.org/10.1371/journal.pone.0191346

Cardone, F., Corriero, G., Longo, C., Mercurio, M., Onen Tarantini, S., Gravina, M.F., Liscio, S., Moretti, M., De Giosa, F., Giangrande, A., Marzano, C.N., Pierri, C. (2020). Massive bioconstructions built by *Neopycnodonte cochlear* (Mollusca, Bivalvia) in a mesophotic environment in the central Mediterranean Sea. *Scientific Reports*, 10(1), 6337. https://doi.org/10.1038/s41598-020-63241-y

Castellan, G., Angeletti, L., Taviani, M., Montagna, P. (2019). The yellow coral *Dendrophyllia cornigera* in a Warming Ocean. *Frontiers in Marine Science*, 6. https://doi.org/10.3389/fmars.2019.00692

Cau, A., Follesa, M.C., Moccia, D., Bellodi, A., Mulas, A., Bo, M., Canese, S., Angiolillo, M., Cannas, R. (2017). *Leiopathes glaberrima* millennial forest from SW Sardinia as nursery ground for the small spotted catshark *Scyliorhinus canicula*. *Aquatic Conservation: Marine and Freshwater Ecosystems*, 27(3), 731–735. https://doi.org/10.1002/aqc.2717

Cerrano, C., Bastari, A., Calcinai, B., Camillo, C.D., Pica, D., Puce, S., Valisano, L., Torsani, F. (2019). Temperate mesophotic ecosystems: gaps and perspectives of an emerging conservation challenge for the Mediterranean Sea. *The European Zoological Journal*, 86(1), 370–388. https://doi.org/10.1080/24750263.2019.1677790

Cerrano, C., Bianchelli, S., Camillo, C.G.D., Torsani, F., Pusceddu, A. (2015). Do colonies of *Lytocarpia myriophyllum*, L. 1758 (Cnidaria, Hydrozoa) affect the biochemical composition and the meiofaunal diversity of surrounding sediments? *Chemistry and Ecology*, 31(1), 1–21. https://doi.org/10.1080/02757540.2014.966699

Chimienti, G. (2020). Vulnerable Forests of the Pink Sea Fan *Eunicella verrucosa* in the Mediterranean Sea. *Diversity*, 12(5), 176. https://doi.org/10.3390/d12050176

Christaki, U., Van Wambeke, F., Lefevre, D., Lagaria, A., Prieur, L., Pujo-Pay, M., Grattepanche, J.D., Colombet, J., Psarra, S., Dolan, J.R., Sime-Ngando, T., Conan, P., Weinbauer, M.G., Moutin, T. (2011). Microbial food webs and metabolic state across oligotrophic waters of the Mediterranean Sea during summer. *Biogeosciences*, 8(7), 1839–1852. https://doi.org/10.5194/bg-8-1839-2011

Corriero, G., Pierri, C., Mercurio, M., Marzano, C.N., Tarantini, S.O., Gravina, M.F., Lisco S., Moretti M., De Giosa F., Valenzano E., Giangrande A., Mastrodonato M., Longo C., Cardone F. (2019). A Mediterranean mesophotic coral reef built by non-symbiotic scleractinians. *Scientific Reports*, 9(1), 3601. https://doi.org/10.1038/s41598-019-40284-4

D'Onghia, G., Sion, L., Capezzuto, F. (2019). Cold-water coral habitats benefit adjacent fisheries along the Apulian margin (central Mediterranean). *Fisheries Research*, 213, 172-179.

D'Ortenzio, F., Ribera d'Alcalà, M. (2009). On the trophic regimes of the Mediterranean Sea: a satellite analysis. *Biogeosciences*, 6(2), 139–148. https://doi.org/10.5194/bg-6-139-2009

Danovaro, R., Fanelli, E., Canals, M., Ciuffardi, T., Fabri, M.-C., Taviani, M., Argyrou, M., Azzurro, E., Bianchelli, S., Cantafaro, A., Carugati, L., Corinaldesi, C., de Haan, W.P., Dell'Anno, A., Evans, J., Foglini, F., Galil, B., Gianni, M., Goren, M., Greco, S., Grimalt, J., Güell-Bujons, Q., Jadaud, A., Knittweis, L., Lopez, J.L., Sanchez-Vidal, A., Schembri, P.J., Snelgrove, P., Vaz, S., Angeletti, L., Barsanti, M., Borg, J.A., Bosso, M., Brind'Amour, A., Castellan, G., Conte, F., Delbono, I., Galgani, F., Morgana, G., Prato, S., Schirone, A., Soldevila, E. (2020). Towards a marine strategy for the deep Mediterranean Sea: Analysis of current ecological status. *Marine Policy*, 112, 103781. https://doi.org/10.1016/j.marpol.2019.103781

Davies, A.J., Guinotte, J.M. (2011). Global habitat suitability for framework-forming cold-water corals. *PLOS ONE*, 6(4), e18483. https://doi.org/10.1371/journal.pone.0018483

Enrichetti, F., Bava, S., Bavestrello, G., Betti, F., Lanteri, L., Bo, M. (2019a). Artisanal fishing impact on deep coralligenous animal forests: A Mediterranean case study of marine vulnerability. *Ocean, Coastal Management*, 177, 112–126. https://doi.org/10.1016/j.ocecoaman.2019.04.021

Enrichetti, F., Dominguez-Carrió, C., Toma, M., Bavestrello, G., Betti, F., Canese, S., Bo, M. (2019b). Megabenthic communities of the Ligurian deep continental shelf and shelf break (NW Mediterranean Sea). *PLOS ONE*, 14(10), e0223949. https://doi.org/10.1371/journal.pone.0223949

Foster, M.M., Amado Filho, G.M., Kamenos, N.A., Riosmena-Rodríguez, R., Steller, D.L. (2013). Rhodoliths and rhodolith beds. *Research and discoveries: The revolution of science through scuba*, 39, 143–55.

Fox, J., Friendly, G.G., Graves, S., Heiberger, R., Monette, G., Nilsson, H., Ripley, B., Weisberg, S., Fox, M.J., Suggests, M. (2007). The car package. R package.

Georgian, S.E., Kramer, K., Saunders, M., Shedd, W., Roberts, H., Lewis, C., Fisher C., Cordes E. 2020 (2020). Habitat suitability modelling to predict the spatial distribution of cold-water coral communities affected by the Deepwater Horizon oil spill. *Journal of Biogeography*, 47(7), 1455–1466. https://doi.org/10.1111/jbi.13844

Gori, A., Reynaud, S., Orejas, C., Gili, J.-M., Ferrier-Pagès, C. (2014). Physiological performance of the cold-water coral *Dendrophyllia cornigera* reveals its preference for temperate environments. *Coral Reefs*, 33(3), 665–674. https://doi.org/10.1007/s00338-014-1167-9

Grinyó, J., Garriga, A., Soler-Membrives, A., Santín, A., Ambroso, S., López-González, P.J., Díaz, D. (2020). Soft corals assemblages in deep environments of the Menorca Channel (Western Mediterranean Sea). *Progress in Oceanography*, 188, 102435. https://doi.org/10.1016/j.pocean.2020.102435

Hijmans, R.J., Van Etten, J., Cheng, J., Mattiuzzi, M., Sumner, M., Greenberg, J.A., Lamigueiro, O.P., Bevan, A., Racine, E.B., Shortridge, A. (2015). Package 'raster'. R package.

Hinderstein, L.M., Marr, J.C.A., Martinez, F.A., Dowgiallo, M.J., Puglise, K.A., Pyle, R.L., Zawada, D.G., Appeldoorn, R. (2010). Theme section on "Mesophotic coral ecosystems: characterization, ecology, and management". *Coral Reefs*, 29(2), 247–251. https://doi.org/10.1007/s00338-010-0614-5

Idan, T., Shefer, S., Feldstein, T., Yahel, R., Huchon, D., Ilan, M. (2018). Shedding light on an East-Mediterranean mesophotic sponge ground community and the regional sponge fauna. *Mediterranean Marine Science,* 19(1), 84–106. https://doi.org/10.12681/mms.13853

Kahng, S.E., Garcia-Sais, J.R., Spalding, H.L., Brokovich, E., Wagner, D., Weil, E., Hinderstein, L., Toonen, R.J. (2010). Community ecology of mesophotic coral reef ecosystems. *Coral Reefs*, 29(2), 255–275. https://doi.org/10.1007/s00338-010-0593-6

Kahng, S.E., Akkaynak, D., Shlesinger, T., Hochberg, E.J., Wiedenmann, J., Tamir, R., Tchernov, D. (2019). Light, temperature, photosynthesis, heterotrophy, and the lower depth limits of mesophotic coral ecosystems. In: *Mesophotic coral ecosystems*. Loya Y, Puglise KA, Bridge TCL (Eds). Springer International Publishing: Cham, pp. 801–828.

Lesser, M.P., Slattery, M., Leichter, J.J. (2009). Ecology of mesophotic coral reefs. *Journal of Experimental Marine Biology and Ecology*, 375(1), 1–8. https://doi.org/10.1016/j.jembe.2009.05.009

Lesser, M.P., Slattery, M., Laverick, J.H., Macartney, K.J., Bridge, T.C. (2019). Global community breaks at 60 m on mesophotic coral reefs. *Global Ecology and Biogeography*, 28(10), 1403–1416. https://doi.org/10.1111/geb.12940

Littler, M.M., Littler, D.S., Dennis Hanisak, M. (1991). Deep-water rhodolith distribution, productivity, and growth history at sites of formation and subsequent degradation. *Journal of Experimental Marine Biology and Ecology*, 150(2), 163–182. https://doi.org/10.1016/0022-0981(91)90066-6

Maldonado, M., Aguilar, R., Bannister, R.J., Bell, J.J., Conway, K.W., Dayton, P.K., Díaz, C., Gutt, J., Kenchington, E.L.R., Leys, D., Pomponi, S.A., Rapp, H.T., Rützler, K., Tendal, O.S., Vacelet, J., Young, C.M. (2017). Sponge grounds as key marine habitats: a synthetic review of types, structure, functional roles, and conservation concerns. https://doi.org/10.1007/978-3-319-17001-5_24-1

Markager, S., Sand-Jensen, K. (1992). Light requirements and depth zonation of marine macroalgae. *Marine Ecology Progress Series*, 88, 83–92. https://doi.org/10.3354/meps088083

Martin, C.S., Giannoulaki, M., De Leo, F., Scardi, M., Salomidi, M., Knittweis, L., Pace, M.L., Garofalo, G., Gristina, M., Ballesteros, E., Bavestrello, G., Belluscio, A., Cebrian, E., Gerakaris, V., Pergent, G., Pergent-Martini, C., Schembri, P.J., Terribile, K., Rizzo, L., Ben Souissi, J., Bonacorsi, M., Guarnieri, G., Krzelj, M., Macic, V., Punzo, E., Valavanis, V., Fraschetti S. (2014). Coralligenous and maërl habitats: predictive modelling to identify their spatial distributions across the Mediterranean Sea. *Scientific Reports*, 4(1), 5073. https://doi.org/10.1038/srep05073

Marty, J.-C., Chiavérini, J. (2002). Seasonal and interannual variations in phytoplankton production at DYFAMED time-series station, northwestern Mediterranean Sea. *Deep Sea Research Part II: Topical Studies in Oceanography*, 49(11), 2017–2030. https://doi.org/10.1016/S0967-0645(02)00025-5

Mayot, N., D'Ortenzio, F., Ribera d'Alcalà, M., Lavigne, H., Claustre, H. (2016). Interannual variability of the Mediterranean trophic regimes from ocean color satellites. *Biogeosciences*, 13(6), 1901–1917. https://doi.org/10.5194/bg-13-1901-2016

Mobley, C.D., Mobley, C.D. (1994). *Light and water: radiative transfer in natural waters*. In: *Bulletin of the American Meteorological Society Vol. 76, No. 1*. Ronald, J, Zaneveld, V. (Eds). American Meteorological Society, pp. 160

Morel, A., André, J.-M. (1991). Pigment distribution and primary production in the western Mediterranean as derived and modeled from coastal zone color scanner observations. *Journal of Geophysical Research: Oceans*, 96(C7), 12685–12698. https://doi.org/10.1029/91JC00788

Morel, A., Huot, Y., Gentili, B., Werdell, P.J., Hooker, S.B., Franz, B.A. (2007). Examining the consistency of products derived from various ocean color sensors in open ocean (Case 1) waters in the perspective of a multi-sensor approach. *Remote Sensing of Environment*, 111(1), 69–88. https://doi.org/10.1016/j.rse.2007.03.012

Pinardi, N., Zavatarelli, M., Arneri, E., Crise, A., Ravaioli, M. (2006). The physical, sedimentary and ecological structure and variability of shelf areas in the Mediterranean Sea.

Puglise, K.A., Hinderstein, L.M., Marr, J.C.A., Dowgiallo, M.J., Martinez, F.A., 1961-. (2009). Mesophotic coral ecosystem research strategy international workshop to prioritize research and management needs for mesophotic coral ecosystems, Jupiter, Florida, 12-15 July, 2009. National Centers for Coastal Research, NOAA Undersea Research Program, NOAA Technical Memorandum NOS NCCOS 98 and OAR OER 2, NOAA Silver Spring, MD, pp. 24.

Pyle, R.L., Copus, J.M. (2019). Mesophotic coral ecosystems: introduction and overview. In: *Mesophotic coral ecosystems*. Loya Y, Puglise KA, Bridge TCL (Eds). Springer International Publishing: Cham, pp. 3–27.

R Core Team. (2020). *R: A Language and Environment for Statistical Computing*. R Foundation for Statistical Computing, Vienna: Austria.

Rodolfo-Metalpa, R., Montagna, P., Aliani, S., Borghini, M., Canese, S., Hall-Spencer, J.M., Foggo, A., Milazzo, M., Taviani, M., Houlbrèque, F. (2015). Calcification is not the Achilles' heel of cold-water corals in an acidifying ocean. *Global Change Biology*, 21(6), 2238–2248. https://doi.org/10.1111/gcb.12867

Rossi, S., Bramanti, L., Gori, A., Orejas, C. (Eds.). (2017). *Marine Animal Forests: The Ecology of Benthic Biodiversity Hotspots*. Springer International Publishing: Cham.

Runcie, J.W., Gurgel, C.F.D., Mcdermid, K.J. (2008). *In situ* photosynthetic rates of tropical marine macroalgae at their lower depth limit. *European Journal of Phycology*, 43(4), 377–388. https://doi.org/10.1080/09670260801979303

Saulquin, B., Hamdi, A., Gohin, F., Populus, J., Mangin, A., d'Andon, O.F. (2013). Estimation of the diffuse attenuation coefficient KdPAR using MERIS and application to seabed habitat mapping. *Remote Sensing of Environment*, 128, 224–233. https://doi.org/10.1016/j.rse.2012.10.002

Slattery, M., Lesser, M.P., Brazeau, D., Stokes, M.D., Leichter, J.J. (2011). Connectivity and stability of mesophotic coral reefs. *Journal of Experimental Marine Biology and Ecology*, 408(1), 32–41. https://doi.org/10.1016/j.jembe.2011.07.024

Spalding, M.D., Fox, H.E., Allen, G.R., Davidson, N., Ferdaña, Z.A., Finlayson, M., Halpern, B., Jorge, M., Lombana, A., Lourie, S., Martin, K., McManus, E., Molnar, J., Recchia, C., Roberston, J. (2007). Marine ecoregions of the world: a bioregionalization of coastal and shelf areas. *BioScience*, 57(7), 573–583. https://doi.org/10.1641/B570707

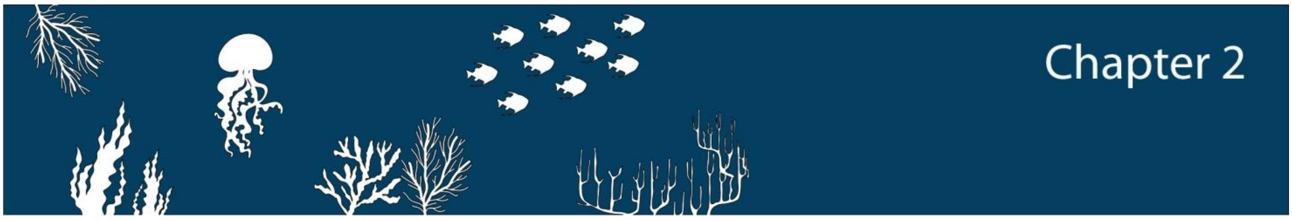

Chapter 2

2. Visual surveys to study mesophotic and deep benthic communities: a comparison between analytical methods

2.1 Introduction

The increasing development and affordability of underwater technologies, such as Remotely Operated Vehicles (ROVs) and Autonomous Underwater Vehicles (AUVs), together with the growth in computing performances permitted the discovery, mapping, and detailed examination of ecosystems at depths that were unimaginable just decades ago (e.g., Cordes et al. 2007; Freiwald et al. 2009; Lundsten et al. 2010; Huvenne et al., 2011; Wynn et al., 2014; Vanreusel et al. 2016; Danovaro et al. 2017). Visual surveys are currently used for exploring the biodiversity associated with biological communities (e.g., Norcross and Mueter 1999; Buhl-Mortensen et al., 2012; Ayma et al. 2016; Consoli et al. 2016; Trotter et al., 2019; Beccari et al., 2020), identifying habitats for priority of conservation (e.g., Fosså et al. 2002; Grasmueck et al., 2006; Bongaerts et al. 2010; Rengstorf et al. 2012; Fabri et al. 2014; Taviani et al., 2017; 2019; IUCN 2019; Angeletti et al., 2020a, 2021 (WATER); Chaniotis et al., 2020), and evaluating the environmental status of ecosystems (e.g., Cánovas-Molina et al. 2016; Fabri et al., 2019; Enrichetti et al., 2019).

When working with visual methods, video surveys should be carried out along linear paths, navigating at constant speed and altitude from the seafloor to guarantee a homogeneous representation of the habitat and biological assemblages under investigation (Eleftheriou and McIntyre 2005, Huvenne et al. 2018). The strength of studying benthic ecosystems through visual surveys is that video footages can be processed using different analytical techniques depending on the aims of the study. Among the most common are manual point-based approaches (Foster, 1991; Meese & Tomich, 1992; Leonard & Clark, 1993; Carleton & Done, 1995) and region-based percentage estimations (Meese & Tomich, 1992; Garrabou et al., 2002; Teixidó et al., 2011; Pech et al., 2004; Guinda et al., 2013). Some of these need a certain degree of overlap among frames to ensure a complete seafloor representation (e.g., 3D reconstructions, Robert et al., 2020), while others avoid frames overlap to reduce analysis replications (e.g., Bo et al., 2014). Despite several automatic and semi-automatic methods have been proposed and tested to faster analysis of benthic video recordings (Stokes and Deane 2009; Aguzzi et al. 2011), their application still requires ad-hoc instrumentation and can be labour-intensive (Foglini et al. 2019; Robert et al. 2020).

In ecological studies, the ROV dive track is divided into multiple partial tracks (i.e., sub-tracks) determined by distance surveyed and a random number of frames is extracted and analyzed. This methodology guarantees to obtain measures (such as mean, standard deviation) which approximate the characteristics of the entire survey and allows statistical comparison between different samples, sites, areas.

Although this variety of possible approaches, the analysis of visual data is challenging in terms of analytical time, often forcing the analysis to only a limited subset of frames, extracted (often manually) at regular time intervals (e.g., Bo et al. 2014; Fabri et al., 2014; Cau et al. 2015). Moreover, visual surveys paths and navigation speeds may be altered by the need for a higher detail, the morphology of the investigated habitat, or external factors (e.g., weather conditions, technical issues).

Some major questions arise: how the video subsampling strategy influence the quality of results? What is an efficient compromise between analytical effort and results' quality?

In this chapter, the coverage of different substrate classes and the taxonomical compositions of biological assemblages obtained by the analyses of a subset of frames are compared with those resulting from the analysis of the entire videos to explore the accuracy of frame-based methods. Two different subsampling techniques are compared: extracting photograms at regular time (4, 10 and 30 s) or distance-intervals (0.5, 1 and 3 m). The methods are applied on three ROV surveys exploring i) a coralligenous formation, ii) a deep-water oyster reef and iii) a cold water corals

(CWC) province. In addition, the influence of the survey speed and the degree of frames overlap on the analysis accuracy are investigated.

2.2 Material and methods

2.2.1 Collection of visual surveys

As part of the Italian Marine Strategy Framework Directive (2008/56/EC MSFD) monitoring program, a coralligenous bioconstruction at mesophotic depth (65-80 m) on the Amendolara Seamount in the Ionian Sea (Angeletti et al., 2017), a deep-water oyster reef at a depth ranging between 95 to 115 m off Santa Maria di Leuca in the Northern Ionian Sea (Castellan et al., 2019; Angeletti and Taviani, 2020), and a CWC province composed by several mounds situated at 400-430 m depth in the Corsica Channel in the Tyrrhenian Sea (Angeletti et al. 2020b) were visually explored by means of the ROV during the MS16_II, MS17_II and MS17_I oceanographic cruises carried out on R/V Minerva Uno (Fig. 2.1 and Tab. 2.1).

The dives were conducted using a Pollux III (Global Electric Italiana) equipped with a low-resolution CCD video camera for navigation and a high resolution (2304 x 1296 pixels) video camera. The ROV was provided with an underwater acoustic tracking system that gives position and depth every 1s. Parallel lasers (with 20 cm separation) were mounted on the ROVs to provide a scale on the videos. Dives point-tracks were smoothed using Adelie Video (© Ifremer) and ArcGIS (© ESRI) software. The Adelie Video tool “points to line” was used to produce a line-format track of ROV dives. Video recordings were performed maintaining ca. 2 m of altitude from the seafloor. In station MS16_II_83, the mean survey speed was equal to 0.14 m/s, in station MS17_II_115 average speed was 0.22 m/s, while in station MS17_I_135 the ROV sailed at 0.21 m/s (Tab. 2.1).

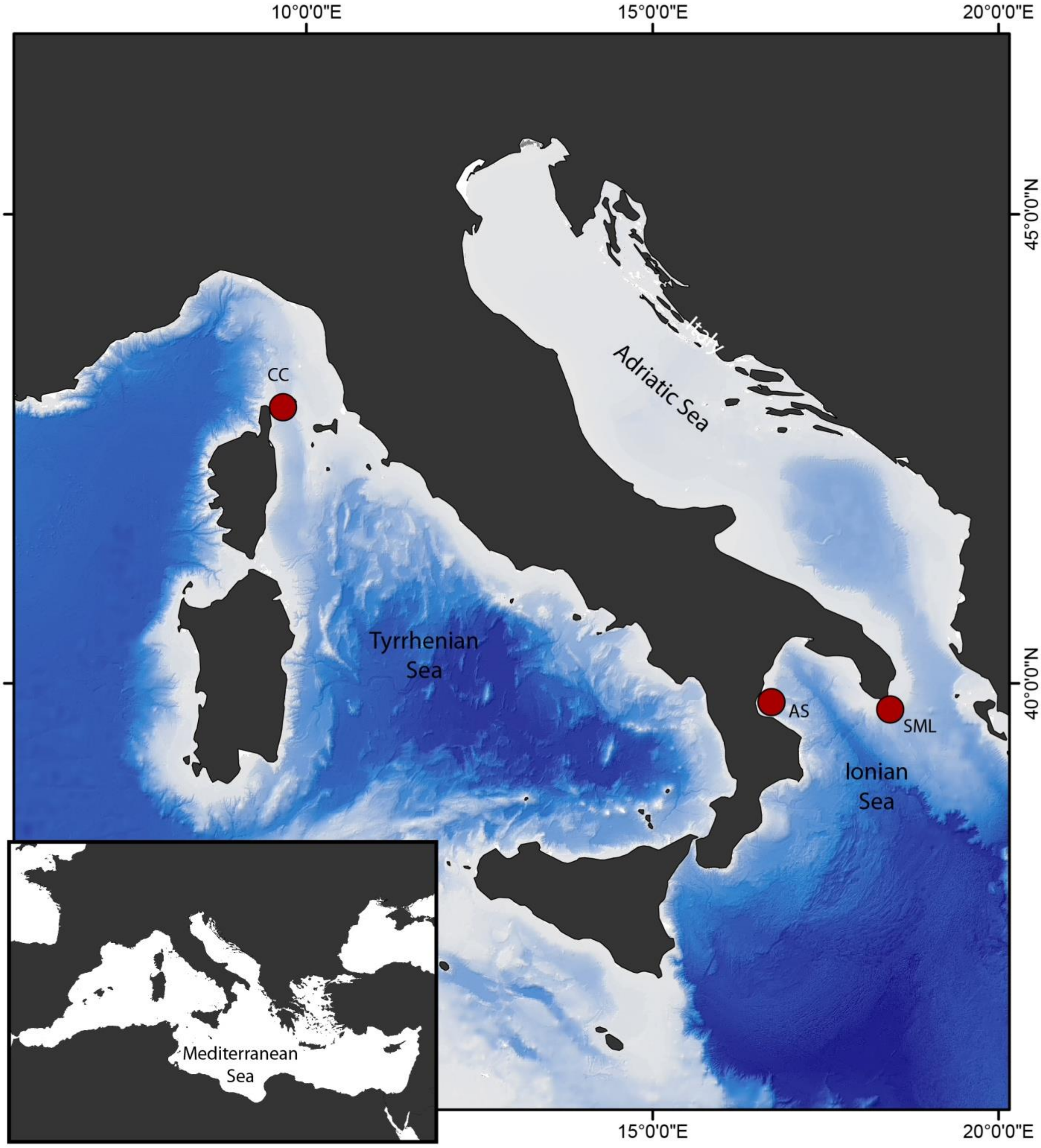

Fig. 2.1. Location of the ROV surveys used in the study; CC: Corsica Channel, AS: Amendolara Seamount, SML: Santa Maria di Leuca.

ROV	Location	Area	Date	Lat	Long	Length (m)	Depth range (m)	Velocity (m/s)	Target
MS16_II_83	Amendolara Seamount	Ionian Sea	10/09/16	39° 51' 32.46"N	16° 41' 59.61"W	647.7	65-80	0.127	Coralligenous formation
MS17_II_115	Off Santa Maria di Leuca	Ionian Sea	31/07/17	37° 56' 59.78"N	12° 7' 15.34"W	896.7	95-115	0.217	Deep-water oyster-reef
MS17_I_135	Corsica Channel	Tyrrhenian Sea	17/07/17	39°44′01.10″ N	18°22′14.90 W	1041.5	400-430	0.212	Cold water corals

Tab. 2.1. ROV dives metadata reporting the location, date, water depth, length and velocity of surveys, and biological targets.

2.2.2 Video analysis and subsampling

The analysis of the entire video footages (hereafter "reference analysis") was performed by extracting a frame every second. The substrate cover was obtained by recording the changes in dominant substrate type (>50% of the frame). The seafloor was classified as "Hard" (geological or biological hard structures), "Mobile" (soft bottoms), or "NA" (bottom not visible). The extensions of each substrate class were calculated using ArcGIS software.

Macro- and mega-benthic organisms were identified to the lowest possible taxonomic rank, counted, and georeferenced by using Adelie Video software. Taxa unidentifiable at the species level were categorized only as morpho-species or morphological categories.

For time-based (TB) subsampling methods, a frame every 4, 10, and 30 seconds was extracted using Adelie Video software. Subsampling intervals for distance-based (DB) methods were selected to obtain a similar number of frames extracted with TB methods, allowing to compare the techniques. A point every 0.5 m, 1 m, and 3 m was generated along the plan view of the ROV tracks using the "Generate points along line" tool in ArcGIS software. The UTM time in correspondence of every point generated was obtained by pairing points with the ROV tracks ("Spatial Join" tool in ArcGIS software, Match option: Intersect; Search Radius: 0.05 m) and used to extract the frames from the videos.

Images extracted with TB and DB methods were analysed for taxonomical composition and substrate type following the methodology described above.

The extents of substrate classes and the number of taxa obtained with every subsampling method were compared with those from the reference analysis to calculate percentage errors (expressed as average ± standard error). The statistical significance among the differences in the percent errors among the sampling intervals (4, 10, 30 s and 0.5, 1, and 3 m) and subsampling methods (TB and DB) was tested with Kruskal-Wallis test and the post hoc Dunn's test using R software (R core team 2019), after checking that data not fulfilled normal distribution and homogeneity of variance assumptions using the Shapiro-Wilk test (package “stats”, version 4.2.0) and Levene’s test (package “car”, version 3.0, Fox et al., 2012), respectively.

With the aim of quantifying the degrees of overlap among frames, a unique serial ID number was assigned to frames extracted with the same technique that displayed a new section of the seafloor. When adjacent frames showed the same portions of the seafloor (>70% of the frame), the same ID was assigned. The ratio between the total number of frames and those presenting a unique ID represented the percentage of overlapping.

2.3 Results

2.3.1 Substrate cover extent

The estimation of substrate classes covers resulting from reference analysis performed on survey MS16_II_83 showed that the 647.7 m of explored seafloor were almost equally composed by “Hard” and “Mobile”, 44.9% (corresponding to 291.1 m) and 41.4% (286.3 m), respectively. The remaining 13.6% (88.3 m) was classified as “NA” (Fig. 2.2 A; Tab.2.2). In survey MS17_II_115, the reference analysis reported 53.7% (481.5 m) of “Hard” substrate, “Mobile” for 30.9% (276.7 m), while “NA” class represented the 15.4% (138.4 m; Fig. 2.2B, Tab. 2.2). The longest ROV survey was MS17_I_135, with 1041.5 m of seafloor explored. Of these, 30% (312.6 m) was classified as “Hard”, 2.1% (542.2 m) as “Mobile” and 17.9% (186.7 m) as “NA” (Fig. 2.2C; Tab. 2.2) from reference analysis.

The TB methods reported strongly larger percent errors on average when compared to DB techniques. “Mobile” was the class reporting the highest average error, reaching 5.44% ± 3.03, the “Hard” class showed an average percent error up to 1.82% ± 0.81, while the “NA” was mainly underestimated with an error of 4.58% ± 2.24 on average (Fig. 2.3D; Tab. 2.3).

In contrast, DB methods showed higher accuracy, with values always below 0.15%. The Kruskal-Wallis test reported significant differences in the accuracy between TB and DB methods (p-value < 0.01).

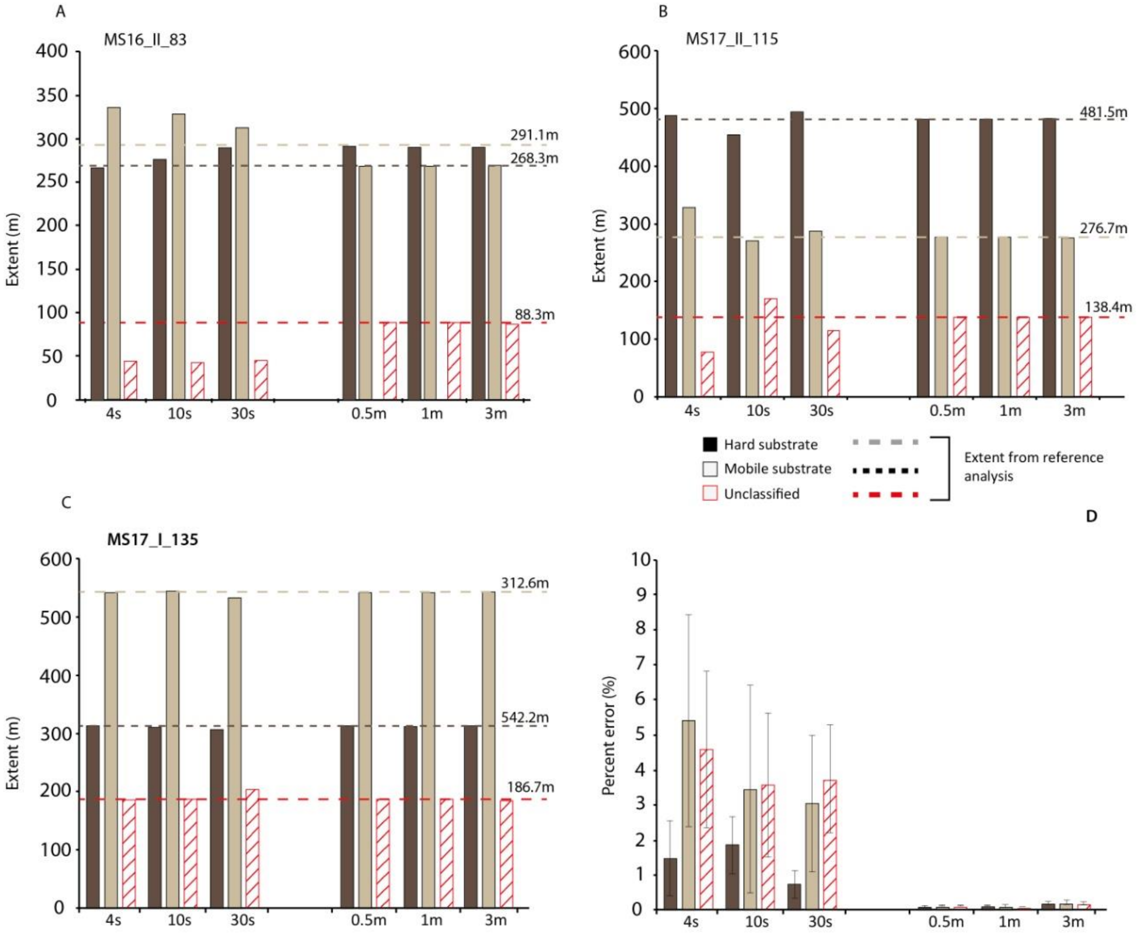

Fig. 2.2. A-C) Bar plots modified from Castellan et al., 2020 showing the spatial cover extent of different substrate classes calculated with the tested techniques. Dashed lines refer to values obtained from reference analysis. D) Average percentage error in the estimation of substrate covering for each method. Error bars represent Standard Errors.

	Method	Frames	Hard (m)	Err (%)	Mobile (m)	Err (%)	NA (m)	Err (%)	Overlap (%)	Taxa	Ident. Taxa (%)	Err (%)
MS16_II_83	Ref.	6840	291.1		268.3		88.3			50		
	4s	1712	267.9	3.57	336.1	10.47	43.6	6.90	85.8	50	100	0
	10s	684	276.5	2.26	328.9	9.35	42.3	7.10	67.3	48	96	4.00
	30s	228	290.1	0.15	313.1	6.92	44.6	6.74	34.0	43	86	14.00
	0.5m	1360	291.6	0.08	268.6	0.04	88.0	0.04	85.8	46	92	8.00
	1m	680	291.1	0	269.1	0.12	88.0	0.04	67.3	45	90	10.00
	3m	251	291.1	0	270.1	0.28	87.0	0.20	33.3	40	80	20.00
MS17_II_115	Ref.	5060	481.5		276.7		138.4			82		
	4s	1264	487.6	0.68	329.2	5.85	78.1	6.73	28.1	71	86.59	13.41
	10s	506	455.0	2.96	270.8	0.65	170.8	3.61	12.3	65	79.27	20.73
	30s	169	494.6	1.45	287.5	1.21	114.6	2.66	1.5	49	59.76	40.24
	0.5m	1486	481.6	0.01	276.6	0.01	138.5	0.01	36.7	74	90.24	9.76
	1m	767	481.8	0.03	276.9	0.02	137.9	0.06	19.2	64	78.05	21.95
	3m	257	482.8	0.14	275.9	0.09	137.9	0.06	4.1	55	67.07	32.93
MS17_I_135	Ref.	5418	312.6	30.01	542.2		186.7			26		
	4s	1355	313.7	0.10	542.2	0.00	185.6	0.10	58.7	25	96.15	3.85
	10s	541	310.0	0.25	544.8	0.24	186.7	0.01	41.7	21	80.77	19.23
	30s	180	306.5	0.58	532.4	0.94	204.1	1.68	16.9	21	80.77	19.23
	0.5m	1543	312.8	0.02	542.1	0.01	186.5	0.02	51.1	23	88.46	11.54
	1m	834	312.3	0.02	542.1	0.01	187.0	0.03	35.6	22	84.62	15.38
	3m	284	313.3	0.07	543.1	0.09	185.0	0.16	13.6	21	80.77	19.23

Tab. 2.2. Comparative ability of TB and DB methods to estimate substrate coverage and detect the taxonomic composition of biological communities in surveyed stations. The number of frames extracted with each technique and the percentage of overlapped frames are also reported. Ref: reference analysis.

Method	Hard		Mobile		NA		Frames		Overlap		Taxa identified	
	Err (%)	SE	Err (%)	SE	Err (%)	SE	Qnt.	SE	(%)	SE	Err (%)	SE
4s	1.45	1.07	5.44	3.03	4.58	2.24	1443.67	136.71	57.56	16.67	7.29	4.17
10s	1.82	0.81	3.41	2.97	3.57	2.05	577.00	54.45	40.45	15.90	15.97	5.99
30s	0.73	0.38	3.02	1.95	3.69	1.55	192.33	18.11	17.46	9.40	25.73	7.98
0.5m	0.04	0.02	0.02	0.01	0.02	0.01	1463.00	54.06	57.88	14.55	11.22	1.98
1m	0.02	0.01	0.05	0.04	0.04	0.01	760.33	44.58	40.71	14.09	17.14	3.79
3m	0.07	0.04	0.15	0.06	0.14	0.04	264.00	10.15	17.03	8.60	25.32	4.26

Tab. 2.3. The average percentage error and standard errors in the estimation of substrate covers and community composition detection for each tested technique. The average number of frames extracted, and percentage of overlapped frames are also reported.

2.3.2 Taxonomic composition

The reference analysis of survey MS16_I_83 exploring a coralligenous community in the Amendolara Seamount identified a total of 50 taxa (Fig. 2.3A-B, Tab. 2.2). TB methods showed high performances in detecting the taxonomical composition of the assemblage at any interval, which decreased with wider subsampling intervals (Fig. 2.4A; Tab. 2.2). The analysis of 1712 frames extracted with the 4s-interval method identified 100% of taxa (n=50, Tab. 2.2). The 10s- and 30s-intervals extracted a lower number of photograms (684 and 228, respectively) and reported lower accuracies, with 96% (n= 48) and 86% (n=43) of total taxa identified, respectively. Although showing good performances, DB methods resulted less accurate compared to TB methods in detecting the taxonomic composition of the explored assemblages: 92% (n=46) of taxa were identified with 0.5m intervals, 90% (n=45) by using 1m intervals, and 80% (n=40) were detected with intervals of 3m (Fig. 2.4A, Tab. 2.2).

Survey MS17_II_115 provided a visual recording of the community populating a deep-water oyster reef offshore Santa Maria di Leuca (Fig. 3C-D). Here, the biological assemblage was highly biodiverse, with 82 taxa identified by reference analysis. The most accurate technique was obtained with the 0.5 m-interval DB method that detected 74 taxa corresponding to 90% of the total. The 10s and 1m methods reported similar results, identifying 65 (79%) and 64 taxa (78%), respectively. With the 3m-interval DB method, 55 taxa were correctly identified (67%), while 49 taxa were detected extracting frames every 30s (60%) (Fig. 2.4A, Tab. 2.2).

The CWC province characterizing the sea bottom in the 400-430 m depth range of the Corsica Channel was explored by the MS17_I_135 survey (Fig. 3E-F). The reference analysis reported a total of 26 different taxa populating the mounds system characterizing the site. The 4s-interval method detected 25 taxa (96% of the total), methods using 10s and 30s intervals identified 21 taxa (81%) (Fig. 2.4; Tab. 2.2).

DB methods reported lower accuracies, with 0.5m-interval method recognizing 23 taxa (88 %), 22 taxa (85%) were detected with 1m-interval and 3m-interval identified 21 taxa (81%)

On average, TB methods missed 7.29% ± 4.17 of total taxa with 4s-interval, 15.97% ± 5.99 were not detected extracting frames every 10s, and the 30s-interval reported an average error of 25.73% ± 7.98. DB methods were less accurate, with the 0.5m-interval method showing an error of 11.22% ± 1.98, 1m-interval missed the 17.14% ± 3.79 of total taxa, and the 25.32% ± 4.26 of the taxa were not detected with the 3m-interval method (Fig. 4B).

No significant differences among sampling intervals and between TB and DB methods in the detection of taxa composition were detected by the Kruskal-Wallis test.

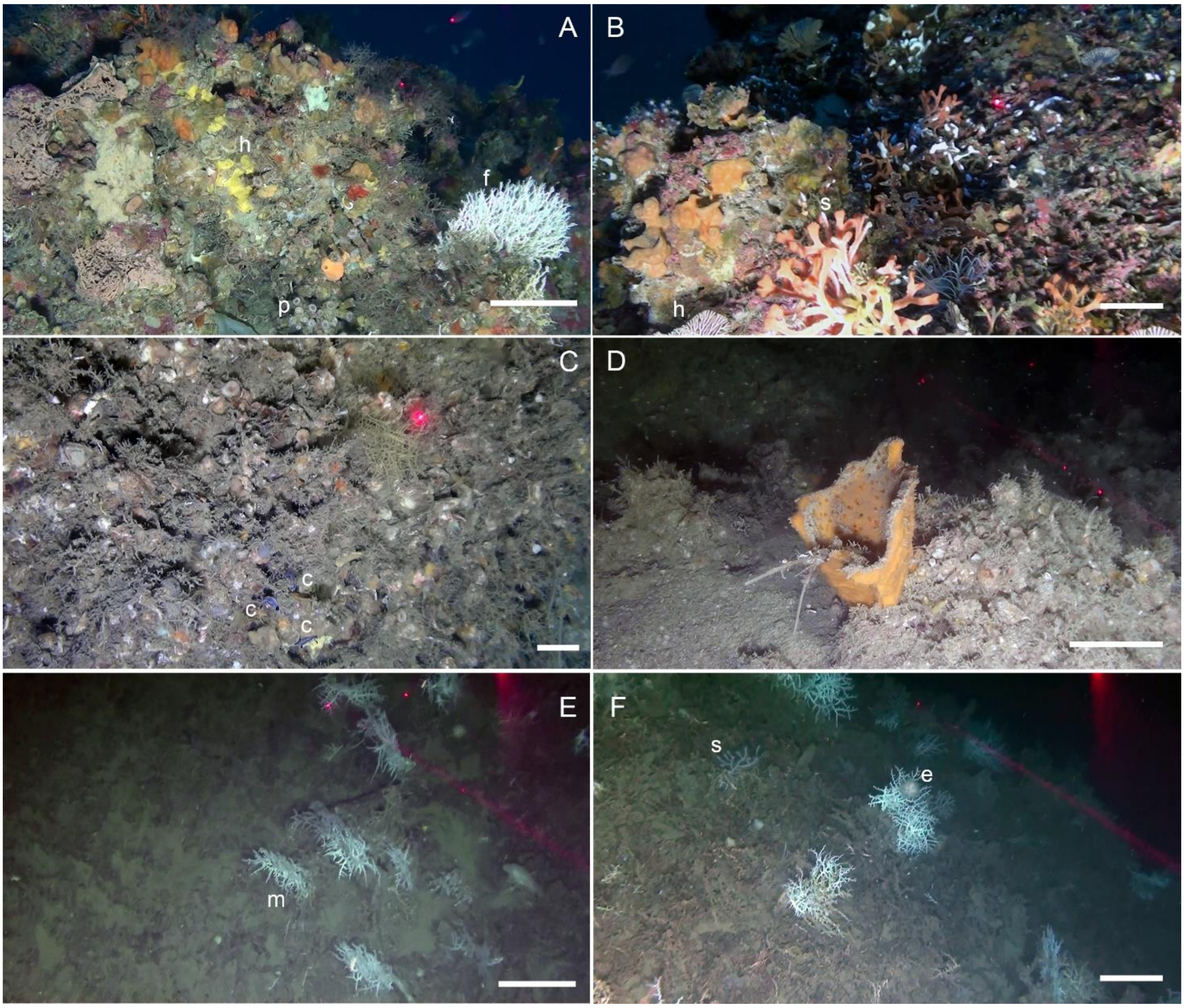

Fig. 2.3. Examples of the different habitats surveyed (from Castellan et al., 2020). A-B) Coralligenous formation at the Amendolara Seamount showing intense faunal cover dominated by several sponges among which *Hexadella detritifera* (h) is easily recognizable, scleractinian corals such as *Phyllangia americana* (p) and *Filograna-Salmacina* complex (f) were also common findings; bar=20 cm. Close-up (B) of Coralligenous formation dominated by the bryozoans *Smittina cervicornis* (s) and *Hornera frondiculata* (h); bar=5 cm. C-D) Deep-water reef dominated by *Neopycnodonte cochlear* at Santa Maria di Leuca. Note the tiny nudibranch *Hypselodoris tricolor* (c) grazing on *Neopycnodonte* shells; bar=3 cm. The large undetermined orange sponge represented the main mega-epifauna at this site; bar=10 cm. E-F) Cold water coral mound at Corsica Channel site showing the colonial scleractinian *Madrepora oculata* (m) characterizing this site; bar=20 cm. F) The octocoral *Swiftia pallida* (s) was present at this site; note the echinoid *Echinus melo* (e) grazing on *M. oculata*; bar=20 cm.

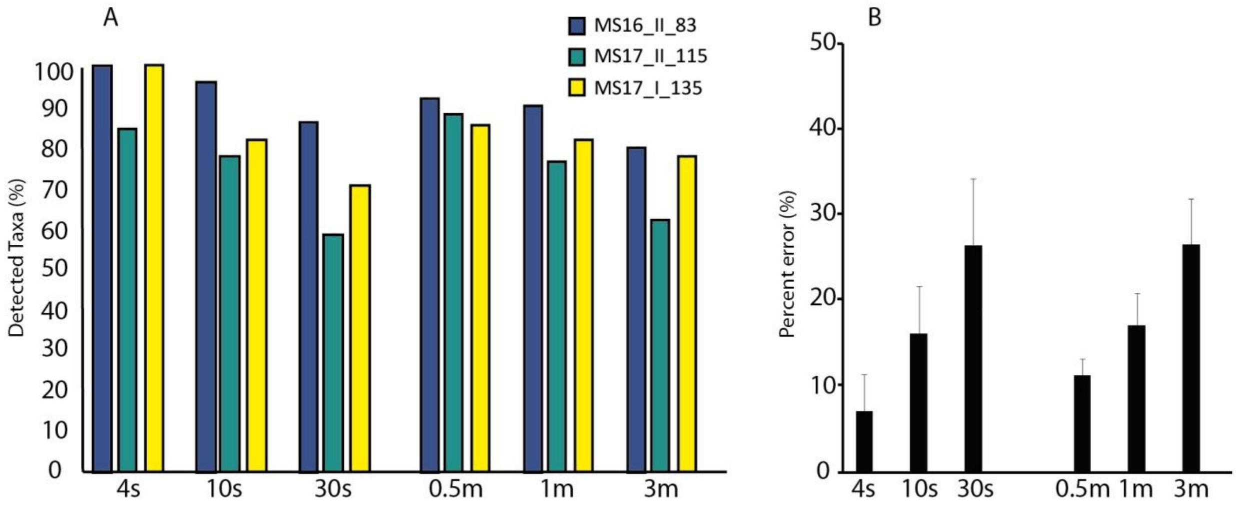

Fig. 2.4. A) Bar plot reporting the percentage of taxa identified with the tested techniques (modified from Castellan et al., 2020). B) Average percentage error in detecting taxa composition of surveyed biological communities. Error bars represent Standard Errors.

2.3.3 The influence of survey velocity

The analysis of the distribution of frames along the ROV paths documented a difference between TB and DB methods (Fig. 2.5). The formers showed peaks of frame densities alternated to segments of the ROV track with rare photograms. Contrarily, DB methods reported a homogeneous distribution of extracted frames along ROV routes at any sampling intervals. Subsampling techniques based on time-interval resulted more affected by the variation of survey velocity, showing an over-sampling in correspondence of survey slowdown and under-sampling when the velocity increased (Fig. 2.6).

The comparison of the accuracy of the methods in the estimation of substrates extents with the coefficient of variation (CV) of velocity (used as a proxy of survey slowdowns) showed that survey velocity was correlated with the average percentage error at any subsampling interval (Fig. 2.7A). In the surveys MS16_II_83, that reported the highest variation in survey velocity along the track, and in MS17_II_115, which was perfomed at the highest survey speed, registered the larger errors in estimating the substrates cover (Fig. 2.7, Tab. 2.3). On the contrary, in survey MS17_I_135 the velocity was constant along the track (low CV) and higher accuracies were documented, which decreased when using wider sampling intervals (Fig. 2.7, Tab. 2.3). In MS16_II_83 and MS17_II_115 surveys, however, the error in substrates extension detection shows a counter-intuitive trend, reporting a decrease of error with wider sampling intervals (Fig. 2.7, Tab. 2.3). The analysis of the CV of the distances among frames, representing the variability of the distance between adjacent photograms, provides a potential explanation, showing a decrease with higher time intervals (Fig. 2.7B). In TB methods, the increase of sampling interval reduced the variation in the distance among the extracted frames, leading to more homogenous distribution of photograms along the track. The use of wider sampling intervals in stations MS16_II_83 and MS17_II_115 may potentially have concurred in reducing the negative influence of the survey speed on the substrates covers estimation.

The survey velocity also influenced the accuracy of TB methods in the taxonomical identification of species composing benthic assemblages. Previous studies suggested that the influence of survey speed variation on the analysis of visual surveys might depend on the morphology of the habitat investigated (e.g., Robert et al., 2020) and the analysis of performances of the methods here tested supports this evidence. Despite surveys MS17_II_115 and MS16_I_83 explored morphologically similar habitats with a patchily spatial distribution (i.e., a deep-water oyster reef and coralligenous formations, respectively), the method performances in defining the taxonomical composition of the assemblages were strongly different, with MS16_I_83 survey reporting the highest accuracies while MS17_II_115 the lowest (Fig. 2.4, Tab. 2.3). MS17_II_115 was performed at a higher (Tab. 2.1) and constant speed (lowest CV value), while MS16_I_83 was collected at a lower speed and with the highest amount of slowdown along the tracks (Fig. 2.5), suggesting that low velocities and higher slowdowns might have increased the accuracy of TB methods in patchily distributed habitats.

In contrast, survey MS17_I_135, that explored a CWC habitat with an almost continuous coverage, showed high accuracies at any TB intervals despite being collected at high velocity (Tab. 2.1) and presenting a lower number of slowdowns along the ROV track (Fig. 2.5).

The analysis of survey velocity also influenced the taxonomical identification accuracy of specimens by affecting the number of overlapped photograms. A larger amount of the latter was, indeed, documented in the slower surveys (Fig. 2.8B-C) that reported the higher community composition detection accuracies (Pearson’s r = 0.86). Percent overlap decreased with wider sampling intervals in both TB and DB methods together with the accuracy of assemblage composition detection. Although having fixed spatial intervals between frames along the track, DB selections showed similar or even higher degrees of overlap when compared to TB methods (Tab. 2.2). This was likely related to the non-linear paths of surveys. In some segments of the surveys, the ROV moved for a few meters, turning around features of interest to collect more detailed images. Therefore, even frames extracted with an interval of 3 m displayed the same portion of the seafloor, producing the higher number of overlapped frames observed. This may potentially have concurred to obtain only slightly lower values of accuracies in community composition detection shown by DB methods when compared to TB methods.

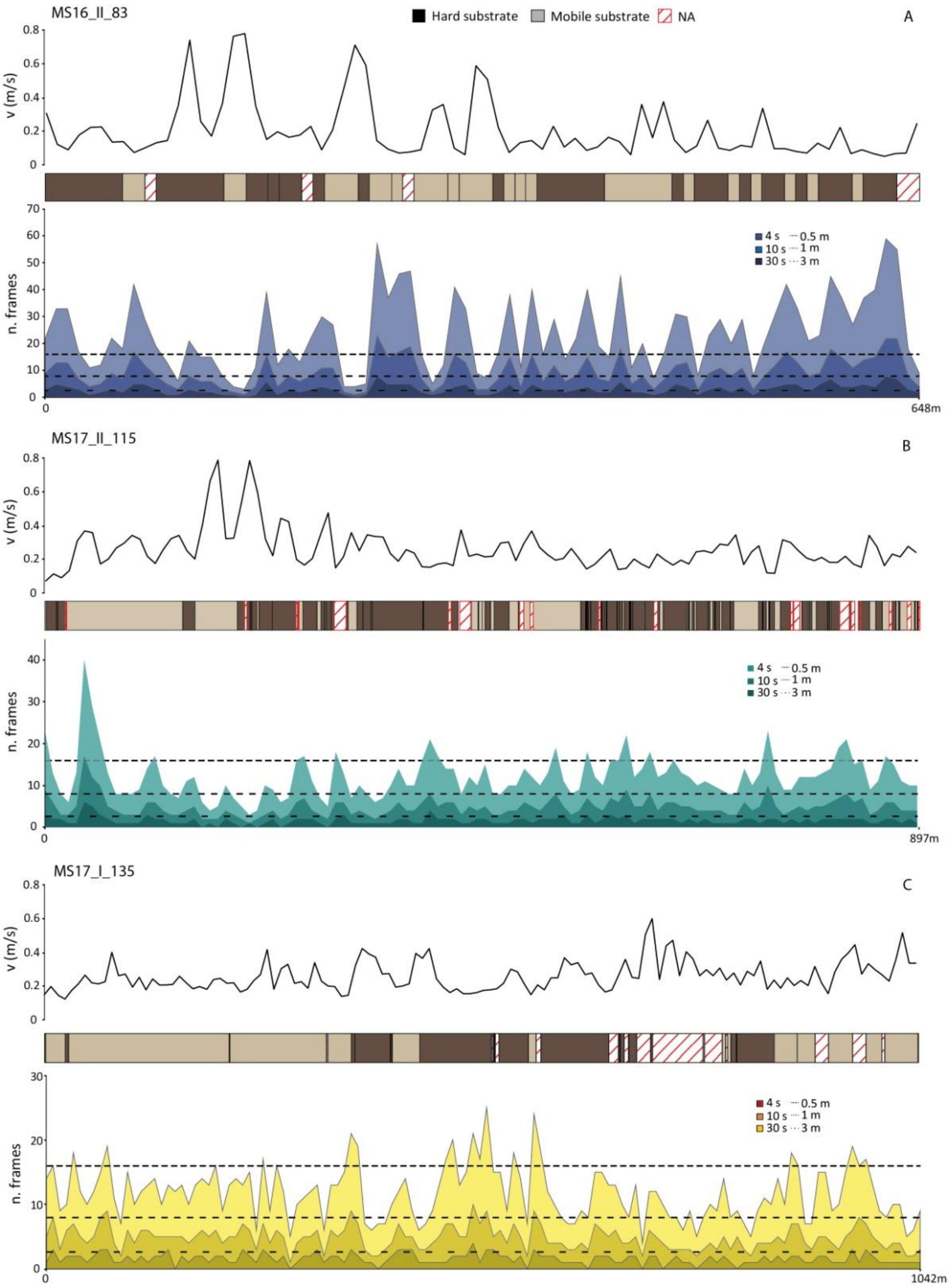

Fig. 2.5. Variation of survey velocity and spatial distribution of frames extracted with the tested techniques along the ROV track. A) Coralligenous formations, B) deep-water oyster reefs, C) CWC mounds. Colored bar represents the different substrate classes characterizing the survey track. Hard substrate: dark-brown bars; mobile substrate: light-brown bars; NA: white bars with red lines. Color distributions refer to frame densities obtained with the TB methods, while dashed lines represent frame distributions from the DB methods. Modified from Castellan et al., 2020.

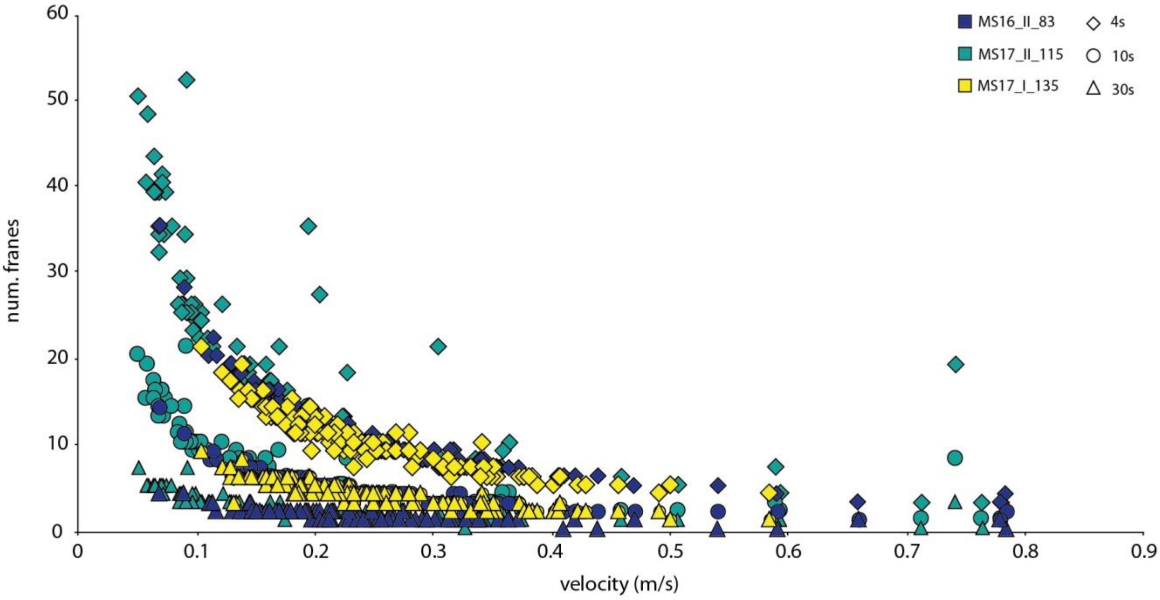

Fig. 2.6. Scatter plot showing the relationship between survey velocity and number of frames extracted with each method (modified from Castellan et al., 2020).

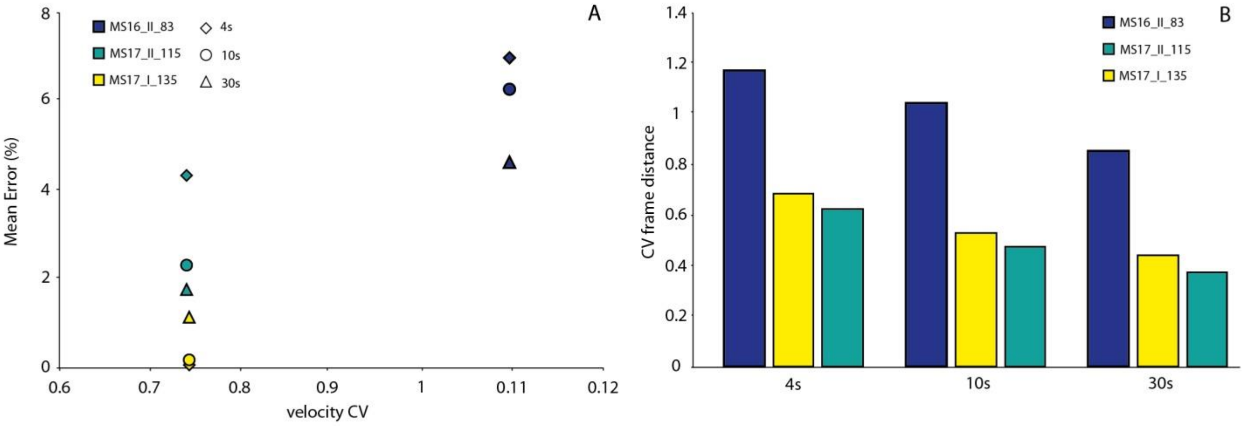

Fig. 2.7. A) Scatter plot displaying the significant positive correlation between the mean percentage error in estimating the substrate covers reported in TB methods and the coefficient of variation of survey speed. B) Bar plot showing the decrease of the CV of distance between adjacent frames with wider sampling TB intervals. Figure modified from Castellan et al., 2020.

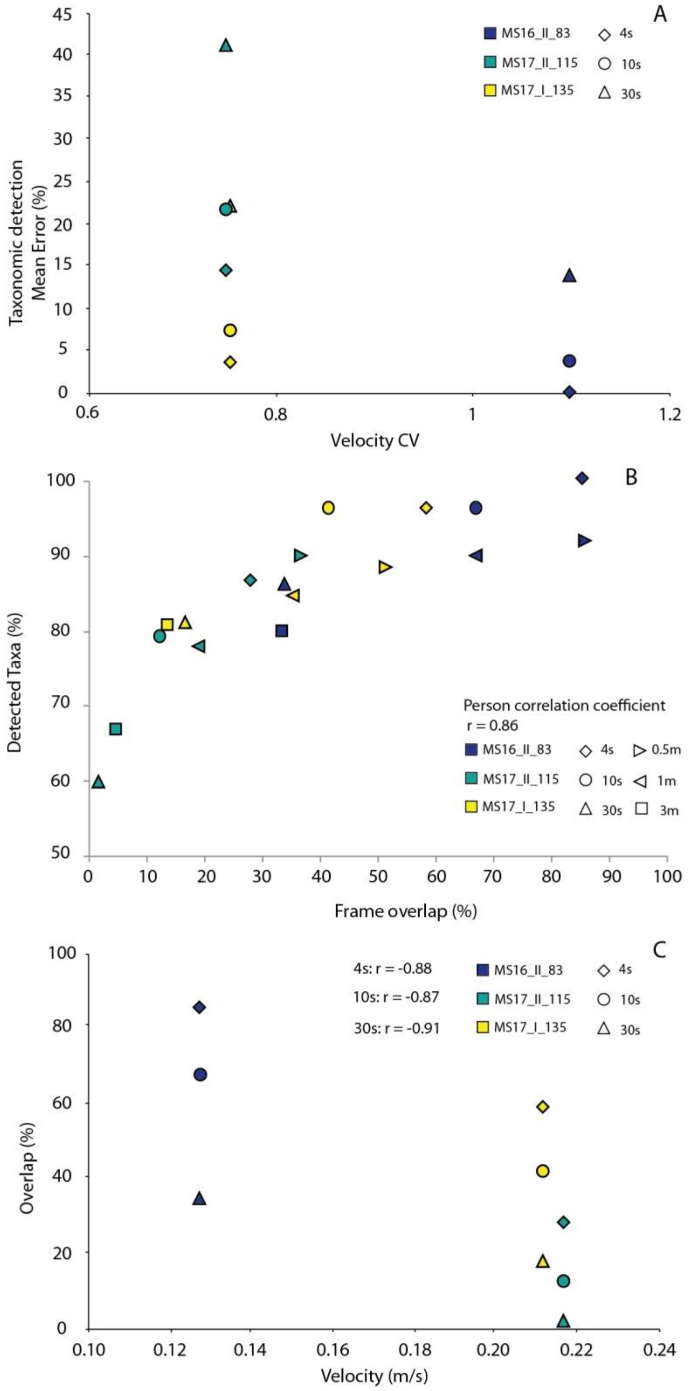

Fig. 2.8. A) scatter plot of the mean percentage error in detecting the taxonomical composition resulting from the TB methods vs. the coefficient of variation of survey velocity. B) scatter plot showing the significant positive correlation between the percent of overlapped frames and percent of taxa detected with each method. C) plot displaying the significant negative relationship between survey velocity and percent of overlapped frames extracted with TB methods. Figure modified from Castellan et al., 2020.

2.4 Discussion

As the human footprint extends deeper into our oceans, information on the seafloor and associated biological communities has become increasingly important to devise appropriate protection actions and achieve national and international conservation goals (e.g., Lundquist and Granek 2005; Davies et al. 2007; Micheli et al. 2013; Zampoukas et al., 2014; Henry and Roberts 2017; Danovaro et al., 2020; Manea et al. 2020). The management of natural resources and the mitigation of anthropic pressure on marine ecosystems (e.g., biodiversity loss, alteration of food webs, and marine pollution) relies on the efficient transfer of scientific knowledge to decision-makers which starts with spatial information (Cvitanovic et al. 2015).

The choice of the processing approach to convert visual surveys into spatial mapping passes through video subsampling techniques that influence the analytic effort and, contemporarily, the quality of results. Selecting a set of sub-tracks generated by splitting the dive track in intervals of equal length and then extracting a number of random frames from this selection is widely used in ecological studies. Such an approach reduces the number of frames analyzed (a set of frames extracted from a set of substrasect) and, thus, the analytical effort and provides repeated measures of taxonomical composition and substrate extent characterizing the explored portion of seafloor. If obtaining repeated measures provide the statistical base for comparing different samples, sites or areas, it arguably results in estimations that might be significantly different from those obtained analyzing the entire survey. For such a reason, selecting random frames from survey sub-tracks might not represent the best method to provide an exhaustive characterization of the investigated habitats.

Among the most used methods to entirely analyze surveys on benthic ecosystems is extracting frames at regular intervals. Nevertheless, the selection of the most appropriate frame extraction technique is strongly linked to data collection modalities. Maintenance of a regular velocity during visual surveys is crucial to guarantee a homogenous recording of the seafloor and of biological targets (Huvenne et al. 2018). Survey navigation velocity, however, may largely vary along the track in relation to technical issues (i.e., navigation against currents) and the need for higher detailed recordings. When using video subsampling techniques based on time intervals, the variation in survey velocity may influence frames distribution along the tracks, over-sampling in correspondence of slowdowns, and under-sampling when the vehicle velocity increases (Fig. 2.5). The alternation of slowdowns and speedups may potentially influence the precise mapping of the spatial limits of the different substratum categories. The variation of survey velocity was, in fact, positively correlated with the error percentages in the estimation of substrates cover resulting in a lower precision of TB methods. In situations with large survey velocity fluctuations, using wider sampling intervals may potentially reduce the negative influence of survey speed variations on the estimation of habitat coverings with TB methods.

In contrast, DB techniques were less affected by survey navigation speed leading to higher accuracy in the estimation of substrate classe extent. The maximum percentage error of 0.3% for DB methods (Tab. 2) ensures a higher confidence, promoting these techniques as the most appropriate for estimating the extent of substrate classes.

However, habitat coverage is just one of the applications of visual survey methods. The analysis of the taxonomical compositions of biological assemblgaes is a primary aspect for the study of biodiversity and ecological functions (e.g., Di Camillo et al. 2013; Chaniotis et al., 2020). TB methods resulted more precise in detecting the taxonomical composition of the explored assemblages compared to DB techniques. The influence of irregular survey velocity on TB methods could have positive unintended advantages: a larger number of frames displaying the same portion of seafloor could facilitate the identification of specimens occurring in highly dense assemblages or less visible (such as infauna inhabiting soft substrate). During visual surveys, specimens may not be clearly identifiable with few frames. Extracting more frames displaying the same specimens could increase the probability of having clearer images, facilitating the taxonomical identification. Consequently, TB methods might be more appropriate for the description of assemblages taxonomical composition, especially by using 4s or 10s intervals, which showed lower errors.

The technique for the analysis of benthic visual recordings collected with unmanned vehicles is related to the aims and the characteristics of the survey. Distance-based frame extraction methods provided a much higher efficiency in the estimation of the spatial extent of the different substrate classes, being less affected by vehicle speed variations during the sampling. On the contrary, the higher density of frame in correspondence of features of interest and a larger overlapping degree obtained when extracting frames with time intervals ensure a more accurate detection of the composition of biological assemblages. The comparable number of frames extracted by both TB and DB low-, intermediate- and wide-intervals, coupled with the percent errors reported in this chapter, provide the context from which to choose the most efficient techniques for the purposes of analysis.

References

Aguzzi, J., Costa, C., Robert, K., Matabos, M., Antonucci, F., Juniper, S.K., Menesatti, P. Automated Image Analysis for the detection of benthic crustaceans and bacterial mat coverage using the VENUS Undersea Cabled Network. *Sensors*. 2011; 11:10534–10556. https://doi.org/10.3390/s111110534

Angeletti, L., Basso, D., Bavestrello, G., Bo, M., Bracchi, V., D’Ambrosio, P., D'Onghia, G., Fraschetti, S., Grande, V., Guarnieri, G., Maiorano, P., Savini, A., Rizzo, L., Taviani, M. (2017). SOTTOPROGRAMMA 2.2 Monitoraggio dell'estensione dell'habitat a coralligeno. Giugno 2017, pp. 1-64

Angeletti, L., Taviani, M. (2020). Offshore *Neopycnodonte* oyster reefs in the Mediterranean Sea. *Diversity*, 12(3), 92. https://doi.org/10.3390/d12030092

Angeletti, L., Canese, S., Cardone, F., Castellan, G., Foglini, F., Taviani, M. (2020a). A brachiopod biotope associated with rocky bottoms at the shelf break in the central Mediterranean Sea: geobiological traits and conservation aspects. *Aquatic Conservation: Marine and Freshwater Ecosystems*, 30:402-411. https://doi.org/10.1002/aqc.3255

Angeletti, L., Castellan, G., Montagna, P., Remia, A., Taviani, M. (2020b). The Corsica Channel Cold Water Coral Province (Mediterranean Sea). *Frontiers in Marine Science*, 7:661. https://10.3389/fmars.2020.00661

Angeletti, L., D'Onghia, G., Otero, M. D. M., Settanni, A., Spedicato, M. T., Taviani, M. (2021). A Perspective for Best Governance of the Bari Canyon Deep-Sea Ecosystems. *Water*, 13(12), 1646. https://doi.org/10.3390/w13121646

Ayma, A., Aguzzi, J., Canals, M., Lastras, G., Bahamon, N., Mecho, A., Company, JB. (2016). Comparison between ROV video and Agassiz trawl methods for sampling deep water fauna of submarine canyons in the Northwestern Mediterranean Sea with observations on behavioural reactions of target species. *Deep-Sea Research Part I: Oceanographic Research Papers*, 114:149–159. https://doi.org/10.1016/j.dsr.2016.05.013

Beccari, V., Basso, D., Spazzaferri, S., Rüggeberg, A., Neuman, A., Makovsky, Y. (2020). Preliminary video-spatial analysis of cold seep bivalve beds at the base of the continental slope of Israel (Palmahim Disturbance). *Deep-*

Sea Research Part II: Topical Studies in Oceanography, 171:104664. https://doi.org/10.1016/j.dsr2.2019.104664

Bo, M., Bava, S., Canese, S., Angiolillo, M., Cattaneo-Vietti, R., Bavestrello, G. (2014). Fishing impact on deep Mediterranean rocky habitats as revealed by ROV investigation. *Biological Conservation*, 171:167–176

Bongaerts, P., Ridgway, T., Sampayo, E.M., Hoegh-Guldberg, O. (2010). Assessing the 'deep reef refugia' hypothesis: focus on Caribbean reefs. *Coral Reefs*, 29(2), 309–327. https://doi.org/10.1007/s00338-009-0581-x

Buhl-Mortensen, L., Buhl-Mortensen, P., Dolan, M.F.J., Dannheim, J., Bellec, V., Holte, B. (2012). Habitat complexity and bottom fauna composition at different scales on the continental shelf and slope of northern Norway. *Hydrobiologia*, 685:191-219. https://doi.org/10.1007/s10750-011-0988-6

Cánovas-Molina, A., Montefalcone, M., Bavestrello, G., Cau, A., Bianchi, C.N., Morri, C., Canese S., Bo, M. (2016). A new ecological index for the status of mesophotic megabenthic assemblages in the Mediterranean based on ROV photography and video footage. *Continental Shelf Research*, 121, 13–20. https://doi.org/10.1016/j.csr.2016.01.008

Carleton, J.H., Done, T.J. (1995). Quantitative video sampling of coral reef benthos: large-scale application. *Coral Reef,* 14:35–46. https://doi.org/10.1007/BF00304070

Castellan, G., Angeletti, L., Taviani, M., Montagna, P. (2019). The yellow coral *Dendrophyllia cornigera* in a warming ocean. *Frontiers in Marine Science*, 6: 692. https://doi.org/10.3389/fmars.2019.00692.

Castellan, G., Angeletti, L., Correggiari, A., Foglini, F., Grande, V., Taviani, M. (2020). Visual methods for monitoring mesophotic-to-deep reefs and animal forests: finding a compromise between analytical effort and result quality. In: *Perspectives on the Marine Animal Forests of the World*, Springer, Cham, pp. 487-514

Cau, A., Follesa, M.C., Moccia, D., Alvito, A., Bo, M., Angiolillo, M., Canese, S., Paliaga, E.M., Orrù, P.E., Sacco, F., Cannas, R. (2015). Deepwater corals biodiversity along roche du large ecosystems with different habitat complexity along the south Sardinia continental margin (CW Mediterranean Sea). *Marine Biology*, 162:1865–1878. https://doi.org/10.1007/s00227-015-2718-5

Chaniotis, P.D., Robson, L.M., Lemasson, A.J., Cornthwaite, A.L., Howell, K.L. (2020). UK deep-sea conservation: progress, lessons learned, and actions for the future. *Aquatic Conservation: Marine and Freshwater Ecosystems*, 30:375-393. https://doi.org/10.1002/aqc.3243

Consoli, P., Esposito, V., Battaglia, P., Altobelli, C., Perzia, P., Romeo, T., Canese, S., Andaloro, F. (2016). Fish distribution and habitat complexity on banks of the Strait of Sicily (Central Mediterranean Sea) from Remotely-Operated Vehicle (ROV) explorations. *PLOS ONE*,11. https://doi.org/10.1371/journal.pone.0167809

Cordes, E.E., Carney, S.L., Hourdez, S., Carney, R.S., Brooks, J.M., Fisher, C.R. (2007). Cold seeps of the deep Gulf of Mexico: Community structure and biogeographic comparisons to Atlantic equatorial belt seep communities. *Deep-Sea Research Part I: Oceanographic Research Papers*, 54:637–653. https://doi.org/10.1016/j.dsr.2007.01.001

Cvitanovic, C., Hobday, A.J., van Kerkhoff, L., Wilson, S.K., Dobbs, K., Marshall, N.A. (2015). Improving knowledge exchange among scientists and decision-makers to facilitate the adaptive governance of marine resources: A review of knowledge and research needs. *Ocean, Coastal Management*, 112, 25–35. https://doi.org/10.1016/j.ocecoaman.2015.05.002

Danovaro, R., Canals, M., Tangherlini, M., Dell'Anno, A., Gambi, C., Lastras, G., Amblas, D., Sanchez-Vidal, A., Frigola, J., Calafat, A.M., Pedrosa-Pàmies, R., Rivera, J., Rayo, X., Corinaldesi, C. (2017). A submarine volcanic eruption leads to a novel microbial habitat. *Nature Ecology & Evolution*, 1:1–9. https://doi.org/10.1038/s41559-017-0144

Danovaro, R., Fanelli, E., Canals, M., Ciuffardi, T., Fabri, M-C., Taviani, M., Argyrou, M., Azzurro, E., Bianchelli, S., Cantafaro, A., Carugati, L., Corinaldesi, C., de Haan, P., Dell'Anno, A., Evans, J., Foglini, F., Galil, B., Gianni, M., Goren, M., Greco, S., Grimalt, J., Güell-Bujons, Q., Jadaud, A., Knittweis, L., Lopez, J.L., Sanchez-Vidal, A., Schembri, P.J., Snelgrove, P., Vaz, S., the IDEM Consortium. (2020). Towards a marine strategy for the deep Mediterranean Sea: Analysis of current ecological status. *Marine Policy,* 112:103781. https://doi.org/10.1016/j.marpol.2019.103781

Davies, A.J., Roberts, J.M., Hall-Spencer, J. (2007). Preserving deep-sea natural heritage: emerging issues in offshore conservation and management. *Biological Conservation*, 138:299–312. https://doi.org/10.1016/j.biocon.2007.05.011

Di Camillo, C.G., Boero, F., Gravili, C., Previati, M., Torsani, F., Cerrano, C. (2013). Distribution, ecology and morphology of *Lytocarpia myriophyllum* (Cnidaria: Hydrozoa), a Mediterranean Sea habitat former to protect. *Biodiversity and Conservation*, 22:773–787. https://doi.org/10.1007/s10531-013-0449-9

Eleftheriou, A., McIntyre, A. (Eds.) (2005). Methods for the study of marine benthos, Third Edition. Wiley-Blackwell Publishing: Oxford.

Enrichetti, F., Dominguez-Carrió, C., Toma, M., Bavestrello, G., Betti, F., Canese, S., Bo, M. (2019b). Megabenthic communities of the Ligurian deep continental shelf and shelf break (NW Mediterranean Sea). *PLOS ONE*, 14(10), e0223949. https://doi.org/10.1371/journal.pone.0223949

Fabri, M-C., Pedel, L., Beuck, L., Galgani, F., Hebbeln, D., Freiwald, A. (2014). Megafauna of vulnerable marine ecosystems in French mediterranean submarine canyons: spatial distribution and anthropogenic impacts. *Deep-Sea Research Part II: Topical Studies in Oceanography*, 104:184–207. https://doi.org/10.1016/j.dsr2.2013.06.016

Fabri, M-C., Vinha, B., Allais, A-G., Bouhier, M-E., Dugornay, O., Gaillot, A., Arnaubec, A. (2019). Evaluating the ecological status of cold-water coral habitats using non-invasive methods: An example from Cassidaigne canyon, northwestern Mediterranean Sea. *Progress in Oceanography*, 178:102172. https://doi.org/10.1016/j.pocean.2019.102172

Foglini, F., Grande, V., Marchese, F., Bracchi, V.A., Prampolini, M., Angeletti, L., Castellan, G., Chimienti, G., Hansen, I.M., Gudmundsen, M., Meroni, A.N., Mercorella, A., Vertino, A., Badalamenti, F., Corselli, C., Erdal, I., Martorelli, E., Savini, A., Taviani, M. (2019). Application of Hyperspectral Imaging to Underwater Habitat Mapping, Southern Adriatic Sea. *Sensors*, 19:2261. https://doi.org/10.3390/s19102261

Fosså, J.H., Mortensen, P.B., Furevik, D.M. (2002). The deep-water coral *Lophelia pertusa* in Norwegian waters: distribution and fishery impacts. *Hydrobiologia*, 471:1–12. https://doi.org/10.1023/A:1016504430684

Foster, M.S., Harrold, C., Hardin, D.D. (1991). Point vs. photo quadrat estimates of the cover of sessile marine organisms. *Journal of Experimental Marine Biology and Ecology*, 146:193–203. https://doi.org/10.1016/0022-0981(91)90025-R

Fox, J., Friendly, G.G., Graves, S., Heiberger, R., Monette, G., Nilsson, H., Ripley, B., Weisberg, S., Fox, M.J., Suggests, M. (2007). The car package. R package.

Freiwald, A., Beuck, L., Rüggeberg, A., Taviani, M., Hebbeln, D. and R/V Meteor M70-1 Participants. (2009). The white coral community in the Central Mediterranean Sea revealed by ROV surveys. *Oceanography*, 22:58–57

Garrabou, J., Ballesteros, E., Zabala, M. (2002). Structure and dynamics of North-western Mediterranean rocky benthic communities along a depth gradient. *Estuarine, Coastal and Shelf Science*, 55:493–508. https://doi.org/10.1006/ecss.2001.0920

Grasmueck, M., Eberli, G.P., Viggiano, D.A., Correa, T., Rathwell, G., Luo, J. (2006). Autonomous underwater vehicle (AUV) mapping reveals coral mound distribution, morphology, and oceanography in deep water of the Straits of Florida. *Geophysical Research Letters*, 33:L23616. https://doi:10.1029/2006GL027734

Guinda, X., Gracia, A., Puente, A., Juanes, J.A., Rzhanov, Y., Mayer, L. (2014). Application of landscape mosaics for the assessment of subtidal macroalgae communities using the CFR index. *Deep-Sea Research Part II: Topical Studies in Oceanography*, 106:207–215. https://doi.org/10.1016/j.dsr2.2013.09.037

Henry, L-A., Roberts, J.M. (2017). Global biodiversity in Cold-Water Coral reef ecosystems. In: *Marine Animal Forests: The Ecology of Benthic Biodiversity Hotspots*. Rossi S, Bramanti L, Gori A, Orejas C (Eds) Cham: Springer, p. 235–256

Huvenne, V.A.I., Tyler, P.A., Masson, D.G., Fisher, E.H., Hauton, C., Hühnerbach, V., Le Bas, T.P., Wolff, G.A. (2011). A picture on the wall: innovative mapping reveals cold-water coral refuge in submarine canyon. *PLOS ONE*, 6:e28755. https://doi.org/10.1371/journal.pone.0028755

Huvenne, V.A.I., Robert, K., Marsh, L., Lo Iacono, C., Le Bas, T., Wynn, R.B. (2019). ROVs and AUVs. In: *Submarine geomorphology*. Micallef A, Krastel S, Savini A (Eds). Cham: Springer, p. 93–108

IUCN. Thematic Report – Conservation overview of Mediterranean deep-sea biodiversity: A strategic assessment. 122 pages. Gland, Switzerland and Malaga: IUCN. 2019.

Leonard, G., Clark, R. (1993). Point quadrat versus video transect estimates of the cover of benthic red algae. *Marine Ecology Progress Series*, 101:203–208. https://doi.org/10.3354/meps101203

Lundquist, C.J., Granek, E.F. (2005). Strategies for successful marine conservation: integrating socioeconomic, political, and scientific factors. *Conservation Biology*, 19:1771–1778. https://doi.org/10.1111/j.1523-1739.2005.00279.x

Lundsten, L., Schlining, K.L., Frasier, K., Johnson, S.B., Kuhnz, L.A., Harvey, J.B.J., Clague, G., Vrijenhoek, R.C. (2010). Time-series analysis of six whale-fall communities in Monterey Canyon, California, USA. *Deep-Sea Research Part I: Oceanographic Research Papers*, 57:1573–1584. https://doi.org/10.1016/j.dsr.2010.09.003

Manea, E., Bianchelli, S., Fanelli, E., Danovaro, R., Gissi, E. (2020). Towards an Ecosystem-Based Marine Spatial Planning in the deep Mediterranean Sea. *Science of the Total Environment*, 715:136884. https://doi.org/10.1016/j.scitotenv.2020.136884

Meese, R.J., Tomich, P.A. (1992) Dots on the rocks: a comparison of percent cover estimation methods. *Journal of Experimental Marine Biology and Ecology*, 165:59–73. https://doi.org/10.1016/0022-0981(92)90289-M

Micheli, F., Levin, N., Giakoumi, S., Katsanevakis, S., Abdulla, A., Coll, M., Fraschetti, S., Kark, S., Koutsoubas, D., Mackelworth, P., Maiorano, L., Possingham, H.P. (2013) Setting Priorities for Regional Conservation Planning in the Mediterranean Sea. *PLOS ONE*, 8:e59038. https://doi.org/10.1371/journal.pone.0059038

Norcross, B.L., Mueter, F-J. (1999). The use of an ROV in the study of juvenile flatfish. *Fisheries Research*, 39:241–251. https://doi.org/10.1016/S0165-7836(98)00200-8

Pech, D., Condal, A.R., Bourget, E., Ardisson, P-L. (2004). Abundance estimation of rocky shore invertebrates at small spatial scale by high-resolution digital photography and digital image analysis. *Journal of Experimental Marine Biology and Ecology*, 299:185–199. https://doi.org/10.1016/j.jembe.2003.08.017

R Core Team. (2020). *R: A Language and Environment for Statistical Computing*. R Foundation for Statistical Computing, Vienna: Austria.

Rengstorf, A.M., Mohn, C., Brown, C., Wisz, M.S., Grehan, A.J. (2014). Predicting the distribution of deep-sea vulnerable marine ecosystems using high-resolution data: considerations and novel approaches. *Deep-Sea Research Part I: Oceanographic Research Papers*, 93:72–82. https://doi.org/10.1016/j.dsr.2014.07.007

Robert, K., Jones, D.O.B., Georgiopoulou, A., Huvenne, V.A.I. (2020). Cold-water coral assemblages on vertical walls from the Northeast Atlantic. *Diversity and Distribution*, 26:284–298. https://doi.org/10.1111/ddi.13011

Rowden AA, Anderson OF, Georgian SE, Bowden DA, Clark MR, Pallentin A, Miller A. High-Resolution Habitat Suitability Models for the Conservation and Management of Vulnerable Marine Ecosystems on the Louisville Seamount Chain, South Pacific Ocean. Front Mar Sci. 2017; 4:335. https://doi.org/10.3389/fmars.2017.00335

Stokes, M.D., Deane, G.B. (2009). Automated processing of coral reef benthic images. *Limnology and Oceanography, Methods*, 7:157–168. https://doi.org/10.4319/lom.2009.7.157

Taviani, M., Angeletti, L., Canese, S., Cannas, R., Cardone, F., Cau, A., Cau, A.B., Follesa, M.C., Marchese, F., Montagna, P., Tessarolo, C. (2017). The “Sardinian cold-water coral province” in the context of the Mediterranean coral ecosystems. *Deep-Sea Research Part II: Topical Studies in Oceanography*,145, 61–78. https://doi.org/10.1016/j.dsr2.2015.12.008

Taviani, M., Angeletti, L., Cardone, F., Montagna, P., Danovaro, R. (2019). A unique and threatened deep water coral-bivalve biotope new to the Mediterranean Sea offshore the Naples megalopolis. *Scientific Reports*, 9:3411. https://doi.org/10.1038/s41598-019-39655-8

Teixidó, N., Albajes-Eizagirre, A., Bolbo, D., Hir, E.L., Demestre, M., Garrabou, J., Guigues, L., Gili, J-M., Piera, J., Prelot, T., Soria-Frisch, A. (2011). Hierarchical segmentation-based software for cover classification analyses of seabed images (Seascape). *Marine Ecology Progress Series*, 431:45–53. https://doi.org/10.3354/meps09127

Trotter J, Pattiaratchi C, Montagna P, Taviani M, Falter J, Threser R, Hosie A, Haig D, Foglini F, Hua Q, McCulloch M. First ROV exploration of the Perth Canyon: canyon setting, faunal observations, and anthropogenic impacts. *Frontiers in Marines Sciences*, 6:193. https://doi.org/10.3389/fmars.2019.00173

Vanreusel, A., Hilario, A., Ribeiro, P.A., Menot, L., Arbizu, P.M. (2016). Threatened by mining, polymetallic nodules are required to preserve abyssal epifauna. *Scientific Reports*, 6:1–6. https://doi.org/10.1038/srep26808

Wynn, R.B., Huvenne, V.A.I., Le Bas, T.P., Murton, B.J., Connelly, D.P., Bett, B.J., Ruhl, H.A., Morris, K.J., Peakall, J., Parsons, D.R., Summer, E.J., Darby, S.E., Dorrel, R.M., Hunt, J.E. (2014). Autonomous Underwater Vehicles (AUVs): their past, present and future contributions to the advancement of marine geoscience. *Marine Geology*, 352:451-468. https://doi.org/10.1016/j.margeo.2014.03.012

Zampoukas, N., Palialexis, A., Duffek, A., Graveland, J., Giorgi, G., Hagebro, C., Hanke, G., Korpinen, S., Tasker, M., Tornero, V., Abaza, V., Battaglia, P., Caparis, M., Dekeling, R., Frias Vega, M., Haarich, M., Katsanevakis, S., Klein, H., Krzyminski, W., Laamanen, M., Le Gac, J.C., Leppanen, J.M., Lips, U., Maes, T., Magaletti, E., Malcolm, S., Marques, J.M., Mihail, O., Moxon, R., O'Brien, C., Panagiotidis, P., Penna, M., Piroddi, C., Probst, W.N., Raicevich, S., Trabucco, B., Tunesi, L., van der Graaf, S., Weiss, A., Wernersson, A.S., Zevenboom, W. (2014). Technical guidance on monitoring for the Marine Strategy Framework Directive. 2014, European Commission EUR 26499 – Joint Research Centre – Institute for Environment and Sustainability, Luxembourg: Publications Office of the European Union pp. 1-166. http://dx.publications.europa.eu/10.2788/70344

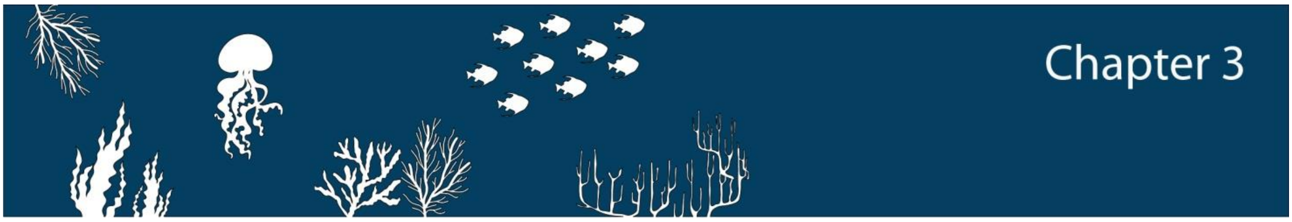

3. Mediterranean mesophotic benthic assemblages: the role of environmental filtering and geographic location on taxonomical and functional diversity

3.1 Introduction

A complex network of environmental and biotic factors shapes the presence and composition of biological assemblages and links biodiversity to the ecological functioning and services (Moritz et al., 2013). Even the “simplest” ecological services depend on complex linkages between biological components (Hughes & Stachowicz, 2004; Palumbi, McLeod & Grünbaum, 2008). Evidence of the relationship between the diversity of biological assemblage and ecosystems productivity, resistance, and resilience at different spatial scales increased over the last decades (Stachowicz et al., 2002; Hilborn et al., 2003; Allison, 2004; Hughes & Stachowicz, 2004; Reusch et al., 2005; Byrnes et al., 2006; Coleman et al., 2006; Sala & Knowlton, 2006; Worm et al., 2006; Palumbi, McLeod & Grünbaum, 2008). Single species play a central ecological role in some situations. Structure-forming species, such as corals, oysters, and seagrasses are especially important because their physical form increases the three-dimensional complexity of habitats, providing additional microhabitats (Sala & Knowlton, 2006). In other cases, important functions may depend on the cumulative action of different components whose presence is influenced by different mechanisms. In this sense, high-diversity assemblages are likely to include species with hidden roles than those with lower diversity levels (Sala & Knowlton, 2006).

The more taxa are present in a system, the more the chance that taxa belong to different functional entities, resulting in a positive relation between taxonomical and functional richness. Coupling species diversity with functional diversity better explains the structure of biological communities, being more representative of species identity and allowing to identify which functions are redundant within the community (e.g., Villéger et al., 2008; Villéger et al., 2010; Mouillot et al., 2013). When high diversity results in the presence of species with similar ecological roles, this redundancy can serve as a reservoir of biological options that help in ensuring that an ecosystem can respond to some level of perturbation without catastrophic loss of functions (Aarts, 1999).

Different processes concur and interact in generating and maintain both taxonomical and functional diversity, in influencing species distributions, and regulating assemblages structure across multiple spatial scales. Evolutionary history and dispersal processes influence the structure of communities at the regional scale (Moritz et al., 2013). The decrease in community similarity with geographic distance has proven to be common to different groups of organisms, with close-located communities presenting higher similarities in terms of species composition than those located further apart (Soininen et al., 2007). At the local scale, stochastic, environmental and ecological (e.g., competition, recruitment) processes are dominant in shaping assemblages composition (Ricklefs, 1987). In some situations, the geographical location may conceal the role of environmental filtering since sites located at short distances are more likely environmentally similar and, thus, suitable for similar biological components (e.g., Quattrini et al., 2017).

Among the major environmental drivers that influence the distribution and composition of mesophotic ecosystems, the light regime is a crucial factor (Kahng et al., 2010, 2019). The correlation between the water clarity and the maximum depth reached by obligate phototrophic organisms, such as algae and zooxanthellate corals, has been documented at different latitudes (Acevedo et al., 1989; Kahng et al., 2010; Muir et al., 2015). Also, the metanalysis in Lesser et al., (2020) reported a "community break" in mesophotic ecosystems occurring around 60 m depth at a global scale, suggesting a major role played by the gradient of light.

A further major factor influencing the composition of mesophotic communities is the thermal regime that can limit the maximum depth reachable for some taxa, favoring the colonization by other sessile components (Baker et al., 2016; Kahng et al., 2019). Although considered more stable compared to shallow counterparts due to the attenuation of climate change stressors, the mesophotic depths may experience rapid changes in water temperature. The so-called “heat waves” documented in many locations may lead to mass mortalities (Garrabou et al., 2009) and bleaching events (Smith et al., 2016).

However, information on how environmental variables influence the structure of mesophotic ecosystems mainly relate to tropical situations (Kahng et al., 2019; Tamir et al., 2019; Laverick et al., 2020) whilst the number of studies focusing on temperate mesophotic ecosystems is comparably scant (Turner et al., 2019).

In this chapter, Remotely Operated Vehicles (ROV) dives surveying 25 mesophotic assemblages along the Italian coast are analyzed to estimate their taxonomical composition and provide information about their biodiversity. Taxa are also classified according to different traits reflecting their biological aspects, like body size, vertical position, movement, feeding strategy, aggregation degree, and habitat-building ability, to explore the functional diversity related to the explored assemblages. Furthermore, this chapter explores whatever the taxonomic and functional composition of mesophotic assemblages is influenced by environmental variables and/or by geographical location. The correlation between taxonomic and functional diversity and environmental and geographical distance is used as an estimation of the role of the environmental setting or the location on the composition of the investigated assemblages. If the environmental setting was important, then assemblage compositions would change along environmental gradients, and it would be possible to assume that environmental factors are dominant drivers in structuring the compositions of assemblages in terms of taxa and functional entities. On the contrary, if the geographical location was dominant, then different assemblages would be found across increasing spatial distances, suggesting a main role of geographic location in shaping assemblages composition.

3.2 Materials and methods

3.2.1 Video survey collection and analyses

A total of 25 ROV surveys were collected during several oceanographic cruises performed in the framework of the Marine Strategy Framework Directive (MSFD 2008/56/CE) monitoring activities along the Italian coasts (Fig. 3.1, Tab. 3.1). Video footages were acquired using a Pollux III (Global Electric Italiana) equipped with a low-resolution CCD video camera and a high-resolution (2304 x 1296 pixels) video camera. The ROV was provided with an underwater acoustic tracking system (USBL, Linkquest, TrackLink 1500 MA) that recorded position every second. The ROV mounted also a high-definition video camera (SONY HDR-HD7, Tokyo, Japan). Three parallel laser beams (with 20 cm separation) provided a scale during recordings.

Dives trackpoints were smoothed utilizing Adelie GIS (©Ifremer) extension for ArcGIS (© ESRI) software. The Adelie Video tool “points to line” was used to produce a line-format track of ROV dives. Frames were extracted from video recordings every 10 s using Adelie Video (© Ifremer) and analyzed for taxonomical identification. When necessary, the images were coupled with low-definition video recording to improve taxonomic identification efficiency. Macrofauna (2 mm – 2 cm) and megafauna (>2 cm) were identified to the lowest possible taxonomic rank. Organisms unidentifiable at the genus or species level were categorized as morpho-species or morphological categories. The abundances of taxa along the ROV tracks were calculated and mapped by counting the number of taxa in each frame (Tab. S3.1). To characterize the taxonomic diversity of the benthic assemblages, differences among sites were investigated in terms of taxa richness, calculated as number of benthic taxa per ROV survey and considering any taxonomic levels (species, genus, or higher taxonomic rank). Since the length of the video footages and, thus, the number of extracted frames were different, species accumulation curves representing the expected number of taxa as a function of sampling effort (number of frames) were generated using function "specaccum" of package "vegan" (version 2.5, Oksanen et al., 2007, method "random", 1000 permutations). The value of expected taxonomic richness with 100 frames was used to compare the diversity associated with explored assemblages. Also, megabenthic diversity was estimated using the Shannon-Wiener diversity index (H) and Pielou's evenness index (J), representing a measure of the relative abundances of species within a community. Information on substrate type was also recorded.

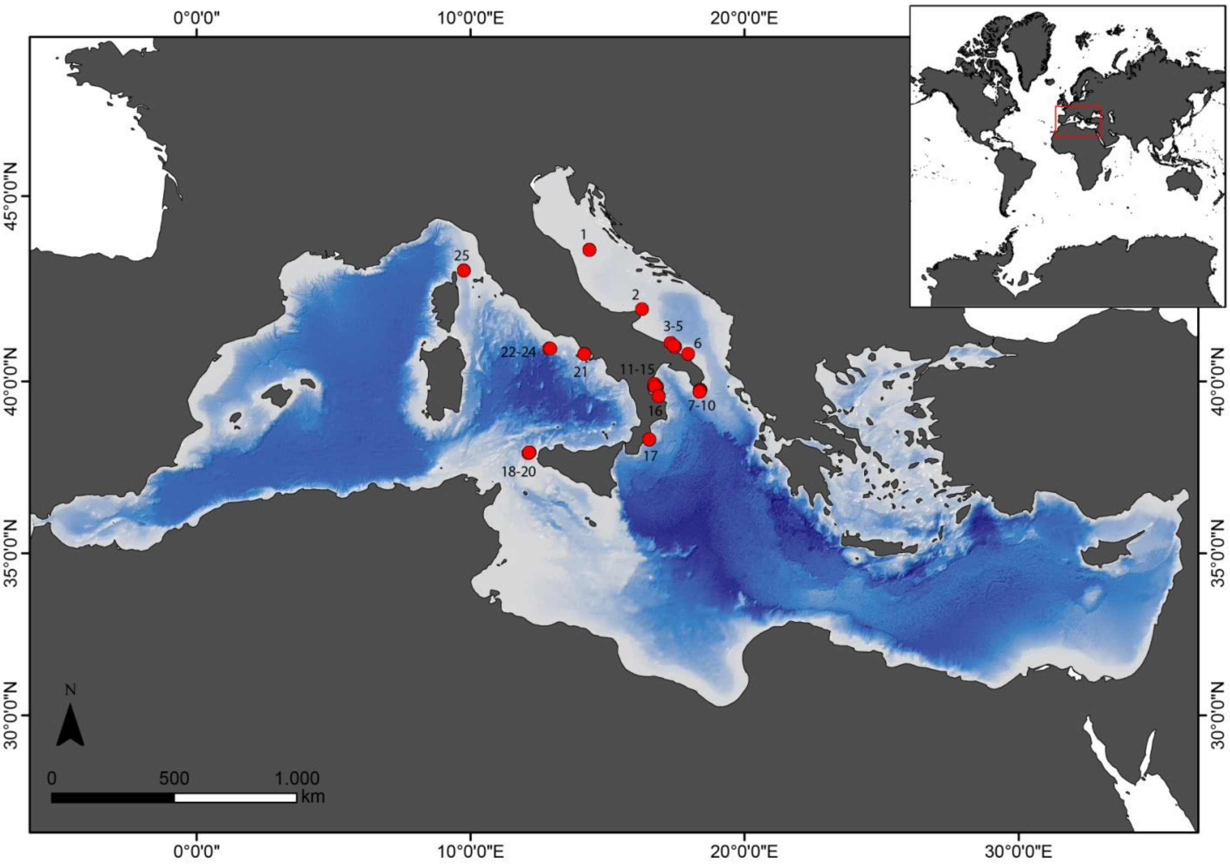

Fig. 3.1. Location of the 25 ROV dives performed at mesophotic depth along the Italian coasts.

ID	ROV	Location	Area	Date	Lat	Long	Lenght (m)	Depth range (m)	Assemblage	Extr. Frames
1	MS17_III_110	Bonaccia field	Adriatic Sea	13/08/2017	41° 59' 37.24"N	16° 15' 8.66"W	862.49	87-90	DWOR	440
2	MS15_47	Off Vieste	Adriatic Sea	10/11/2015	40° 57' 44.56"N	17° 27' 34.57"W	1127.32	50-60	DWOR	296
3	MS17_III_115	Off Monopoli	Adriatic Sea	15/08/2017	39° 45' 50.71"N	18° 23' 25.83"W	984.76	100-103	DWOR	449
4	MS15_79	Off Monopoli	Adriatic Sea	12/11/2015	39° 45' 16.39"N	18° 21' 59.03"W	994.92	72-80	MB	614
5	MS17_II_180	Off Monopoli	Adriatic Sea	05/08/2017	39° 35' 11.73"N	16° 52' 6.84"W	1564.42	92-110	MB	644
6	MS17_II_165	Off Brindisi	Adriatic Sea	04/08/2017	38° 20' 37.82"N	16° 31' 13.99"W	1359.06	102-105	MB	737
7	MS15_127	Off Santa Maria di Leuca	Ionian Sea	16/11/2015	40° 54' 41.63"N	12° 52' 59.28"W	1230.8	70-95	DWOR	727
8	MS15_118	Off Santa Maria di Leuca	Ionian Sea	15/11/2015	40° 54' 30.55"N	12° 52' 6.37"W	1129.15	90-98	DWOR	455
9	MS17_II_117	Off Santa Maria di Leuca	Ionian Sea	31/07/2017	37° 58' 31.29"N	12° 8' 24.23"W	1179.23	124-138	DWOR	599
10	MS17_II_115	Off Santa Maria di Leuca	Ionian Sea	31/07/2017	37° 56' 59.78"N	12° 7' 15.34"W	896.67	108-126	DWOR	507
11	MS17_II_83	Amendolara Seamount	Ionian Sea	28/07/2017	37° 58' 27.72"N	12° 8' 53.24"W	1424.7	91-97	MB	561
12	MS16_II_89	Amendolara Seamount	Ionian Sea	10/09/2016	40° 54' 46.31"N	12° 54' 29.29"W	1151.07	67-88	C	680
13	MS16_II_83	Amendolara Seamount	Ionian Sea	10/09/2016	39° 51' 32.46"N	16° 41' 59.61"W	647.65	67-83	C	653
14	MS17_II_93	Amendolara Seamount	Ionian Sea	29/07/2017	40° 45' 59.2"N	14° 9' 24.18"W	1370.36	132-168	CN	669
15	MS17_II_92	Amendolara Seamount	Ionian Sea	29/07/2017	43° 2' 19.91"N	9° 45' 1.81"W	859.29	170-190	CN	489
16	MS15_144	Off Crotone	Ionian Sea	18/11/2015	39° 55' 57.17"N	16° 42' 42.99"W	855.98	60-65	MB	905
17	MS15_184	Off Rocella Ionica	Ionian Sea	20/11/2015	39° 49' 48.75"N	16° 48' 7.5"W	986.38	68-79	C	570
18	MS16_186	Egadi Islands	Tyrrhenian Sea	01/08/2016	39° 50' 49.94"N	16° 47' 47.87"W	840.76	104-118	CN	705
19	MS16_197	Egadi Islands	Tyrrhenian Sea	02/08/2016	39° 44' 0.87"N	18° 22' 15.13"W	1086.01	70-75	RB	550
20	MS16_203	Egadi Islands	Tyrrhenian Sea	03/08/2016	39° 42' 19.07"N	18° 21' 19.25"W	1448.76	95-115	CN	877
21	MS17_I_103	Gulf of Naples	Tyrrhenian Sea	13/07/2017	40° 45' 47.31"N	17° 56' 32.11"W	1522.48	113-119	MB	842
22	MS16_21	Pontine Islands	Tyrrhenian Sea	18/07/2016	41° 0' 11.31"N	17° 24' 15.93"W	670.68	45-68	RB	520
23	MS16_128	Pontine Islands	Tyrrhenian Sea	27/07/2016	43° 35' 29.4"N	14° 20' 7.91"W	827.24	65-72	RB	678
24	MS16_142	Pontine Islands	Tyrrhenian Sea	27/07/2016	41° 4' 9.69"N	17° 18' 9.76"W	1240.14	55-80	RB	638
25	MS17_I_136	Off Capraia	Tyrrhenian Sea	17/07/2017	39° 50' 38.28"N	16° 43' 49.02"W	1376.04	98-105	MB	876

Tab. 3.1. Technical information of the 25 ROV videos performed on mesophotic assemblages. Table reports the assemblage category and number of frames extracted. C: coralligenous assemblages; MB: mobile-bottom assemblages; CN: cnidarians assemblages; DWOR: deep-water oyster-reef assemblages; Rrhodolith-bed assemblages.

3.2.2 Functional traits analyses

To explore the functional diversity of mesophotic assemblages, a biological traits analysis was performed on the benthic fauna associated to each site following the methods described by Mouillot et al., 2013. The chosen functional traits focused on key characteristics, such as foraging methods, modes of locomotion, and habitat construction (Tab. S3.2). All traits were categorical and coded as follows. Maximum body size (total length): meiofauna (<2 mm), macrofauna (2mm - 2 cm) and megafauna (>2 cm); domain of adult stage: benthic or pelagic; adult motility: sessile, facultatively motile, vagile, swimmer; feeding strategy (most frequent diet in adults): deposit feeder, grazer, filter feeder, suspension feeder, scavenger/predator, and photosynthetic metabolism; sociability (aggregation degree): solitary, gregarious, and colonial; ability to build habitat: habitat-builder, non habitat-builder.

Information on biological traits related to life-cycle characteristics (reproduction, larval development, and half-life) which drive connectivity between spatially distinct populations or assemblages was not available for every taxon identified. For such a reason, these traits were not considered for the functional analysis.

Traits' assignment was based on published accounts of the biology of each taxon, books, and websites of various scientific institutions (e.g., World Register of Marine Species (https://www.marinespecies.org), Encyclopaedia of Life (http://eol.org) databases).

Several indexes have been used to represent the functional diversity depending on the type of biological traits used to classify the biological community (Villéger et al., 2008 with reference therein). When using categorical traits, only functional richness and evenness can be calculated (Petchey & Gaston, 2002). The first is measured as the number of unique trait value combinations in a community while the latter describes the evenness of abundance distribution in functional trait space (i.e., it quantifies the regularity with which the functional space is filled by species) and decreases when different taxa belong to the same FE (Functional Entity, Villéger et al., 2008). The Functional

Richness (FRic) and Functional Evenness (FEve) for each assemblage explored were calculated by using the “FD” package (version 1.0, Laliberté et al., 2014) in R software.

3.2.3 Environmental variables

A set of physical and biochemical variables (Tab. 3.2) was used to explore environmental difference among locations hosting different mesophotic assemblages and to test the influence of environmental factors on their presence and composition. Data within a period of 20 years, from 1999 to 2018, were obtained from the European Coperincus open-access repository (marine.copernicus.eu) with a resolution of 4 km. The currents velocity was calculated as the sum of the square of eastward (uo) and westward (vo) components in R software (R Core Team, 2019). For every variable, the values at the location and depth of frames extracted from ROV videos was obtained using the function “extract” of the package “raster” (version 3.3-13) in R software, and the average value for each dive was calculated. The depth values were extracted from the bathymetry provided by EMODnet repository (https://www.emodnet-bathymetry.eu) at a horizontal resolution of 115m, while information on light regime is source from estimation presented in Chapter 1.

Variable	Units	Native Resolution	Reference
Depth	meters	115 m	EMODnet
Light at seabed	mmol. phot. m^{-2} day^{-1}	-	Derived (Chapter 1)
Concentration Chl-a	mg m^{-3}	4km	Marine Copernicus
Currents velocity	m/s	-	-
Concentration of nitrates NO_{3-}	mmol m^{-3}	-	-
Concentration of nitrates PO_3^{4-}	mmol m^{-3}	-	-
Dissolved O_2	mmol $m^{-3}day^{-1}$	-	-
Salinity	psu	-	-
Temperature	°C	-	-

Tab. 3.2. Environmental variables considered for statistical analysis with resolution and source.

3.2.4 Statistical analyses

3.2.4.1 Diversity of assemblages

The taxonomic (richness, H and J) and functional (FRic, FEve) diversity indexes were tested for difference amongst different explored assemblages using one-way analysis of variance (ANOVA, fixed, orthogonal, 5 levels) and *post-hoc* Tukey's honest significance test in R software (R Core Team, 2019). The ANOVA assumptions for normal distribution and homogeneity of variance were checked using the Shapiro-Wilk test (package "stats", version 4.2.0) and Levene's test (package "car", version 3.0, Fox et al., 2012), respectively. When the assumptions were not fulfilled, Kruskal–Wallis test and non-parametric pairwise comparisons Dunn's test were used. The potential correlation between taxonomic composition and depth was tested using Pearson's correlation (function "corr", package "stats", version 4.0), detecting no significance.

To test weather the investigated mesophotic assemblages were significantly different in the taxonomic and functional composition the ANOSIM (analysis of similarities) was performed in R software (n=5 assemblages, package: vegan, version 2.5-7, Oksanen et al., 2007) considering the entire dataset. In addition, the ANOSIM test was performed on dives divided in two groups, 30-100 m and 100-200 m, to exclude a potential effect of the depth in the observed differences.

Further insight into similarities among assemblages was provided by the cluster analysis based on clustering algorithm Ward's minimum variance method (package "stats", version 2.15.3) on Bray-Curtis dissimilarity measures over square root transformed density data. Data were square root transformed to decrease the contribution of dominant species (Mirto et al., 2014). The number of groups was determined using the silhouette function included in the "cluster" package (Maechler et al., 2013) representing a measure of the similarity of objects within a cluster (cohesion) rather than among clusters (separation).

3.2.4.2 Environmental characterization

After checking for normal distribution and homogeneity of variance, the differences in each environmental variable extracted in correspondence of the assemblage typologies were tested using one-way ANOVA (fixed, orthogonal, 5 levels) and *post-hoc* Tukey's honest significance test or Kruskal–Wallis test and non-parametric pairwise comparisons Dunn’s test, according to the methodology described above. The correlation among environmental variables was explored using function “corr” in package “stats” (version 4.0). Variables with Pearson’s r greater or lower than ±0.75 were excluded from further analysis.

Two Mantel test were used to test whether there was a significant correlation of taxonomic and functional dissimilarity with environmental distance given geographical distance and with geographical distance given environmental distance (999 permutations, 500 bootstraps; package “ecodist”, version 2.0.7, Goslee et al., 2020). Since Mantel test have been demonstrated to be prone to Type I error when space is investigated along with other variables (Guillot & Rousset, 2013), partial distance correlations were also performed using package “energy” in R software (version 1.7-8, Rizzo & Székely, 2016). In case partial Mantel test reported statistical significance, a distance-based redundancy analysis (Db-RDA) was used to explore the importance of environmental variables on the composition of assemblages (package “vegan”, version 2.5).

3.3 Results

3.3.1 Diversity associated with mesophotic assemblages

3.3.1.1 Habitat characterization and taxonomic composition

The 25 ROV dives were performed along 27.64 km of the seabed resulting in more than 12500 frames extracted (Tab. 3.1). The 76.7% of frames imaged portions of the seafloor dominated by soft bottoms, 53.7% of which constituted by mud and sands while 23% hosted rhodolith beds. The 23.3% of remaining extracted images showed seafloor characterized by hard substrate, either in form of continuous hard bottom or blocks elevating from the seabed. Of these, 3.2% and 4.7% hosted coralligenous formations and oysters bioconstructions, respectively. The analysis of frames extracted from video recordings for taxonomic identification registered a total of 17,263 megabenthic organisms belonging to 291 different taxa. The 78.3% of the taxa were classified at the species level (49.8%) or genus level (28.5%), while the remaining were identified as morphospecies and classified with higher taxonomic levels: family (6.5%), order (2.7%), and class (12.3%). The complete list of identified taxa is provided in Tab. S3.1. Sponges and cnidarians represented the major contributors to the biodiversity of the explored sites, corresponding to 30.9% and 15.1% of taxa identified, respectively. Echinoderms were frequently observed (10.3%), together with mollusks (8.6%), crustaceans (6.5%), ascidians (5.2%), and bryozoans (4.8%). Also, annelids colonizing the substrate and epibionts on other sessile fauna were abundant (4.5%). Although not included for further analysis, the nektonic fauna was well represented, with 34 taxa identified. In terms of individuals or colonies, sponges were the most abundant group (38.2%), followed by cnidarians (24.4%), bryozoans (14.9%), and echinoderms (12.3%). The remaining groups counted approximately 8% of the total number of organisms.

The assemblages were classified based on principal/dominant taxonomic component, identifying 5 groups:

- coralligenous assemblages (C): outcrops built by Corallinales algae populated by bryozoans (*Smittina cervicornis*, *Pentapora fascialis*), solitary corals (Caryophyllidae) and sponges (*Hexadella* spp. and *Axinella* spp.);
- mobile-bottom assemblages (MB): soft substrates mainly populated by echinoderms (e.g., *Spatangus purpureus*, *Ophiura fragilis*), soft corals (e.g., *Alcyonium palmatum*, *Pennatula rubra*) and ceriantids (*Cerianthus membranaceus*);
- cnidarians assemblages (CN): hard bottoms dominated by octocorals (e.g., *Acanthogorgia hirsuta*, *Callogorgia verticillata*) forming also dense forests, or by the scleratinian coral *Dendrophyllia cornigera*;

- deep-water oyster-reef assemblages (DWOR): reefs built by *Neopycnodonte cochlear* populated by sponges (e.g., *Hexadella* spp. and *Axinella* spp.), bryozoans (*Schizomavella mamillata*, *S. cervicornis*), ascidians (*Halocynthia papillosa*) and polychetes (*Filograna*/*Salmacina* complex);
- rhodolith-bed assemblages (RB): mobile bottoms covered by living and dead non-geniculate coralline red algae characterized by the presence of echinoderms (*Stylocidaris affinis*), bryozoans (*Myriapora truncata*) and sporadic octocorals (*Eunicella singularis*).

The ANOSIM analyses provided evidence that the assemblages were significantly different in terms of taxonomic composition both when analyzed together ($p<0.01$, Fig. 3.2A) and grouped by depth range (group 30-100 m, $p<0.01$; group 100-200 m, $p<0.01$). The C and CN assemblages presented the highest taxonomic richness (Fig. 2B), with 24.15 ± 4.6 and 21.16 ± 4.2 taxa identified with 100 frames (Tab. S3.3). The DWOR reported slightly lower values, counting on average 18.40 ± 2.6 taxa with the same number of samples. The richness of taxa associated with RB and MB was strongly lower, showing values of 6.83 ± 2.5 and 5.2 ± 0.2, respectively (Fig 3.2B). The difference in richness of taxa among assemblages was significant (ANOVA test, $p<0.01$). The Tukey post hoc test showed that these differences were significant between CN, C, DWOR, and MB and RB.

The Shannon diversity index calculated for the assemblages reached the highest values in DWOR, CN, and C (Fig. 3.2C). The ANOVA and Tukey tests reported significant differences ($p<0.01$) in the Shannon index between DWOR and MB. The evenness index, expressing the distribution of specimens among the taxa, showed similar values among the assemblages (Fig. 3.2D), and no significant differences were observed.

The hierarchical clustering exploring the similarity showed segregation of sites not matching that from visual analysis, reporting three major groups (Fig. 3.3). A first group was mainly formed DWOR and C, the CN constituted a second cluster, while MB and RB represented the third group.

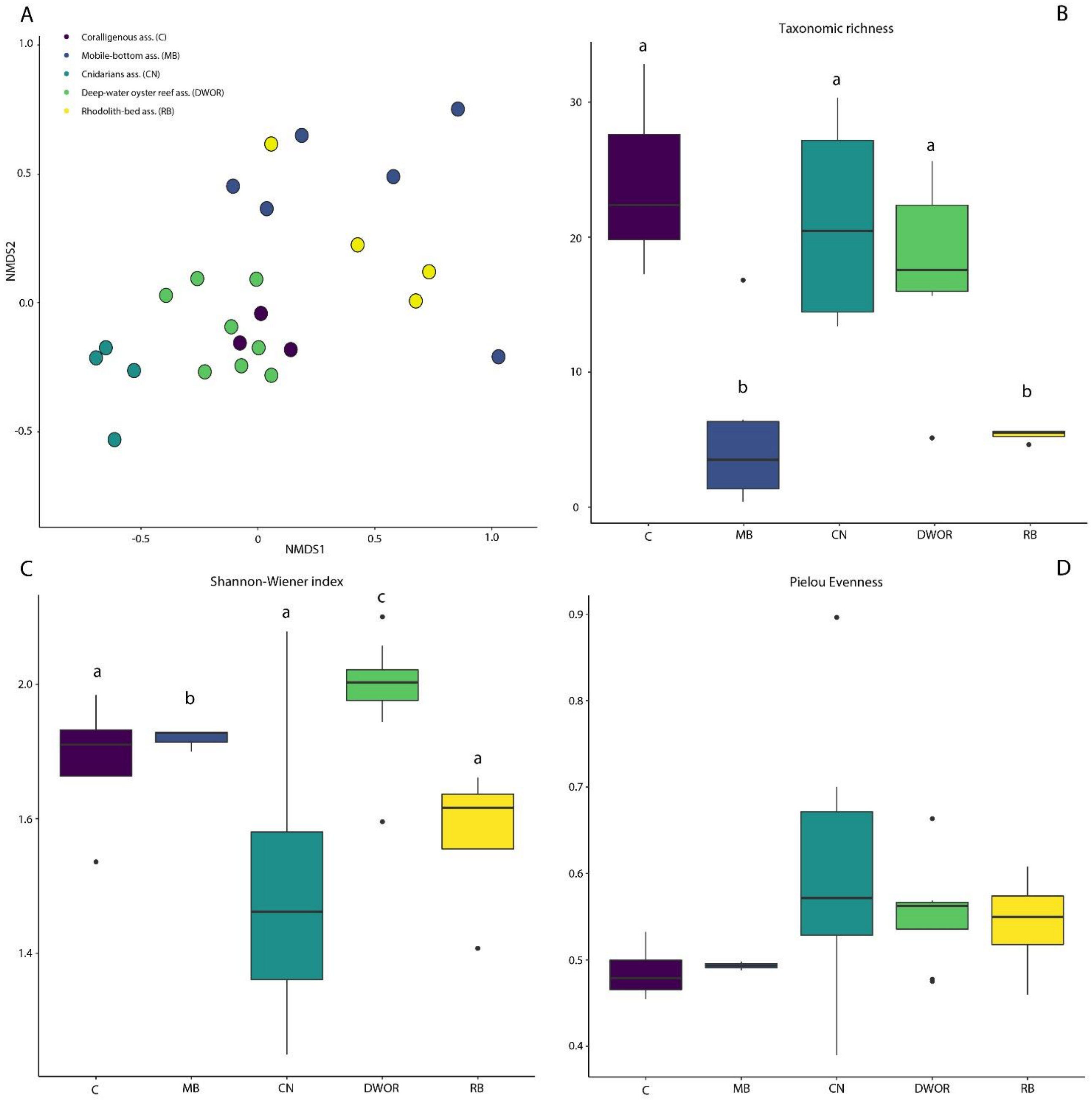

Fig. 3.2 A) Non-metric multidimensional scaling (NMDS) plot of taxonomic composition in the explored sites colored by assemblage category; B) boxplot of richness of taxa identified in mesophotic assemblages; C) boxplot of diversity (Shannon-Wiener index) among assemblages; D) boxplot of evenness (Pielou's J) for the taxa identified in the investigated assemblages. Letters refer to significant differences.

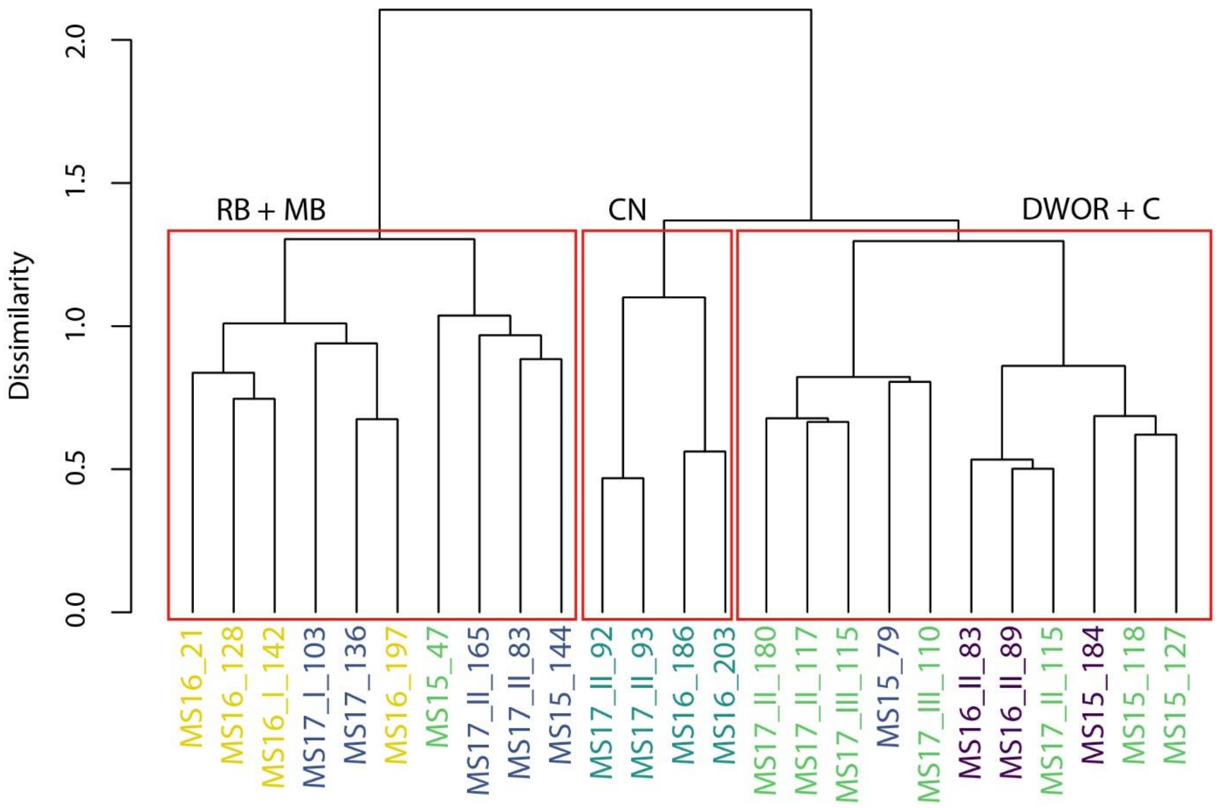

Fig. 3.3 Dendrogram showing Ward's clustering constructed over Bray-Curtis dissimilarity of square-root transformed abundance data of identified taxa. Red squares delineate groups identified with silhouette function.

3.3.1.2 Functional composition of assemblages

The analysis of functional diversity associated with explored assemblages resulted in 22 different functional entities (FE, Tab. S3.4). The classification of taxa depending on their functional characteristics registered (i) two categories of adult body dimension (macro- and megafauna), (ii) four adult motility categories (sessile, facultatively motile, vagile, and swimmers), (iii) six different strategies of feeding (deposit feeders, grazers, filter feeders, suspension feeders, scavenger/predators, and photosynthetic organisms), (iv) two types of adult habits (benthic and pelagic), (v) three categories of organism aggregation (single, colonial and gregarious), either (vi) capable to build habitat or not.

The ANOSIM analysis reported significant differences among assemblages in terms of functional composition ($p<0.01$, Fig. 3.4A). The coralligenous assemblages reported the highest functional richness (Frich), with an average of 12.75 ± 0.25 FE (Fig. 3.4B). Similar richness values were observed for cnidarians assemblages, which presented 12.5 ± 1.6 FE on average. A slightly lower Frich was detected in deep-water oyster reef assemblages, hosting an average of 10.88 ± 1.3 FE. Rhodolith-bed and mobile-bottom assemblages presented the lowest Frich values and were characterized by 8.25 ± 0.25 and 5.80 ± 1.16 Fes, respectively.

The Kruskal-Wallis and post hoc Dunn tests revealed significant differences in the functional richness between C, CN, DWOR, and MB.

The Feve, expressing the distribution of taxa among the identified Fes, reported comparable values for CN, C, DWOR, and RB, with values between 0.2-0.35 on average (Fig. 3.4C). MB represented an exception, showing high variability among sites and resulting in an average value of 0.46 ± 0.13. No significant differences were observed through the Kruskal-Wallis test.

The hierarchical clustering exploring the similarity between sites in terms of functional composition reported results similar to those observed for taxonomic composition, with silhouette function detecting two major clusters (Fig. 3.4D). The C, CN, and DWOR assemblages composed the first cluster, while the second grouped RB and MB assemblages.

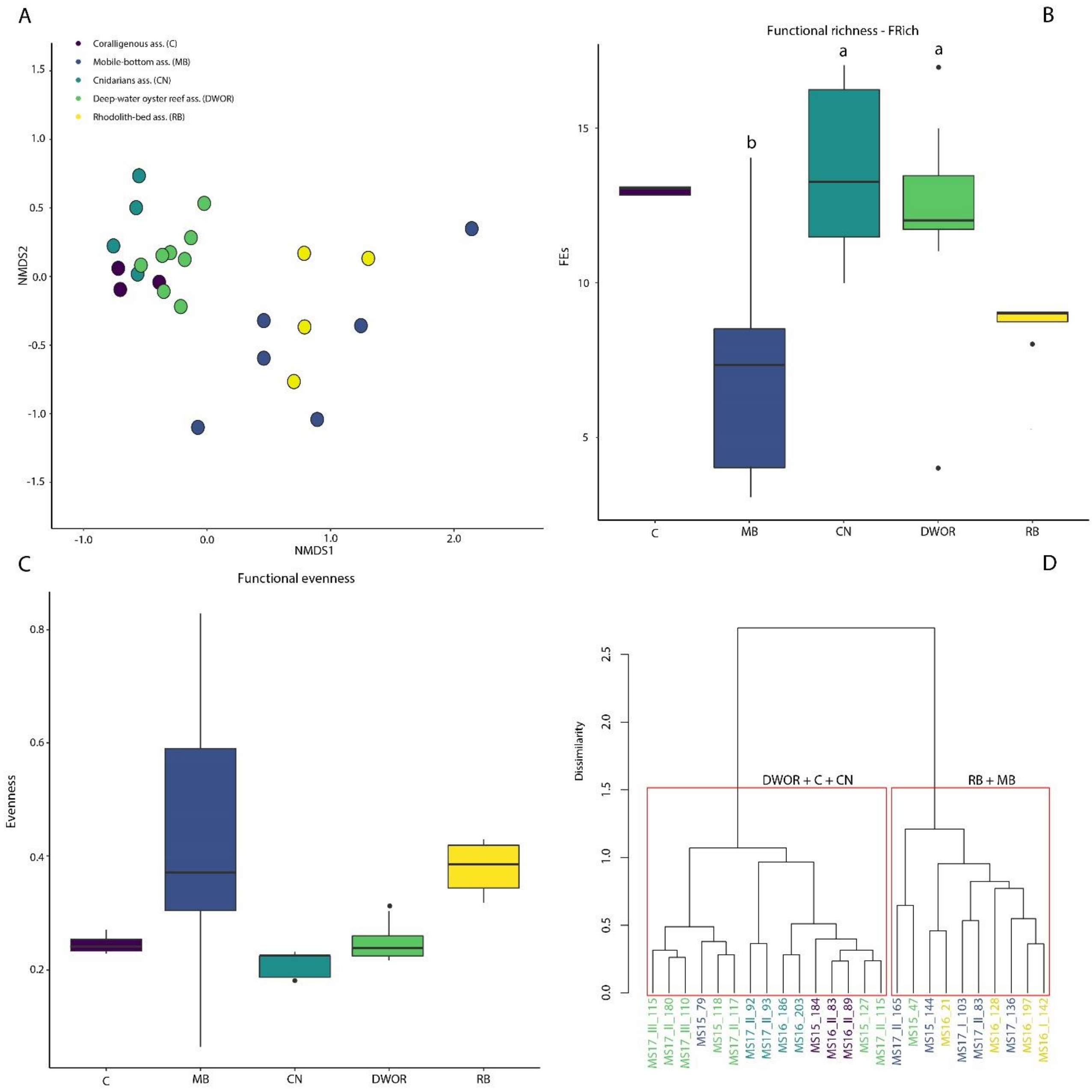

Fig. 3.4 A) Non-metric multidimensional scaling (NMDS) plot of functional composition of explored sites colored by assemblage category; B) boxplot of functional richness (Frich) of the different categories of mesophotic assemblages; C) boxplot of functional evenness (Feve) for Fes identified in the investigated assemblages; Boxes extend from the 25th to the 75th percentile with the horizontal line representing median value. The vertical lines indicate the most extreme values within 1.5 interquartile range of the 25th and 75th percentile; D) Dendrogram representation of Ward's clustering on Bray-Curtis dissimilarity of square-root transformed abundance of Fes identified in the explored assemblages. Letters refer to significant differences.

3.3.2 Environmental characterization

The visual surveys explored portions of seabed in a depth range spanning from ca. 55 m to 200 m (Tab. 3.1). The RB sites were the shallowest, reporting an average depth of 72.05 ± 3.01 m, followed by C and MB, located at average depths of 80.27 ± 5.21 m and 94.27 ± 7.90 m, respectively (Fig. 3.5A). The surveys imaging DWOR and CN were situated at 100.95 ± 7.78 m and 153.95 ± 21.41, representing the deepest mesophotic assemblages explored. The depth of occurrence of CN resulted significantly different from the other assemblages from ANOVA and Tukey post hoc tests.

The analysis of environmental factors showed that the different assemblages investigated were located within diverse environmental settings (Fig. 3.5). The light intensity extracted in correspondence of survey sites ranged between 0.21% and 0.34% (Fig. 3.5B). Despite that the amount of light reaching the seabed decreases with depth (Saulquin et al., 2013), no such relation was observed, with the shallowest sites hosting RB showing, instead, the lowest light intensity. Significant differences were documented only between RB and DWOR. Contrarily, concentrations of Chl-a linearly decreased with depth (Fig. 3.5C), showing a negative correlation (Pearson's r = -0.75, $p<0.01$).

No significant differences were observed in the velocity of currents at seabed among assemblages, showing similar values ranging from 0.001 to 0.06 m/s (Fig. 3.5D). The highest value was detected in DWOR, reporting 0.03 ± 0.002 m/s on average.

Sites hosting CN showed a significantly higher concentration of nutrients (NO_{3-} and PO_3^{4-}) with respect to C and RB (Fig. 3.5 E,F), and a significantly lower concentration of dissolved oxygen (Fig. 3.5G) than DWOR and C.

Salinity was significantly lower values in of RB with respect to other assemblages (Fig. 3.5H), likely due to their geographic locations: sites hosting RB were located in the Tyrrhenian Sea, which is characterized by lower salinity values with respect to the central and eastern Mediterranean Sea due to the influence of Atlantic currents (Astraldi & Gasparini, 1992). Finally, no differences were observed in temperature among explored assemblages, which showed values ranging from ca. 13 to 16 °C (Fig. 3.5 I).

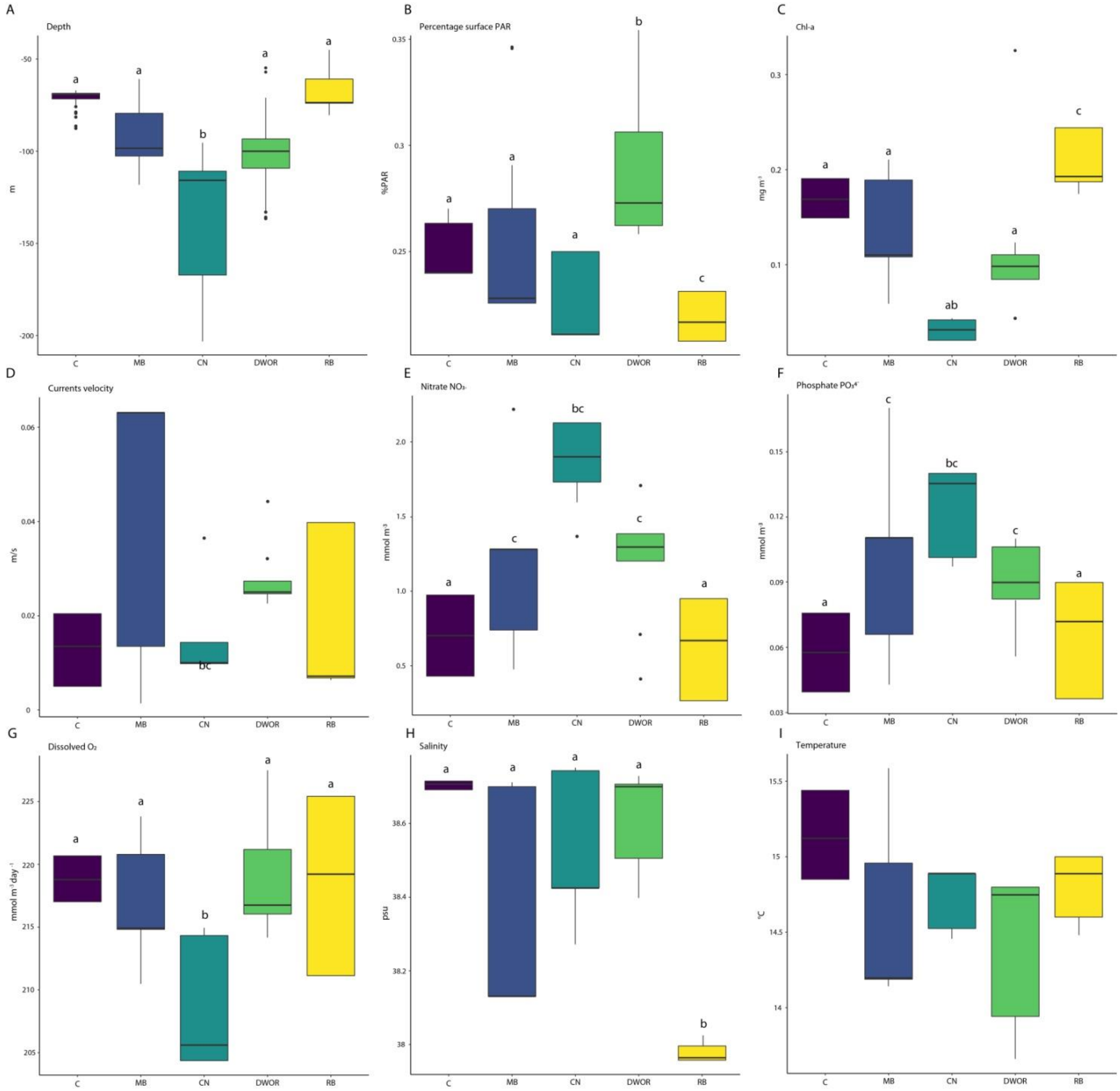

Fig. 3.5 Boxplots of the environmental variables extracted in correspondence of ROV survey sites. Within each box the horizontal line represents median value. Boxes extend from the 25th to the 75th percentile. The vertical lines indicate the most extreme values within 1.5 interquartile range of the 25th and 75th percentile. Letters refer to significant differences.

3.3.3 The role of environmental filtering and geographic location on taxonomic and functional diversity

Dissimilarity of assemblages in terms of taxonomic composition increased with increasing environmental distance rather than with geographical distance. The taxonomic diversity was significantly correlated with environmental distance given geographical distance (partial mantel, p = 0.04), but not with geographical distance given environmental distance (partial mantel, p = 0.21).

Based on the dbRDA, the selected variables explained 56% of the variability in taxa composition among assemblages, with the first two axes explaining ca. 46% of the constrained variance (CAP1: 24.9%, CAP2: 20.9%; Fig. 3.6). Light regime was the most significant predictor, together with depth and temperature. The NO_{3-} concentration and dissolved O_2 were also significant factors explaining the difference in taxonomic composition among the assemblages. The concentration of Chl-a was correlated with depth while PO_3^{4-} with NO_{3-} and, consequently, these variables were excluded. In addition, salinity was excluded due to a potential basin effect on the observed salinity values.

The dissimilarity of assemblages in terms of functional composition was not correlated with either abiotic distance given geographical distance (partial mantel, p = 0.5) or with geographical distance given environmental distance (partial mantel, p = 0.3).

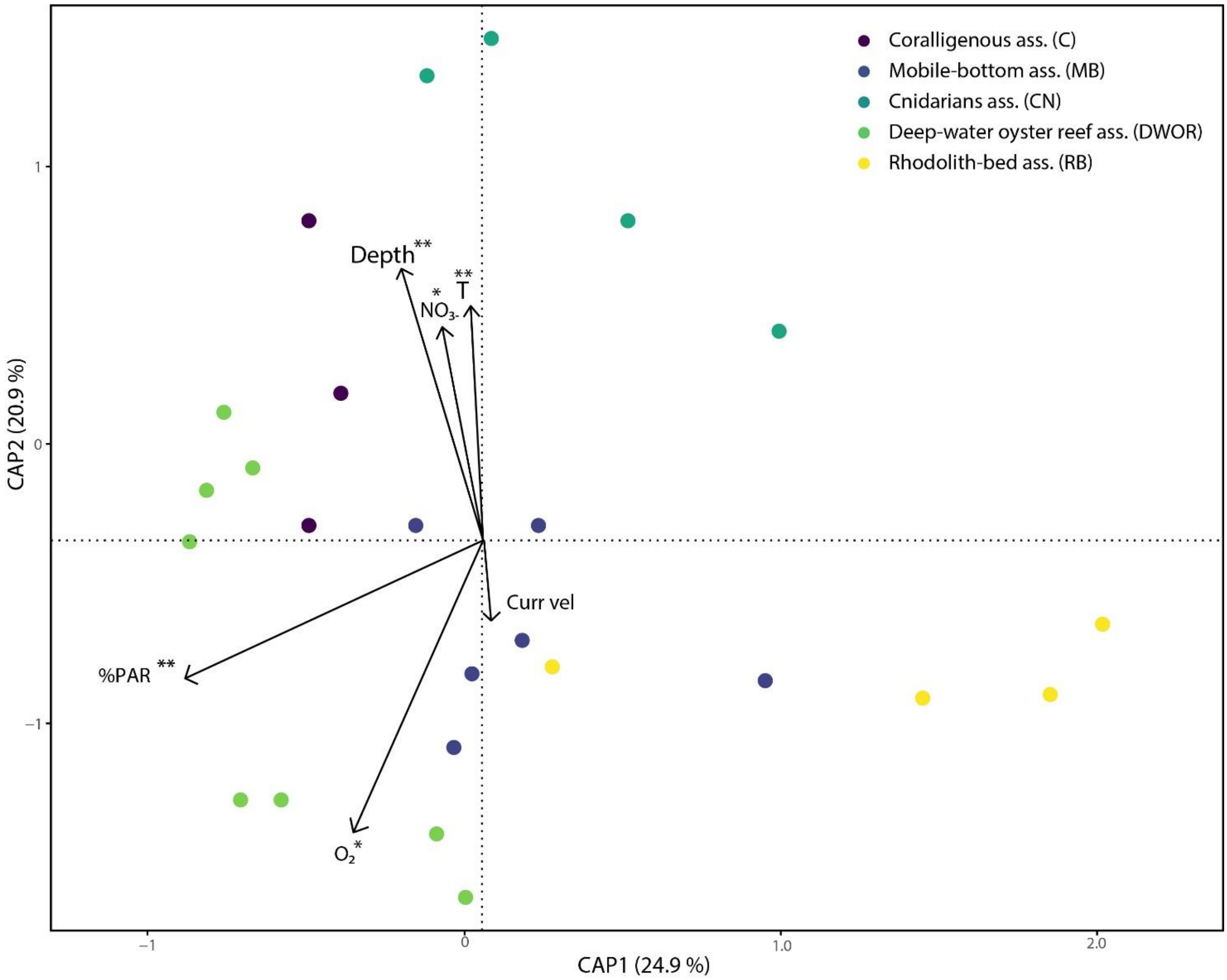

Fig. 3.6 Distance-based redundancy analysis (dbRDA) plot of composition of mesophotic assemblages showing environmental factors with significance represented by asterisks.

3.4 Discussion

3.4.1 Diversity of mesophotic assemblages

The recent development of marine technology allowed the direct observation mesophotic ecosystems, providing information on their composition and functions (Loya, et al., 2018). Regarding the Mediterranean Sea, local or sub-regional studies evaluated the diversity of mesophotic benthic assemblages based on video recordings (e.g., Bo et al., 2011; Grinyó et al., 2018; Idan et al., 2018; Corriero et al., 2019; Angeletti & Taviani, 2020; Cardone et al., 2020; Chimienti et al., 2020). Large-scale studies are, however, still scant and focused on a few taxonomical groups, mainly cnidarians, or habitats, such as coralligenous formations (Cerrano et al., 2019; Enrichetti et al., 2019). The ecological value of CN and C is long since recognized, representing hotspots of biodiversity, and delivering important ecosystem services (Ballesteros, 2006). The analysis of ROV videos collected along the Italian coasts at mesophotic depth provided further evidence of the diversity associated with these biological assemblages, which presented the highest diversity values. Despite sponges and cnidarians were the major contributors to the biodiversity of C and CN in terms of the number of taxa identified and number of individuals or colonies (Tab. S3.1), organisms were quite homogeneously distributed among taxa (Pielou's J ca. 0.5).

Moreover, the taxonomic richness of C and CN was associated with a high functional diversity (i.e., functional richness). Several studies documented the ecological functions and services that coralligenous and cnidarians-dominated associations provide, representing refuge/nursery areas, and concentrating food resources palatable for vagile species (e.g., Gibson et al., 2006, Rossi et al., 2017). Echinoderms and fish fauna (although not considered for diversity indexes calculations) were, indeed, frequently observed in C and CN while feeding or hiding in the bioconstructions crevices.

Noticeably, DWOR reported diversity levels, in terms of taxa and functions, comparable to those documented for C and CN. The few records in the literature reported high levels of biodiversity associated with DWOR in the Mediterranean Sea (e.g., Angeletti & Taviani, 2020; Cardone et al., 2020). The results represent further evidence suggesting DWOR may represent hotspots of biodiversity at mesophotic depths in the Mediterranean basin. The complex three-dimensional structures built mainly by *N. cochlear* provide secondary hard substrates suitable for other sessile fauna. Sponges and cnidarians were frequently observed on dead portions of reef structure, together with annelids colonizing both the hard substrate and fouling other megafauna, ascidians, and bryozoans. In DWOR, the biome not only was taxonomically rich, but taxa were different in a functional perspective, registering values of functional richness comparable to those of C and CN. Also, the hierarchical clustering was not able to distinguish DWOR from C assemblages in terms of taxonomic composition, and from C and CN in terms of functional composition. Similarly to C and

CN situations, DWOR might, thus, represent hotspots of functions, ultimately playing a relevant ecological role at mesophotic depths.

Like for taxonomic composition, functional richness is a sensitive indicator when studying the potential consequences of biodiversity loss on ecological functions provided by biological assemblages. However, functional richness saturates increasing the number of taxa, so beyond that threshold, a rise in taxonomic richness is not coupled with an increase in FRich (e.g., Schumm et al., 2019 with reference therein). Moreover, perturbations can also lead to changes in the assemblage structure, modifying the effective dominance of functional entities and redundancy of functions within biological assemblages. The FRich by itself does not provide information on how taxa are distributed across functional groups, i.e., functional evenness (FE). A low number of taxa within a certain functional group limits the biological options capable of providing the same function if taxa are lost due to perturbations (Aarts, 1999). The C, CN, and DWOR showed the lowest functional evenness among explored assemblages, suggesting the high functional richness observed might base on weak reed: if a perturbation removed functional-unique taxa from the assemblage, those functions would be entirely lost.

Coupling richness with information on the composition of biological associations and functional redundancy ensures a more complete evaluation of explored ecosystems also in situations with low diversity levels. The MB and RB, for instance, reported the highest taxonomical and functional evenness but the richness values were largely lower with respect to other assemblages. Here, the few functions documented were provided by different taxa, each counting many specimens. Whilst the equal distribution of individuals among taxonomic functional groups is usually interpreted as an ecologically stable situation, the dominance of some taxa and functional entities might be the result of previous or ongoing disturbances influencing the composition of the associations. The trawling scars and lost fishing gears observed in surveys on MB and RB assemblages suggest that human activities were and/or are in act in the investigated areas and might have influenced the composition of the associations. The MB and RB were mainly represented by echinoderms, encrusting sponges and bryozoans and few erected soft cnidarians colonizing the hard substrates. Previous studies have already evidenced high abundances of echinoderms in benthic habitats impacted by trawling activities, likely due to the higher potential survival capacity of high-motility taxa as well as to the increased availability of food resources for scavengers in the form of animals damaged by the fishing gears. Hence, the loss of taxa may not only drive a loss of functional groups, but also an increase in the evenness of those remaining.

3.4.2 Environmental filtering and geographic location

The increase in the dissimilarity of composition of communities with geographic distances have been observed for certain taxonomic groups (e.g., corals, Hubble, 2001; bivalves, McClain et al., 2012; marine bacteria, Martiny et al., 2011; plankton, Chust et al., 2013), with close-located associations generally more similar than those located further apart (Soininen et al., 2007). The analysis of the dissimilarity of mesophotic assemblages, however, indicated that geographic location is not the main driver influencing how taxa assemble in the explored mesophotic situations, with no observed correlation. Matter of fact, the investigated assemblages and associated taxa are present in different areas within and outside the Mediterranean Sea.

Contrarily, the results suggest that environmental setting is an important factor shaping the composition of mesophotic assemblages in the Mediterranean Sea. Those occurring within comparable environmental characteristics were more taxonomic similar than those environmentally different. The composition of the investigated mesophotic assemblages might, therefore, be the result of the environmental characterization rather than processes related with geographical location.

Among the environmental variables mostly influencing the taxonomic difference of the explored mesophotic assemblages, the light regime played a main role. The penetration of light along the water column unavoidably influences the distribution of obligate phototrophic components, limiting their presence to areas where light radiation satisfies the physiological requirements. Despite identified in the shallowest explored areas, the C and RB were present at medium-low light intensity in terms of percent surface PAR at seabed, ranging between 0.20-0.35 % and 0.21-0.23%, respectively. These values are in line with previous evidence in the Mediterranean Sea (Ballesteros, 1994, 2006) and within the irradiance range resulting as potentially associated with the mesophotic conditions (10-0.0005% of surface PAR, see Chapter 1).

Light probably influenced the presence of coralline algae structuring C and RB but it might also act in concert with other factors in sorting taxa associated with explored mesophotic assemblages. The variation of depth frequently synthetizes changes in the environmental conditions, because other abiotic factors (temperature, salinity, food supply) co-vary with depth. The depth, indeed, resulted major factor contributing to the variance in the taxonomic composition of the assemblages.

The temperature delineated the the axis separating CN from other assemblages, suggesting a role in explaining the taxa composition of assemblages dominated by cnidarians. Similarily, nutrients concentration (represented by NO_{3-} concentration) presented a pattern suggesting a relevant contribution in determining the taxonomic composition of CN, showing the highest values in correspondence of area hosting these assemblages. Studies suggested that mesophotic and deep corals might settle in areas characterized by hydrodynamic processes leading to the upwelling of nutrient-rich deep waters producing re-suspension of organic particles and favoring suspension-feeders (Bo et al., 2011; Corriero et al., 2019).

Contratily, the functional composition of the investigated assemblages resulted as not affect by both environmental and geographical distance. If taxa might comprise organisms with similar environmental preferences, the same may not be true for functional entities which count individuals from different Families and Phyla (Tab. 3.1). Consequently, specimens with different environmental requirements may fall within the same functional entity.

Despite environmental variables and geographical location are known to play a major role in influencing the distribution of benthic taxa, stochastic processes and set of different biotic interactions among individuals shape the composition of benthic assemblages by limiting or facilitating the presence of taxa. The considered environmental variables, indeed, explained only a portion (56%) of the variance in the taxonomic composition of explored assemblages, suggesting that different processes probably act in concert to structure these assemblages. To disentangle the relative roles of deterministic niche-based processes and stochastic processes such as chance colonization, random extinction, and ecological shifts (random changes in species relative abundance) it undoubtedly hard, or even not be possible, when studying benthic associations with visual surveys. However, the results reported in this chapter provide evidence of the major filtering role of environmental settings on the dispersal and presence of benthic taxa, contributing to more than half the variability observed in the taxonomic composition of the investigated mesophotic assemblages.

References

Aarts, B.G.W. (1999). Ecological sustainability and biodiversity. *International Journal of Sustainable Development, World Ecology*, 6(2), 89–102. https://doi.org/10.1080/13504509909469998

Acevedo, R., Morelock, J., Olivieri, R.A. (1989). Modification of coral reef zonation by terrigenous sediment Stress. *PALAIOS*, 4(1), 92–100. https://doi.org/10.2307/3514736

Allison, G. (2004). The influence of species diversity and stress intensity on community resistance and resilience. *Ecological Monographs*, 74(1), 117–134. https://doi.org/10.1890/02-0681

Angeletti, L. Taviani, M. (2020). Offshore *Neopycnodonte* Oyster Reefs in the Mediterranean Sea. *Diversity*, 12(3), 92. https://doi.org/10.3390/d12030092

Astraldi, M., Gasparini, G.P. (1992). The seasonal characteristics of the circulation in the north Mediterranean basin and their relationship with the atmospheric-climatic conditions. *Journal of Geophysical Research: Oceans*, 97(C6), 9531–9540. https://doi.org/10.1029/92JC00114

Baker, E.K., Puglise, K.A., Harris, P.T. (2016). *Mesophotic coral ecosystems: a lifeboat for coral reefs?* The United Nations Environment Programme and GRID-Arendal, Nairobi and Arenal: Nairobi, Kenya, 98 pp.

Ballesteros, E. (1994). The deep-water *Peyssonnelia* beds from the Balearic Islands (Western Mediterranean). *Marine Ecology*, 15(3–4), 233–253. https://doi.org/10.1111/j.1439-0485.1994.tb00055.x

Ballesteros, E. (2006). Mediterranean coralligenous assemblages: a synthesis of present knowledge. *Oceanography and Marine Biology: An Annual Review*, 123–195.

Bo, M., Bertolino, M., Borghini, M., Castellano, M., Harriague, A.C., Di Camillo, C.G., Gasparini, G.P., Misic, C., Povero, P., Schroeder, K., Bavestrello, G. (2011). Characteristics of the mesophotic megabenthic assemblages of the Vercelli Seamount (North Tyrrhenian Sea). *PLOS ONE*, 6(2), e16357. https://doi.org/10.1371/journal.pone.0016357

Byrnes, J., Stachowicz, J.J., Hultgren, K.M., Randall Hughes, A., Olyarnik, S.V., Thornber, C.S. (2006). Predator diversity strengthens trophic cascades in kelp forests by modifying herbivore behaviour. *Ecology Letters*, 9(1), 61–71. https://doi.org/10.1111/j.1461-0248.2005.00842.x

Cardone, F., Corriero, G., Longo, C., Mercurio, M., Onen Tarantini, S., Gravina, M.F., Liscio, S., Moretti, M., De Giosa, F., Giangrande, A., Marzano, C.N., Pierri, C. (2020). Massive bioconstructions built by *Neopycnodonte cochlear* (Mollusca, Bivalvia) in a mesophotic environment in the central Mediterranean Sea. *Scientific Reports*, 10(1), 6337. https://doi.org/10.1038/s41598-020-63241-y

Cerrano, C., Bastari, A., Calcinai, B., Camillo, C.D., Pica, D., Puce, S., Valisano, L., Torsani, F. (2019). Temperate mesophotic ecosystems: gaps and perspectives of an emerging conservation challenge for the Mediterranean Sea. *The European Zoological Journal*, 86(1), 370–388. https://doi.org/10.1080/24750263.2019.1677790

Chimienti, G., De Padova, D., Mossa, M., Mastrototaro, F. (2020). A mesophotic black coral forest in the Adriatic Sea. *Scientific Reports*, 10(1), 8504. https://doi.org/10.1038/s41598-020-65266-9

Chust, G., Irigoien, X., Chave, J., Harris, R.P. (2013). Latitudinal phytoplankton distribution and the neutral theory of biodiversity. *Global Ecology and Biogeography*, 22(5), 531–543. https://doi.org/10.1111/geb.12016

Coleman, M.L., Sullivan, M.B., Martiny, A.C., Steglich, C., Barry, K., DeLong, E.F., et al. (2006). Genomic islands and the ecology and evolution of *Prochlorococcus*. *Science*, 311(5768), 1768–1770. https://doi.org/10.1126/science.1122050

Corriero, G., Pierri, C., Mercurio, M., Marzano, C.N., Tarantini, S.O., Gravina, M.F., Lisco S., Moretti M., De Giosa F., Valenzano E., Giangrande A., Mastrodonato M., Longo C., Cardone F. (2019). A Mediterranean mesophotic coral reef built by non-symbiotic scleractinians. *Scientific Reports*, 9(1), 3601. https://doi.org/10.1038/s41598-019-40284-4

Enrichetti, F., Dominguez-Carrió, C., Toma, M., Bavestrello, G., Betti, F., Canese, S., Bo, M. (2019). Megabenthic communities of the Ligurian deep continental shelf and shelf break (NW Mediterranean Sea). *PLOS ONE*, 14(10), e0223949. https://doi.org/10.1371/journal.pone.0223949

Fox, J., Friendly, G.G., Graves, S., Heiberger, R., Monette, G., Nilsson, H., Ripley, B., Weisberg, S., Fox, M.J., Suggests, M. (2007). The car package. R package.

Garrabou, J., Coma, R., Bensoussan, N., Bally, M., Chevaldonné, P., Cigliano, M., Díaz, D., Harmelin, J.-G., Gambi, M.C., Kersting, D.K. (2009). Mass mortality in Northwestern Mediterranean rocky benthic communities: effects of the 2003 heat wave. *Global change biology*, 15(5), 1090–1103.

Gibson, R.N., Atkinson, R.J.A., Gordon, J.D.M. (2006). Oceanography and Marine Biology: An Annual Review, Volume 44. CRC Press: New York, USA.

Goslee, S., Urban, D., Goslee, M.S. (2020). Package ‘ecodist’. R package.

Grinyó, J., Viladrich, N., Díaz, D., Muñoz, A., Mallol, S., Salazar, J., Castillo, R., Gili, J.-M., Gori, A. (2018). Reproduction, energy storage and metabolic requirements in a mesophotic population of the gorgonian *Paramuricea macrospina*. *PLOS ONE*, 13(9), e0203308. https://doi.org/10.1371/journal.pone.0203308

Guillot, G., Rousset, F. (2013). Dismantling the Mantel tests. *Methods in Ecology and Evolution*, 4(4), 336–344.

Hilborn, R., Quinn, T.P., Schindler, D.E., Rogers, D.E. (2003). Biocomplexity and fisheries sustainability. *Proceedings of the National Academy of Sciences*, 100(11), 6564–6568. https://doi.org/10.1073/pnas.1037274100

Hughes, A.R., Stachowicz, J.J. (2004). Genetic diversity enhances the resistance of a seagrass ecosystem to disturbance. *Proceedings of the National Academy of Sciences*, 101(24), 8998–9002. https://doi.org/10.1073/pnas.0402642101

Idan, T., Shefer, S., Feldstein, T., Yahel, R., Huchon, D., Ilan, M. (2018). Shedding light on an East-Mediterranean mesophotic sponge ground community and the regional sponge fauna. *Mediterranean Marine Science*, 19(1), 84–106. https://doi.org/10.12681/mms.13853

Kahng, S.E., Garcia-Sais, J.R., Spalding, H.L., Brokovich, E., Wagner, D., Weil, E., Hinderstein, L., Toonen, R.J. (2010). Community ecology of mesophotic coral reef ecosystems. *Coral Reefs*, 29(2), 255–275. https://doi.org/10.1007/s00338-010-0593-6

Kahng, S.E., Akkaynak, D., Shlesinger, T., Hochberg, E.J., Wiedenmann, J., Tamir, R., Tchernov, D. (2019). Light, temperature, photosynthesis, heterotrophy, and the lower depth limits of mesophotic coral ecosystems. In: *Mesophotic coral ecosystems*. Loya Y, Puglise KA, Bridge TCL (Eds). Springer International Publishing: Cham, pp. 801–828.

Laliberté, E., Legendre, P., Shipley, B., Laliberté, M.E. (2014). Package 'FD'. *Measuring functional diversity from multiple traits, and other tools for functional ecology*. R. package.

Laverick, J.H., Tamir, R., Eyal, G., Loya, Y. (2020). A generalized light-driven model of community transitions along coral reef depth gradients. *Global Ecology and Biogeography*, 29(9), 1554–1564. https://doi.org/10.1111/geb.13140

Lesser, M.P., Slattery, M., Leichter, J.J. (2009). Ecology of mesophotic coral reefs. *Journal of Experimental Marine Biology and Ecology*, 375(1), 1–8. https://doi.org/10.1016/j.jembe.2009.05.009

Loya, Y., Puglise, K.A., Bridge, T.C.L. (2018). *Mesophotic coral ecosystems*. Springer Berlin Heidelberg: New York, NY.

Maechler, M., Rousseeuw, P., Struyf, A., Hubert, M., Hornik, K., Studer, M. (2013). Package 'cluster'. R package.

Martiny, J.B.H., Eisen, J.A., Penn, K., Allison, S.D., Horner-Devine, M.C. (2011). Drivers of bacterial β-diversity depend on spatial scale. *Proceedings of the National Academy of Sciences*, 108(19), 7850–7854. https://doi.org/10.1073/pnas.1016308108

McClain, C.R., Stegen, J.C., Hurlbert, A.H. (2012). Dispersal, environmental niches and oceanic-scale turnover in deep-sea bivalves. *Proceedings of the Royal Society B: Biological Sciences*, 279(1735), 1993–2002. https://doi.org/10.1098/rspb.2011.2166

Mirto, S., Arigò, C., Genovese, L., Pusceddu, A., Gambi, C., & Danovaro, R. (2014). Nematode assemblage response to fish-farm impact in vegetated (*Posidonia oceanica*) and non-vegetated habitats. *Aquaculture Environment Interactions*, 5(1), 17-28.

Moritz, C., Meynard, C.N., Devictor, V., Guizien, K., Labrune, C., Guarini, J.-M., et al. (2013). Disentangling the role of connectivity, environmental filtering, and spatial structure on metacommunity dynamics. *Oikos*, 122(10), 1401–1410. https://doi.org/10.1111/j.1600-0706.2013.00377.x

Mouillot, D., Graham, N.A.J., Villéger, S., Mason, N.W.H., Bellwood, D.R. (2013). A functional approach reveals community responses to disturbances. *Trends in Ecology, Evolution*, 28(3), 167–177. https://doi.org/10.1016/j.tree.2012.10.004

Muir, P.R., Wallace, C.C., Done, T., Aguirre, J.D. (2015). Limited scope for latitudinal extension of reef corals. *Science*, 348(6239), 1135–1138. https://doi.org/10.1126/science.1259911

Oksanen, J., Kindt, R., Legendre, P., O'Hara, B., Stevens, M.H.H., Oksanen, M.J., Suggests, M. (2007). The vegan package. *Community ecology package*, 10(631–637), 719.

Palumbi, S.R., McLeod, K.L., Grünbaum, D. (2008). Ecosystems in action: lessons from marine ecology about recovery, resistance, and reversibility. *BioScience*, 58(1), 33–42. https://doi.org/10.1641/B580108

Petchey, O.L., Gaston, K.J. (2002). Functional diversity (FD), species richness and community composition. *Ecology Letters*, 5(3), 402–411. https://doi.org/10.1046/j.1461-0248.2002.00339.x

Quattrini, A.M., Gómez, C.E., Cordes, E.E. (2017). Environmental filtering and neutral processes shape octocoral community assembly in the deep sea. *Oecologia*, 183(1), 221–236. https://doi.org/10.1007/s00442-016-3765-4

R Core Team. (2020). *R: A Language and Environment for Statistical Computing*. R Foundation for Statistical Computing, Vienna: Austria.

Reusch, T.B.H., Ehlers, A., Hämmerli, A., Worm, B. (2005). Ecosystem recovery after climatic extremes enhanced by genotypic diversity. *Proceedings of the National Academy of Sciences*, 102(8), 2826–2831. https://doi.org/10.1073/pnas.0500008102

Ricklefs, R.E. (1987). Community Diversity: Relative Roles of Local and Regional Processes. *Science*, 235(4785), 167–171. https://doi.org/10.1126/science.235.4785.167

Rizzo, M.L., Székely, G.J. (2016). Energy distance. *Wiley interdisciplinary reviews: Computational statistics*, 8(1), 27–38.

Rossi, S., Bramanti, L., Gori, A., Orejas, C. (Eds.). (2017). *Marine Animal Forests: The Ecology of Benthic Biodiversity Hotspots*. Springer International Publishing: Cham.

Sala, E., Knowlton, N. (2006). Global Marine Biodiversity Trends. *Annual Review of Environment and Resources*, 31(1), 93–122. https://doi.org/10.1146/annurev.energy.31.020105.100235

Saulquin, B., Hamdi, A., Gohin, F., Populus, J., Mangin, A., d’Andon, O.F. (2013). Estimation of the diffuse attenuation coefficient KdPAR using MERIS and application to seabed habitat mapping. *Remote Sensing of Environment*, 128, 224–233. https://doi.org/10.1016/j.rse.2012.10.002

Schumm, M., Edie, S.M., Collins, K.S., Gómez-Bahamón, V., Supriya, K., White, A.E., Price, T.D., Jablonski, D. (2019). Common latitudinal gradients in functional richness and functional evenness across marine and terrestrial systems. *Proceedings of the Royal Society B: Biological Sciences*, 286(1908), 20190745. https://doi.org/10.1098/rspb.2019.0745

Smith, T.B., Gyory, J., Brandt, M.E., Miller, W.J., Jossart, J., Nemeth, R.S. (2016). Caribbean mesophotic coral ecosystems are unlikely climate change refugia. *Global Change Biology*, 22(8), 2756–2765. https://doi.org/10.1111/gcb.13175

Soininen, J., McDonald, R., Hillebrand, H. (2007). The distance decay of similarity in ecological communities. *Ecography*, 30(1), 3–12. https://doi.org/10.1111/j.0906-7590.2007.04817.x

Stachowicz, J.J., Fried, H., Osman, R.W., Whitlatch, R.B. (2002). Biodiversity, invasion resistance, and marine ecosystem function: reconciling pattern and process. *Ecology*, 83(9), 2575–2590. https://doi.org/10.1890/0012-9658(2002)083[2575:BIRAME]2.0.CO;2

Tamir, R., Eyal, G., Kramer, N., Laverick, J.H., Loya, Y. (2019). Light environment drives the shallow-to-mesophotic coral community transition. *Ecosphere*, 10(9), e02839. https://doi.org/10.1002/ecs2.2839

Turner, J.A., Andradi-Brown, D.A., Gori, A., Bongaerts, P., Burdett, H.L., Ferrier-Pagès, C., Voolstra, C.R., Weinstein, D.K., Bridge, T., Costantini, F., Gress, E., Laverick, J., Loya, Y., Goodbody-Gringley, G., Rossi, S., Taylor, M.L., Viladrich, N., Voss, J., Williams, J., Woodall, L.C., Eyal, G. (2019). Key questions for research and conservation of mesophotic coral ecosystems and temperate mesophotic ecosystems. In: *Mesophotic coral ecosystems*. Loya Y, Puglise KA, Bridge TCL (Eds). Springer International Publishing: Cham, pp. 989–1003.

Villéger, S., Mason, N.W.H., Mouillot, D. (2008). New Multidimensional Functional Diversity Indices for a Multifaceted Framework in Functional Ecology. *Ecology*, 89(8), 2290–2301. https://doi.org/10.1890/07-1206.1

Villéger, S., Miranda, J.R., Hernández, D.F., Mouillot, D. (2010). Contrasting changes in taxonomic vs. functional diversity of tropical fish communities after habitat degradation. *Ecological Applications*, 20(6), 1512–1522. https://doi.org/10.1890/09-1310.1

Worm, B., Barbier, E.B., Beaumont, N., Duffy, J.E., Folke, C., Halpern, B.S., Jackson, J.B.C., Lotze, H.K., Micheli, F., Palumbi, S.R., Sala, E., Selkoe, K.A., Stachowicz, J.J., Watson, R. (2006). Impacts of biodiversity loss on ocean ecosystem services. *Science*, 314(5800), 787–790. https://doi.org/10.1126/science.1132294

Supplementary material

Tab. S3.1. Comprehensive list of the species identified during video analysis, with their abundance values and occurrence in the assemblage categories.

Phylum	Class	Order	Family	Genus	Species	Author	ind.	CN	C	MB	DWOR	RB
Rhodophyta	Florideophyceae	Corallinales			spp.	P.C. Silva & H.W. Johansen, 1986		X				X
Ochrophyta	Phaeophyceae	Dictyotales	Dictyotaceae	*Dictyota*	*Dictyota dichotoma*	(Hudson) J.V. Lamouroux, 1809	2				X	
Ochrophyta	Phaeophyceae	Ectocarpales	Acinetosporaceae	*Acinetospora*	*Acinetospora crinita*	(Carmichael) Sauvageau, 1899	31					X
Chlorophyta	Pyramimonadophyceae	Palmophyllales	Palmophyllaceae	*Palmophyllum*	*Palmophyllum crassum*	(Naccari) Rabenhorst, 1868	64		X			
Chlorophyta	Ulvophyceae	Bryopsidales	Codiaceae	*Codium*	spp.		1					X
Chlorophyta	Ulvophyceae	Bryopsidales	Codiaceae	*Codium*	*Codium bursa*	(Olivi) C. Agardh, 1817	2					X
Foraminifera	Globothalamea	Rotaliida	Homotrematidae	*Miniacina*	*Miniacina miniacea*	Pallas, 1766	51		X			
Porifera	Calcarea	Clathrinida	Clathrinidae	*Clathrina*	spp.		11				X	
Porifera	Calcarea	Clathrinida	Clathrinidae	*Clathrina*	*Clathrina blanca*	Miklucho-Maclay, 1868	75				X	
Porifera	Demospongiae	Agelasida	Agelasidae	*Agelas*	*Agelas oroides*	Schmidt, 1864	28		X		X	
Porifera	Demospongiae	Axinellida	Axinellidae	*Axinella*	*Axinella polypoides*	Schmidt, 1862	45				X	
Porifera	Demospongiae	Axinellida	Axinellidae	*Axinella*	sp. 1		1		X			
Porifera	Demospongiae	Axinellida	Axinellidae	*Axinella*	sp. 2		33	X			X	
Porifera	Demospongiae	Axinellida	Axinellidae	*Axinella*	sp. 3		2	X				
Porifera	Demospongiae	Axinellida	Raspailiidae	*Raspailia*	*Raspailia hispida*	Montagu, 1814	59		X		X	
Porifera	Demospongiae	Axinellida	Raspailiidae	*Raspailia*	*Raspailia viminalis*	Schmidt, 1862	6				X	
Porifera	Demospongiae	Bubarida	Dictyonellidae	*Dictyonella*	*Dictyonella incisa*	Schmidt, 1880	3		X		X	
Porifera	Demospongiae	Chondrosiida	Chondrosiidae	*Chondrosia*	*Chondrosia reniformis*	Nardo, 1847	67	X	X		X	
Porifera	Demospongiae	Clionaida	Clionaidae	*Cliona*	sp. 1		3	X				
Porifera	Demospongiae	Clionaida	Spirastrellidae	*Spirastrella*	*Spirastrella cunctatrix*	Schmidt, 1868	40	X			X	
Porifera	Demospongiae	Dictyoceratida	Dysideidae	*Dysidea*	sp. 1		34	X	X			
Porifera	Demospongiae	Dictyoceratida	Irciniidae	*Ircinia*	spp.		1	X				
Porifera	Demospongiae	Dictyoceratida	Irciniidae	*Ircinia*	*Ircinia variabilis*	Schmidt, 1862	1				X	
Porifera	Demospongiae	Dictyoceratida	Spongiidae	*Spongia*	spp.		3	X				X
Porifera	Demospongiae	Dictyoceratida	Spongiidae	*Spongia*	*Spongia agaricina*	Pallas, 1766	1				X	
Porifera	Demospongiae	Dictyoceratida	Spongiidae	*Spongia*	*Spongia lamella*	Schulze, 1879	2				X	

Porifera	Demospongiae	Dictyoceratida	Spongiidae	*Spongia*	*Spongia officinalis*	Linnaeus, 1759	8		X		
Porifera	Demospongiae	Dictyoceratida	Thorectidae	*Scalarispongia*	spp.		1	X			
Porifera	Demospongiae	Haplosclerida	Petrosiidae	*Petrosia*	*Petrosia ficiformis*	Poiret, 1789	107	X	X	X	
Porifera	Demospongiae	Haplosclerida	Chalinidae	*Haliclona*	*Haliclona fulva*	Topsent, 1893	1			X	
Porifera	Demospongiae	Haplosclerida	Chalinidae	*Haliclona*	sp. 1		230	X	X	X	
Porifera	Demospongiae	Haplosclerida	Chalinidae	*Haliclona*	sp. 2		209	X	X	X	
Porifera	Demospongiae	Haplosclerida	Chalinidae	*Haliclona*	sp. 3		26		X	X	
Porifera	Demospongiae	Haplosclerida	Chalinidae	*Haliclona*	sp. 4		104	X			
Porifera	Demospongiae	Haplosclerida	Chalinidae	*Haliclona*	sp. 5		4	X			
Porifera	Demospongiae	Haplosclerida	Chalinidae	*Haliclona*	sp. 6		66	X			
Porifera	Demospongiae	Haplosclerida	Chalinidae	*Haliclona*	sp. 7		9	X			
Porifera	Demospongiae	Haplosclerida	Chalinidae	*Haliclona*	sp. 8		16	X			
Porifera	Demospongiae	Haplosclerida	Chalinidae	*Haliclona*	sp. 9		12			X	
Porifera	Demospongiae	Haplosclerida	Chalinidae	*Haliclona*	sp. 10		46			X	
Porifera	Demospongiae	Haplosclerida	Chalinidae	*Haliclona*	sp. 11		111	X	X	X	
Porifera	Demospongiae	Haplosclerida	Chalinidae	*Haliclona*	sp. 12		6		X		
Porifera	Demospongiae	Poecilosclerida	Crambeidae	*Crambe*	spp.		2				X
Porifera	Demospongiae	Poecilosclerida	Crambeidae	*Crambe*	*Crambe crambe*	Schmidt, 1862	1		X		
Porifera	Demospongiae	Poecilosclerida	Esperiopsidae	*Ulosa*	*Ulosa digitata*	Schmidt, 1866	25	X	X	X	
Porifera	Demospongiae	Poecilosclerida	Hymedesmiidae	*Hemimycale*	*Hemimycale columella*	Bowerbank, 1874	1				X
Porifera	Demospongiae	Poecilosclerida	Hymedesmiidae	*Phorbas*	*Phorbas tenacior*	Topsent, 1925	279	X	X	X	
Porifera	Demospongiae	Poecilosclerida	Microcionidae	*Clathria*	*Clathria compressa*	Schmidt, 1862	8			X	
Porifera	Demospongiae	Poecilosclerida	Mycalidae	*Mycale*	sp. 1		10			X	
Porifera	Demospongiae	Poecilosclerida	Tedaniidae	*Tedania*	sp. 1		18	X			
Porifera	Demospongiae	Polymastiida	Polymastiidae	*Polymastia*	spp.		1			X	
Porifera	Demospongiae	Suberitida	Halichondriidae	*Halichondria*	sp. 1		342	X			
Porifera	Demospongiae	Suberitida	Halichondriidae	*Halichondria*	sp. 2		85			X	
Porifera	Demospongiae	Suberitida	Halichondriidae	*Topsentia*	*Topsentia vaceleti*	Kefalas & Castritsi-Catharios, 2012	6	X		X	
Porifera	Demospongiae	Suberitida	Suberitidae	*Suberites*	spp.		20			X	
Porifera	Demospongiae	Suberitida	Suberitidae	*Suberites*	*Suberites domuncula*	Olivi, 1792	1			X	
Porifera	Demospongiae	Tethyida	Tethyidae	*Tethya*	sp. 1		1			X	

Porifera	Demospongiae	Tethyida	Tethyidae	*Tethya*	*Tethya aurantium*	Pallas, 1766	1				X	
Porifera	Demospongiae	Tethyida	Tethyidae	*Tethya*	*Tethya citrina*	Sarà & Melone, 1965	13	X	X		X	
Porifera	Demospongiae	Tetractinellida	Geodiidae	*Geodia*	*Geodia cydonium*	Linnaeus, 1767	1				X	
Porifera	Demospongiae	Tetractinellida	Geodiidae	*Geodia*	sp. 1		1				X	
Porifera	Demospongiae	Tetractinellida	Pachastrellidae	*Pachastrella*	*Pachastrella monilifera*	Schmidt, 1868	210	X			X	
Porifera	Demospongiae	Tetractinellida	Theneidae	*Thenea*	*Thenea muricata*	Bowerbank, 1858	1				X	
Porifera	Demospongiae	Tetractinellida	Vulcanellidae	*Poecillastra*	*Poecillastra compressa*	Bowerbank, 1866	245	X			X	
Porifera	Demospongiae	Verongiida	Aplysinidae	*Aplysina*	sp. 1		2	X				
Porifera	Demospongiae	Verongiida	Ianthellidae	*Hexadella*	*Hexadella racovitzai*	Topsent, 1896	255	X	X		X	X
Porifera	Demospongiae	Verongiida	Ianthellidae	*Hexadella*	sp. 1		1	X				
Porifera	Demospongiae				sp. 1		16		X		X	
Porifera	Demospongiae				sp. 2		65		X		X	
Porifera	Demospongiae				sp. 3		1		X			
Porifera	Demospongiae				sp. 4		1852	X	X		X	
Porifera	Demospongiae				sp. 5		42		X			
Porifera	Demospongiae				sp. 6		1				X	
Porifera	Demospongiae				sp. 7		1		X			
Porifera	Demospongiae				sp. 8		3	X			X	
Porifera	Demospongiae				sp. 9		27	X				
Porifera	Demospongiae				sp. 10		26	X				
Porifera	Demospongiae				sp. 11		32	X	X		X	
Porifera	Demospongiae				sp. 12		18				X	
Porifera	Demospongiae				sp. 13		357	X	X		X	X
Porifera	Demospongiae				sp. 14		14				X	
Porifera	Demospongiae				sp. 15		412	X	X		X	
Porifera	Demospongiae				sp. 16		17		X			
Porifera	Demospongiae				sp. 17		144				X	
Porifera	Demospongiae				sp. 18		3		X			
Porifera	Demospongiae				sp. 19		1					X
Porifera	Demospongiae				sp. 20		50		X		X	
Porifera	Demospongiae				sp. 21		210	X				

Porifera	Demospongiae				sp. 22		11				X	
Porifera	Demospongiae				sp. 23		346	X			X	
Porifera	Demospongiae				sp. 24		1				X	
Porifera	Demospongiae				sp. 25		2		X			
Porifera	Demospongiae				sp. 26		37				X	
Porifera	Demospongiae				sp. 27		2				X	
Porifera	Hexactinellida	Lyssacinosida	Rossellidae	*Sympagella*	*Sympagella delauzei*	Boury-Esnault, Vacelet, Reiswig & Chevaldonné, 2015	3	X				
Porifera	Homoscleromorpha	Homosclerophorida	Plakinidae	*Corticium*	spp.		1					X
Porifera	Homoscleromorpha	Homosclerophorida	Plakinidae	*Corticium*	*Corticium candelabrum*	Schmidt, 1862	2	X				
Cnidaria	Anthozoa	Actiniaria	Aliciidae	*Alicia*	*Alicia mirabilis*	Johnson, 1861	1					X
Cnidaria	Anthozoa	Actiniaria	Andresiidae	*Andresia*	*Andresia partenopea*	Andrès, 1883	3		X	X		
Cnidaria	Anthozoa	Actiniaria			spp.		3					X
Cnidaria	Anthozoa	Alcyonacea	Acanthogorgiidae	*Acanthogorgia*	*Acanthogorgia hirsuta*	Gray, 1857	1441	X	X			
Cnidaria	Anthozoa	Alcyonacea	Acanthogorgiidae	*Acanthogorgia*	*Acanthogorgia hirsuta*	Gray, 1857	2	X				
Cnidaria	Anthozoa	Alcyonacea	Alcyoniidae	*Alcyonium*	*Alcyonium coralloides*	Pallas, 1766	17	X				
Cnidaria	Anthozoa	Alcyonacea	Alcyoniidae	*Alcyonium*	*Alcyonium palmatum*	Pallas, 1766	50		X	X	X	
Cnidaria	Anthozoa	Alcyonacea	Coralliidae	*Corallium*	*Corallium rubrum*	Linnaeus, 1758	5	X				
Cnidaria	Anthozoa	Alcyonacea	Cornulariidae	*Cornularia*	*Cornularia cornucopiae*	Pallas, 1766	432	X	X			X
Cnidaria	Anthozoa	Alcyonacea	Gorgoniidae	*Eunicella*	spp.		7	X				
Cnidaria	Anthozoa	Alcyonacea	Gorgoniidae	*Eunicella*	*Eunicella cavolini*	Koch, 1887	6				X	
Cnidaria	Anthozoa	Alcyonacea	Gorgoniidae	*Eunicella*	*Eunicella singularis*	Esper, 1791	54					X
Cnidaria	Anthozoa	Alcyonacea	Gorgoniidae	*Eunicella*	*Eunicella verrucosa*	Pallas, 1766	9	X				
Cnidaria	Anthozoa	Alcyonacea	Nidaliidae	*Nidalia*	*Nidalia studeri*	von Koch, 1891	7	X				
Cnidaria	Anthozoa	Alcyonacea	Paralcyoniidae	*Paralcyonium*	*Paralcyonium spinulosum*	Delle Chiaje, 1822	29	X	X	X		X
Cnidaria	Anthozoa	Alcyonacea	Plexauridae	*Paramuricea*	*Paramuricea clavata*	Risso, 1826	8				X	
Cnidaria	Anthozoa	Alcyonacea	Plexauridae	*Paramuricea*	*Paramuricea macrospina*	Koch, 1882	2	X				
Cnidaria	Anthozoa	Alcyonacea	Plexauridae	*Swiftia*	*Swiftia pallida*	Madsen, 1970	63		X			
Cnidaria	Anthozoa	Alcyonacea	Primnoidae	*Callogorgia*	*Callogorgia verticillata*	Pallas, 1766	87	X				
Cnidaria	Anthozoa	Alcyonacea			sp. 1		12	X				
Cnidaria	Anthozoa	Antipatharia	Myriopathidae	*Antipathella*	*Antipathella subpinnata*	Ellis & Solander, 1786	3	X				
Cnidaria	Anthozoa	Penicillaria	Arachnactidae	*Arachnanthus*	*Arachnanthus oligopodus*	Cerfontaine, 1891	4		X		X	

Cnidaria	Anthozoa	Pennatulacea	Funiculinidae	*Funiculina*	*Funiculina quadrangularis*	Pallas, 1766	5			X	X	
Cnidaria	Anthozoa	Pennatulacea	Pennatulidae	*Pennatula*	*Pennatula phosphorea*	Linnaeus, 1758	19	X				X
Cnidaria	Anthozoa	Pennatulacea	Pennatulidae	*Pennatula*	*Pennatula rubra*	Ellis, 1761	167			X	X	
Cnidaria	Anthozoa	Pennatulacea	Virgulariidae	*Virgularia*	*Virgularia mirabilis*	Müller, 1776	2		X			
Cnidaria	Anthozoa	Scleractinia	Caryophylliidae	*Caryophyllia*	sp. 1		197	X	X		X	
Cnidaria	Anthozoa	Scleractinia	Caryophylliidae	*Caryophyllia*	sp. 2		152	X	X		X	
Cnidaria	Anthozoa	Scleractinia	Caryophylliidae		spp.	Lamarck, 1801	2		X			
Cnidaria	Anthozoa	Scleractinia	Caryophylliidae		sp. 1		938	X	X		X	
Cnidaria	Anthozoa	Scleractinia	Caryophylliidae		sp. 2		85				X	
Cnidaria	Anthozoa	Scleractinia	Dendrophylliidae	*Balanophyllia*	*Balanophyllia europaea*	Risso, 1826	1		X			
Cnidaria	Anthozoa	Scleractinia	Dendrophylliidae	*Balanophyllia*	sp. 1		2				X	
Cnidaria	Anthozoa	Scleractinia	Dendrophylliidae	*Dendrophyllia*	*Dendrophyllia cornigera*	Lamarck, 1816	148	X			X	
Cnidaria	Anthozoa	Spirularia	Cerianthidae	*Cerianthus*	spp.	Delle Chiaje, 1841	1		X			
Cnidaria	Anthozoa	Spirularia	Cerianthidae	*Cerianthus*	*Cerianthus membranaceus*	Gmelin, 1791	41		X	X	X	X
Cnidaria	Anthozoa	Spirularia	Cerianthidae		spp.		3				X	
Cnidaria	Anthozoa	Spirularia	Cerianthidae		sp. 1		2		X			
Cnidaria	Anthozoa	Zoantharia	Epizoanthidae	*Epizoanthus*	sp. 1		16	X	X			
Cnidaria	Anthozoa	Zoantharia	Epizoanthidae	*Epizoanthus*	sp. 2		2					X
Cnidaria	Anthozoa	Zoantharia	Parazoanthidae	*Parazoanthus*	sp. 1		22		X		X	
Cnidaria	Hydrozoa	Leptothecata	Aglaopheniidae	*Aglaophenia*	sp. 1		24	X			X	
Cnidaria	Hydrozoa	Leptothecata	Aglaopheniidae	*Lytocarpia*	*Lytocarpia myriophyllum*	Linnaeus, 1758	105			X	X	
Cnidaria	Hydrozoa	Leptothecata	Plumulariidae	*Nemertesia*	spp.	Lamouroux, 1812	30	X	X		X	
Mollusca	Bivalvia	Cardiida	Cardiidae	*Acanthocardia*	*Acanthocardia aculeata*	Linnaeus, 1758	3				X	
Mollusca	Bivalvia	Cardiida	Cardiidae	*Acanthocardia*	sp. 1		1				X	
Mollusca	Bivalvia	Ostreida	Gryphaeidae	*Neopycnodonte*	*Neopycnodonte cochlear*	Poli, 1795	115			X	X	X
Mollusca	Bivalvia	Ostreida	Pteriidae	*Pteria*	*Pteria hirundo*	Linnaeus, 1758	2		X	X		
Mollusca	Bivalvia	Pectinida	Pectinidae	*Pecten*	spp.		1					X
Mollusca	Cephalopoda	Octopoda	Eledonidae	*Eledone*	*Eledone cirrhosa*	Lamarck, 1798	4			X		
Mollusca	Cephalopoda	Octopoda	Octopodidae	*Callistoctopus*	*Callistoctopus macropus*	Risso, 1826	1				X	
Mollusca	Cephalopoda	Octopoda	Octopodidae	*Octopus*	*Octopus vulgaris*	Cuvier, 1797	2			X	X	
Mollusca	Cephalopoda	Sepiida	Sepiidae	*Sepia*	spp.		2	X		X		

Mollusca	Gastropoda	Littorinimorpha	Cypraeidae	*Naria*	spp.		3	X				
Mollusca	Gastropoda	Neogastropoda	Columbellidae	*Columbella*	*Columbella rustica*	Linnaeus, 1758	1					X
Mollusca	Gastropoda	Neogastropoda	Fasciolariidae	*Fusinus*	spp.		1				X	
Mollusca	Gastropoda	Neogastropoda	Fasciolariidae	*Tarantinaea*	spp.		1				X	
Mollusca	Gastropoda	Neogastropoda	Muricidae	*Hexaplex*	*Hexaplex trunculus*	Linnaeus, 1758	1				X	
Mollusca	Gastropoda	Nudibranchia	Chromodorididae	*Felimare*	*Felimare tricolor*	Cantraine, 1835	4				X	X
Mollusca	Gastropoda	Nudibranchia	Discodorididae	*Discodoris*	spp.		5		X			
Mollusca	Gastropoda	Nudibranchia	Discodorididae	*Platydoris*	*Platydoris argo*	Linnaeus, 1767	2		X			
Mollusca	Gastropoda	Nudibranchia	Myrrhinidae	*Dondice*	*Dondice banyulensis*	Portmann & Sandmeier, 1960	1				X	
Mollusca	Gastropoda	Pleurobranchida	Pleurobranchidae	*Pleurobranchus*	*Pleurobranchus testudinarius*	Cantraine, 1835	1				X	
Mollusca	Gastropoda	Trochida	Calliostomatidae	*Calliostoma*	spp.		2	X			X	
Mollusca	Gastropoda	Trochida	Turbinidae	*Bolma*	*Bolma rugosa*	Linnaeus, 1767	1		X			
Mollusca	Gastropoda		Plakobranchidae	*Elysia*	sp. 1		1		X			
Mollusca	Gastropoda				spp.	"						
Mollusca	Gastropoda				sp. 1							
Mollusca	Gastropoda				sp. 2		3				X	
Annelida	Polychaeta	Echiuroidea	Bonelliidae	*Bonellia*	*Bonellia viridis*		1				X	
Annelida	Polychaeta	Sabellida	Sabellidae	*Sabella*	spp.	Rolando, 1822	58	X	X		X	X
Annelida	Polychaeta	Sabellida	Sabellidae	*Sabella*	*Sabella pavonina*	Linnaeus, 1767	7			X	X	
Annelida	Polychaeta	Sabellida	Sabellidae	*Sabella*	sp. 1	Savigny, 1822	111		X	X	X	X
Annelida	Polychaeta	Sabellida	Sabellidae		spp.		37	X	X	X	X	X
Annelida	Polychaeta	Sabellida	Sabellidae		sp. 1	Latreille, 1825	5		X			X
Annelida	Polychaeta	Sabellida	Serpulidae	*Filograna*	*Filograna implexa*		2		X			
Annelida	Polychaeta	Sabellida	Serpulidae	*Protula*	sp. 1	Berkeley, 1835	395	X	X	X	X	
Annelida	Polychaeta	Sabellida	Serpulidae	*Serpula*	*Serpula vermicularis*		110	X	X		X	X
Annelida	Polychaeta	Sabellida	Serpulidae	*Vermiliopsis*	sp. 1	Linnaeus, 1767	1				X	
Annelida	Polychaeta	Sabellida	Serpulidae		spp.		4		X		X	
Annelida	Polychaeta	Terebellida	Terebellidae	*Lanice*	*Lanice conchilega*	Rafinesque, 1815	9	X	X	X	X	
Annelida	Polychaeta	Terebellida	Trichobranchidae	*Terebellides*	sp. 1	Pallas, 1766	48	X	X		X	
Arthropoda	Malacostraca	Decapoda	Calappidae	*Calappa*	*Calappa granulata*		7	X			X	
Arthropoda	Malacostraca	Decapoda	Inachidae	*Inachus*	*Inachus phalangium*	Linnaeus, 1758	1				X	

Arthropoda	Malacostraca	Decapoda	Inachidae	*Macropodia*	*Macropodia longirostris*	Fabricius, 1775	7		X	X	X	
Arthropoda	Malacostraca	Decapoda	Munididae	*Munida*	spp.	Fabricius, 1775	1				X	
Arthropoda	Malacostraca	Decapoda	Munididae	*Munida*	*Munida tenuimana*		11		X		X	
Arthropoda	Malacostraca	Decapoda	Paguridae	*Paguristes*	*Paguristes longirostris*	Sars, 1872	8		X			
Arthropoda	Malacostraca	Decapoda	Paguridae		spp.	Dana, 1851	1				X	
Arthropoda	Malacostraca	Decapoda	Paguridae		sp. 1	Latreille, 1802	4		X	X	X	
Arthropoda	Malacostraca	Decapoda	Paguridae		sp. 2		3				X	
Arthropoda	Malacostraca	Decapoda	Paguridae		sp. 3		3		X			X
Arthropoda	Malacostraca	Decapoda	Paguridae		sp. 4		1					X
Arthropoda	Malacostraca	Decapoda	Palinuridae	*Palinurus*	*Palinurus elephas*		2				X	
Arthropoda	Malacostraca	Decapoda	Parthenopidae	*Spinolambrus*	spp.	Fabricius, 1787	7	X	X		X	
Arthropoda	Malacostraca	Decapoda	Polybiidae	*Liocarcinus*	spp.		1					X
Arthropoda	Malacostraca	Decapoda	Polybiidae	*Liocarcinus*	*Liocarcinus depurator*		2		X			
Arthropoda	Malacostraca	Decapoda			spp.	Linnaeus, 1758	1				X	
Arthropoda	Malacostraca	Decapoda			sp. 1	Latreille, 1802	2				X	
Arthropoda	Malacostraca	Decapoda			sp. 2		2	X				
Arthropoda	Malacostraca	Euphausiacea			spp.	Latreille, 1802	13	X		X	X	
Bryozoa	Gymnolaemata	Cheilostomatida	Adeonidae	*Adeonella*	*Adeonella calveti*		1				X	
Bryozoa	Gymnolaemata	Cheilostomatida	Bitectiporidae	*Pentapora*	*Pentapora fascialis*	Canu & Bassler, 1930	2				X	
Bryozoa	Gymnolaemata	Cheilostomatida	Bitectiporidae	*Schizomavella*	*Schizomavella linearis*	Pallas, 1766	80		X		X	
Bryozoa	Gymnolaemata	Cheilostomatida	Bitectiporidae	*Schizomavella*	*Schizomavella mamillata*	Hassall, 1841	1					X
Bryozoa	Gymnolaemata	Cheilostomatida	Bitectiporidae	*Schizomavella*	sp. 1	Hincks, 1880	2076		X		X	X
Bryozoa	Gymnolaemata	Cheilostomatida	Bugulidae	*Bugula*	spp.		2				X	
Bryozoa	Gymnolaemata	Cheilostomatida	Celleporidae	*Turbicellepora*	*Turbicellepora avicularis*		1		X			
Bryozoa	Gymnolaemata	Cheilostomatida	Myriaporidae	*Myriapora*	spp.	Hincks, 1860	1		X			
Bryozoa	Gymnolaemata	Cheilostomatida	Myriaporidae	*Myriapora*	*Myriapora truncata*		4				X	
Bryozoa	Gymnolaemata	Cheilostomatida	Phidoloporidae	*Reteporella*	spp.	Pallas, 1766	16		X		X	X
Bryozoa	Gymnolaemata	Cheilostomatida	Phidoloporidae	*Reteporella*	*Reteporella grimaldii*	Busk, 1884	2	X				
Bryozoa	Gymnolaemata	Cheilostomatida	Phidoloporidae	*Reteporella*	sp. 1	Jullien, 1903	42	X	X		X	
Bryozoa	Gymnolaemata	Cheilostomatida	Smittinidae	*Smittina*	*Smittina cervicornis*		2		X			
Bryozoa	Stenolaemata	Cyclostomatida	Horneridae	*Hornera*	*Hornera frondiculata*	Pallas, 1766	296	X	X		X	

Echinodermata	Asteroidea	Forcipulatida	Asteriidae	*Coscinasterias*	*Coscinasterias tenuispina*	Lamarck, 1816	61		X		X	
Echinodermata	Asteroidea	Forcipulatida	Asteriidae	*Marthasterias*	*Marthasterias glacialis*	Lamarck, 1816	1				X	
Echinodermata	Asteroidea	Paxillosida	Astropectinidae	*Astropecten*	spp.	Linnaeus, 1758	8				X	X
Echinodermata	Asteroidea	Paxillosida	Astropectinidae	*Astropecten*	*Astropecten aranciacus*		3			X		X
Echinodermata	Asteroidea	Paxillosida	Luidiidae	*Luidia*	*Luidia ciliaris*	Linnaeus, 1758	1					X
Echinodermata	Asteroidea	Spinulosida	Echinasteridae	*Echinaster*	*Echinaster sepositus*	Philippi, 1837	1				X	
Echinodermata	Asteroidea	Valvatida	Chaetasteridae	*Chaetaster*	*Chaetaster longipes*	Retzius, 1783	45	X	X		X	X
Echinodermata	Asteroidea	Valvatida	Goniasteridae	*Peltaster*	*Peltaster placenta*	Bruzelius, 1805	5	X			X	
Echinodermata	Asteroidea	Valvatida	Ophidiasteridae	*Hacelia*	*Hacelia attenuata*	Müller & Troschel, 1842	42	X	X		X	
Echinodermata	Crinoidea	Comatulida	Antedonidae	*Antedon*	*Antedon mediterranea*	Gray, 1840	5	X				
Echinodermata	Crinoidea	Comatulida	Antedonidae	*Leptometra*	*Leptometra phalangium*	Lamarck, 1816	127	X	X		X	X
Echinodermata	Echinoidea	Camarodonta	Echinidae	*Echinus*	*Echinus melo*	Müller, 1841	11			X	X	
Echinodermata	Echinoidea	Cidaroida	Cidaridae	*Cidaris*	*Stylocidaris affinis*	Lamarck, 1816	12	X	X			
Echinodermata	Echinoidea	Cidaroida	Cidaridae	*Cidaris*	*Cidaris cidaris*	Philippi, 1845	751	X	X	X		X
Echinodermata	Echinoidea	Diadematoida	Diadematidae	*entrostephanus*	*Centrostephanus longispinus*	Linnaeus, 175	59	X		X	X	
Echinodermata	Echinoidea	Holothuriida	Holothuriidae	*Holothuria*	spp.	Philippi, 1845	14		X		X	X
Echinodermata	Echinoidea	Holothuriida	Holothuriidae	*Holothuria*	*Holothuria forskali*		1			X		
Echinodermata	Echinoidea	Holothuriida	Holothuriidae	*Holothuria*	*Holothuria poli*	Delle Chiaje, 1823	5	X			X	X
Echinodermata	Echinoidea	Holothuriida	Holothuriidae	*Holothuria*	*Holothuria tubulosa*	Delle Chiaje, 1824	5	X			X	
Echinodermata	Echinoidea	Spatangoida	Brissidae	*Brissus*	*Brissus unicolor*	Gmelin, 1788	2		X			
Echinodermata	Echinoidea	Spatangoida	Spatangidae	*Spatangus*	*Spatangus purpureus*	Leske, 1778	1					X
Echinodermata	Holothuroidea	Dendrochirotida	Cucumariidae	*Cucumaria*	sp. 1	O.F. Müller, 1776	82			X		X
Echinodermata	Holothuroidea	Holothuriida	Mesothuriidae	*Mesothuria*	spp.		2				X	
Echinodermata	Holothuroidea	Synallactida	Stichopodidae	*Parastichopus*	*Parastichopus regalis*		1		X			
Echinodermata	Ophiuroidea	Amphilepidida	Ophiopsilidae	*Ophiopsila*	spp.	Cuvier, 1817	1			X		
Echinodermata	Ophiuroidea	Amphilepidida	Ophiotrichidae	*Ophiothrix*	*Ophiothrix fragilis*		2					X
Echinodermata	Ophiuroidea	Euryalida	Gorgonocephalidae	*Astrospartus*	*Astrospartus mediterraneus*	Abildgaard in O.F. Müller, 1789	890		X	X	X	X
Echinodermata	Ophiuroidea	Ophiacanthida	Ophiodermatidae	*Ophioderma*	spp.	Risso, 1826	5	X				
Echinodermata	Ophiuroidea	Ophiacanthida	Ophiomyxidae	*Ophiomyxa*	*Ophiomyxa pentagona*		1		X			
Echinodermata	Ophiuroidea				sp. 1	Lamarck, 1816	1			X		
Chordata	Actinopterygii	Anguilliformes	Congridae	*Ariosoma*	*Ariosoma balearicum*		35				X	

Chordata	Actinopterygii	Anguilliformes	Muraenidae	*Muraena*	*Muraena helena*	Delaroche, 1809	3				X	
Chordata	Actinopterygii	Anguilliformes	Ophichthidae	*Ophisurus*	*Ophisurus serpens*	Linnaeus, 1758	23	X	X		X	
Chordata	Actinopterygii	Anguilliformes			spp.	Linnaeus, 1758	1			X		
Chordata	Actinopterygii	Gadiformes	Phycidae	*Phycis*	spp.		6				X	
Chordata	Actinopterygii	Gadiformes	Phycidae	*Phycis*	*Phycis blennoides*		3	X			X	
Chordata	Actinopterygii	Gadiformes	Phycidae	*Phycis*	*Phycis phycis*	Brünnich, 1768	3	X				
Chordata	Actinopterygii	Perciformes	Callanthiidae	*Callanthias*	*Callanthias ruber*	Linnaeus, 1766	1				X	
Chordata	Actinopterygii	Perciformes	Gobiidae		spp.	Rafinesque, 1810	161	X	X		X	X
Chordata	Actinopterygii	Perciformes	Labridae	*Ctenolabrus*	*Ctenolabrus rupestris*		9			X		
Chordata	Actinopterygii	Perciformes	Labridae	*Lappanella*	*Lappanella fasciata*	Linnaeus, 1758	2				X	
Chordata	Actinopterygii	Perciformes	Mullidae	*Mullus*	spp.	Cocco, 1833	2				X	
Chordata	Actinopterygii	Perciformes	Mullidae	*Mullus*	*Mullus barbatus*		2				X	X
Chordata	Actinopterygii	Perciformes	Pomacentridae	*Chromis*	spp.	Linnaeus, 1758	4				X	
Chordata	Actinopterygii	Perciformes	Scorpaenidae	*Scorpaena*	*Scorpaena scrofa*		43					X
Chordata	Actinopterygii	Perciformes	Serranidae	*Serranus*	spp.	Linnaeus, 1758	21	X	X	X	X	
Chordata	Actinopterygii	Perciformes	Serranidae	*Serranus*	*Serranus cabrilla*		3				X	
Chordata	Actinopterygii	Perciformes	Serranidae	*Serranus*	*Serranus hepatus*	Linnaeus, 1758	31	X	X	X	X	X
Chordata	Actinopterygii	Perciformes	Serranidae		sp. 1	Linnaeus, 1758	4			X		
Chordata	Actinopterygii	Perciformes	Sparidae	*Pagellus*	spp.		2				X	
Chordata	Actinopterygii	Perciformes	Sparidae	*Pagellus*	*Pagellus erythrinus*		5		X		X	
Chordata	Actinopterygii	Perciformes	Sparidae	*Spondyliosoma*	*Spondyliosoma cantharus*	Linnaeus, 1758	1				X	
Chordata	Actinopterygii	Perciformes	Sparidae		spp.	Linnaeus, 1758	1				X	
Chordata	Actinopterygii	Perciformes	Synodontidae	*Synodus*	*Synodus saurus*		1				X	
Chordata	Actinopterygii	Perciformes	Trachinidae	*Trachinus*	spp.	Linnaeus, 1758	1				X	
Chordata	Actinopterygii	Perciformes	Trachinidae	*Trachinus*	*Trachinus araneus*		1					X
Chordata	Actinopterygii	Perciformes	Triglidae	*Eutrigla*	sp. 1	Cuvier, 1829	2			X		
Chordata	Actinopterygii	Pleuronectiformes	Soleidae	*Solea*	*Solea solea*		1			X		
Chordata	Actinopterygii	Scorpaeniformes	Sebastidae	*Helicolenus*	*Helicolenus dactylopterus*	Linnaeus, 1758	1				X	
Chordata	Actinopterygii	Scorpaeniformes	Triglidae	*Chelidonichthys*	*Chelidonichthys lastoviza*	Delaroche, 1809	17	X		X		
Chordata	Actinopterygii	Scorpaeniformes	Triglidae	*Chelidonichthys*	*Chelidonichthys lucerna*	Bonnaterre, 1788	8					X
Chordata	Actinopterygii	Scorpaeniformes	Triglidae	*Lepidotrigla*	*Lepidotrigla cavillone*	Linnaeus, 1758	1	X				

Chordata	Actinopterygii	Zeiformes	Zeidae	*Zeus*	*Zeus faber*	Lacepède, 1801	3		X	X		
Chordata	Actinopterygii				sp. 1	Linnaeus, 1758	4	X			X	X
Chordata	Ascidiacea	Aplousobranchia	Clavelinidae	*Clavelina*	sp. 1		15					X
Chordata	Ascidiacea	Aplousobranchia	Diazonidae	*Rhopalaea*	spp.		4	X				
Chordata	Ascidiacea	Aplousobranchia	Diazonidae	*Rhopalaea*	*Rhopalaea neapolitana*		7		X			
Chordata	Ascidiacea	Aplousobranchia	Didemnidae	*Diplosoma*	*Diplosoma spongiforme*	Philippi, 1843	4		X			
Chordata	Ascidiacea	Aplousobranchia	Didemnidae	*Polysyncraton*	*Polysyncraton lacazei*	Giard, 1872	9		X		X	
Chordata	Ascidiacea	Aplousobranchia	Didemnidae		sp. 1	Giard, 1872	4		X		X	
Chordata	Ascidiacea	Aplousobranchia	Didemnidae		sp. 2		41		X		X	
Chordata	Ascidiacea	Aplousobranchia	Didemnidae		sp. 3		6				X	
Chordata	Ascidiacea	Aplousobranchia	Polyclinidae	*Aplidium*	sp. 1		18	X			X	
Chordata	Ascidiacea	Phlebobranchia	Cionidae	*Ciona*	spp.		4	X				
Chordata	Ascidiacea	Stolidobranchia	Pyuridae	*Halocynthia*	*Halocynthia papillosa*		3		X			
Chordata	Ascidiacea				spp.	Linnaeus, 1767	66	X	X		X	X
Chordata	Ascidiacea				sp. 1		1			X	X	
Chordata	Ascidiacea				sp. 2		8		X		X	
Chordata	Ascidiacea				sp. 3		5	X				
Chordata	Ascidiacea				sp. 4		6				X	

Tab. S3.2. Biological traits with relative categories used for functional analysis.

Trait	Category
Adult body dimension	Meiofauna (<2 mm)
	Macrofauna (2mm - 2 cm)
	Megafauna (>2 cm)
	Macroalgae
Domain of adult stage	Benthic
	Pelagic
Adult motility	Sessile
	Facultatively motile
	Vagile
	Swimmer
Feeding strategy (most frequent in adult stage)	Deposit feeder
	Grazer
	Filter feeder
	Suspension feeder
	Scavenger/predator
	Photosynthetic metabolism
Sociability (aggregation degree)	Solitary
	Gregarious
	Colonial
Ability to build habitat	Habitat-builder
	Non habitat-builder

Tab. S3.3. Taxonomic richness and standard errors with 100 frames resulting from species accumulation curves for ROV dives and assemblage categories. “Mean n. Taxa” refers to the mean number of taxa for the different assemblages.

ROV	Assemblage	n. Taxa	Mean n. Taxa / assemblage
MS15_184	C	17.25 ± 3.4	24.15 ± 4.6
MS16_II_83	C	32.83 ± 2.1	
MS16_II_89	C	22.38 ± 3.1	
MS16_186	CN	30.33 ± 3.6	21.16 ± 4.2
MS16_203	CN	26.12 ± 3.9	
MS17_II_92	CN	13.39 ± 1.6	
MS17_II_93	CN	14.81 ± 1.8	
MS15_47	DWOR	5.13 ± 1.9	18.4 ± 2.7
MS15_118	DWOR	16.1 ± 3.2	
MS15_127	DWOR	25.5 ± 4.4	
MS17_II_115	DWOR	25.64 ± 2.8	
MS17_II_117	DWOR	18.81 ± 3.7	
MS17_III_110	DWOR	16.32 ± 3.2	
MS17_III_115	DWOR	21.33 ± 3.2	
MS15_79	MB	16.82 ± 4.2	6.83 ± 2.5
MS15_144	MB	1.45 ± 0.5	
MS17_I_103	MB	3.7 ± 1.3	
MS17_I_136	MB	6.48 ± 1.4	
MS17_II_165	MB	0.41 ± 0.6	
MS17_II_180	MB	15.66 ± 2.5	
MS17_II_83	MB	3.32 ± 1.1	
MS16_21	RB	5.61 ± 1.6	5.33 ± 0.2
MS16_128	RB	5.65 ± 1.9	
MS16_197	RB	5.43 ± 1.4	
MS16_142	RB	4.64 ± 2.5	

Tab. S3.4. Classification of identified taxa using functional traints. NHB: non habitat builder; HB: habitat builder.

Phylum	Class	Order	Family	Genus	Species	Adult dimension	Domain	Adult motility	Feeding strategy	Sociability	Ability to build habitat
Chlorophyta	Pyramimonadophyceae	Palmophyllales	Palmophyllaceae	*Palmophyllum*	*Palmophyllum crassum*	Macroalgae	Benthic	Sessile	Photosynthetic	Single	NHB
Chlorophyta	Ulvophyceae	Bryopsidales	Codiaceae	*Codium*	spp.	Macroalgae	Benthic	Sessile	Photosynthetic	Single	NHB
Chlorophyta	Ulvophyceae	Bryopsidales	Codiaceae	*Codium*	*Codium bursa*	Macroalgae	Benthic	Sessile	Photosynthetic	Single	NHB
Ochrophyta	Phaeophyceae	Dictyotales	Dictyotaceae	*Dictyota*	*Dictyota dichotoma*	Macroalgae	Benthic	Sessile	Photosynthetic	Single	NHB
Ochrophyta	Phaeophyceae	Ectocarpales	Acinetosporaceae	*Acinetospora*	*Acinetospora crinita*	Macroalgae	Benthic	Sessile	Photosynthetic	Single	NHB
Rhodophyta	Florideophyceae	Corallinales			spp.	Macroalgae	Benthic	Sessile	Photosynthetic	Single	NHB
Foraminifera	Globothalamea	Rotaliida	Homotrematidae	*Miniacina*	*Miniacina miniacea*	Macrofauna	Benthic	Vagile	Scavenger/Predator	Single	NHB
Porifera	Calcarea	Clathrinida	Clathrinidae	*Clathrina*	*Clathrina blanca*	Megafauna	Benthic	Sessile	Filter feeder	Single	NHB
Porifera	Calcarea	Clathrinida	Clathrinidae	*Clathrina*	spp.	Megafauna	Benthic	Sessile	Filter feeder	Single	NHB
Porifera	Demospongiae	Agelasida	Agelasidae	*Agelas*	*Agelas oroides*	Megafauna	Benthic	Sessile	Filter feeder	Single	NHB
Porifera	Demospongiae	Axinellida	Axinellidae	*Axinella*	*Axinella polypoides*	Megafauna	Benthic	Sessile	Filter feeder	Single	HB
Porifera	Demospongiae	Axinellida	Axinellidae	*Axinella*	sp. 1	Megafauna	Benthic	Sessile	Filter feeder	Single	HB
Porifera	Demospongiae	Axinellida	Axinellidae	*Axinella*	sp. 2	Megafauna	Benthic	Sessile	Filter feeder	Single	HB
Porifera	Demospongiae	Axinellida	Axinellidae	*Axinella*	sp. 3	Megafauna	Benthic	Sessile	Filter feeder	Single	HB
Porifera	Demospongiae	Axinellida	Raspailiidae	*Raspailia*	*Raspailia hispida*	Megafauna	Benthic	Sessile	Filter feeder	Single	NHB
Porifera	Demospongiae	Axinellida	Raspailiidae	*Raspailia*	*Raspailia viminalis*	Megafauna	Benthic	Sessile	Filter feeder	Single	NHB
Porifera	Demospongiae	Bubarida	Dictyonellidae	*Dictyonella*	*Dictyonella incisa*	Megafauna	Benthic	Sessile	Filter feeder	Single	NHB
Porifera	Demospongiae	Chondrosiida	Chondrosiidae	*Chondrosia*	*Chondrosia reniformis*	Megafauna	Benthic	Sessile	Filter feeder	Single	NHB
Porifera	Demospongiae	Clionaida	Clionaidae	*Cliona*	sp. 1	Megafauna	Benthic	Sessile	Filter feeder	Single	NHB
Porifera	Demospongiae	Clionaida	Spirastrellidae	*Spirastrella*	*Spirastrella cunctatrix*	Megafauna	Benthic	Sessile	Filter feeder	Single	NHB
Porifera	Demospongiae	Dictyoceratida	Dysideidae	*Dysidea*	sp. 1	Megafauna	Benthic	Sessile	Filter feeder	Single	NHB
Porifera	Demospongiae	Dictyoceratida	Irciniidae	*Ircinia*	*Ircinia variabilis*	Megafauna	Benthic	Sessile	Filter feeder	Single	NHB
Porifera	Demospongiae	Dictyoceratida	Irciniidae	*Ircinia*	spp.	Megafauna	Benthic	Sessile	Filter feeder	Single	NHB
Porifera	Demospongiae	Dictyoceratida	Spongiidae	*Spongia*	spp.	Megafauna	Benthic	Sessile	Filter feeder	Single	NHB
Porifera	Demospongiae	Dictyoceratida	Spongiidae	*Spongia*	*Spongia agaricina*	Megafauna	Benthic	Sessile	Filter feeder	Single	NHB
Porifera	Demospongiae	Dictyoceratida	Spongiidae	*Spongia*	*Spongia lamella*	Megafauna	Benthic	Sessile	Filter feeder	Single	NHB
Porifera	Demospongiae	Dictyoceratida	Spongiidae	*Spongia*	*Spongia officinalis*	Megafauna	Benthic	Sessile	Filter feeder	Single	NHB
Porifera	Demospongiae	Dictyoceratida	Thorectidae	*Scalarispongia*	spp.	Megafauna	Benthic	Sessile	Filter feeder	Single	NHB
Porifera	Demospongiae	Haplosclerida	Petrosiidae	*Petrosia*	*Petrosia ficiformis*	Megafauna	Benthic	Sessile	Filter feeder	Single	NHB
Porifera	Demospongiae	Haplosclerida	Chalinidae	*Haliclona*	*Haliclona fulva*	Megafauna	Benthic	Sessile	Filter feeder	Single	NHB
Porifera	Demospongiae	Haplosclerida	Chalinidae	*Haliclona*	sp. 1	Megafauna	Benthic	Sessile	Filter feeder	Single	NHB
Porifera	Demospongiae	Haplosclerida	Chalinidae	*Haliclona*	sp. 2	Megafauna	Benthic	Sessile	Filter feeder	Single	NHB
Porifera	Demospongiae	Haplosclerida	Chalinidae	*Haliclona*	sp. 3	Megafauna	Benthic	Sessile	Filter feeder	Single	NHB
Porifera	Demospongiae	Haplosclerida	Chalinidae	*Haliclona*	sp. 4	Megafauna	Benthic	Sessile	Filter feeder	Single	NHB
Porifera	Demospongiae	Haplosclerida	Chalinidae	*Haliclona*	sp. 5	Megafauna	Benthic	Sessile	Filter feeder	Single	NHB
Porifera	Demospongiae	Haplosclerida	Chalinidae	*Haliclona*	sp. 6	Megafauna	Benthic	Sessile	Filter feeder	Single	NHB
Porifera	Demospongiae	Haplosclerida	Chalinidae	*Haliclona*	sp. 7	Megafauna	Benthic	Sessile	Filter feeder	Single	NHB

Porifera	Demospongiae	Haplosclerida	Chalinidae	*Haliclona*	sp. 8	Megafauna	Benthic	Sessile	Filter feeder	Single	NHB
Porifera	Demospongiae	Haplosclerida	Chalinidae	*Haliclona*	sp. 9	Megafauna	Benthic	Sessile	Filter feeder	Single	NHB
Porifera	Demospongiae	Haplosclerida	Chalinidae	*Haliclona*	sp. 10	Megafauna	Benthic	Sessile	Filter feeder	Single	NHB
Porifera	Demospongiae	Haplosclerida	Chalinidae	*Haliclona*	sp. 11	Megafauna	Benthic	Sessile	Filter feeder	Single	NHB
Porifera	Demospongiae	Haplosclerida	Chalinidae	*Haliclona*	sp. 12	Megafauna	Benthic	Sessile	Filter feeder	Single	NHB
Porifera	Demospongiae	Poecilosclerida	Crambeidae	*Crambe*	*Crambe crambe*	Megafauna	Benthic	Sessile	Filter feeder	Single	NHB
Porifera	Demospongiae	Poecilosclerida	Crambeidae	*Crambe*	spp.	Megafauna	Benthic	Sessile	Filter feeder	Single	NHB
Porifera	Demospongiae	Poecilosclerida	Esperiopsidae	*Ulosa*	*Ulosa digitata*	Megafauna	Benthic	Sessile	Filter feeder	Single	NHB
Porifera	Demospongiae	Poecilosclerida	Hymedesmiidae	*Hemimycale*	*Hemimycale columella*	Megafauna	Benthic	Sessile	Filter feeder	Single	NHB
Porifera	Demospongiae	Poecilosclerida	Hymedesmiidae	*Phorbas*	*Phorbas tenacior*	Megafauna	Benthic	Sessile	Filter feeder	Single	NHB
Porifera	Demospongiae	Poecilosclerida	Microcionidae	*Clathria*	*Clathria compressa*	Megafauna	Benthic	Sessile	Filter feeder	Single	NHB
Porifera	Demospongiae	Poecilosclerida	Mycalidae	*Mycale*	sp. 1	Megafauna	Benthic	Sessile	Filter feeder	Single	NHB
Porifera	Demospongiae	Poecilosclerida	Tedaniidae	*Tedania*	sp. 1	Megafauna	Benthic	Sessile	Filter feeder	Single	NHB
Porifera	Demospongiae	Polymastiida	Polymastiidae	*Polymastia*	spp.	Megafauna	Benthic	Sessile	Filter feeder	Single	NHB
Porifera	Demospongiae	Suberitida	Halichondriidae	*Halichondria*	sp. 1	Megafauna	Benthic	Sessile	Filter feeder	Single	NHB
Porifera	Demospongiae	Suberitida	Halichondriidae	*Halichondria*	sp. 2	Megafauna	Benthic	Sessile	Filter feeder	Single	NHB
Porifera	Demospongiae	Suberitida	Halichondriidae	*Topsentia*	*Topsentia vaceleti*	Megafauna	Benthic	Sessile	Filter feeder	Single	NHB
Porifera	Demospongiae	Suberitida	Suberitidae	*Suberites*	spp.	Megafauna	Benthic	Sessile	Filter feeder	Single	NHB
Porifera	Demospongiae	Suberitida	Suberitidae	*Suberites*	*Suberites domuncula*	Megafauna	Benthic	Sessile	Filter feeder	Single	NHB
Porifera	Demospongiae	Tethyida	Tethyidae	*Tethya*	sp. 1	Megafauna	Benthic	Sessile	Filter feeder	Single	NHB
Porifera	Demospongiae	Tethyida	Tethyidae	*Tethya*	*Tethya aurantium*	Megafauna	Benthic	Sessile	Filter feeder	Single	NHB
Porifera	Demospongiae	Tethyida	Tethyidae	*Tethya*	*Tethya citrina*	Megafauna	Benthic	Sessile	Filter feeder	Single	NHB
Porifera	Demospongiae	Tetractinellida	Geodiidae	*Geodia*	*Geodia cydonium*	Megafauna	Benthic	Sessile	Filter feeder	Single	NHB
Porifera	Demospongiae	Tetractinellida	Geodiidae	*Geodia*	sp. 1	Megafauna	Benthic	Sessile	Filter feeder	Single	NHB
Porifera	Demospongiae	Tetractinellida	Pachastrellidae	*Pachastrella*	*Pachastrella monilifera*	Megafauna	Benthic	Sessile	Filter feeder	Single	HB
Porifera	Demospongiae	Tetractinellida	Theneidae	*Thenea*	*Thenea muricata*	Megafauna	Benthic	Sessile	Filter feeder	Single	NHB
Porifera	Demospongiae	Tetractinellida	Vulcanellidae	*Poecillastra*	*Poecillastra compressa*	Megafauna	Benthic	Sessile	Filter feeder	Single	HB
Porifera	Demospongiae	Verongiida	Aplysinidae	*Aplysina*	sp. 1	Megafauna	Benthic	Sessile	Filter feeder	Single	NHB
Porifera	Demospongiae	Verongiida	Ianthellidae	*Hexadella*	*Hexadella racovitzai*	Megafauna	Benthic	Sessile	Filter feeder	Single	NHB
Porifera	Demospongiae	Verongiida	Ianthellidae	*Hexadella*	sp. 1	Megafauna	Benthic	Sessile	Filter feeder	Single	NHB
Porifera	Demospongiae				sp. 1	Megafauna	Benthic	Sessile	Filter feeder	Single	NHB
Porifera	Demospongiae				sp. 2	Megafauna	Benthic	Sessile	Filter feeder	Single	NHB
Porifera	Demospongiae				sp. 3	Megafauna	Benthic	Sessile	Filter feeder	Single	NHB
Porifera	Demospongiae				sp. 4	Megafauna	Benthic	Sessile	Filter feeder	Single	NHB
Porifera	Demospongiae				sp. 5	Megafauna	Benthic	Sessile	Filter feeder	Single	NHB
Porifera	Demospongiae				sp. 6	Megafauna	Benthic	Sessile	Filter feeder	Single	NHB
Porifera	Demospongiae				sp. 7	Megafauna	Benthic	Sessile	Filter feeder	Single	NHB
Porifera	Demospongiae				sp. 8	Megafauna	Benthic	Sessile	Filter feeder	Single	NHB
Porifera	Demospongiae				sp. 9	Megafauna	Benthic	Sessile	Filter feeder	Single	NHB
Porifera	Demospongiae				sp. 10	Megafauna	Benthic	Sessile	Filter feeder	Single	NHB
Porifera	Demospongiae				sp. 11	Megafauna	Benthic	Sessile	Filter feeder	Single	NHB

Porifera	Demospongiae				sp. 12	Megafauna	Benthic	Sessile	Filter feeder	Single	NHB
Porifera	Demospongiae				sp. 13	Megafauna	Benthic	Sessile	Filter feeder	Single	NHB
Porifera	Demospongiae				sp. 14	Megafauna	Benthic	Sessile	Filter feeder	Single	NHB
Porifera	Demospongiae				sp. 15	Megafauna	Benthic	Sessile	Filter feeder	Single	NHB
Porifera	Demospongiae				sp. 16	Megafauna	Benthic	Sessile	Filter feeder	Single	NHB
Porifera	Demospongiae				sp. 17	Megafauna	Benthic	Sessile	Filter feeder	Single	NHB
Porifera	Demospongiae				sp. 18	Megafauna	Benthic	Sessile	Filter feeder	Single	NHB
Porifera	Demospongiae				sp. 19	Megafauna	Benthic	Sessile	Filter feeder	Single	NHB
Porifera	Demospongiae				sp. 20	Megafauna	Benthic	Sessile	Filter feeder	Single	NHB
Porifera	Demospongiae				sp. 21	Megafauna	Benthic	Sessile	Filter feeder	Single	NHB
Porifera	Demospongiae				sp. 22	Megafauna	Benthic	Sessile	Filter feeder	Single	NHB
Porifera	Demospongiae				sp. 23	Megafauna	Benthic	Sessile	Filter feeder	Single	NHB
Porifera	Demospongiae				sp. 24	Megafauna	Benthic	Sessile	Filter feeder	Single	NHB
Porifera	Demospongiae				sp. 25	Megafauna	Benthic	Sessile	Filter feeder	Single	NHB
Porifera	Demospongiae				sp. 26	Megafauna	Benthic	Sessile	Filter feeder	Single	NHB
Porifera	Demospongiae				sp. 27	Megafauna	Benthic	Sessile	Filter feeder	Single	NHB
Porifera	Hexactinellida	Lyssacinosida	Rossellidae	*Sympagella*	*Sympagella delauzei*	Megafauna	Benthic	Sessile	Filter feeder	Single	NHB
Porifera	Homoscleromorpha	Homosclerophorida	Plakinidae	*Corticium*	spp.	Megafauna	Benthic	Sessile	Filter feeder	Single	NHB
Porifera	Homoscleromorpha	Homosclerophorida	Plakinidae	*Corticium*	*Corticium candelabrum*	Megafauna	Benthic	Sessile	Filter feeder	Single	NHB
Cnidaria	Anthozoa	Actiniaria			spp.	Megafauna	Benthic	Sessile	Suspension feeder	Single	NHB
Cnidaria	Anthozoa	Actiniaria	Aliciidae	*Alicia*	*Alicia mirabilis*	Megafauna	Benthic	Sessile	Suspension feeder	Single	NHB
Cnidaria	Anthozoa	Actiniaria	Andresiidae	*Andresia*	*Andresia partenopea*	Megafauna	Benthic	Sessile	Suspension feeder	Single	NHB
Cnidaria	Anthozoa	Alcyonacea	Acanthogorgiidae	*Acanthogorgia*	*Acanthogorgia hirsuta*	Megafauna	Benthic	Sessile	Suspension feeder	Colonial	NHB
Cnidaria	Anthozoa	Alcyonacea	Alcyoniidae	*Alcyonium*	*Alcyonium coralloides*	Megafauna	Benthic	Sessile	Suspension feeder	Colonial	NHB
Cnidaria	Anthozoa	Alcyonacea	Alcyoniidae	*Alcyonium*	*Alcyonium palmatum*	Megafauna	Benthic	Sessile	Suspension feeder	Colonial	NHB
Cnidaria	Anthozoa	Alcyonacea	Coralliidae	*Corallium*	*Corallium rubrum*	Megafauna	Benthic	Sessile	Suspension feeder	Colonial	HB
Cnidaria	Anthozoa	Alcyonacea	Cornulariidae	*Cornularia*	*Cornularia cornucopiae*	Macrofauna	Benthic	Sessile	Suspension feeder	Colonial	NHB
Cnidaria	Anthozoa	Alcyonacea	Gorgoniidae	*Eunicella*	spp.	Megafauna	Benthic	Sessile	Suspension feeder	Colonial	NHB
Cnidaria	Anthozoa	Alcyonacea	Gorgoniidae	*Eunicella*	*Eunicella cavolini*	Megafauna	Benthic	Sessile	Suspension feeder	Colonial	HB
Cnidaria	Anthozoa	Alcyonacea	Gorgoniidae	*Eunicella*	*Eunicella singularis*	Megafauna	Benthic	Sessile	Suspension feeder	Colonial	HB
Cnidaria	Anthozoa	Alcyonacea	Gorgoniidae	*Eunicella*	*Eunicella verrucosa*	Megafauna	Benthic	Sessile	Suspension feeder	Colonial	HB
Cnidaria	Anthozoa	Alcyonacea	Nidaliidae	*Nidalia*	*Nidalia studeri*	Megafauna	Benthic	Sessile	Suspension feeder	Colonial	NHB
Cnidaria	Anthozoa	Alcyonacea	Paralcyoniidae	*Paralcyonium*	*Paralcyonium spinulosum*	Megafauna	Benthic	Sessile	Suspension feeder	Colonial	NHB
Cnidaria	Anthozoa	Alcyonacea	Plexauridae	*Paramuricea*	*Paramuricea clavata*	Megafauna	Benthic	Sessile	Suspension feeder	Colonial	HB
Cnidaria	Anthozoa	Alcyonacea	Plexauridae	*Paramuricea*	*Paramuricea macrospina*	Megafauna	Benthic	Sessile	Suspension feeder	Colonial	HB
Cnidaria	Anthozoa	Alcyonacea	Plexauridae	*Swiftia*	*Swiftia pallida*	Megafauna	Benthic	Sessile	Filter feeder	Single	NHB
Cnidaria	Anthozoa	Alcyonacea	Primnoidae	*Callogorgia*	*Callogorgia verticillata*	Megafauna	Benthic	Sessile	Suspension feeder	Colonial	HB
Cnidaria	Anthozoa	Alcyonacea			sp. 1	Megafauna	Benthic	Sessile	Suspension feeder	Colonial	NHB
Cnidaria	Anthozoa	Antipatharia	Myriopathidae	*Antipathella*	*Antipathella subpinnata*	Megafauna	Benthic	Sessile	Suspension feeder	Colonial	HB
Cnidaria	Anthozoa	Penicillaria	Arachnactidae	*Arachnanthus*	*Arachnanthus oligopodus*	Megafauna	Benthic	Sessile	Suspension feeder	Single	NHB
Cnidaria	Anthozoa	Pennatulacea	Funiculinidae	*Funiculina*	*Funiculina quadrangularis*	Megafauna	Benthic	Sessile	Suspension feeder	Colonial	HB

Cnidaria	Anthozoa	Pennatulacea	Pennatulidae	*Pennatula*	*Pennatula phosphorea*	Megafauna	Benthic	Sessile	Suspension feeder	Colonial	HB
Cnidaria	Anthozoa	Pennatulacea	Pennatulidae	*Pennatula*	*Pennatula rubra*	Megafauna	Benthic	Sessile	Suspension feeder	Colonial	HB
Cnidaria	Anthozoa	Pennatulacea	Virgulariidae	*Virgularia*	*Virgularia mirabilis*	Megafauna	Benthic	Sessile	Suspension feeder	Colonial	HB
Cnidaria	Anthozoa	Scleractinia	Caryophylliidae		spp.	Megafauna	Benthic	Sessile	Suspension feeder	Single	HB
Cnidaria	Anthozoa	Scleractinia	Caryophylliidae	*Caryophyllia*	sp. 1	Megafauna	Benthic	Sessile	Suspension feeder	Single	HB
Cnidaria	Anthozoa	Scleractinia	Caryophylliidae	*Caryophyllia*	sp. 2	Megafauna	Benthic	Sessile	Suspension feeder	Single	HB
Cnidaria	Anthozoa	Scleractinia	Caryophylliidae		sp. 1	Megafauna	Benthic	Sessile	Suspension feeder	Single	HB
Cnidaria	Anthozoa	Scleractinia	Caryophylliidae		sp. 2	Megafauna	Benthic	Sessile	Suspension feeder	Single	HB
Cnidaria	Anthozoa	Scleractinia	Dendrophylliidae	*Balanophyllia*	*Balanophyllia europaea*	Megafauna	Benthic	Sessile	Suspension feeder	Single	HB
Cnidaria	Anthozoa	Scleractinia	Dendrophylliidae	*Balanophyllia*	sp. 1	Megafauna	Benthic	Sessile	Suspension feeder	Single	HB
Cnidaria	Anthozoa	Scleractinia	Dendrophylliidae	*Dendrophyllia*	*Dendrophyllia cornigera*	Megafauna	Benthic	Sessile	Suspension feeder	Colonial	HB
Cnidaria	Anthozoa	Spirularia	Cerianthidae	*Cerianthus*	*Cerianthus membranaceus*	Megafauna	Benthic	Sessile	Scavenger/Predator	Single	NHB
Cnidaria	Anthozoa	Spirularia	Cerianthidae		spp.	Megafauna	Benthic	Sessile	Scavenger/Predator	Single	NHB
Cnidaria	Anthozoa	Spirularia	Cerianthidae	*Cerianthus*	spp.	Megafauna	Benthic	Sessile	Scavenger/Predator	Single	NHB
Cnidaria	Anthozoa	Spirularia	Cerianthidae		sp. 1	Megafauna	Benthic	Sessile	Scavenger/Predator	Single	NHB
Cnidaria	Anthozoa	Zoantharia	Epizoanthidae	*Epizoanthus*	sp. 1	Megafauna	Benthic	Sessile	Suspension feeder	Single	NHB
Cnidaria	Anthozoa	Zoantharia	Epizoanthidae	*Epizoanthus*	sp. 2	Megafauna	Benthic	Sessile	Suspension feeder	Single	NHB
Cnidaria	Anthozoa	Zoantharia	Parazoanthidae	*Parazoanthus*	sp. 1	Megafauna	Benthic	Sessile	Suspension feeder	Single	NHB
Cnidaria	Hydrozoa	Leptothecata	Aglaopheniidae	*Aglaophenia*	sp. 1	Megafauna	Benthic	Sessile	Suspension feeder	Colonial	NHB
Cnidaria	Hydrozoa	Leptothecata	Aglaopheniidae	*Lytocarpia*	*Lytocarpia myriophyllum*	Megafauna	Benthic	Sessile	Suspension feeder	Colonial	HB
Cnidaria	Hydrozoa	Leptothecata	Plumulariidae	*Nemertesia*	spp.	Megafauna	Benthic	Sessile	Suspension feeder	Colonial	NHB
Mollusca	Bivalvia	Cardiida	Cardiidae	*Acanthocardia*	*Acanthocardia Aculeata*	Megafauna	Benthic	Sessile	Filter feeder	Single	NHB
Mollusca	Bivalvia	Cardiida	Cardiidae	*Acanthocardia*	sp. 1	Megafauna	Benthic	Sessile	Filter feeder	Single	NHB
Mollusca	Bivalvia	Ostreida	Gryphaeidae	*Neopycnodonte*	*Neopycnodonte cochlear*	Megafauna	Benthic	Sessile	Suspension feeder	Single	HB
Mollusca	Bivalvia	Ostreida	Pteriidae	*Pteria*	*Pteria hirundo*	Megafauna	Benthic	Sessile	Suspension feeder	Single	NHB
Mollusca	Bivalvia	Pectinida	Pectinidae	*Pecten*	spp.	Megafauna	Benthic	Sessile	Suspension feeder	Single	HB
Mollusca	Cephalopoda	Octopoda	Eledonidae	*Eledone*	*Eledone cirrhosa*	Megafauna	Benthic	Swimmer	Scavenger/Predator	Single	NHB
Mollusca	Cephalopoda	Octopoda	Octopodidae	*Callistoctopus*	*Callistoctopus macropus*	Megafauna	Benthic	Swimmer	Scavenger/Predator	Single	NHB
Mollusca	Cephalopoda	Octopoda	Octopodidae	*Octopus*	*Octopus vulgaris*	Megafauna	Benthic	Swimmer	Scavenger/Predator	Single	NHB
Mollusca	Cephalopoda	Sepiida	Sepiidae	*Sepia*	spp.	Megafauna	Benthic	Swimmer	Scavenger/Predator	Single	NHB
Mollusca	Gastropoda		Plakobranchidae	*Elysia*	sp. 1	Megafauna	Benthic	Vagile	Grazer	Single	NHB
Mollusca	Gastropoda				spp.	Megafauna	Benthic	Vagile	Scavenger/Predator	Single	NHB
Mollusca	Gastropoda				sp. 1	Megafauna	Benthic	Vagile	Scavenger/Predator	Single	NHB
Mollusca	Gastropoda				sp. 2	Megafauna	Benthic	Vagile	Scavenger/Predator	Single	NHB
Mollusca	Gastropoda	Littorinimorpha	Cypraeidae	*Naria*	spp.	Megafauna	Benthic	Vagile	Scavenger/Predator	Single	NHB
Mollusca	Gastropoda	Neogastropoda	Columbellidae	*Columbella*	*Columbella rustica*	Macrofauna	Benthic	Vagile	Grazer	Single	NHB
Mollusca	Gastropoda	Neogastropoda	Fasciolariidae	*Fusinus*	spp.	Megafauna	Benthic	Vagile	Scavenger/Predator	Single	NHB
Mollusca	Gastropoda	Neogastropoda	Fasciolariidae	*Tarantinaea*	spp.	Megafauna	Benthic	Vagile	Scavenger/Predator	Single	NHB
Mollusca	Gastropoda	Neogastropoda	Muricidae	*Hexaplex*	*Hexaplex trunculus*	Megafauna	Benthic	Vagile	Scavenger/Predator	Single	NHB
Mollusca	Gastropoda	Nudibranchia	Chromodorididae	*Felimare*	*Felimare tricolor*	Megafauna	Benthic	Vagile	Scavenger/Predator	Single	NHB
Mollusca	Gastropoda	Nudibranchia	Discodorididae	*Discodoris*	spp.	Megafauna	Benthic	Vagile	Scavenger/Predator	Single	NHB

Mollusca	Gastropoda	Nudibranchia	Discodorididae	*Platydoris*	*Platydoris argo*	Megafauna	Benthic	Vagile	Scavenger/Predator	Single	NHB
Mollusca	Gastropoda	Nudibranchia	Myrrhinidae	*Dondice*	*Dondice banyulensis*	Megafauna	Benthic	Vagile	Scavenger/Predator	Single	NHB
Mollusca	Gastropoda	Pleurobranchida	Pleurobranchidae	*Pleurobranchus*	*Pleurobranchus testudinarius*	Megafauna	Benthic	Vagile	Scavenger/Predator	Single	NHB
Mollusca	Gastropoda	Trochida	Calliostomatidae	*Calliostoma*	spp.	Macrofauna	Benthic	Vagile	Scavenger/Predator	Single	NHB
Mollusca	Gastropoda	Trochida	Turbinidae	*Bolma*	*Bolma rugosa*	Megafauna	Benthic	Vagile	Grazer	Single	NHB
Annelida	Polychaeta	Echiuroidea	Bonelliidae	*Bonellia*	*Bonellia viridis*	Megafauna	Benthic	Vagile	Deposit feeder	Single	NHB
Annelida	Polychaeta	Sabellida	Sabellidae		spp.	Megafauna	Benthic	Sessile	Suspension feeder	Single	NHB
Annelida	Polychaeta	Sabellida	Sabellidae		sp. 1	Megafauna	Benthic	Sessile	Suspension feeder	Single	NHB
Annelida	Polychaeta	Sabellida	Sabellidae	*Sabella*	spp.	Megafauna	Benthic	Sessile	Suspension feeder	Single	NHB
Annelida	Polychaeta	Sabellida	Sabellidae	*Sabella*	sp. 1	Megafauna	Benthic	Sessile	Suspension feeder	Single	NHB
Annelida	Polychaeta	Sabellida	Sabellidae	*Sabella*	*Sabella pavonina*	Megafauna	Benthic	Sessile	Suspension feeder	Single	NHB
Annelida	Polychaeta	Sabellida	Serpulidae		spp.	Megafauna	Benthic	Sessile	Suspension feeder	Single	NHB
Annelida	Polychaeta	Sabellida	Serpulidae	*Filograna*	*Filograna implexa*	Macrofauna	Benthic	Sessile	Filter feeder	Gregarious	HB
Annelida	Polychaeta	Sabellida	Serpulidae	*Protula*	sp. 1	Megafauna	Benthic	Sessile	Filter feeder	Single	NHB
Annelida	Polychaeta	Sabellida	Serpulidae	*Serpula*	*Serpula vermicularis*	Megafauna	Benthic	Sessile	Suspension feeder	Single	NHB
Annelida	Polychaeta	Sabellida	Serpulidae	*Vermiliopsis*	sp. 1	Megafauna	Benthic	Sessile	Filter feeder	Single	NHB
Annelida	Polychaeta	Terebellida	Terebellidae	*Lanice*	*Lanice conchilega*	Megafauna	Benthic	Facultatively motile	Suspension feeder	Single	NHB
Annelida	Polychaeta	Terebellida	Trichobranchidae	*Terebellides*	sp. 1	Megafauna	Benthic	Facultatively motile	Deposit feeder	Single	NHB
Arthropoda	Malacostraca	Decapoda	Calappidae	*Calappa*	*Calappa granulata*	Megafauna	Benthic	Vagile	Scavenger/Predator	Single	NHB
Arthropoda	Malacostraca	Decapoda	Inachidae	*Inachus*	*Inachus phalangium*	Megafauna	Benthic	Vagile	Scavenger/Predator	Single	NHB
Arthropoda	Malacostraca	Decapoda	Inachidae	*Macropodia*	*Macropodia longirostris*	Megafauna	Benthic	Vagile	Scavenger/Predator	Single	NHB
Arthropoda	Malacostraca	Decapoda	Munididae	*Munida*	spp.	Megafauna	Benthic	Vagile	Scavenger/Predator	Single	NHB
Arthropoda	Malacostraca	Decapoda	Munididae	*Munida*	*Munida tenuimana*	Megafauna	Benthic	Vagile	Scavenger/Predator	Single	NHB
Arthropoda	Malacostraca	Decapoda	Paguridae	*Paguristes*	*Paguristes longirostris*	Megafauna	Benthic	Vagile	Scavenger/Predator	Single	NHB
Arthropoda	Malacostraca	Decapoda	Paguridae		spp.	Megafauna	Benthic	Vagile	Scavenger/Predator	Single	NHB
Arthropoda	Malacostraca	Decapoda	Paguridae		sp. 1	Megafauna	Benthic	Vagile	Scavenger/Predator	Single	NHB
Arthropoda	Malacostraca	Decapoda	Paguridae		sp. 2	Megafauna	Benthic	Vagile	Scavenger/Predator	Single	NHB
Arthropoda	Malacostraca	Decapoda	Paguridae		sp. 3	Megafauna	Benthic	Vagile	Scavenger/Predator	Single	NHB
Arthropoda	Malacostraca	Decapoda	Paguridae		sp. 4	Megafauna	Benthic	Vagile	Scavenger/Predator	Single	NHB
Arthropoda	Malacostraca	Decapoda	Palinuridae	*Palinurus*	*Palinurus elephas*	Megafauna	Benthic	Vagile	Scavenger/Predator	Single	NHB
Arthropoda	Malacostraca	Decapoda	Parthenopidae	*Spinolambrus*	spp.	Megafauna	Benthic	Vagile	Scavenger/Predator	Single	NHB
Arthropoda	Malacostraca	Decapoda	Polybiidae	*Liocarcinus*	*Liocarcinus depurator*	Megafauna	Benthic	Vagile	Scavenger/Predator	Single	NHB
Arthropoda	Malacostraca	Decapoda	Polybiidae	*Liocarcinus*	spp.	Megafauna	Benthic	Vagile	Scavenger/Predator	Single	NHB
Arthropoda	Malacostraca	Decapoda			spp.	Megafauna	Benthic	Vagile	Scavenger/Predator	Single	NHB
Arthropoda	Malacostraca	Decapoda			sp. 1	Megafauna	Benthic	Vagile	Scavenger/Predator	Single	NHB
Arthropoda	Malacostraca	Decapoda			sp. 2	Megafauna	Benthic	Vagile	Scavenger/Predator	Single	NHB

Arthropoda	Malacostraca	Euphausiacea			spp.	Megafauna	Pelagic	Vagile	Scavenger/Predator	Single	NHB
Bryozoa	Gymnolaemata	Cheilostomatida	Adeonidae	*Adeonella*	*Adeonella calveti*	Megafauna	Benthic	Sessile	Suspension feeder	Colonial	NHB
Bryozoa	Gymnolaemata	Cheilostomatida	Bitectiporidae	*Pentapora*	*Pentapora fascialis*	Megafauna	Benthic	Sessile	Suspension feeder	Colonial	NHB
Bryozoa	Gymnolaemata	Cheilostomatida	Bitectiporidae	*Schizomavella*	*Schizomavella linearis*	Megafauna	Benthic	Sessile	Suspension feeder	Colonial	NHB
Bryozoa	Gymnolaemata	Cheilostomatida	Bitectiporidae	*Schizomavella*	*Schizomavella mamillata*	Megafauna	Benthic	Sessile	Suspension feeder	Colonial	NHB
Bryozoa	Gymnolaemata	Cheilostomatida	Bitectiporidae	*Schizomavella*	sp. 1	Megafauna	Benthic	Sessile	Suspension feeder	Colonial	NHB
Bryozoa	Gymnolaemata	Cheilostomatida	Bugulidae	*Bugula*	spp.	Megafauna	Benthic	Sessile	Suspension feeder	Colonial	NHB
Bryozoa	Gymnolaemata	Cheilostomatida	Celleporidae	*Turbicellepora*	*Turbicellepora avicularis*	Megafauna	Benthic	Sessile	Suspension feeder	Colonial	NHB
Bryozoa	Gymnolaemata	Cheilostomatida	Myriaporidae	*Myriapora*	*Myriapora truncata*	Megafauna	Benthic	Sessile	Suspension feeder	Colonial	NHB
Bryozoa	Gymnolaemata	Cheilostomatida	Myriaporidae	*Myriapora*	spp.	Megafauna	Benthic	Sessile	Suspension feeder	Colonial	NHB
Bryozoa	Gymnolaemata	Cheilostomatida	Phidoloporidae	*Reteporella*	*Reteporella grimaldii*	Megafauna	Benthic	Sessile	Suspension feeder	Single	NHB
Bryozoa	Gymnolaemata	Cheilostomatida	Phidoloporidae	*Reteporella*	spp.	Megafauna	Benthic	Sessile	Suspension feeder	Single	NHB
Bryozoa	Gymnolaemata	Cheilostomatida	Phidoloporidae	*Reteporella*	sp. 1	Megafauna	Benthic	Sessile	Suspension feeder	Single	NHB
Bryozoa	Gymnolaemata	Cheilostomatida	Smittinidae	*Smittina*	*Smittina cervicornis*	Megafauna	Benthic	Sessile	Suspension feeder	Colonial	NHB
Bryozoa	Stenolaemata	Cyclostomatida	Horneridae	*Hornera*	*Hornera frondiculata*	Megafauna	Benthic	Sessile	Suspension feeder	Colonial	NHB
Echinodermata	Asteroidea	Forcipulatida	Asteriidae	*Coscinasterias*	*Coscinasterias tenuispina*	Megafauna	Benthic	Sessile	Scavenger/Predator	Single	NHB
Echinodermata	Asteroidea	Forcipulatida	Asteriidae	*Marthasterias*	*Marthasterias glacialis*	Megafauna	Benthic	Sessile	Scavenger/Predator	Single	NHB
Echinodermata	Asteroidea	Paxillosida	Astropectinidae	*Astropecten*	spp.	Megafauna	Benthic	Sessile	Scavenger/Predator	Single	NHB
Echinodermata	Asteroidea	Paxillosida	Astropectinidae	*Astropecten*	*Astropecten aranciacus*	Megafauna	Benthic	Sessile	Scavenger/Predator	Single	NHB
Echinodermata	Asteroidea	Paxillosida	Luidiidae	*Luidia*	*Luidia ciliaris*	Megafauna	Benthic	Sessile	Scavenger/Predator	Single	NHB
Echinodermata	Asteroidea	Spinulosida	Echinasteridae	*Echinaster*	*Echinaster sepositus*	Megafauna	Benthic	Sessile	Scavenger/Predator	Single	NHB
Echinodermata	Asteroidea	Valvatida	Chaetasteridae	*Chaetaster*	*Chaetaster longipes*	Megafauna	Benthic	Sessile	Scavenger/Predator	Single	NHB
Echinodermata	Asteroidea	Valvatida	Goniasteridae	*Peltaster*	*Peltaster placenta*	Megafauna	Benthic	Sessile	Deposit feeder	Single	NHB
Echinodermata	Asteroidea	Valvatida	Ophidiasteridae	*Hacelia*	*Hacelia attenuata*	Megafauna	Benthic	Sessile	Deposit feeder	Single	NHB
Echinodermata	Crinoidea	Comatulida	Antedonidae	*Antedon*	*Antedon mediterranea*	Megafauna	Benthic	Facultatively motile	Suspension feeder	Single	NHB
Echinodermata	Crinoidea	Comatulida	Antedonidae	*Leptometra*	*Leptometra phalangium*	Megafauna	Benthic	Facultatively motile	Suspension feeder	Single	NHB
Echinodermata	Echinoidea	Camarodonta	Echinidae	*Echinus*	*Echinus melo*	Megafauna	Benthic	Vagile	Grazer	Single	NHB
Echinodermata	Echinoidea	Cidaroida	Cidaridae	*Cidaris*	*Stylocidaris affinis*	Megafauna	Benthic	Vagile	Scavenger/Predator	Single	NHB
Echinodermata	Echinoidea	Cidaroida	Cidaridae	*Cidaris*	*Cidaris cidaris*	Megafauna	Benthic	Vagile	Grazer	Single	NHB
Echinodermata	Echinoidea	Diadematoida	Diadematidae	*Centrostephanus*	*Centrostephanus longispinus*	Megafauna	Benthic	Vagile	Grazer	Single	NHB
Echinodermata	Echinoidea	Holothuriida	Holothuriidae	*Holothuria*	*Holothuria forskali*	Megafauna	Benthic	Vagile	Deposit feeder	Single	NHB
Echinodermata	Echinoidea	Holothuriida	Holothuriidae	*Holothuria*	*Holothuria poli*	Megafauna	Benthic	Vagile	Deposit feeder	Single	NHB
Echinodermata	Echinoidea	Holothuriida	Holothuriidae	*Holothuria*	spp.	Megafauna	Benthic	Vagile	Deposit feeder	Single	NHB
Echinodermata	Echinoidea	Holothuriida	Holothuriidae	*Holothuria*	*Holothuria tubulosa*	Megafauna	Benthic	Vagile	Deposit feeder	Single	NHB
Echinodermata	Echinoidea	Spatangoida	Brissidae	*Brissus*	*Brissus unicolor*	Megafauna	Benthic	Vagile	Deposit feeder	Single	NHB
Echinodermata	Echinoidea	Spatangoida	Spatangidae	*Spatangus*	*Spatangus purpureus*	Megafauna	Benthic	Vagile	Deposit feeder	Single	NHB
Echinodermata	Holothuroidea	Dendrochirotida	Cucumariidae	*Cucumaria*	*Cucumaria piperata*	Megafauna	Benthic	Vagile	Deposit feeder	Single	NHB
Echinodermata	Holothuroidea	Holothuriida	Mesothuriidae	*Mesothuria*	spp.	Megafauna	Benthic	Vagile	Deposit feeder	Single	NHB
Echinodermata	Holothuroidea	Synallactida	Stichopodidae	*Parastichopus*	*Parastichopus regalis*	Megafauna	Benthic	Vagile	Deposit feeder	Single	NHB
Echinodermata	Ophiuroidea				sp. 1	Megafauna	Benthic	Vagile	Scavenger/Predator	Single	NHB

Echinodermata	Ophiuroidea	Amphilepidida	Ophiopsilidae	*Ophiopsila*	spp.	Megafauna	Benthic	Vagile	Suspension feeder	Single	NHB
Echinodermata	Ophiuroidea	Amphilepidida	Ophiotrichidae	*Ophiothrix*	*Ophiothrix fragilis*	Megafauna	Benthic	Vagile	Scavenger/Predator	Single	NHB
Echinodermata	Ophiuroidea	Euryalida	Gorgonocephalidae	*Astrospartus*	*Astrospartus mediterraneus*	Megafauna	Benthic	Vagile	Suspension feeder	Single	NHB
Echinodermata	Ophiuroidea	Ophiacanthida	Ophiodermatidae	*Ophioderma*	spp.	Megafauna	Benthic	Vagile	Scavenger/Predator	Single	NHB
Echinodermata	Ophiuroidea	Ophiacanthida	Ophiomyxidae	*Ophiomyxa*	*Ophiomyxa pentagona*	Megafauna	Benthic	Vagile	Scavenger/Predator	Single	NHB
Chordata	Actinopterygii	Anguilliformes			spp.	Megafauna	Pelagic	Swimmer	Scavenger/Predator	Single	NHB
Chordata	Actinopterygii				sp. 1	Megafauna	Pelagic	Swimmer	Scavenger/Predator	Single	NHB
Chordata	Actinopterygii	Anguilliformes	Congridae	*Ariosoma*	*Ariosoma balearicum*	Megafauna	Pelagic	Swimmer	Scavenger/Predator	Single	NHB
Chordata	Actinopterygii	Anguilliformes	Muraenidae	*Muraena*	*Muraena helena*	Megafauna	Pelagic	Swimmer	Scavenger/Predator	Single	NHB
Chordata	Actinopterygii	Anguilliformes	Ophichthidae	*Ophisurus*	*Ophisurus serpens*	Megafauna	Pelagic	Swimmer	Scavenger/Predator	Single	NHB
Chordata	Actinopterygii	Gadiformes	Phycidae	*Phycis*	*Phycis blennoides*	Megafauna	Pelagic	Swimmer	Scavenger/Predator	Single	NHB
Chordata	Actinopterygii	Gadiformes	Phycidae	*Phycis*	spp.	Megafauna	Pelagic	Swimmer	Scavenger/Predator	Single	NHB
Chordata	Actinopterygii	Gadiformes	Phycidae	*Phycis*	*Phycis phycis*	Megafauna	Pelagic	Swimmer	Scavenger/Predator	Single	NHB
Chordata	Actinopterygii	Perciformes	Callanthiidae	*Callanthias*	*Callanthias ruber*	Megafauna	Pelagic	Swimmer	Scavenger/Predator	Single	NHB
Chordata	Actinopterygii	Perciformes	Gobiidae		spp.	Megafauna	Pelagic	Swimmer	Scavenger/Predator	Single	NHB
Chordata	Actinopterygii	Perciformes	Labridae	*Ctenolabrus*	*Ctenolabrus rupestris*	Megafauna	Pelagic	Swimmer	Scavenger/Predator	Single	NHB
Chordata	Actinopterygii	Perciformes	Labridae	*Lappanella*	*Lappanella fasciata*	Megafauna	Pelagic	Swimmer	Scavenger/Predator	Single	NHB
Chordata	Actinopterygii	Perciformes	Mullidae	*Mullus*	spp.	Megafauna	Pelagic	Swimmer	Scavenger/Predator	Single	NHB
Chordata	Actinopterygii	Perciformes	Mullidae	*Mullus*	*Mullus barbatus*	Megafauna	Pelagic	Swimmer	Scavenger/Predator	Single	NHB
Chordata	Actinopterygii	Perciformes	Pomacentridae	*Chromis*	spp.	Megafauna	Pelagic	Swimmer	Scavenger/Predator	Single	NHB
Chordata	Actinopterygii	Perciformes	Scorpaenidae	*Scorpaena*	*Scorpaena scrofa*	Megafauna	Pelagic	Swimmer	Scavenger/Predator	Single	NHB
Chordata	Actinopterygii	Perciformes	Serranidae	*Serranus*	spp.	Megafauna	Pelagic	Swimmer	Scavenger/Predator	Single	NHB
Chordata	Actinopterygii	Perciformes	Serranidae	*Serranus*	*Serranus cabrilla*	Megafauna	Pelagic	Swimmer	Scavenger/Predator	Single	NHB
Chordata	Actinopterygii	Perciformes	Serranidae	*Serranus*	*Serranus hepatus*	Megafauna	Pelagic	Swimmer	Scavenger/Predator	Single	NHB
Chordata	Actinopterygii	Perciformes	Serranidae		sp. 1	Megafauna	Pelagic	Swimmer	Scavenger/Predator	Single	NHB
Chordata	Actinopterygii	Perciformes	Sparidae		spp.	Megafauna	Pelagic	Swimmer	Scavenger/Predator	Single	NHB
Chordata	Actinopterygii	Perciformes	Sparidae	*Pagellus*	spp.	Megafauna	Pelagic	Swimmer	Scavenger/Predator	Single	NHB
Chordata	Actinopterygii	Perciformes	Sparidae	*Pagellus*	*Pagellus erythrinus*	Megafauna	Pelagic	Swimmer	Scavenger/Predator	Single	NHB
Chordata	Actinopterygii	Perciformes	Sparidae	*Spondyliosoma*	*Spondyliosoma cantharus*	Megafauna	Pelagic	Swimmer	Scavenger/Predator	Single	NHB
Chordata	Actinopterygii	Perciformes	Synodontidae	*Synodus*	*Synodus saurus*	Megafauna	Pelagic	Swimmer	Scavenger/Predator	Single	NHB
Chordata	Actinopterygii	Perciformes	Trachinidae	*Trachinus*	spp.	Megafauna	Pelagic	Swimmer	Scavenger/Predator	Single	NHB
Chordata	Actinopterygii	Perciformes	Trachinidae	*Trachinus*	*Trachinus araneus*	Megafauna	Pelagic	Swimmer	Scavenger/Predator	Single	NHB
Chordata	Actinopterygii	Perciformes	Triglidae	*Eutrigla*	*Eutrigla*	Megafauna	Pelagic	Swimmer	Scavenger/Predator	Single	NHB
Chordata	Actinopterygii	Pleuronectiformes	Soleidae	*Solea*	*Solea solea*	Megafauna	Pelagic	Swimmer	Scavenger/Predator	Single	NHB
Chordata	Actinopterygii	Scorpaeniformes	Sebastidae	*Helicolenus*	*Helicolenus dactylopterus*	Megafauna	Benthic	Swimmer	Scavenger/Predator	Single	NHB
Chordata	Actinopterygii	Scorpaeniformes	Triglidae	*Chelidonichthys*	*Chelidonichthys lastoviza*	Megafauna	Benthic	Swimmer	Scavenger/Predator	Single	NHB
Chordata	Actinopterygii	Scorpaeniformes	Triglidae	*Chelidonichthys*	*Chelidonichthys lucerna*	Megafauna	Benthic	Swimmer	Scavenger/Predator	Single	NHB
Chordata	Actinopterygii	Scorpaeniformes	Triglidae	*Lepidotrigla*	*Lepidotrigla cavillone*	Megafauna	Benthic	Swimmer	Scavenger/Predator	Single	NHB
Chordata	Actinopterygii	Zeiformes	Zeidae	*Zeus*	*Zeus faber*	Megafauna	Pelagic	Swimmer	Scavenger/Predator	Single	NHB
Chordata	Ascidiacea	Aplousobranchia	Clavelinidae	*Clavelina*	sp. 1	Megafauna	Benthic	Sessile	Filter feeder	Single	NHB
Chordata	Ascidiacea	Aplousobranchia	Didemnidae		sp. 1	Megafauna	Benthic	Sessile	Filter feeder	Colonial	NHB

Chordata	Ascidiacea	Aplousobranchia	Didemnidae		sp. 2	Megafauna	Benthic	Sessile	Filter feeder	Colonial	NHB
Chordata	Ascidiacea	Aplousobranchia	Didemnidae		sp. 3	Megafauna	Benthic	Sessile	Filter feeder	Colonial	NHB
Chordata	Ascidiacea	Aplousobranchia	Diazonidae	*Rhopalaea*	spp.	Megafauna	Benthic	Sessile	Filter feeder	Single	NHB
Chordata	Ascidiacea	Aplousobranchia	Diazonidae	*Rhopalaea*	*Rhopalaea neapolitana*	Megafauna	Benthic	Sessile	Filter feeder	Single	NHB
Chordata	Ascidiacea	Aplousobranchia	Didemnidae	*Diplosoma*	*Diplosoma spongiforme*	Megafauna	Benthic	Sessile	Filter feeder	Colonial	NHB
Chordata	Ascidiacea	Aplousobranchia	Didemnidae	*Polysyncraton*	*Polysyncraton lacazei*	Megafauna	Benthic	Sessile	Filter feeder	Colonial	NHB
Chordata	Ascidiacea	Aplousobranchia	Polyclinidae	*Aplidium*	sp. 1	Megafauna	Benthic	Sessile	Filter feeder	Colonial	NHB
Chordata	Ascidiacea	Phlebobranchia	Cionidae	*Ciona*	spp.	Megafauna	Benthic	Sessile	Filter feeder	Single	NHB
Chordata	Ascidiacea	Stolidobranchia	Pyuridae	*Halocynthia*	*Halocynthia papillosa*	Megafauna	Benthic	Sessile	Filter feeder	Single	NHB
Chordata	Ascidiacea				spp.	Megafauna	Benthic	Sessile	Filter feeder	Single	NHB
Chordata	Ascidiacea				sp. 1	Megafauna	Benthic	Sessile	Filter feeder	Single	NHB
Chordata	Ascidiacea				sp. 2	Megafauna	Benthic	Sessile	Filter feeder	Single	NHB
Chordata	Ascidiacea				sp. 3	Megafauna	Benthic	Sessile	Filter feeder	Single	NHB
Chordata	Ascidiacea				sp. 4	Megafauna	Benthic	Sessile	Filter feeder	Single	NHB

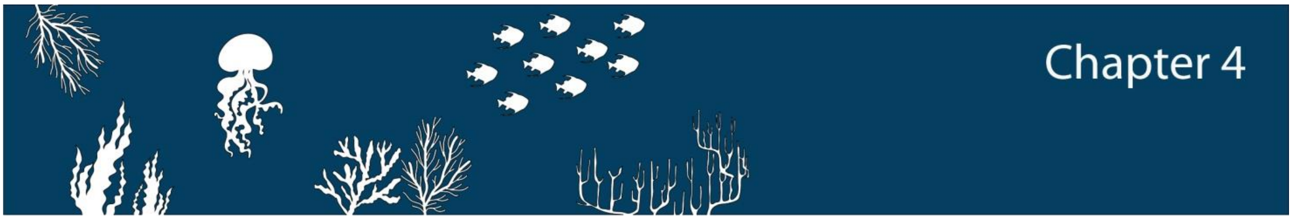

Chapter 4

4. Predictive modeling to identify areas suitable for the presence of deep-water oyster reefs at mesophotic depth in the Adriatic-northern Ionian Sea

4.1 Introduction

Oysters are important ecosystem engineers at tidal and subtidal depths, creating biogenic structures (i.e., reefs) in estuarine, bay, or lagoonal situations (Stenzel, 1971; Bahr & Lanier, 1981; Drinkwaard, 1998; Bayne, 2017). In the Mediterranean Sea, the main reef-builders in the depth range 0-20 m are members of the Ostreidae (*Ostrea edulis* Linnaeus, 1758, and *Crassostrea* spp., (Agius et al., 1978; Parenzan, 1989; Launey et al., 2002; Carlucci et al., 2010; Stagličić et al., 2020). To date, the few evidence of oyster aggregations below 20 m depth in the Mediterranean Sea concerns two species in the *Neopycnodonte* genus: *Neopycnodonte cochlear* and *Neopycnodonte zibrowii* (Corriero et al., 2019; Angeletti and Taviani, 2020; Cardone et al., 2020). Despite these biocontructions remaining still largely unexplored, an increase in the volume of information regarding deep-water oyster reefs (DWOR) is taking place in the last few years, also due to the development of technologies for the exploration of deep waters, such as ROVs.

N. zibrowii aggregations are frequent in the Atlantic Ocean but seldom documented in the Mediterranean Sea, forming encrustations, rims, and occasional small reefs on hard substrates at bathyal depths (ca. 300–800 m, Freiwald et al., 2009; Wisshak et al., 2009; Gofas et al., 2010; Van Rooij et al., 2010; Beuck et al., 2016; Aguilar et al., 2017; Fourt et al., 2017; Taviani et al., 2019) *N. cochlear*, instead, shows a wider distribution, forming aggregations at intermediate waters (ca. 30–

150 m), also in dark submarine caves (Onorato et al., 2003; Taviani et al., 2012; Corriero et al., 2019; Angeletti and Taviani, 2020; Cardone et al., 2020; Belmonte et al., 2021). However, there is a substantial lack of knowledge regarding the distribution of *N. cochlear* reefs and the environmental setting favoring their presence.

Habitat suitability models (HSM) are increasingly used to map areas presenting environmental characteristics suitable for the presence of species or assemblages, especially in intermediate-to-deep situations where data availability is often poor (Rengstorf et al., 2012). HSMs compare the environmental setting of sites where the species has been observed to the conditions of a certain area, in order to identify how the environmental characteristics suitable for the presence of the species are distributed in the space (Elith & Leathwick, 2009).

Such modeling techniques have been developed for a variety of habitats in the Mediterranean Sea, such as seagrasses (e.g., Beca-Carretero et al., 2020), coralligenous bioconstructions (e.g., Martin et al., 2014), stony corals (e.g., Bargain et al., 2017, 2018; Matos et al., 2021), black corals (Lauria et al., 2021) and gorgonians (Giusti et al., 2014; Boavida et al., 2016). By identifying the areas suitable for the presence of a target biological feature, within a certain degree (=suitability index), the model outputs are also extremely useful to explore the factors influencing the distribution patterns and environmental preferences of species and assemblages (Sundahl, Buhl-Mortensen & Buhl-Mortensen, 2020).

The definition of suitable areas provided by HSM represent spatial information that can be included in management plans and that might orient conservation actions aimed at preserving ecological relevant ecosystems (Rengstorf et al., 2012). Recent studies on DWOR, and the present thesis (Chapter 3) provided evidence of their role as biodiversity hotspots by increasing the structural complexity of habitats and attracting a diversified associated fauna (Angeletti & Taviani, 2020). Moreover, a large number of benthic species attributable to different taxonomic groups have been documented occurring in the microhabitats created by oysters bioconstruction (Cardone et al., 2020).

In this chapter, a habitat suitability model is developed to predict the distribution of areas potentially suitable for the presence of DWOR in the Adriatic Sea and in the northern Ionian Sea. Sites of occurrence were obtained from the analysis of ROV videos collected within the study area. Mapping the potential distribution of DWOR provides important insights into the environmental setting suitable for their presence, also identifying novel sites for exploration, and ultimately orienting conservation efforts.

4.2 Materials and methods

4.2.1 Occurrence data

The occurrence sites for DWOR were obtained from the analysis of ROV videos performed in Chapter 3. Location points were obtained from the analysis of frames extracted every 10 seconds (following methodology developed by Castellan et al., 2020 and Chapter 3) from 7 dives were located at mesophotic depth in the Adriatic and northern Ionian Sea (Fig. 3.1 and Tab. 3.1 in Chapter 3). Every frame imaging DWOR was used as occurrence, resulting in 3237 records. Since the amount of literature information on DWOR available for the Mediterranean Sea is exiguous, no further occirrences from literature were integrated. A total of 10,000 random points were generated with package “raster” (version 3.3-13, Hijmans et al., 2015) in R software (R Core Team, 2020) and used as pseudo-absences, following method in Phillips & Dudik (2008).

4.2.2 Environmental data

A subset of the environmental variables used in the Chapter 3 were considered for inclusion in modeling efforts (Tab. 4.1). Information on dissolved oxygen, concentrations of Chl-a and nutrients (NO_3^-, PO_3^{4-}) at the seafloor together with the velocity of currents were extrapolated from satellite data obtained from the open-access database Copernicus (copernicus.marine.eu) at a horizontal resolution of 4 km. The amount of PAR at seabed was obtained from the estimation performed in the Chapter 1, at a horizontal resolution of 115 m. The bathymetry at horizontal resolution of 115 m was downloaded from Emodnet database (emodnet-bathymetry.eu). A suite of topographic variables was calculated from this bathymetry layer, i.e., slope, curvature, and the topographic position index (TPI). Slope was calculated using the tool “spatial analyst” Tool ArcGIS 10.5 (©ESRI). The curvatures (general and profile) were calculated using the DEM Surface Tool (v2.1.292; Jenness, 2013). General curvature describes the shape of the seafloor assuming positive values in correspondence of convex surfaces and negative values concave surfaces. Profile curvature is used as a proxy of the speed of water across a surface, with positive values indicating currents deceleration, and negative values indicating acceleration. TPI quantifies the relative elevation of a location relative to the surrounding seafloor, with positive values indicating locally elevated features and negative values indicating depressions. TPI was calculated using the package “raster” at scales of 3, 5, 10, 20 pixels, corresponding to ca. 345, 575, 1150 and 2300 m.

Every environmental variable used in modeling effort was restricted to the spatial extent of the mesophotic zone in the area, using the polygon produced in the Chapter 1. The layers were clipped using the package “raster” in R software.

The variables were transformed to match the resolution of the bathymetry data using an upscaling approach that approximates conditions at the seafloor (Davies & Guinotte, 2011 and Chapter 3).

Variable	Units	Native Resolution	Reference
Seafloor characteristics			
Depth	meters	115 m	EMODnet bathymetry
Plan curvature	-	-	Derived
Profile curvature	-	-	Derived
Slope	°	-	Derived
TPI	-	345, 575, 1150 and 2300 m	Derived
Water column characteristics			
Light at seabed	-	-	Derived (Chapter 1)
Concentration Chl-a	mg m^{-3}	4km	Marine Copernicus
Currents velocity	m/s	-	-
Concentration of nitrate NO_{3-}	mmol m^{-3}	-	-
Concentration of phosphate PO_4^{3-}	-	-	-
Dissolved O_2	mmol $m^{-3}day^{-1}$	-	-
Salinity	psu	-	-
Temperature	°C	-	-

Tab. 4.1. Environmental variables considered for inclusion in the DWOR habitat suitability model.

4.2.3 Variable selection

A MaxEnt (Phillips et al., 2006) model including only the different TPI generated from the bathymetry was run and the variable importance was analyzed to select the TPI resolution most significant for the presence of DWOR to be considered in the final model.

Since the inclusion of highly correlated variables may affect model performance and variables contributions (e.g., Huang et al., 2011), a variable selection process was performed to identify a more parsimonious variable set. Variables were retained based on correlation and their performance in preliminary MaxEnt models. Among highly correlated variables (Pearson's r greater or lower than ±0.75, Fig. S4.2), those with the highest percent contribution in the preliminary models were retained.

4.2.4 Model generation

Presence-only ecological niche models were generated using MaxEnt (Phillips et al., 2006), which has been shown to consistently outperform a variety of other modeling approaches (e.g., Robert et al., 2016). Models were run using a random subset of occurrence points for model calibration (70%) and evaluation (30%) during each run. The results are habitat suitability maps providing a probability of habitat suitability within the study area, ranging from 0 to 1, with higher values indicating more suitable habitat. Models performance was assessed using a threshold-independent receiver operating characteristic (ROC) curve, evaluated by the area under the curve (AUC) metric describing the ability of models to correctly rank a known occurrences location, with higher AUC values closer to one indicating better model performance. Variables importance was determined by using the function “var.importance” (package: ENMEval, v. 0.3.1) in R software. Variables are randomly permuted among the calibration points and the decrease in training AUC is estimated. Larger decrease indicates higher importance of the variable in the model.

4.3 Results

4.3.1 Predictor variable selection

The analysis of variable contribution of the MaxEnt model predicting the suitability areas for DWOR presence generated by including only the TPI calculated at different scales showed that TPI-5 (5 pixels) was the most significant variable (Fig. 4.1). Thus, it was included in the final model.

Correlations among variables in the final set were considerably lower than among the variables in the initial set (Fig. 4.2), with the highest remaining correlation between temperature and currents velocity (Pearson's r = -0.56). Of the 13 environmental predictor variables originally considered, six were ultimately retained for use in the final MaxEnt model: concentration of NO_3^-, TPI-5, currents velocity, light regime, slope and temperature (Fig. 4.3).

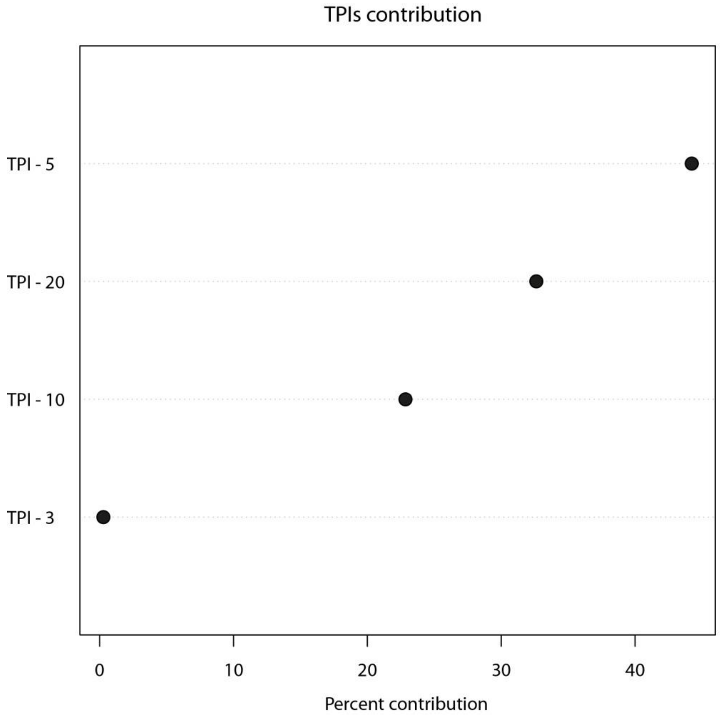

Fig. 4.1. Percentage contribution of variables to the MaxEnt model run including only the different TPI resolutions.

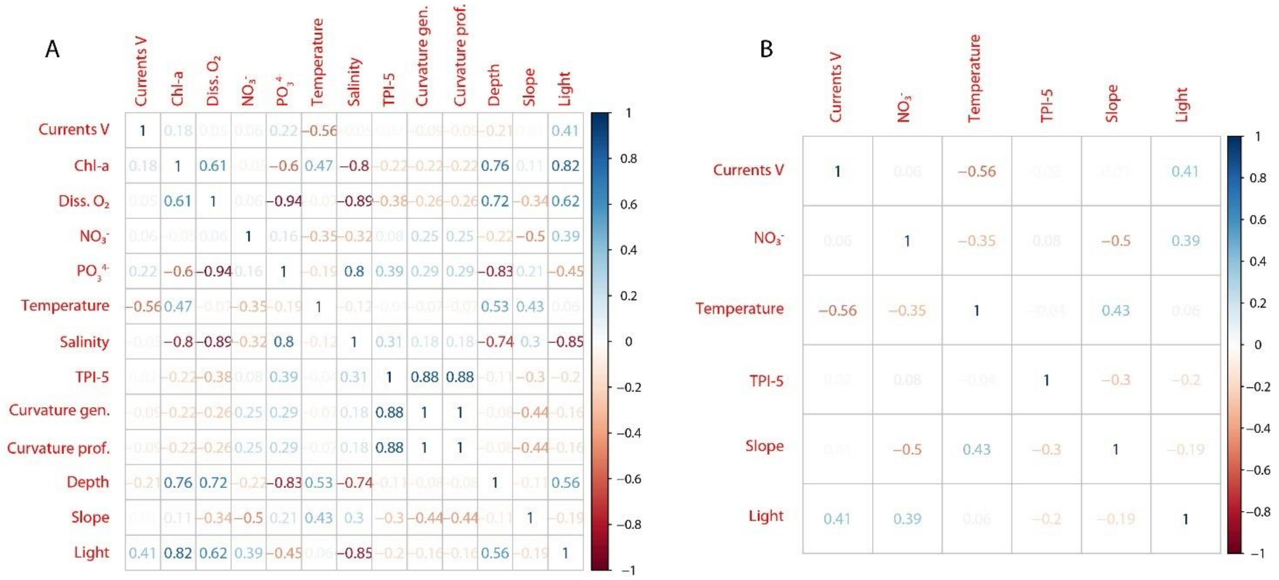

A

	Currents V	Chl-a	Diss. O_2	NO_3^-	PO_3^{4-}	Temperature	Salinity	TPI-5	Curvature gen.	Curvature prof.	Depth	Slope	Light
Currents V	1	0.18	0.05	0.06	0.22	−0.56	−0.05	0.02	−0.09	−0.09	−0.21	0.01	0.41
Chl-a	0.18	1	0.61	−0.05	−0.6	0.47	−0.8	−0.22	−0.22	−0.22	0.76	0.11	0.82
Diss. O_2	0.05	0.61	1	0.06	−0.94	−0.07	−0.89	−0.38	−0.26	−0.26	0.72	−0.34	0.62
NO_3^-	0.06	−0.05	0.06	1	0.16	−0.35	−0.32	0.08	0.25	0.25	−0.22	−0.5	0.39
PO_3^{4-}	0.22	−0.6	−0.94	0.16	1	−0.19	0.8	0.39	0.29	0.29	−0.83	0.21	−0.45
Temperature	−0.56	0.47	−0.07	−0.35	−0.19	1	−0.12	−0.04	−0.07	−0.07	0.53	0.43	0.06
Salinity	−0.05	−0.8	−0.89	−0.32	0.8	−0.12	1	0.31	0.18	0.18	−0.74	0.3	−0.85
TPI-5	0.02	−0.22	−0.38	0.08	0.39	−0.04	0.31	1	0.88	0.88	−0.11	−0.3	−0.2
Curvature gen.	−0.09	−0.22	−0.26	0.25	0.29	−0.07	0.18	0.88	1	1	−0.08	−0.44	−0.16
Curvature prof.	−0.09	−0.22	−0.26	0.25	0.29	−0.07	0.18	0.88	1	1	−0.08	−0.44	−0.16
Depth	−0.21	0.76	0.72	−0.22	−0.83	0.53	−0.74	−0.11	−0.08	−0.08	1	−0.11	0.56
Slope	0.01	0.11	−0.34	−0.5	0.21	0.43	0.3	−0.3	−0.44	−0.44	−0.11	1	−0.19
Light	0.41	0.82	0.62	0.39	−0.45	0.06	−0.85	−0.2	−0.16	−0.16	0.56	−0.19	1

B

	Currents V	NO_3^-	Temperature	TPI-5	Slope	Light
Currents V	1	0.06	−0.56	0.02	0.01	0.41
NO_3^-	0.06	1	−0.35	0.08	−0.5	0.39
Temperature	−0.56	−0.35	1	−0.04	0.43	0.06
TPI-5	0.02	0.08	−0.04	1	−0.3	−0.2
Slope	0.01	−0.5	0.43	−0.3	1	−0.19
Light	0.41	0.39	0.06	−0.2	−0.19	1

Fig. 4.2. Pearson's Correlation Coefficient among all variables considered for inclusion in modeling efforts (A) and included in the final model (B).

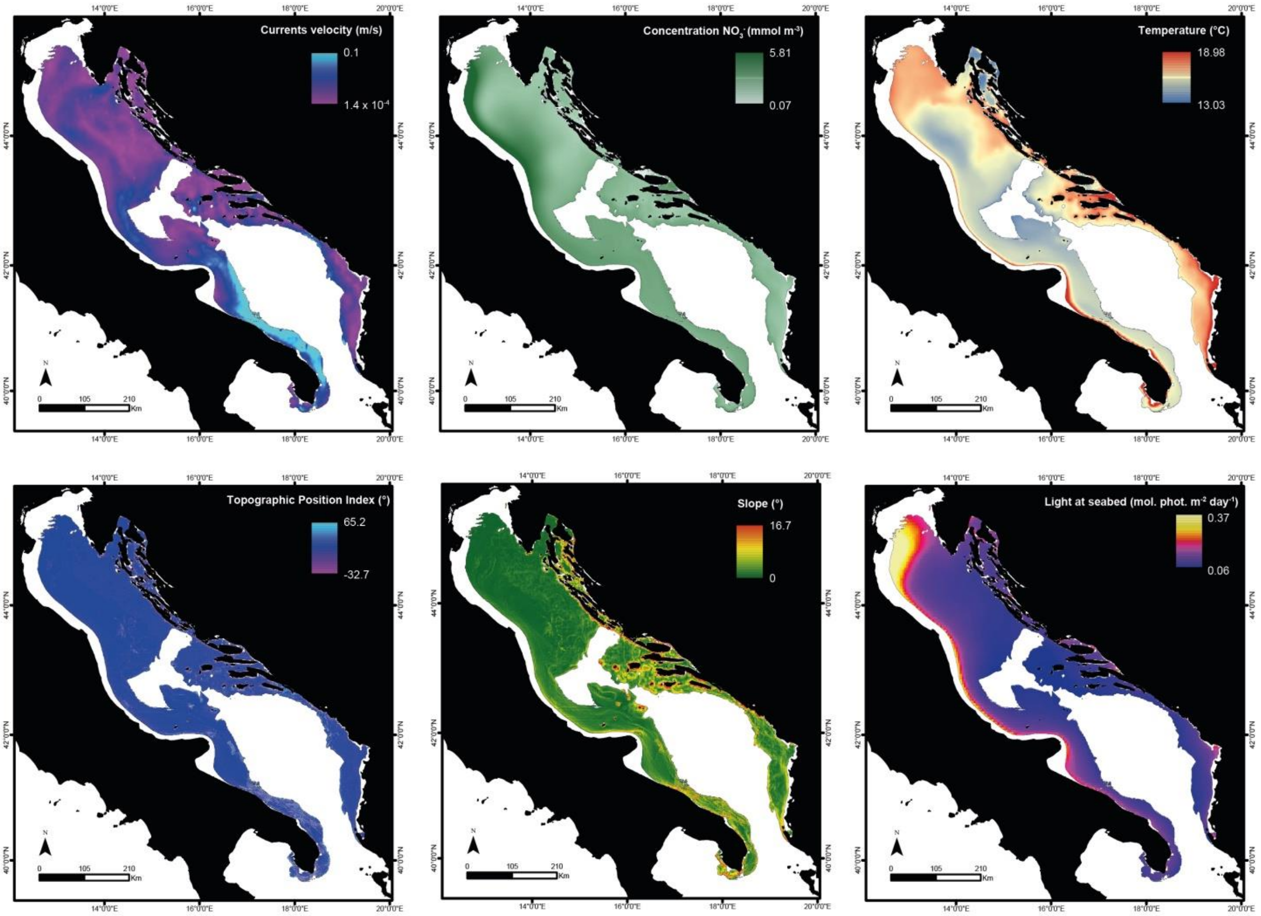

Fig. 4.3. Values at bottom for environmental variables included in the final MaxEnt model.

4.3.2 Habitat suitability model

Areas presenting environmental settings suitable for the presence of DWOR in the Adriatic and the north-Ionian Sea regions of the Mediterranean Sea were identified using a MaxEnt model (Fig. 4.4). The performance was excellent, with a training AUC of 0.99 and a test AUC of 0.98.

The slope contributed the most to the final prediction, with a percent contribution of 41.65% (Tab. 4.2). Most of highly suitable areas were in correspondence with steep slopes (Fig. 4.5). The light regime at the seabed contributed 28.41% to the predicted distribution of suitable areas. The temperature was the next highest relevant variable, with a percent contribution of 18.28%. Predicted habitat suitability was low in areas with colder situations (about 15°C) and rose rapidly with temperature. The currents velocity and concentration of NO_3^- contributed less to the final prediction, with 7.82%, and 3.62%, respectively. Topographic position index, calculated at a scale of 5 pixels (TPI-5) was the variable that contributed the least to the final model.

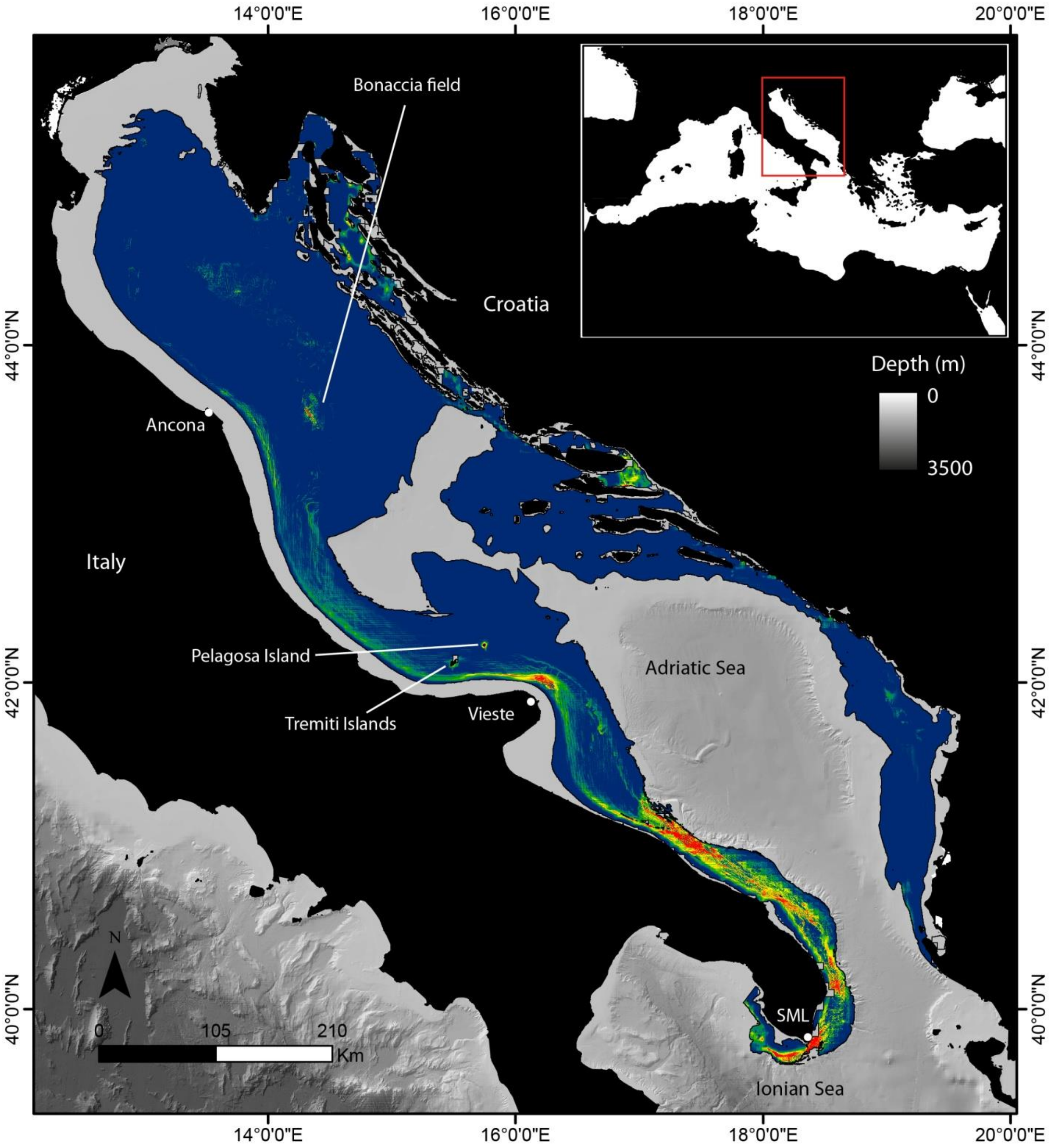

Fig. 4.4. Predicted habitat suitability map for DWOR within the modeled area. Warmer colours indicate more suitable habitat. Grey tones indicate depth. SML: Santa Maria di Leuca.

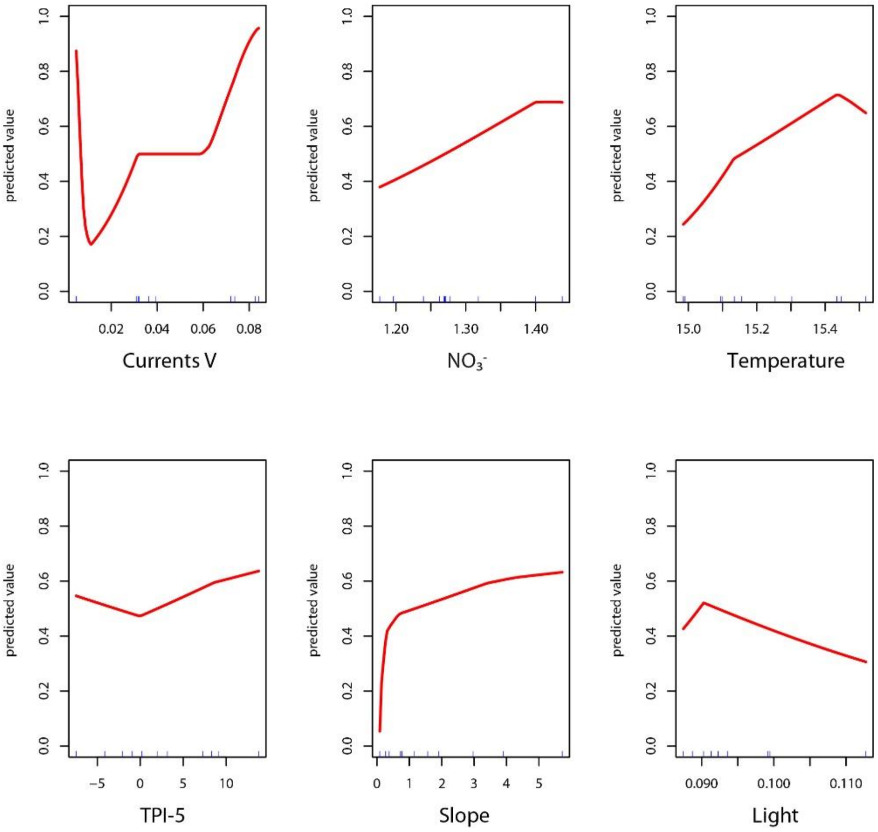

Fig. 4.5. Response curves showing how predicted habitat suitability for DWOR changes over the range of each environmental variable included in the final model.

Variable	Percent contribution
Slope	41.65
Light	28.42
Temperature	18.27
Currents V	7.82
NO_3^-	3.62
TPI-5	0.22

Tab. 4.2. Percent contribution of variables included in the final Maxent model.

4.3.3 Distribution of areas suitable for DWOR

The model predicted as suitable (suitability>0.4) an area of 1280.86 km^2 (Fig. 4.4). Environmental conditions favorable for the presence of DWOR were predicted to occur over a small fraction of the entire study area, corresponding to 1.8%. The northern and central sectors of the Adriatic Sea resulted mainly not suitable for the presence of DWOR with only a few portions of seabed characterized by low-medium suitability (<30%) detected along the Croatian coast. As an exception, the area in correspondence of the Bonaccia field represented a hotspot of medium-high suitability, with small areas exceeding 0.6 of suitability. The model identified segments of low-medium suitability along the Italian coast in the central Adriatic Sea offshore Ancona and extending to the southern sector. Here, the large portions of the seafloor along the Italian shelf were predicted as suitable for DWOR. The southernmost sector of the Adriatic Sea along the Italian side presented large portions of seafloor characterized by high suitability, also exceeding 0.7. Spots of medium-high suitability were also detected at north of the Gargano promontory, around Tremiti Islands. Also, the area off Santa Maria di Leuca (northern Ionian Sea) resulted as presenting environmental setting able to host DWOR, with suitability values over 0.7.

4.4 Discussion

A habitat suitability model was developed to predict the distribution of areas presenting environmental characteristics able to host DWOR within the mesophotic depth range across a region encompassing the Adriatic Sea and a portion of the northeastern Ionian Sea. Only small sections of the study area, covering about 1.8% of the modeled region and mainly distributed in the southwestern Adriatic Sea and off Santa Maria di Leuca (Ionian Sea), were predicted as suitable for DWOR. Although the rarity of areas predicted as presenting a combination of environmental factors suitable for the presence of DWOR might be a consequence of a modeling approach relying only on records collected on the field, this could also represent the peculiar environmental setting required by these associations to settle and survive. The information on the biological communities populating the mesophotic depth range of the modeled region is, in fact, increasing in the last decade (e.g., Ponti et al., 2018; Castellan et al., 2019; Bandelj et al., 2020; Chimienti, 2020; Chimienti et al., 2020) but evidence of the presence of DWOR is scarce (Corriero et al., 2019; Angeletti & Taviani, 2020; Cardone et al., 2020).

Our model suggests that DWOR niches in the study region might be constrained by the requirement for gently sloped and shaded reliefs, lapped by water masses rich in nutrients and within a certain temperature range. The slope contributed the most information to the model (41.64%), indicating that topography is an effective predictor of DWOR presence. Predicted habitat suitability increased with seafloor inclination likely related to the presence of bare hard substrate suitable for the recruitment and settlement of oysters.

Light regime was also a major factor in creating suitable conditions for the presence of DWOR in the modeled area, contributing 28.41% to the final prediction. DWOR were predicted to occur in areas presenting lower light intensity at the seabed, delineating a preference for shaded situations. The increasing attenuation of light penetration with depth limits the presence of algal components colonizing the hard substrates to areas characterized by light intensity able to sustain photosynthetic metabolism. Consequently, the covering of algal concretions declines with depth, leaving space for the colonization of benthic sessile invertebrates that become the main habitat builder (Cardone et al., 2020). No photosynthetic components were, in facts, observed in correspondence of DWOR sites, suggesting that hard substrates might be availabile for oysters colonization.

The temperature was the third-most important variable in creating favorable conditions for DWOR presence. Within the study area, the temperature ranged from ca. 13 to 19°C, whilst DWOR suitable areas were predicted to occur within the range 15°C–15.5 °C. If such a narrow interval might suggest that DWOR require specific thermal conditions for long-term survival at mesophotic depth in the study area, it may nevertheless be representative of DWOR preferences for water masses with certain properties. Albeit to a lesser extent, in fact, also the concentration of nutrients (represented by NO_3^-) and the velocity of the currents cumulatively played a relevant role in the model, contributing to 11.43%. The properties of the water mass are likely among the main factors concurring to create the environmental setting able to support the presence of DWOR, which seem to prefer areas with warmer, NO_3^--rich waters and moving at a greater velocity. Despite areas characterized by small currents velocity were predicted as highly suitable (Fig. 4.5), the majority of portions of seabed with high suitability values were located in the southwestern Adriatic Sea and in the Ionian sector of the study area that presented the fastest currents velocity observed (Fig. 4.3). Although the modeling approach here reported was developed including the variables that may be relevant in creating the environmental setting suitable for the presence of DWOR, habitat suitability models can only provide a view of their fundamental niche by spatially identifying areas environmentally similar, with a certain degree (suitability index), to those hosting the target feature. A complex combination of factors, however, concur in determining the distribution of species and benthic assemblages, such as dispersal, competition for food and substrate, and ecosystems perturbations (Moritz et al., 2013). Consequently, it is likely that some areas that were predicted to be suitable for DWOR might be, instead, unoccupied. On the contrary, not involving the entire suite of variables controlling the presence of DWOR, some areas predicted as not suitable might somewhat present bioconstructions built by oysters as a result of dynamic not considered in modeling effort (e.g., stochastic processes).

Nevertheless, the paucity of evidence in the literature regarding DWOR in the modeled area lends support to the restricted environmental setting resulting as likely needed by oysters to settle and survive from modeling efforts. The recent evidence on the role of DWOR as hotspots of biodiversity (Angeletti & Taviani, 2020; Cardone et al., 2020) and ecological functions (see Chapter 3), and the limited spatial extension of areas suitable for their presence from the modeling approach emphasize the potential ecological relevance of losing even relatively few sites hosting DWOR and the need for further exploration and mapping activities.

References

Agius, C., Jaccarini, V., Ritz, D.A. (1978). Growth trials of *Crassostrea gigas* and *Ostrea edulis* in inshore waters of Malta (Central Mediterranean). *Aquaculture*, 15(3), 195–218. https://doi.org/10.1016/0044-8486(78)90031-5

Aguilar, R.; Pilar, M.; Gerovasileiou, V. (2017). *Draft Guidelines for Inventoring and Monitoring of Dark Habitats*. UNEP(DEPI)/MED WG. 431/Inf.12, Thirteenth Meeting of Focal Points for Specially Protected Areas. Agenda Item 4: Progress report on activities carried out by SPA/RAC since the twelfth meeting of Focal Points for SPAs. United Nations Environment Programme/Mediterranean Action Plan (UN Environment /MAP); Specially Protected Areas Regional Activity Centre (SPA/RAC): Alexandria, Egypt, pp. 1–55.

Angeletti, L., Taviani, M. (2020). Offshore *Neopycnodonte* Oyster Reefs in the Mediterranean Sea. *Diversity*, 12(3), 92. https://doi.org/10.3390/d12030092

Bahr, L.M., Lanier, W.P. (1981). *The Ecology of Intertidal Oyster Reefs of the South Atlantic Coast: A Community Profile*. U.S. Fish and Wildlife Service, Office of Biological Services, Washington D.C., FWS/OBS-81/15, 105 pp.

Bandelj, V., Solidoro, C., Laurent, C., Querin, S., Kaleb, S., Gianni, F., Falace, A. (2020). Cross-scale connectivity of macrobenthic communities in a patchy network of habitats: The Mesophotic Biogenic Habitats of the Northern Adriatic Sea. *Estuarine, Coastal and Shelf Science*, 245, 106978. https://doi.org/10.1016/j.ecss.2020.106978

Bargain, A., Foglini, F., Pairaud, I., Bonaldo, D., Carniel, S., Angeletti, L., Taviani, M., Rochette, S., Fabri, M.C. (2018). Predictive habitat modeling in two Mediterranean canyons including hydrodynamic variables. *Progress in Oceanography*, 169, 151–168. https://doi.org/10.1016/j.pocean.2018.02.015

Bargain, A., Marchese, F., Savini, A., Taviani, M., Fabri, M.-C. (2017). Santa Maria di Leuca Province (Mediterranean Sea): identification of suitable mounds for Cold-Water Coral settlement using geomorphometric proxies and MaxEnt methods. *Frontiers in Marine Science*, 4. https://doi.org/10.3389/fmars.2017.00338

Bayne, B.L. (2017). *Biology of oysters*. Academic Press: London, United Kingdom.

Beca-Carretero, P., Teichberg, M., Winters, G., Procaccini, G., Reuter, H. (2020). Projected rapid habitat expansion of tropical seagrass species in the Mediterranean Sea as climate change progresses. *Frontiers in Plant Science*, 11, 1762. https://doi.org/10.3389/fpls.2020.555376

Belmonte, G., Guido, A., Mastandrea, A., Onorato, R., Rosso, A., Sanfilippo, R. (2020). Animal Forests in Submarine Caves. In: *Perspectives on the Marine Animal Forests of the World*. Rossi S, Bramanti L (Eds). Springer International Publishing: Cham, pp. 129–145.

Beuck, L., Aguilar, R., Fabri, M., Freiwald, A., Gofas, S., Hebbeln, D., López Correa, M., Ramos Martos, A., Ramil, F. & Sánchez, D.F. (2016). Biotope characterisation and compiled geographical distribution of the deep-water oyster *Neopycnodonte zibrowii* in the Atlantic Ocean and Mediterranean Sea. *Rapp. Comm. int. Mer Médit*, 41, 462.

Boavida, J., Assis, J., Silva, I., Serrão, E.A. (2016). Overlooked habitat of a vulnerable gorgonian revealed in the Mediterranean and Eastern Atlantic by ecological niche modelling. *Scientific Reports*, 6, 36460. https://doi.org/10.1038/srep36460

Cardone, F., Corriero, G., Longo, C., Mercurio, M., Onen Tarantini, S., Gravina, M.F., Liscio, S., Moretti, M., De Giosa, F., Giangrande, A., Marzano, C.N., Pierri, C. (2020). Massive bioconstructions built by *Neopycnodonte cochlear* (Mollusca, Bivalvia) in a mesophotic environment in the central Mediterranean Sea. *Scientific Reports*, 10(1), 6337. https://doi.org/10.1038/s41598-020-63241-y

Carlucci, R., Sassanelli, G., Matarrese, A., Giove, A., D’Onghia, G. (2010). Experimental data on growth, mortality and reproduction of Ostrea edulis (L., 1758) in a semi-enclosed basin of the Mediterranean Sea. *Aquaculture*, 306(1), 167–176. https://doi.org/10.1016/j.aquaculture.2010.05.026

Castellan, G., Angeletti, L., Taviani, M., Montagna, P. (2019). The Yellow Coral Dendrophyllia cornigera in a Warming Ocean. *Frontiers in Marine Science*, 6. https://doi.org/10.3389/fmars.2019.00692

Chimienti, G. (2020). Vulnerable Forests of the Pink Sea Fan *Eunicella verrucosa* in the Mediterranean Sea. *Diversity*, 12(5), 176. https://doi.org/10.3390/d12050176

Chimienti, G., De Padova, D., Mossa, M., Mastrototaro, F. (2020). A mesophotic black coral forest in the Adriatic Sea. *Scientific Reports*, 10(1), 8504. https://doi.org/10.1038/s41598-020-65266-9

Corriero, G., Pierri, C., Mercurio, M., Marzano, C.N., Tarantini, S.O., Gravina, M.F., Lisco S., Moretti M., De Giosa F., Valenzano E., Giangrande A., Mastrodonato M., Longo C., Cardone F. (2019). A Mediterranean mesophotic coral reef built by non-symbiotic scleractinians. *Scientific Reports*, 9(1), 3601. https://doi.org/10.1038/s41598-019-40284-4

Davies, A.J., Guinotte, J.M. (2011). Global Habitat Suitability for Framework-Forming Cold-Water Corals. *PLOS ONE*, 6(4), e18483. https://doi.org/10.1371/journal.pone.0018483

Drinkwaard, A.C. (1998). Introductions and developments of oysters in the North Sea area: a review. *Helgoländer Meeresuntersuchungen*, 52(3–4), 301–308. https://doi.org/10.1007/BF02908904

Elith, J., Leathwick, J.R. (2009). Species distribution models: ecological explanation and prediction across space and time. *Annual Review of Ecology, Evolution, and Systematics*, 40(1), 677–697. https://doi.org/10.1146/annurev.ecolsys.110308.120159

Fourt, M., Goujard, A., Perez, T., Chevaldonné, P. (2017). *Guide de la faune profonde de la mer Méditerranée. Exploration des roches et canyons sous-marins des côtes françaises*. Museum national d'Histoire naturelle, Paris, pp. 184.

Freiwald, A., Beuck, L., Rüggeberg, A., Taviani, M., Hebbeln, D. and R/V Meteor M70-1 Participants. (2009). The white coral community in the Central Mediterranean Sea revealed by ROV surveys. *Oceanography*, 22:58–57

Giusti, M., Innocenti, C., Canese, S. (2014). Predicting suitable habitat for the gold coral *Savalia savaglia* (Bertoloni, 1819) (Cnidaria, Zoantharia) in the South Tyrrhenian Sea. *Continental Shelf Research*, 81, 19–28. https://doi.org/10.1016/j.csr.2014.03.011

Gofas, S., Rueda, J.L., Salas, C., Díaz-Del-Río, V. (2010). A new record of the giant deep-sea oyster *Neopycnodonte zibrowii* in the Gulf of Cadiz (south-western Iberian Peninsula). *Marine Biodiversity Records*, 3. https://doi.org/10.1017/S1755267210000618

Hijmans, R.J., Van Etten, J., Cheng, J., Mattiuzzi, M., Sumner, M., Greenberg, J.A., Lamigueiro, O.P., Bevan, A., Racine, E.B., Shortridge, A. (2015). Package ‘raster’. R package.

Huang, Z., Brooke, B., Li, J. (2011). Performance of predictive models in marine benthic environments based on predictions of sponge distribution on the Australian continental shelf. *Ecological Informatics*, 6(3), 205–216. https://doi.org/10.1016/j.ecoinf.2011.01.001

Jenness, J. (2013). Dem surface tools for ARCGIS. Jenness Enterprises. http://www.jennessent.com/arcgis/surface:area.htm

Launey, S., Ledu, C., Boudry, P., Bonhomme, F., Naciri-Graven, Y. (2002). Geographic structure in the European flat oyster (*Ostrea edulis* L.) as revealed by microsatellite polymorphism. *Journal of Heredity*, 93(5), 331–351. https://doi.org/10.1093/jhered/93.5.331

Lauria, V., Massi, D., Fiorentino, F., Milisenda, G., Cillari, T. (2021). Habitat suitability mapping of the black coral *Leiopathes glaberrima* to support conservation of vulnerable marine ecosystems. *Scientific Reports*, 11(1), 15661. https://doi.org/10.1038/s41598-021-95256-4

Martin, C.S., Giannoulaki, M., De Leo, F., Scardi, M., Salomidi, M., Knittweis, L., Pace, M.L., Garofalo, G., Gristina, M., Ballesteros, E., Bavestrello, G., Belluscio, A., Cebrian, E., Gerakaris, V., Pergent, G., Pergent-Martini, C., Schembri, P.J., Terribile, K., Rizzo, L., Ben Souissi, J., Bonacorsi, M., Guarnieri, G., Krzelj, M., Macic, V., Punzo, E., Valavanis, V., Fraschetti S. (2014). Coralligenous and maërl habitats: predictive modelling to identify their spatial distributions across the Mediterranean Sea. *Scientific Reports*, 4(1), 5073. https://doi.org/10.1038/srep05073

Matos, F.L., Company, J.B., Cunha, M.R. (2021). Mediterranean seascape suitability for Lophelia pertusa: Living on the edge. *Deep Sea Research Part I: Oceanographic Research Papers*, 170, 103496. https://doi.org/10.1016/j.dsr.2021.103496

Moritz, C., Meynard, C.N., Devictor, V., Guizien, K., Labrune, C., Guarini, J.-M., Mouquet, N. (2013). Disentangling the role of connectivity, environmental filtering, and spatial structure on metacommunity dynamics. *Oikos*, 122(10), 1401–1410. https://doi.org/10.1111/j.1600-0706.2013.00377.x

Onorato, R., Forti, P., Belmonte, G., Poto, M., Costantini, A. (2003). La grotta sottomarina lu Lampiùne: novità esplorative e prime indagini ecologiche. *Thalassia Salentina*, 26(Suppl), 55–64.

Parenzan, P. (1989). Storia della *Crassostrea gigas* (Thunb.) spontanea nel Mediterraneo. *Thalassia Salentina*, 19, 39–48.

Phillips, S.J., Anderson, R.P., Schapire, R.E. (2006). Maximum entropy modeling of species geographic distributions. *Ecological Modelling*, 190(3), 231–259. https://doi.org/10.1016/j.ecolmodel.2005.03.026.

Phillips, S.J. and Dudík M. (2008). Modeling of species distributions with Maxent: new extensions and a comprehensive evaluation. *Ecography* 31(2), 161-175.

Ponti, M., Turicchia, E., Ferro, F., Cerrano, C., Abbiati, M. (2018). The understorey of gorgonian forests in mesophotic temperate reefs. *Aquatic Conservation: Marine and Freshwater Ecosystems*, 28(5), 1153–1166. https://doi.org/10.1002/aqc.2928

R Core Team. (2020). *R: A Language and Environment for Statistical Computing*. R Foundation for Statistical Computing, Vienna: Austria.

Rengstorf, A.M., Grehan, A., Yesson, C., Brown, C. (2012). Towards high-resolution habitat suitability modeling of vulnerable marine ecosystems in the deep-sea: resolving terrain attribute dependencies. *Marine Geodesy*, 35(4), 343–361. https://doi.org/10.1080/01490419.2012.699020

Robert, K., Jones, D.O., Roberts, J.M., Huvenne, V.A. (2016). Improving predictive mapping of deep-water habitats: Considering multiple model outputs and ensemble techniques. *Deep Sea Research Part I: Oceanographic Research Papers*, 113, 80–89. https://doi.org/10.1016/j.dsr.2016.04.008

Stagličić, N., Šegvić-Bubić, T., Ezgeta-Balić, D., Bojanić Varezić, D., Grubišić, L., Žuvić, L., Lin, Y., Briski, E. (2020). Distribution patterns of two co-existing oyster species in the northern Adriatic Sea: The native European flat oyster *Ostrea edulis* and the non-native Pacific oyster *Magallana gigas*. *Ecological Indicators*, 113, 106233. https://doi.org/10.1016/j.ecolind.2020.106233

Stenzel, H.B. (1971). Oysters. *Treatise on Invertebrate Paleontology, Part N, Mollusca 6, Bivalvia 3*, N953–N1224.

Sundahl, H., Buhl-Mortensen, P., Buhl-Mortensen, L. (2020). Distribution and suitable habitat of the cold-water corals *Lophelia pertusa*, *Paragorgia arborea*, and *Primnoa resedaeformis* on the Norwegian continental shelf. *Frontiers in Marine Science*, 7, 213. https://doi.org/10.3389/fmars.2020.00213

Taviani, M., Angeletti, L., Campiani, E., Ceregato, A., Foglini, F., Maselli, V., Morsilli, M., Parise, M., Trincardi, F. (2012). Drowned karst landscape offshore the Apulian Margin (Southern Adriatic Sea, Italy). *Journal of cave and karst studies the National Speleological Society bulletin*, 74, 197–212. https://doi.org/10.4311/2011JCKS0204

Taviani, M., Angeletti, L., Cardone, F., Montagna, P., Danovaro, R. (2019). A unique and threatened deep water coral-bivalve biotope new to the Mediterranean Sea offshore the Naples megalopolis. *Scientific Reports*, 9(1), 3411. https://doi.org/10.1038/s41598-019-39655-8

Van Rooij, D., De Mol, L., Le Guilloux, E., Wisshak, M., Huvenne, V.A.I., Moeremans, R., Henriet, J.-P. (2010). Environmental setting of deep-water oysters in the Bay of Biscay. *Deep Sea Research Part I: Oceanographic Research Papers*, 57(12), 1561–1572. https://doi.org/10.1016/j.dsr.2010.09.002

Wisshak, M., López Correa, M., Gofas, S., Salas, C., Taviani, M., Jakobsen, J., Freiwald, A. (2009). Shell architecture, element composition, and stable isotope signature of the giant deep-sea oyster Neopycnodonte zibrowii sp. n. from the NE Atlantic. *Deep Sea Research Part I: Oceanographic Research Papers*, 56(3), 374–407. https://doi.org/10.1016/j.dsr.2008.10.002

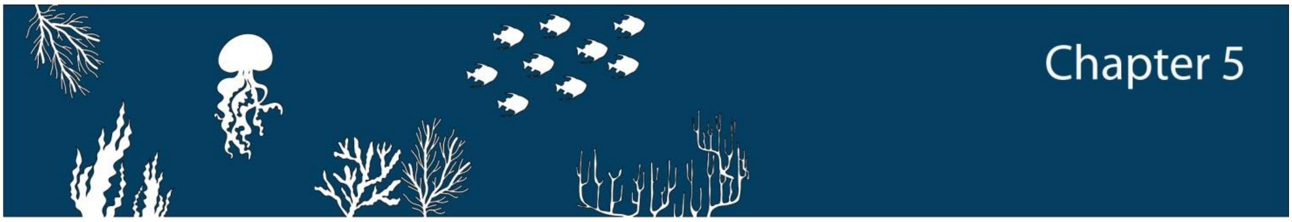

5. Out of the Mediterranean Sea: the mesophotic zone of the Gulf of Mexico

5.1 Introduction

The continental shelf in the northern Gulf of Mexico (GoM) is largely characterized by flat bottoms covered by soft sediment (Sammarco et al., 2016). In many areas, however, hard-bottom banks rise from the seabottom up to 17 m of the sea surface (Rezak et al., 1985). At mesophotic depths, these banks host flourish biological associations, encompassing a diverse set of taxonomic groups, including green and coralline algae, corals and other benthic invertebrates (Gittings et al., 1992; Precht et al., 2008). These ecosystems have been documented in 4 main areas in the Gulf: the Pinnacles Reefs, the Flower Garden Banks and other hard-ground features off-shore of Texas, the Florida Middle Ground reef system, and Pulley Ridge (Locker et al., 2010). Aiming at increasing the knowledge about the distribution of mesophotic ecosystems, efforts have been made to define the spatial and bathymetric extension of the mesophotic zone in the GoM using fixed depth range (Locker et al., 2010) or predictive models (Silva & MacDonald, 2017; Sterne et al., 2020). However, approaches integrating the light regime are still missing.

The extension of the mesophotic zone is defined by the intensity of light reaching the sea bottom, which is influenced by the incident sunlight radiation and turbidity of the water column (Locker et al., 2010). The penetration of light along the water column in the northern Gulf is unavoidably influenced by the runoff of the rivers flowing into its waters. Among these, the Mississippi River discharges around 380 km^3 year^{-1} of freshwater and ca. 150×109 kg year^{-1} of sediment in waters surrounding its mouth (Meade et al., 1990; Dagg & Breed, 2003), generating a buoyant plume that spreads over the receiving ocean waters. The suspended sediments increase stratification influencing the turbidity and restricts light penetration in the surroundings of the river mouth. The amount of light reaching the seabed limits the distribution of light-dependent taxonomic groups and, together with a set of environmental and ecological factors, and stochastic processes, ultimately concurs to influence the composition of mesophotic assemblages.

Several ROV surveys carried out in the GoM provided information on mesophotic ecosystems populating the complex banks system that characterizes the geomorphology of the northwest sector, documenting a conspicuous presence of deep-water octocorals (mainly Ellisellidae, Paramuriceidae, and antipatharians) and associated fauna (Cairns & Bayer, 2009; Etnoyer et al., 2016; Silva & MacDonald, 2017; Frometa et al., 2021). These associations provide structural complexity, representing hotspots of biodiversity and refuge for vagile invertebrates and fish fauna of commercial interest, such as grouper, snapper, amberjack, and mackerel (Etnoyer, 2014).

The diversity of situations dominated by cnidarians in the deep GoM (200-2500 m) has been widely studied to explore the factors influencing how they assemble, documenting a potential role of depth, intended as proxy of other environmental gradients, in shaping the composition of assemblages (Quattrini et al., 2014; Quattrini et al., 2017). Sammarco et al. (2016) suggest that the diversity of the mesophotic community populating banks might be related to the relief of the banks, with deeper situation presenting the higher diversity. However, the relationship between depth and assemblages diversity has not been specifically tested.

In this chapter, the seabed portion under mesophotic conditions for the northern GoM is provided by estimating the quantity of PAR reaching the seafloor and compared with the location of 37 ROV surveys performed on 8 banks (Fig. 5.1, Tab. 5.1), known to host benthic mesophotic assemblages. In addition, a set of 8 videos (one per each bank) was selected and analyzed for taxonomic identification to explore the composition of mesophotic cnidarians assemblages. The diversity and abundance of specimens were tested for correlation with depth to investigate patterns of assembling and distribution of cnidarian-dominated assemblages in the surveyed area.

5.2 Materials and methods

5.2.1 Bathymetric and spatial definition of the mesophotic zone

Satellite data on PAR at sea surface and diffuse attenuation coefficient at 490nm were obtained from NASA Ocean Color database (https://oceancolor.gsfc.nasa.gov/) with a horizontal resolution of 5 km for the period 2002-2018, used also in Chapter 1 (Fig. 5.2). Bathymetric data were acquired from NOAA repository (https://www.ncei.noaa.gov/maps/bathymetry/) at a horizontal resolution of 100 m. The 17-years mean of k_{d490} was calculated and used to estimate K_{dPAR} and the quantity of light reaching the seabed following the methodology developed in the first chapter of this thesis. The percent surface PAR at seabed was, then, estimated as the ratio between the light at the seabed with the correspondence surface PAR value in each pixel, multiplied by 100. All calculations were performed by using the package “raster” (version 3.3-13, Hijmans et al., 2015) in R software (R Core Team, 2020). Satellite data were processed to match the resolution of bathymetry data.

The upper limit for the mesophotic zone was set at 30 m, excluding shallower areas from further analysis. The 0.0005% of surface PAR was used as the lower border of the mesophotic zone. The resulting raster dataset was then classified using the tool “Reclassify” in ArcGIS 10.5 (ESRI©) and converted to a polygon using the “Raster to Polygon” tool.

Points every 20 km along the upper and the lower borders were generated and used to provide ranges (average ± standard error) of percent surface PAR and depth of the estimated mesophotic zone.

To validate the estimation, the area resulting as under mesophotic condition was compared with position of 37 ROV surveys collected in correspondence of known mesophotic communities in the north-western sector of the GoM carried out within the NOAA RESTORE Science Program.

5.2.2 Video surveys

A total of 37 ROV surveys were collected in 2017 and 2018 in the Flower Garden Banks National Marine Sanctuary in the framework of the ‘Research Priority: Population Connectivity of Deepwater Corals in the Northern Gulf of Mexico’, funded by the NOAA RESTORE Science Program. Video footages were acquired using the ROV Mohawk provided with a high-definition video camera and a digital stills camera. A pair of lasers spaced 10 cm apart were utilized as size scale. Once on the bottom, the ROV was driven at ~0.5 knots and approximately 0.5-1 m above the seafloor. The acoustic tracking system was an ultra-short baseline (USBL) telemetry system providing the ROV location every two seconds and the depth.

From each bank, one ROV video was randomly selected and analyzed for taxonomical identification. The surveys explored: Eastern Flower Garden Bank, Western Flower Garden Bank, Stetson Bank, Sonnier Bank, Bouma Bank, Elvers Bank, Bright Bank and McNeil Bank (Fig. 5.1, Tab. 5.1). A frames every 10 s was extracted from video footages following the methodology from Castellan et al., 2020 and Chapter 2. The images were coupled with video footages to improve taxonomic identification efficiency, when necessary. Macrofauna and megafauna were identified to the lowest possible taxonomic rank. Organisms unidentifiable at the genus or species level were categorized as morpho-species or morphological categories. The abundances of taxa along the ROV tracks were calculated by counting the number of taxa in each frame. To overcome sampling differences related to the different length of the surveys and frames extracted, species accumulation curves were generated in R software (package "vegan", version 2.5-7 Oksanen et al., 2007). The value of expected taxonomic richness with 100 still images was used to compare the diversity associated with explored assemblages. For each dive, the number of frames needed to document 75% of the identified taxa was used to sub-sample the video footages, generating 3 sub-tracks per video.

5.2.3 Statistical analysis

The significant difference in the composition of mesophotic assemblages explored was tested using ANOSIM in R software (package "vegan"). The Shannon-Wiener diversity index of communities and the octocorals abundance were calculated considering only taxa in the Anthipatharia and Alcyonacea. The mantel was used to test for significant correlation of cnidarians diversity and cumulative abundance with vertical distance. The results of Mantel tests were validated with distance correlations (package "energy", version 1.7; Rizzo & Székely, 2016).

5.3 Results

5.3.1 Extension of the estimated mesophotic zone

The average intensity of PAR at surface in the GoM for the period 2002-2018 showed a gradient related to the latitude. Values ranged between 36.15 to 44.48 mol. phot. m^{-2} d^{-1}, increasing moving towards south (Fig. 5.2A). A reverse was observed in the diffuse attenuation coefficient at 490 nm (k_{d490}) that decreased with distance from the coast (Fig. 5.2B). In the area surrounding the Mississippi River mouth, the attenuation was the strongest documented, presenting values up to 2.73 m^{-1}. Similarly, the estimated attenuation coefficients for PAR (K_{dPAR}) showed higher values along the coastline with maximum attenuation in the central-northern part of the Gulf (Fig. 5.2C).

On average, the area estimated as under mesophotic conditions in the GoM extended in the depth range 30 – 187.3 m ± 50.4 and in the light range 4.85 ± 3.9 – 0.0005% of surface PAR. The analysis of the amount of PAR at the seabed showed a trend related to the geomorphology and hydrological processes. The light regime decreased with distance from the coast as a result of the increasing depth, with the exception of the area characterized by the Mississippi River runoff, where attenuation was strong enough to limit the penetration of light to areas above ca. 40 m depth (Fig. 5.2D). Consequently, the depth of the lower limit of the mesophotic zone was significantly shallower in the area close to the Mississippi mouth (Fig. 5.3A)

The spatial extension of the area estimated as under mesophotic conditions was larger in the eastern sector of the GoM, reflecting the gradients in attenuation coefficients and PAR at surface, and the seafloor morphology (Fig. 5.2E). Along the west side of Florida, in fact, the values of the attenuation coefficients were lower, the intensity of surface PAR was the highest observed and the shelf was broad and gently sloped.

Similarly, the percent PAR at the upper mesophotic border (i.e., 30 m depth) showed an increasing west-east pattern, with the highest values documented along the Florida margin (Fig. 5.3). The areas corresponding to the Mississippi River and Rio Grande mouths reported the lowest percentage of

PAR at the upper border potentially as consequence of the augmented attenuation of light penetration (Fig. 5.3B).

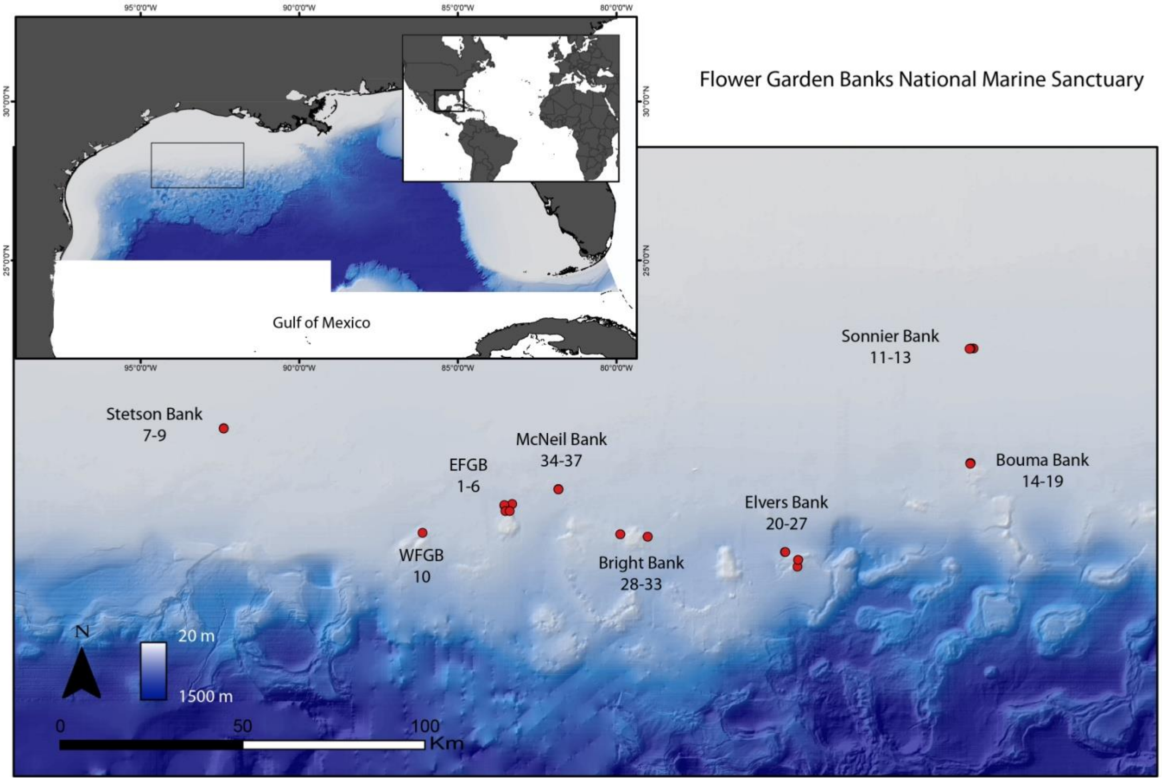

Fig. 5.1. Location of ROV videos used to validate the light penetration model. One video from each bank were also analyzed for taxonomical identification. The IDs refer to Tab. 5.1.

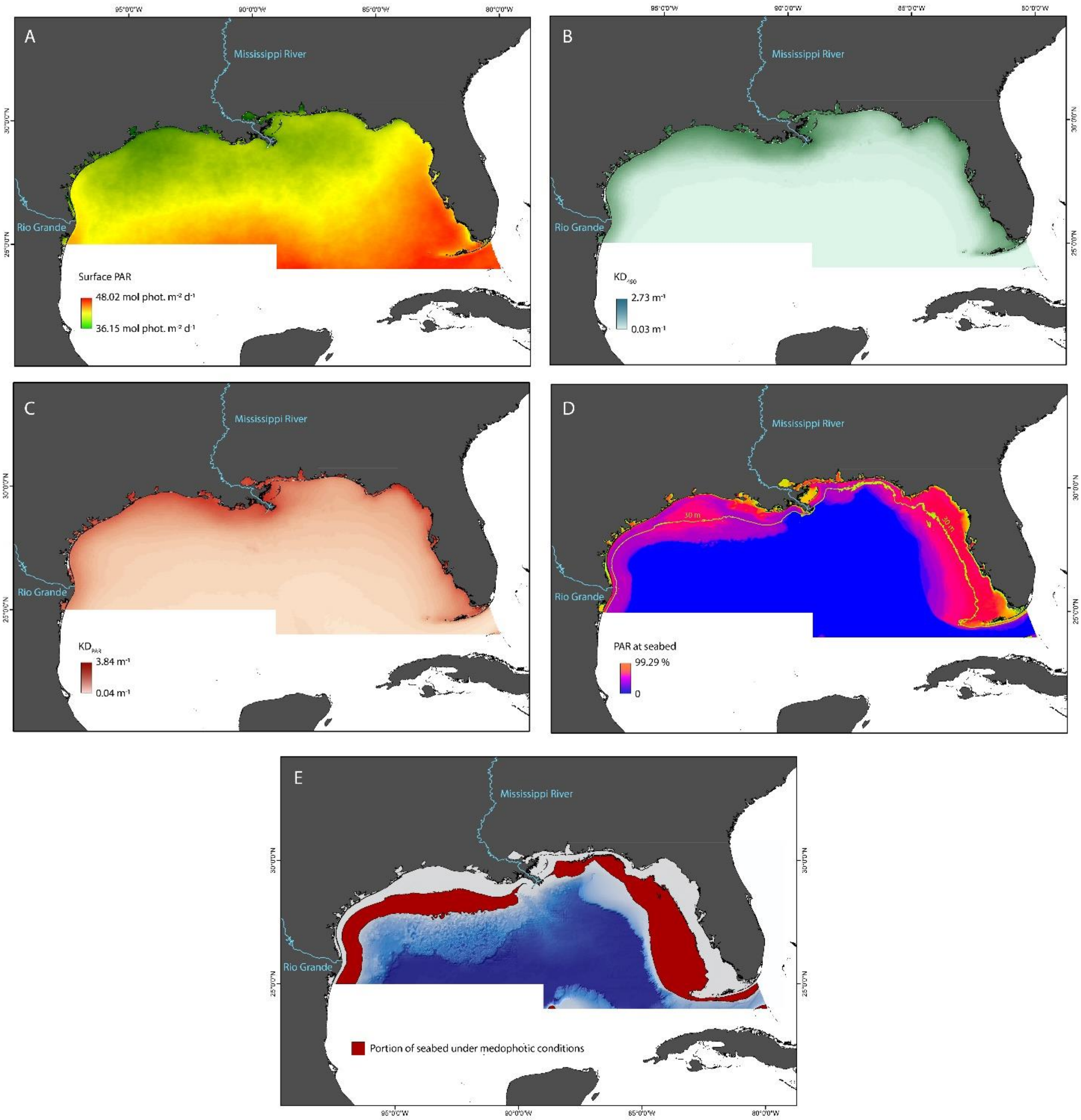

Fig. 5.2. Satellite data on surface PAR (A) and diffuse attenuation coefficient at 490 nm (K_{d490}, B); C) diffuse attenuation coefficient for PAR light (K_{dPAR}) calculated from concentration of K_{d490}; D) percentage of surface PAR reaching the seabed; E) portion of seabed under mesophotic condition (30 m – 0.0005% of surface PAR).

ID	Cruise	Location	ROV	Date	Lat	Long	Depth range (m)
1	RESTORE_MT17	EFGB	**Dive 553**	**10/10/2017**	**27° 58' 15.93'' N**	**93° 35' 38.06'' W**	**98 - 110**
2			Dive554	10/10/2017	27° 58' 5.13" N	93° 36' 45.7" W	68 - 74
3			Dive555	10/10/2017	27° 58' 5.55" N	93° 36' 46.77" W	70 - 77
4			Dive556	10/10/2017	27° 58' 6.13" N	93° 36' 47.46" W	74 - 90
5			Dive557	10/10/2017	27° 57' 14.94" N	93° 36' 38.67" W	81 - 90
6			Dive558	10/10/2017	27° 57' 12.66" N	93° 36' 0.28" W	62 - 78
7		Stetson Bank	Dive559	12/10/2017	28° 9' 26.78" N	94° 18' 8.61" W	53 - 57
8			Dive560	12/10/2017	28° 9' 25.52" N	94° 18' 9.49" W	55 - 57
9			**Dive561**	**12/10/2017**	**28° 9' 25.53'' N**	**94° 18' 11.54'' W**	**52 - 60**
10		WFGB	**Dive562**	**12/10/2017**	**27° 54' 0.87'' N**	**93° 48' 50.63'' W**	**71 - 95**
11	RESTORE_MT18	Sonnier Bank	Dive673	18/09/2018	28° 21' 13.71" N	92° 27' 35.4" W	57 - 58
12			Dive674	18/09/2018	28° 21' 13.53" N	92° 28' 1.39" W	52 - 55
13			**Dive675**	**18/09/2018**	**28° 21' 9.96'' N**	**92° 28' 8.82'' W**	**52 - 55**
14		Bouma Bank	Dive676	19/09/2018	28° 4' 17.89" N	92° 28' 2.24" W	78 - 80
15			Dive677	19/09/2018	28° 4' 17.92" N	92° 28' 2.54" W	79 - 90
16			Dive678	19/09/2018	28° 4' 17.71" N	92° 28' 2.32" W	78 - 90
17			Dive679	19/09/2018	28° 4' 17.58" N	92° 28' 2.47" W	79 - 95
18			**Dive680**	**19/09/2018**	**28° 4' 17.34'' N**	**92° 28' 2.04'' W**	**77 - 95**
19			DIve681	19/09/2018	28° 4' 13.53" N	92° 28' 2.34" W	78 - 80
20		Elvers Bank	Dive682	20/09/2018	27° 49' 2.14" N	92° 53' 33.91" W	98 - 125
21			Dive683	20/09/2018	27° 51' 10.47" N	92° 55' 24.06" W	98 - 120
22			Dive684	20/09/2018	27° 51' 12.59" N	92° 55' 22.59" W	95 - 120
23			Dive685	20/09/2018	27° 51' 10.9" N	92° 55' 23.07" W	90 - 115
24			Dive686	20/09/2018	27° 51' 10.9" N	92° 55' 20.01" W	80 - 110
25			Dive687	20/09/2018	27° 50' 3.98" N	92° 53' 26.34" W	96 - 120
26			**Dive688**	**20/09/2018**	**27° 50' 3.26'' N**	**92° 53' 26.66'' W**	**95 - 120**
27			Dive689	20/09/2018	27° 50' 3.33" N	92° 53' 26.94" W	95 - 100
28		Bright Bank	Dive690	21/09/2018	27° 53' 27.08" N	93° 15' 38.22" W	115 - 120
29			Dive691	21/09/2018	27° 53' 27.41" N	93° 15' 39.31" W	105 - 120
30			**Dive692**	**21/09/2018**	**27° 53' 27.84'' N**	**93° 15' 39.26'' W**	**113 - 130**
31			Dive693	21/09/2018	27° 53' 50.43" N	93° 19' 39.37" W	83 - 85
32			Dive694	21/09/2018	27° 53' 50.19" N	93° 19' 39.3" W	82 - 84
33			Dive695	21/09/2018	27° 53' 50.13" N	93° 19' 39.45" W	82 - 84
34		McNeil Bank	Dive696	22/09/2018	28° 0' 27.51" N	93° 28' 47.41" W	84 - 85
35			Dive697	22/09/2018	28° 0' 27.69" N	93° 28' 47.79" W	83 - 90
36			**Dive698**	**22/09/2018**	**28° 0' 26.61'' N**	**93° 28' 48.68'' W**	**85 - 95**
37			Dive699	22/09/2018	28° 0' 25.31" N	93° 28' 48.6" W	83 - 90

Tab. 5.1. Metadata of ROV videos imaging mesophotic assemblages in the Flower Garden Banks Marine National Sanctuary. Bold characters identify the dives selected for taxonomical analysis.

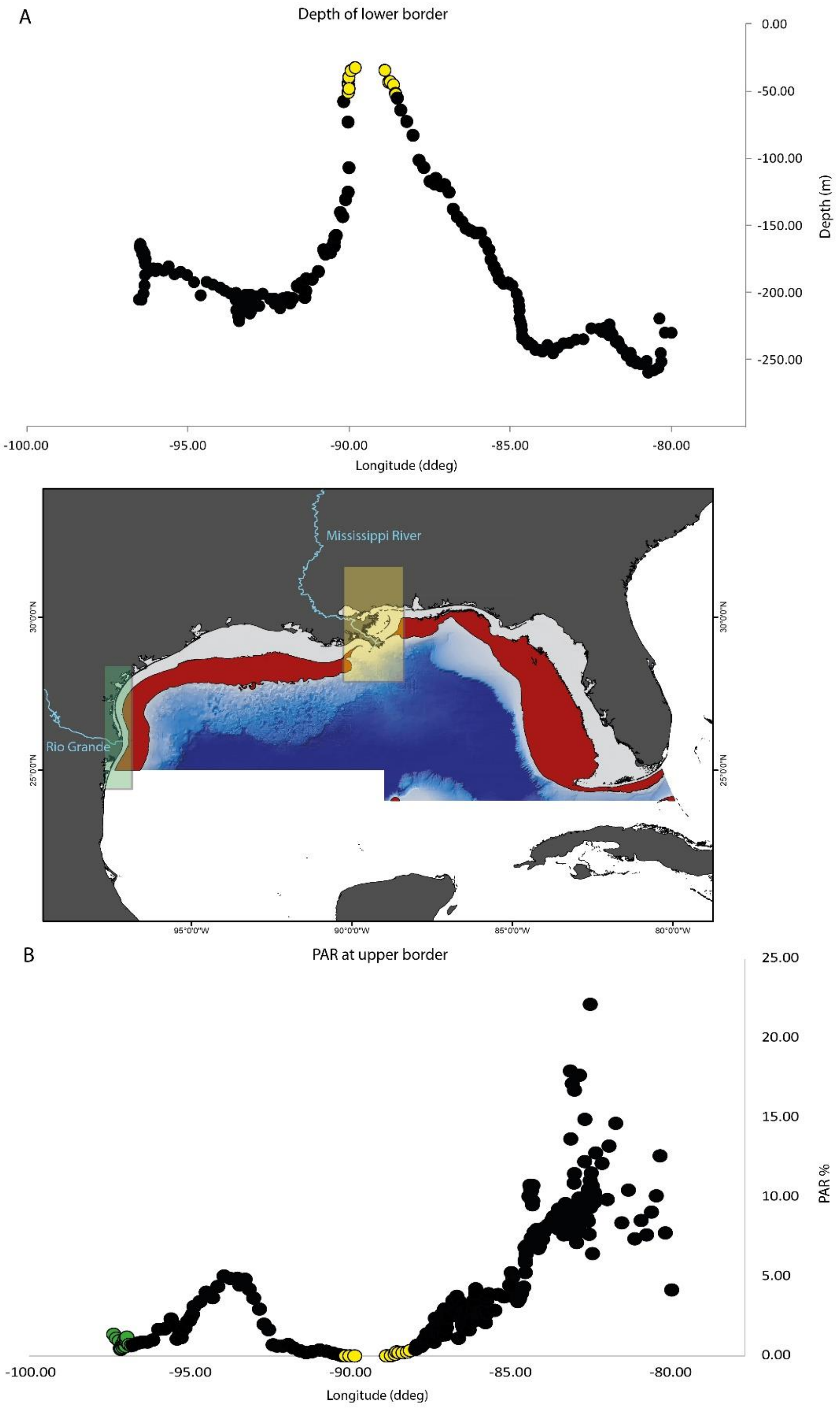

Fig. 5.3. A) Variation in the depth of the lower border (i.e., 0.0005% surface PAR) of the mesophotic zone with longitude; B) variation in the percentage of surface PAR at the upper border (i.e., 30 m depth) with longitude. Yellow square and dots identify the area close to Mississippi River mouth, whilst green color refers to the area influenced by Rio Grande runoff.

5.3.2 Diversity of the explored mesophotic assemblages

The dives explored the mesophotic assemblages populating 8 banks in the north-western Gulf of Mexico imaging 7.6 km of seafloor in linear distance in the depth range 50-130 m (Tab. 5.1). The substrate varied from mobile bottoms (EFGB, Bright Bank, McNeil Bank), also characterized by sparse hard blocks with coralline algae covering (Stetson Bank, Sonnier Bank, Bouma Bank), to hard bottoms, nude or colonized by green (Chlorophyta) and coralline algae (WFGB, Elvers Bank). The taxonomic composition of the assemblages was significantly different among banks (ANOSIM test, $p<0.01$). These were dominated by cnidarians, representing 70% of the entire taxonomic diversity with 49 different taxa identified (Tab. S5.1). Anthipatharians and alcyonaceans were the major contributors, counting 1296 and 1286 colonies, respectively. Black corals (Order: Anthipatharia) comprised specimens of the *Stichopathes*, *Elatopathes* and *Tanacetipathes* and were observed both on hard substrates and erecting from mobile bottoms.

Alcyonaceans were represented by ellisellids of the genera *Nicella* and *Ellisella* (Family: Ellisellidae) which were frequent in the explored sites, colonizing bare or partially buried hard substrates emerging from mobile bottoms. Also, plexaurids such as *Swiftia exserta* and *Hypnogorgia pendula* were regularly observed, forming large fan-shaped colonies often fouled by basket stars (Order: Euryalida). The highest number of cnidarians taxa was observed in the Bright Bank (15 taxa, 254.3 ind. on average), whilst the lowest in Stetson Bank (4 taxa, 15 ind. on average, Fig. 5.4).

Albeit less abundant, sponges were present in the explored sites with a total of 14 taxa of identified, representing the second most taxonomic diverse group in the explored banks (ca. 20% of the taxonomic diversity, Tab. S5.1). Specimens populated the hard bottoms, bare or covered by a thin layer of sediment, and counted 213 colonies.

Although with only 2 taxa identified, echinoderms were abundant, mainly as epibionts on cnidarians, with more than 270 individuals recognized.

The remaining portion of taxonomic diversity was constituted by bryozoans (3 taxa, 9 colonies) and the arthropods of the Families Pycnogonidae and Inachoididae counting 1 individual each (Tab. S5.1).

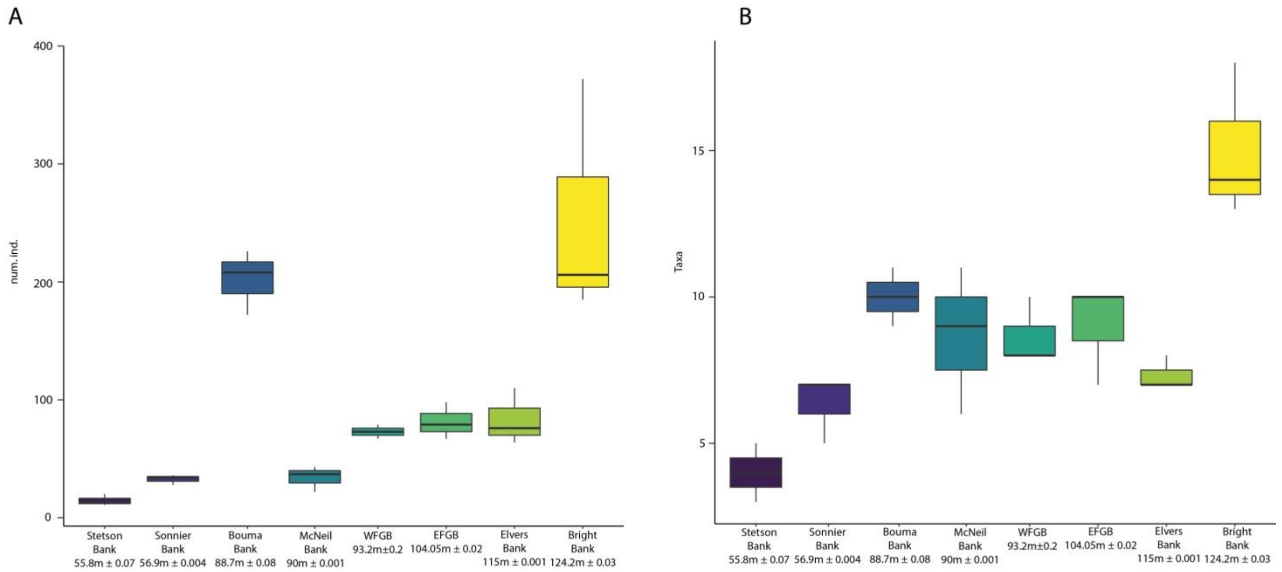

Fig. 5.4. Boxplots of abundance (A) and diversity (B) of mesophotic octocorals community in the explored banks. The average depth (± standard deviation) of dives is reported.

5.3.3 The relation between cnidarians diversity and abundance with depth

The diversity of cnidarians was significantly correlated with vertical distance (mantel, r = 0.43, p = 0.001). The dissimilarity in the composition of explored assemblages in terms of number of taxa was higher in sites vertically distant from each other, with those located at greater depth presenting a larger number of taxa (Fig. 5.4A).

Similarly, the number of individuals was significantly correlated with vertical distance (mantel, r = 0.48, p = 0.01). The number of individuals of cnidarians showed the highest values in Bright Bank, the deepest location surveyed (Fig. 5.4A).

Within the study area, the cnidarians assemblages not only presented a higher number of individuals but was also a higher taxonomic diversity in the deeper areas with respect to those located at shallower depths.

5.4 Discussion

5.4.1 The mesophotic zone of the GoM

In the literature, opinions differ regarding the bathymetric interval associated with the mesophotic zone in the GoM. Some studies suggest that mesophotic conditions might range between 30 and 150-200 m depth expecting no light penetration below 200 m depth (e.g., Semmler et al., 2017; Mayorga-Martínez et al., 2021). Contrarily, other authors adopt the bathymetric interval 30-100 m as range of occurrence of mesophotic conditions (Locker et al., 2010).

The estimated spatial and bathymetric extent for the mesophotic zone in the GoM based on the quantity of light reaching the seabed revealed that mesophotic conditions might occur in the depth range 30-187.3 m ± 50.4 m, on average. The analysis of the depth of the lower border, however, showed the extent of the mesophotic zone largely varied across the Gulf. In the areas comprised between the Rio Grande and the Mississippi River, the lower border of the mesophotic zone reached 220 m depth, extending even much deeper along the western Florida coast, trespassing 250 m in the southern part. In contrast, only areas above 40 m depth resulted as under mesophotic conditions in the area surrounding the Mississippi River mouth. River runoff affects the water transparency by driving great volumes of sediment to the ocean that generate turbid plumes that impede the penetration of light beyond certain depths (Dagg & Breed, 2003), ultimately influencing the average value calculated for the entire GoM. When the area around the Mississippi River mouth was excluded, the average depth for the lower mesophotic border not only increased but also showed a lower variance (207.46 m ± 25.6).

Similarly, the rivers outflow also affected the estimated percent surface PAR at the upper mesophotic border, which showed the lowest values in the surroundings of the Mississippi River and the Rio Grande mouths. Excluding these areas, the average percentage of PAR at the upper border was increased to 6.94 % ± 3.97.

Not only the values of light and depth associated with the borders of the mesophotic zone varied with distance from the areas affected by rivers runoff but also the spatial extension of the portion of seafloor estimated as under mesophotic conditions, which was higher in the area between the two rivers and in the eastern sector of the GoM. The seafloor geomorphology surely acted in concert with water transparency. The shelf of eastern Texas and western Florida is broader and characterized by gentle slopes, resulting in a greater horizontal extension of seafloor reached by light intensities in the photic range (up to 0.0005% surface PAR).

5.4.2 Diversity of the mesophotic assemblages

As mentioned above, the GoM harbors diverse benthic ecosystems populating the many topographic features characterizing the seafloor (Sammarco et al., 2016). Corals represent the major taxonomic group whose diversity is widely documented in the literature (e.g., Cairns & Bayer, 2009; Etnoyer, 2014; Quattrini et al., 2014). Such accounts, it is known that at least 162 octocoral species occur at depths up to 3000 m in the entire GoM, and 51% of these are found in waters shallower than 200 m (Cairns & Bayer, 2009). The mesophotic assemblages explored by ROV confirm previous observations, hosting lush cnidarian assemblages dominated by anthipatharians and alcyonaceans. Black corals (*Stichopathes*, *Elatopathes,* and *Tanacetipathes*) together with ellisellids and plexaurids were densely present colonizing bare and partially buried hard substrates or erecting from mobile bottoms. The observed taxonomic diversity is in line with evidence from exploration performed in the area (Schmahl et al., 2008), on other banks (e.g., Etnoyer et al., 2016) or from whole GoM e.g., (Quattrini et al., 2014; Quattrini et al., 2017).

The composition of cnidarian assemblages and the cumulative number of individuals varied with depth, with sites located much deeper presenting a higher diversity (number of taxa) and number of individuals. The change in species abundance and community composition with depth is a common phenomenon and has been already identified in several taxa including amphipods (France & Kocher, 1996), bivalves (Chase et al., 1998; Zardus et al., 2006), polychaetes (Schüller, 2011) and stylasterid corals (Lindner et al., 2008). Moreover, recent studies have documented the change in the taxonomic composition of the octocoral community of GoM related to depth gradient in the range 250-2500 m (Quattrini et al., 2014; Quattrini et al., 2017). The results provide evidence that a similar pattern might occur on a smaller scale within the mesophotic depth range of the GoM.

The factors and processes concurring to shape the abundance of taxonomic groups and the composition of biological assemblages are, however, different. For instance, dispersal processes are relevant at a regional scale and determine the possible combinations of biological assemblages by governing the presence of species and their distribution. At a smaller scale, the ecological relationships among taxa, such as competition for food, substrate, and predation, become crucial, limiting the abundance/presence of some taxa, and ultimately influencing the structure of assemblages. Finally, stochastic processes act at both large and small scales by determining how species assemble in benthic ecosystems, with taxa arriving first that present more chances for successful recruitment and establishment, potentially limiting the colonization by other taxonomic groups. In addition, the relative abundance of taxa could also result from local disturbances such as the re-suspension of sediments and slope instability (Tripsanas et al., 2004; Brooke, Holmes & Young, 2009).

The structure of the mesophotic assemblages explored in the GoM is, arguably, the result of the combination of environmental, ecological, and stochastic processes that occur throughout the mesophotic depth range. However, the observed variation in the abundance and diversity of cnidarians with depth could ultimately be a consequence of depth-related environmental gradients. Many environmental factors, such as food supply, temperature, light, water mass characteristic, and oxygen, indeed, co-vary with depth, creating habitats with environmental characteristics suitable for certain taxa rather than others.

References

Brooke, S., Holmes, M., Young, C.M. (2009). Effects of sediment on two morphotypes of *Lophelia pertusa* from the Gulf of Mexico. *Mar Ecol Prog Ser*, 390, 137–144.

Cairns, S.D., Bayer, F.M. (2009). Octocorallia (Cnidaria) of the Gulf of Mexico. *Gulf of Mexico–origins, waters, and biota*, 1, 321–331.

Castellan, G., Angeletti, L., Correggiari, A., Foglini, F., Grande, V., Taviani, M. (2020). Visual methods for monitoring mesophotic-to-deep reefs and animal forests: finding a compromise between analytical effort and result quality. In: *Perspectives on the Marine Animal Forests of the World*, Springer, Cham, pp. 487-514

Chase, M.R., Etter, R.J., Rex, M.A., Quattro, J.M. (1998). Bathymetric patterns of genetic variation in a deep-sea protobranch bivalve, *Deminucula atacellana*. *Marine Biology*, 131(2), 301–308. https://doi.org/10.1007/s002270050323

Dagg, M.J., Breed, G.A. (2003). Biological effects of Mississippi River nitrogen on the northern gulf of Mexico—a review and synthesis. *Journal of Marine Systems*, 43(3), 133–152. https://doi.org/10.1016/j.jmarsys.2003.09.002

Etnoyer, P. (2014). Distribution and diversity of octocorals in the Gulf of Mexico. Ph.D. Dissertation, Texas A&M University, U.S.

Etnoyer, P.J., Wickes, L.N., Silva, M., Dubick, J.D., Balthis, L., Salgado, E., MacDonald, I.R. (2016). Decline in condition of gorgonian octocorals on mesophotic reefs in the northern Gulf of Mexico: before and after the Deepwater Horizon oil spill. *Coral Reefs*, 35(1), 77–90. https://doi.org/10.1007/s00338-015-1363-2

France, S.C., Kocher, T.D. (1996). Geographic and bathymetric patterns of mitochondrial 16S rRNA sequence divergence among deep-sea amphipods, *Eurythenes gryllus*. *Marine Biology*, 126(4), 633–643. https://doi.org/10.1007/BF00351330

Frometa, J., Etnoyer, P.J., Quattrini, A.M., Herrera, S., Greig, T.W. (2021). Genetic divergence and polyphyly in the octocoral genus *Swiftia* [Cnidaria: Octocorallia], including a species impacted by the DWH Oil Spill. *Diversity*, 13(4), 172. https://doi.org/10.3390/d13040172

Gittings, S.R., Bright, T., Schroeder, W., Sager, W., Laswell, S., Rezak, R. (1992). Invertebrate assemblages and ecological controls on topographic features in the Northeast Gulf of Mexico. *Bulletin of Marine Science*, 50, 435–455.

Lindner, A., Cairns, S.D., Cunningham, C.W. (2008). From offshore to onshore: multiple origins of shallow-water corals from deep-Sea ancestors. *PLOS ONE*, 3(6), e2429. https://doi.org/10.1371/journal.pone.0002429

Locker, S.D., Armstrong, R.A., Battista, T.A., Rooney, J.J., Sherman, C., Zawada, D.G. (2010). Geomorphology of mesophotic coral ecosystems: current perspectives on morphology, distribution, and mapping strategies. *Coral Reefs*, 29(2), 329–345. https://doi.org/10.1007/s00338-010-0613-6

Mayorga-Martínez, M., Bello-Pineda, J., Perales-Valdivia, H., Pérez-España, H., Heyman, W.D. (2021). Characterizing geomorphology of mesophotic coral reef ecosystems in the Southwestern Gulf of Mexico: implications for conservation and management. *Frontiers in Marine Science*, 8, 631. https://doi.org/10.3389/fmars.2021.639359

Meade, R.H., Yuzyk, T.R., Day, T.J. (1990). Movement and storage of sediment in rivers of the United States and Canada. In: *Surface Water Hydrology.* Geological Society of America, Boulder, Colorado, pp. 255-280.

Oksanen, J., Kindt, R., Legendre, P., O'Hara, B., Stevens, M.H.H., Oksanen, M.J., Suggests, M. (2007). The vegan package. *Community ecology package*, 10(631–637), 719.

Precht, W.F., Aronson, R.B., Deslarzes, K.J., Robbart, M.L., Evans, D.J., Zimmer, B., Duncan, L. (2008). Long-Term Monitoring at the East and West Flower Garden Banks, 2004-2005–Interim Report, Volume 1: Technical Report.

Quattrini, A.M., Etnoyer, P.J., Doughty, C., English, L., Falco, R., Remon, N., Rittinghouse, M., Cordes, E.E. (2014). A phylogenetic approach to octocoral community structure in the deep Gulf of Mexico. *Deep Sea Research Part II: Topical Studies in Oceanography*, 99, 92–102. https://doi.org/10.1016/j.dsr2.2013.05.027

Quattrini, A.M., Gómez, C.E., Cordes, E.E. (2017). Environmental filtering and neutral processes shape octocoral community assembly in the deep sea. *Oecologia*, 183(1), 221–236. https://doi.org/10.1007/s00442-016-3765-4

R Core Team. (2020). *R: A Language and Environment for Statistical Computing*. R Foundation for Statistical Computing, Vienna: Austria.

Rezak, R., Bright, T.J., McGrail, D.W. (1985). *Reefs and banks of the northwestern Gulf of Mexico: their geological, biological, and physical dynamics*. Wiley-Interscience: New York, U.S., pp. 259

Rizzo, M.L., Székely, G.J. (2016). Energy distance. *Wiley interdisciplinary reviews: Computational statistics*, 8(1), 27–38.

Sammarco, P., Nuttall, M., Beltz, D., Hickerson, E., Schmahl, G.P. (2016). Patterns of mesophotic benthic community Structure on banks off vs inside the continental shelf edge, Gulf of Mexico. *Gulf of Mexico Science*, 33(1). https://doi.org/10.18785/goms.3301.07

Schmahl, G.P., Hickerson, E.L., Precht, W.F. (2008). Biology and ecology of coral reefs and coral communities in the Flower Garden Banks Region, Northwestern Gulf of Mexico. In: *Coral Reefs of the USA*. Riegl BM,, , Dodge RE (Eds). Springer Netherlands: Dordrecht, pp. 221–261.

Schüller, M. (2011). Evidence for a role of bathymetry and emergence in speciation in the genus *Glycera* (Glyceridae, Polychaeta) from the deep Eastern Weddell Sea. *Polar Biology*, 34(4), 549–564. https://doi.org/10.1007/s00300-010-0913-x

Semmler, R.F., Hoot, W.C., Reaka, M.L. (2017). Are mesophotic coral ecosystems distinct communities and can they serve as refugia for shallow reefs? *Coral Reefs*, 36(2), 433–444. https://doi.org/10.1007/s00338-016-1530-0

Silva, M., MacDonald, I.R. (2017). Habitat suitability modeling for mesophotic coral in the northeastern Gulf of Mexico. *Marine Ecology Progress Series*, 583, 121–136.

Sterne, T.K., Retchless, D., Allee, R., Highfield, W. (2020). Predictive modelling of mesophotic habitats in the north-western Gulf of Mexico. *Aquatic Conservation: Marine and Freshwater Ecosystems*, 30(4), 846–859.

Tripsanas, E.K., Bryant, W.R., Phaneuf, B.A. (2004). Slope-instability processes caused by salt movements in a complex deep-water environment, Bryant Canyon area, northwest Gulf of Mexico. *AAPG Bulletin*, 88(6), 801–823. https://doi.org/10.1306/01260403106

Zardus, J.D., Etter, R.J., Chase, M.R., Rex, M.A., Boyle, E.E. (2006). Bathymetric and geographic population structure in the pan-Atlantic deep-sea bivalve *Deminucula atacellana* (Schenck, 1939). *Molecular Ecology*, 15(3), 639–651. https://doi.org/10.1111/j.1365-294X.2005.02832.x

Supplementary materials

Tab. S5.1. Comprehensive list of the species identified during video analysis, with their abundance values and occurrence in the assemblage categories.

Phyum	Class	Order	Family	Genus	Species	Author	n. ind
Porifera	Demospongiae				spp.		13
Porifera	Demospongiae				sp. 1		25
Porifera	Demospongiae				sp. 2		1
Porifera	Demospongiae				sp. 3		1
Porifera	Demospongiae				sp. 4		85
Porifera	Demospongiae				sp. 5		9
Porifera	Demospongiae				sp. 6		1
Porifera	Demospongiae				sp. 7		27
Porifera	Demospongiae				sp. 8		19
Porifera	Demospongiae				sp. 9		4
Porifera	Demospongiae				sp. 10		20
Porifera	Demospongiae				sp. 11		2
Porifera	Demospongiae				sp. 12		1
Porifera	Demospongiae	Tethyida	Tethyidae	*Tethya*	spp.		5
Cnidaria	Anthozoa	Alcyonacea	Clavulariidae	*Carijoa*	sp. 1		2
Cnidaria	Anthozoa	Alcyonacea	Ellisellidae	*Ellisella*	*Ellisella elongata*	Pallas, 1766	41
Cnidaria	Anthozoa	Alcyonacea	Ellisellidae	*Ellisella*	sp. 1		11
Cnidaria	Anthozoa	Alcyonacea	Ellisellidae	*Nicella*	sp. 1		1
Cnidaria	Anthozoa	Alcyonacea	Ellisellidae	*Nicella*	sp. 2		395
Cnidaria	Anthozoa	Alcyonacea	Ellisellidae	*Nicella*	sp. 3		1
Cnidaria	Anthozoa	Alcyonacea	Gorgoniidae	*Leptogorgia*	sp. 1		32
Cnidaria	Anthozoa	Alcyonacea	Isididae	*Acanella*	sp. 1		2
Cnidaria	Anthozoa	Alcyonacea	Nephtheidae	*Gersemia*	sp. 1		3
Cnidaria	Anthozoa	Alcyonacea	Nidaliidae	*Nidalia*	sp. 1		3
Cnidaria	Anthozoa	Alcyonacea	Plexauridae	*Bebryce*	spp.		3
Cnidaria	Anthozoa	Alcyonacea	Plexauridae	*Bebryce*	sp. 1		125
Cnidaria	Anthozoa	Alcyonacea	Plexauridae	*Hypnogorgia*	*Hypnogorgia pendula*	Duchassaing & Michelotti, 1864	140
Cnidaria	Anthozoa	Alcyonacea	Plexauridae	*Muricea*	*Muricea pendula*	Verrill, 1868	16
Cnidaria	Anthozoa	Alcyonacea	Plexauridae	*Muriceides*	sp. 1		8
Cnidaria	Anthozoa	Alcyonacea	Plexauridae	*Swiftia*	spp.		1
Cnidaria	Anthozoa	Alcyonacea	Plexauridae	*Placogorgia*	sp. 1		51
Cnidaria	Anthozoa	Alcyonacea	Plexauridae	*Placogorgia*	sp. 2		4
Cnidaria	Anthozoa	Alcyonacea	Plexauridae	*Swiftia*	*Swiftia exserta*	Ellis & Solander, 1786	141
Cnidaria	Anthozoa	Alcyonacea	Plexauridae	*Thesea*	sp. 1		4
Cnidaria	Anthozoa	Alcyonacea	Plexauridae	*Thesea*	*Thesea nivea*	Deichmann, 1936	18
Cnidaria	Anthozoa	Alcyonacea	Plexauridae	*Thesea*	*Thesea rubra*	Deichmann, 1936	19
Cnidaria	Anthozoa	Alcyonacea	Plexauridae		spp.		24
Cnidaria	Anthozoa	Alcyonacea	Plexauridae		sp. 1		172
Cnidaria	Anthozoa	Alcyonacea	Plexauridae		sp. 2		7
Cnidaria	Anthozoa	Alcyonacea	Plexauridae		sp. 3		27

Cnidaria	Anthozoa	Alcyonacea	Plexauridae		sp. 4		0
Cnidaria	Anthozoa	Alcyonacea	Primnoidae	*Callogorgia*	sp. 1		25
Cnidaria	Anthozoa	Alcyonacea	Primnoidae	*Primnoa*	*Primnoa resedaeformis*	Gunnerus, 1763	7
Cnidaria	Anthozoa	Alcyonacea			sp. 1		3
Cnidaria	Anthozoa	Antipatharia	Antipathidae	*Antipathes*	*Antipathes furca*	Gray, 1857	5
Cnidaria	Anthozoa	Antipatharia	Antipathidae	*Stichopathes*	sp. 1		453
Cnidaria	Anthozoa	Antipatharia	Antipathidae	*Stichopathes*	sp. 2		41
Cnidaria	Anthozoa	Antipatharia	Aphanipathidae	*Aphanipathes*	*Aphanipathes pedata*	Gray, 1857	10
Cnidaria	Anthozoa	Antipatharia	Aphanipathidae	*Elatopathes*	*Elatopathes abietina*	Pourtalès, 1874	57
Cnidaria	Anthozoa	Antipatharia	Aphanipathidae	*Elatopathes*	sp. 1		282
Cnidaria	Anthozoa	Antipatharia	Myriopathidae	*Tanacetipathes*	sp. 1		155
Cnidaria	Anthozoa	Antipatharia	Myriopathidae	*Tanacetipathes*	sp. 2		26
Cnidaria	Anthozoa	Antipatharia			sp. 1		221
Cnidaria	Anthozoa	Antipatharia			sp. 2		21
Cnidaria	Anthozoa	Antipatharia			sp. 3		25
Cnidaria	Anthozoa	Scleractinia	Agariciidae	*Agaricia*	sp. 1		1
Cnidaria	Anthozoa	Scleractinia	Caryophylliidae		sp. 1		2
Cnidaria	Anthozoa	Scleractinia	Oculinidae	*Madrepora*	*Madrepora carolina*	Pourtalès, 1871	39
Cnidaria	Anthozoa	Scleractinia	Oculinidae	*Madrepora*	sp. 1		14
Cnidaria	Anthozoa	Scleractinia	Pocilloporidae	*Madracis*	*Madracis myriaster*	Milne Edwards & Haime, 1850	37
Cnidaria	Hydrozoa	Anthoathecata	Stylasteridae	*Stylaster*	sp. 1		174
Cnidaria	Hydrozoa	Anthoathecata	Stylasteridae		sp. 1		63
Cnidaria	Hydrozoa				sp. 1		27
Arthropoda	Malacostraca	Decapoda	Inachoididae	*Stenorhynchus*	*Stenorhynchus seticornis*	Herbst, 1788	1
Arthropoda	Pycnogonida	Pantopoda	Pycnogonidae		spp.		1
Bryozoa					sp. 1		5
Bryozoa					sp. 2		3
Bryozoa					spp.		1
Echinodermata	Crinoidea				spp.		245
Echinodermata	Ophiuroidea	Euryalina			spp.		29

Conclusions

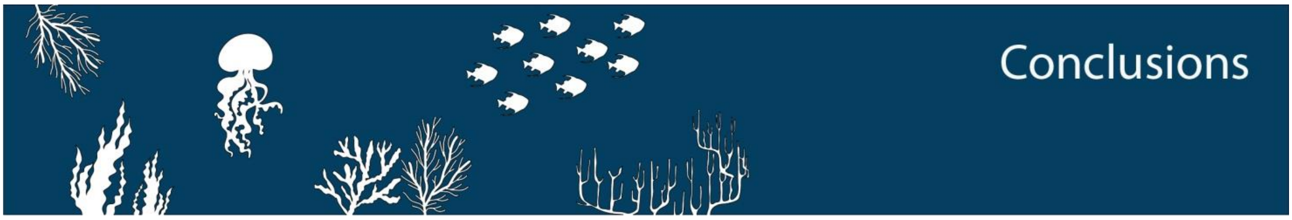

This thesis analyzes the knowledge about the mesophotic zone, focusing particularly on the Mediterranean Sea but with an insight at also extra-Mediterranean situations, to identify information gaps, help overcome discrepancies in the spatial definition of “mesophotic zone”, provide a quantitative characterization of the diversity associated with mesophotic assemblages of different composition, with the ultimate aim of increasing our understanding of the mesophotic zone and identify gaps in the conservation measures targeting the mesophotic natural heritage.

The first chapter provides the first assessment of the spatial and bathymetrical extent of the mesophotic zone in the Mediterranean Sea based on a physical approach by modeling the penetration of light along the water column. Using the light regime to draw the borders of the mesophotic zone would concur overcoming uncertainties related to the definition of the mesophotic domain based on a fixed depth range, ensuring to appreciate the variability in its bathymetric and spatial extension related to local factors and providing quantitative estimation of the portion of seabed under mesophotic conditions.

From the approach here presented, about 15% of the Mediterranean Sea might be under mesophotic conditions. However, the analysis of the literature on mesophotic ecosystems highlighted that most of the information concerns benthic assemblages dominated by cnidarians whilst situations characterized by other taxonomic groups are still poorly explored, suggesting that part of the biodiversity associated with mesophotic ecosystems might be largely undisclosed.

In this context, the Chapter 2 aims at helping to choose the most appropriate approach to process visual data when studying the diversity associated with mesophotic and deep benthic ecosystems and quantifying the extension of the different substrate classes. Techniques to select a subset of frames from video surveys based on time and distance intervals are compared, identifying strengths and weaknesses, and quantifying the confidence related to every method. The study highlights that the variation of survey velocity is the factors influencing the most the quality of the estimations, affecting the distribution of frames along the survey. The results provided suggest that methods based of time intervals might be most appropriate when the aim is the study of the biodiversity associated with benthic assemblages, while methods based on distance intervals might be the best choice when estimating the extent of substrate classes.

In Chapter 3, a set of ROV videos imaging different mesophotic assemblages along the Italian coasts are analyzed using the most appropriate technique to explore their diversity and the environmental factors influencing their distribution and composition. In total, more than 290 taxa were identified in the 25 explored sites, composing 5 different typologies of assemblage: cnidarians associations, coralligenous associations, mobile-bottom associations, deep-water oyster reefs associations and rhodolith-bed associations. Cnidarians and coralligenous assemblages presented the highest taxonomic richness together with deep-water oyster reefs that showed comparable biodiversity values. Moreover, deep-water oyster reefs presented values of functional richness similar to those of coralligenous and cnidarians assemblages, ultimately suggesting that situations characterized by oyster biocontructions might represent hotspot of biodiversity and play a relevant ecological role at mesophotic depths in the Mediterranean Sea.

The analysis of the dissimilarity in the taxonomic composition of assemblages revealed that geographic location is not the main structuring factor at mesophotic depths but, instead, that environmental setting might play a crucial role. Assemblages occurring within comparable environmental characteristics were more taxonomic similar than those environmentally different. Mesophotic taxa are, therefore, probably assemble along environmental gradients rather than geographical distance. Contrarily, environmental variables are not affecting the functional composition of mesophotic assemblages. Functional entities, in fact, might comprise individuals from different taxonomic ranks with different environmental requirements.

However, stochastic processes along with set of different biotic interactions among individuals are of primary importance in shaping the structure of benthic assemblages by limiting or facilitating the presence of taxa. Part of the variability of the composition of mesophotic assemblages surely relies on more complex dynamics and it may not be possible to distinguish the contribution of deterministic processes related to environmental preferences from biotic or stochastic processes.

The results here presented aim at providing information on the diversity associated with mesophotic benthic assemblages in the Mediterranean Sea and the factor influencing this diversity, in order to support future protection actions. As a matter of fact, of the 247 taxa identified in this study, considering those classified at least at Family level, only 26% are currently included in national and international conservation measures (Tab. 1). If situations presenting biogenic or geogenic structure rising from the seafloor such as coralligenous formations, rhodolith beds and deep-water oyster reefs are protected under the Habitat Directive (Council Directive 92/43/EEC; “Reefs – 1170”), the fauna associated to these bioconstructions is mostly not considered by conservation efforts. This is also true for assemblages of soft bottoms that, despite hosting a lower taxonomic and functional richness with respect to the other explored assemblages, might comprises taxa worthy for protection actions.

Phylum	**Family**	**Genus**	**Species**	**Habitat Directive**	**Barcelona Convention**	**Bern Convention**	**CITES**	**IUCN Red List**	**SPAMI species**	**VME Indicator species**	**GFCM priority species**
Ochrophyta	Acinetosporaceae	*Acinetospora*	*Acinetospora crinita*					NE			
Porifera	Axinellidae	*Axinella*	*Axinella polypoides*		Annex II	Annex II			x		
Porifera	Axinellidae	*Axinella*	sp. 3					LC			
Porifera	Spongiidae	*Spongia*	*Spongia agaricina*			Annex III			x		
Porifera	Spongiidae	*Spongia*	*Spongia officinalis*			Annex III			x	x	
Porifera	Tethyidae	*Tethya*	*Tethya aurantium*		Annex II				x		
Porifera	Tethyidae	*Tethya*	*Tethya citrina*		Annex II				x		
Porifera	Geodiidae	*Geodia*	*Geodia cydonium*		Annex II				x		
Porifera	Theneidae	*Thenea*	*Thenea muricata*							x	
Cnidaria	Aliciidae	*Alicia*	*Alicia mirabilis*					LC			
Cnidaria	Andresiidae	*Andresia*	*Andresia partenopea*					DD			
Cnidaria	Acanthogorgiidae	*Acanthogorgia*	*Acanthogorgia hirsuta*					LC			
Cnidaria	Acanthogorgiidae	*Acanthogorgia*	*Acanthogorgia hirsuta*					LC			
Cnidaria	Alcyoniidae	*Alcyonium*	*Alcyonium coralloides*					LC			
Cnidaria	Alcyoniidae	*Alcyonium*	*Alcyonium palmatum*					LC			
Cnidaria	Coralliidae	*Corallium*	*Corallium rubrum*	Annex V		Annex III		EN	x		x
Cnidaria	Cornulariidae	*Cornularia*	*Cornularia cornucopiae*					LC			
Cnidaria	Gorgoniidae	*Eunicella*	*Eunicella cavolini*					NT			
Cnidaria	Gorgoniidae	*Eunicella*	*Eunicella singularis*					NT			
Cnidaria	Gorgoniidae	*Eunicella*	*Eunicella verrucosa*					NT			
Cnidaria	Paralcyoniidae	*Paralcyonium*	*Paralcyonium spinulosum*					LC			
Cnidaria	Plexauridae	*Paramuricea*	*Paramuricea clavata*					VU		x	
Cnidaria	Plexauridae	*Paramuricea*	*Paramuricea macrospina*					DD		x	
Cnidaria	Plexauridae	*Swiftia*	*Swiftia pallida*					DD			
Cnidaria	Primnoidae	*Callogorgia*	*Callogorgia verticillata*					NT	x		
Cnidaria	Myriopathidae	*Antipathella*	*Antipathella subpinnata*				Annex II	NT	x		
Cnidaria	Arachnactidae	*Arachnanthus*	*Arachnanthus oligopodus*					DD			
Cnidaria	Funiculinidae	*Funiculina*	*Funiculina quadrangularis*					VU		x	
Cnidaria	Pennatulidae	*Pennatula*	*Pennatula phosphorea*					VU		x	
Cnidaria	Pennatulidae	*Pennatula*	*Pennatula rubra*					VU		x	
Cnidaria	Virgulariidae	*Virgularia*	*Virgularia mirabilis*					LC		x	
Cnidaria	Dendrophylliidae	*Dendrophyllia*	*Dendrophyllia cornigera*				Annex II	EN			
Cnidaria	Cerianthidae	*Cerianthus*	*Cerianthus membranaceus*					LC			
Cnidaria	Aglaopheniidae	*Lytocarpia*	*Lytocarpia myriophyllum*					LC			
Mollusca	Cardiidae	*Acanthocardia*	*Acanthocardia aculeata*					NE			
Mollusca	Eledonidae	*Eledone*	*Eledone cirrhosa*					LC			
Mollusca	Octopodidae	*Callistoctopus*	*Callistoctopus macropus*					LC			
Mollusca	Octopodidae	*Octopus*	*Octopus vulgaris*					LC			

Arthropoda	Palinuridae	*Palinurus*	*Palinurus elephas*			Annex III		x	
Bryozoa	Adeonidae	*Adeonella*	*Adeonella calveti*				NE		
Echinodermata	Astropectinidae	*Astropecten*	*Astropecten aranciacus*				NE		
Echinodermata	Diadematidae	*Centrostephanus*	*Centrostephanus longispinus*	Annex IV	Annex II	Annex II		x	
Echinodermata	Holothuriidae	*Holothuria*	*Holothuria forskali*				LC		
Echinodermata	Holothuriidae	*Holothuria*	*Holothuria poli*				LC		
Echinodermata	Holothuriidae	*Holothuria*	*Holothuria tubulosa*				LC		
Echinodermata	Stichopodidae	*Parastichopus*	*Parastichopus regalis*				LC		
Chordata	Congridae	*Ariosoma*	*Ariosoma balearicum*				LC		
Chordata	Muraenidae	*Muraena*	*Muraena helena*				LC		
Chordata	Ophichthidae	*Ophisurus*	*Ophisurus serpens*				LC		
Chordata	Phycidae	*Phycis*	*Phycis blennoides*				LC		
Chordata	Phycidae	*Phycis*	*Phycis phycis*				LC		
Chordata	Callanthiidae	*Callanthias*	*Callanthias ruber*				LC		
Chordata	Labridae	*Ctenolabrus*	*Ctenolabrus rupestris*				LC		
Chordata	Mullidae	*Mullus*	*Mullus barbatus*						x
Chordata	Scorpaenidae	*Scorpaena*	*Scorpaena scrofa*				LC		
Chordata	Serranidae	*Serranus*	*Serranus cabrilla*				LC		
Chordata	Serranidae	*Serranus*	*Serranus hepatus*				LC		
Chordata	Sparidae	*Pagellus*	*Pagellus erythrinus*				LC		
Chordata	Sparidae	*Spondyliosoma*	*Spondyliosoma cantharus*				LC		
Chordata	Synodontidae	*Synodus*	*Synodus saurus*				LC		
Chordata	Trachinidae	*Trachinus*	*Trachinus araneus*				LC		
Chordata	Soleidae	*Solea*	*Solea solea*				LC		x
Chordata	Sebastidae	*Helicolenus*	*Helicolenus dactylopterus*				LC		
Chordata	Triglidae	*Chelidonichthys*	*Chelidonichthys lastoviza*				LC		
Chordata	Triglidae	*Chelidonichthys*	*Chelidonichthys lucerna*				LC		
Chordata	Zeidae	*Zeus*	*Zeus faber*				LC		

Tab. 1. List of identified species included in National and International conservation measures. CITES: Convention on International Trade in Endangered Species of Wild Fauna and Flora; VME: Vulnerable Marine Ecosystems; SPAMII: Specially Protected Areas of Mediterranean Importance; GFCM: General Fisheries Commission for the Mediterranean.

Increasing the knowledge about sensitive species or habitats providing spatial information is, thus, of a paramount importance to support proper conservation measures. In this context, Chapter 4 aims at providing a large-scale spatial information on the distribution of areas with environmental settings able to host deep-water oyster reefs at mesophotic depth in the Adriatic-northern Ionian Sea. The results show that only small sections of the modeled region (about 1.8%) might be suitable for deep-water oyster reef assemblages, suggesting that their presence might be constrained by strict environmental requirements such as gently sloped and shaded reliefs, water masses rich in nutrients and a specific temperature range.

We are only beginning to appreciate the diversity and magnitude of benefits that mesophotic ecosystems provide. Much work is still needed to assess the profusion of life in this vast region whose extent largely vary with local climatic and hydrological factors.

In this sense, Chapter 5 focuses on the mesophotic zone of the Gulf of Mexico, used as case study for extra-Mediterranean situations, assessing its bathymetric and spatial extension and the diversity associated with mesophotic assemblages The Gulf of Mexico presents strongly different climatic and oceanographic conditions with respect to the Mediterranean Sea. Here, the outflows of the large rivers characterizing the Gulf, the Mississippi and Rio Grande, influence the water clarity in areas surrounding the rivers mouths, generating huge variations in the bathymetric extent of the mesophotic zone. Including the light regime in the estimation of the spatial extent of the mesophotic zone rather than a fixed depth interval ensures to appreciate how the mesophotic conditions vary across the Gulf. The method developed in the first Chapter is successfully applied to map the mesophotic zone of the Gulf of Mexico, confirming the flexibility of the approach integrating light penetration that can be used in different geographic locations.

Not only the extension of the mesophotic vary with geographic position but also the assemblages that can be found. The main taxonomic groups at mesophotic depths in the Gulf of Mexico is represented by cnidarians, with a dominance of ellisellids and plexaurids, and black corals in the *Stichopathes*, *Elatopathes*, and *Tanacetipathes*. The environmental setting seems to play a major role in shaping the composition of mesophotic assemblages also in the Gulf of Mexico, whose composition vary in relation to depth, with deeper sites presenting a higher diversity and number of individuals.

Acknowledgments

Vorrei esprimere la mia gratitudine al personale del Dipartimento di Beni Culturali dell'Università di Bologna, dai professori allo staff amministrativo, per la loro gentilezza e disponibilità durante questi anni. In particolare, ringrazio il Prof. Marco Abbiati per i consigli che hanno contributito a migliorare il lavoro svolto.

Vorrei ringraziare tutto il personale CNR-ISMAR della sede di Bologna, che mi ha accolto calorosamente e coinvolto in tante attività che hanno reso ancora più ricca questa esperienza. Grazie, soprattutto, a Mariacristina, Alessandra, Andrea, Caterina, Ilaria, Giacomo, Camilla e tanti altri che, tra caffè e risate, hanno portato un po' di leggerezza nelle mie giornate.

Vorrei ringraziare Paolo, per la constante gentilezza e disponibilità, e per avermi guidato con originalità in molte delle attività collaterali al mio percorso di dottorato che abbiamo condiviso.

Ringrazio Erik Cordes per avermi ospitato nel suo laboratoro della Temple University di Philadelphia e avermi dedicato un po' del suo prezioso tempo, dandomi l'opportunità di estendere questo lavoro di tesi oltre il Mediterraneo. Ricorderò per sempre il meraviglioso tempo trascorso con i ragazzi del Cordes Lab.

A Valentina va tutta la mia gratitudine per avermi insegnato lo strano modo dei dati spaziali con pazienza, per essermi sempre stata vicina, mai stanca di aiutare. La sua simpatia ha arricchito questi anni di lavoro in modo indescrivibile diventando per me un punto di riferimento e un'importante amica.

Ringrazio Federica, tutor di questa tesi e amica, senza la quale questo percorso non sarebbe stato possibile. Con la sua positività ed il suo coinvolgente entusiasmo mi ha supportato in ogni iniziativa, permettendo la realizzazione di questo progetto e insegnandomi a non temere quello che non si conosce.

Un grazie particolare va a Lorenzo, tutor e amico, per essere stato sempre presente indirizzando le mie attività, per essere riuscito - col suo tocco pragmatico - a far funzionare meglio le cose e per avermi inseganto a ricercare sempre la miglior qualità in ciò che si fa.

Il mio ringraziamento più grande va a Marco Taviani, tutor di questa tesi sulla carta ma mentore e amico nella realtà, con il quale ho trascorso molto tempo dentro e fuori l'ufficio, tra mercatini, sushi e gite fuoriporta. Le sue idee, unite alla sua passione e al suo entusiasmo, hanno plasmato il mio lavoro, trasmettendomi l'ambizione di sognare in grande pur mantenendo i piedi per terra. Molto di quello che ho imparato in questi anni è merito suo. Grazie per aver avuto fiducia in me e per non aver mai esitato a mandarmi nella mischia. Quanto ci hai messo?!

Ringrazio tutti gli amici, quelli di una vita e quelli più recenti, per avermi fatto senire la loro vicinanza in questi anni, sopportando i miei borbotii e lamentele, e per avermi distratto quando ne avevo più bisogno.

Infine, questo lavoro è dedicato alla mia Famiglia, a mia madre Margherita, mio padre Gabriele, mia sorella Sara e a "i zii" Enrico e Loredana, che mi hanno sempre supportato e, nonstante la distanza, mi sono sempre stati vicini. Grazie per esser stati e per essere al mio fianco nel particolare e complesso percorso che ho scelto di perseguire.